
**Early phase clinical studies of novel
immunotherapeutics in oncology**

Willeke Ros

Publication of this thesis was financially supported by:

Oncology Graduate School Amsterdam

Utrecht Institute for Pharmaceutical Sciences

Book design & layout:

Willeke Ros

Printing:

Gildeprint

© Wilhelmina Ros, 2019

The research described in this thesis was performed at the Division of Pharmacology and the Department of Clinical Pharmacology, Division of Medical Oncology of The Netherlands Cancer Institute, Amsterdam, the Netherlands.

Early phase clinical studies of novel immunotherapeutics in oncology

Vroege fase klinische studies van nieuwe immunotherapieën in de oncologie

(met een samenvatting in het Nederlands)

Proefschrift

ter verkrijging van de graad van doctor aan de
Universiteit Utrecht
op gezag van de
rector magnificus, prof.dr. H.R.B.M. Kummeling,
ingevolge het besluit van het college voor promoties
in het openbaar te verdedigen op

woensdag 18 september 2019 des middags te 12.45 uur

door

Wilhelmina Ros

geboren op 28 februari 1990
te Leiden

Promotor: Prof. dr. J.H. Beijnen

TABLE OF CONTENTS

Preface

Chapter 1 Tumor targeting immunotherapies

Chapter 1.1 Preliminary efficacy, safety, pharmacokinetics and pharmacodynamics of a T-cell bispecific antibody cibatamab (CEA-TCB) administered alone and in combination with atezolizumab in patients with metastatic colorectal cancer.....**15**
Interim analysis

Chapter 1.2 Preliminary efficacy and safety of the novel tumor targeting immunocytokines CEA-IL2v (in combination with atezolizumab) and FAP-IL2v, which contain a variant of interleukin-2.....**33**
Interim analysis

Chapter 2 Monoclonal antibodies targeting co-stimulatory receptor molecules

Chapter 2.1 Preliminary clinical activity and safety of OX40 agonistic monoclonal antibody GSK3174998 administered alone and in combination with pembrolizumab in selected advanced solid tumors.....**53**
Interim analysis

Chapter 2.2 Preliminary efficacy, safety, pharmacokinetics and pharmacodynamics data from a phase I dose-escalation study of OX40 agonistic monoclonal antibody PF-04518600 administered alone and in combination with utomilumab, a 4-1BB agonistic monoclonal antibody.....**67**
Interim analysis

Chapter 2.3 Preliminary efficacy and safety of CD40 agonistic monoclonal antibody selicrelumab administered in combination with atezolizumab or vanucizumab.....**89**
Interim analysis

Chapter 3 Pembrolizumab in rare cancers

Chapter 3.1 Efficacy and Safety of Pembrolizumab in Previously Treated Advanced Cervical Cancer: Results From the Phase 2 KEYNOTE-158 Study.....**117**
Journal of Clinical Oncology 2019;37:1470-1478

Chapter 3.2 Preliminary efficacy and safety of pembrolizumab in selected advanced solid tumors.....**139**
Interim analysis

Chapter 4 Development of assays for immunotherapy

Chapter 4.1 Enzyme linked immunosorbent assay for the quantification of nivolumab and pembrolizumab in human serum and cerebrospinal fluid.....**155**
Journal of Pharmaceutical and Biomedical Analysis 2019;164:128-134.

Chapter 4.2	Multiparameter flow cytometry assay for quantification of immune cell subsets, PD-1 expression levels and PD-1 receptor occupancy by nivolumab and pembrolizumab.....	177
	<i>Cytometry: Part A [In press]</i>	

Chapter 5. Antidrug antibodies

Chapter 5.1	Antidrug Antibody Formation in Oncology: Clinical Relevance and Challenges.....	215
	<i>The Oncologist 2016;21:1260-1268.</i>	

Chapter 6 Combining immunotherapy with chemotherapy

Chapter 6.1	Enhancing anti-tumor response by combining immune checkpoint inhibitors with chemotherapy in solid tumors.....	237
	<i>Annals of Oncology 2019;30:219-235.</i>	

Chapter 7 Conclusions and future perspectives.....267

Appendix

Author affiliations

Summary

Nederlandse samenvatting

Overview of publications

Dankwoord

Curriculum vitae

Preface

Immunotherapy is quickly becoming one of the most effective ways to combat cancer for certain tumor types. The rise of immunotherapy started with the anti-CTLA-4 antibody ipilimumab, which showed significant increase of survival for patients with metastatic melanoma. Three years later, the anti-PD-1 antibodies nivolumab and pembrolizumab were approved for the same indication. Now, in 2019, the anti-PD-1 monoclonal antibodies are approved for metastatic melanoma, non-small cell lung cancer, renal cell carcinoma, Hodgkin's Lymphoma, head and neck cancer, small cell lung cancer, urothelial carcinoma, colorectal cancer, hepatocellular carcinoma, gastric cancer, cervical cancer and mismatch repair deficient tumors. Investigation to further broaden immunotherapy across indications is currently ongoing. Novel immunotherapies are emerging, including monoclonal antibodies that target co-stimulatory receptor molecules or checkpoint molecules, and antibodies which aim to improve targeting of immune cells to the tumor site. This thesis describes the early phase studies of novel immunotherapies in advanced solid tumors.

In **chapter 1** we describe novel immunotherapies which aim to improve the targeting of immunotherapy to the cancer site. **Chapter 1.1** describes a bispecific monoclonal antibody which targets the tumor-specific antigen carcinoembryonic antigen (CEA), while simultaneously binding to CD3 on T-cells. **Chapter 1.2** describes two modified versions of interleukin-2 which are coupled to a monoclonal antibody. These monoclonal antibodies target CEA or fibroblast activating protein (FAP).

Co-stimulatory receptor molecules act to amplify the activation signals of T-cells. Targeting these molecules may be an effective way to increase an ongoing immune response. In **chapter 2** we describe clinical trials investigating monoclonal antibodies that target co-stimulatory receptor molecules. **Chapter 2.1** summarizes the preliminary results of a clinical trial investigating an OX40 agonistic monoclonal antibody GSK3174998 alone and in combination with pembrolizumab. **Chapter 2.2** discusses the dose escalation phase of the anti-OX40 antibody PF-04518600 alone and in combination with utomilumab, an anti-4-1BB agonistic antibody. **Chapter 2.3** reports the preliminary results of two trials of a monoclonal antibody targeting CD40, selicrelumab. Selicrelumab is combined with the anti-PD-L1 antibody atezolizumab and the VEGF/ANG-2 bispecific antibody vanucizumab.

Pembrolizumab has been approved for a wide variety of cancers. However, exploration for further broadening of indications is still being performed. In KEYNOTE-158, pembrolizumab is investigated in rare cancer types. **Chapter 3.1** describes the efficacy of pembrolizumab in cervical cancer. **Chapter 3.2** describes an interim analysis of the efficacy of pembrolizumab in ten rare cancer types investigated at the Netherlands Cancer Institute.

In addition to investigating novel immunotherapies and expansion across tumor types, efforts are also made into identifying those patients that benefit from immunotherapy. For this, identifying novel biomarkers is essential. Chapter 4 describes assays which may help to identify these novel biomarkers. **Chapter 4.1** describes an enzyme linked immunosorbent assay which measures serum concentrations of pembrolizumab and nivolumab. **Chapter 4.2** describes a multi-parameter flow cytometry assay which quantifies PD-1 expression on various immune cells. In addition, this assay measures the PD-1 receptor occupancy by nivolumab or pembrolizumab.

Monoclonal antibodies are biological agents to which the immune system of the host can generate an unwanted response in the form of anti-drug antibodies (ADAs). These ADAs can affect the pharmacokinetics, pharmacodynamics or safety of the therapeutic drug. **Chapter 5** describes ADAs in oncology.

To further broaden checkpoint inhibition therapy, it can be combined with other immunotherapies, as has been explored in this thesis. However, chemotherapy has also been shown to exert beneficial immunological effects. **Chapter 6** describes these immunological aspects and discusses them in the light of combination therapy with checkpoint inhibitors.

Finally, **chapter 7** reflects on the findings of the research described in this thesis. Future perspectives and challenges of the described anticancer immunotherapies are discussed in this chapter.

Chapter 1

Tumor targeting immunotherapies

Chapter 1.1

Preliminary efficacy, safety, pharmacokinetics and pharmacodynamics of a T-cell bispecific antibody cibisatamab (CEA-TCB) administered alone and in combination with atezolizumab in patients with metastatic colorectal cancer.
A summary of published data from early analysis of BP29541 and WP29945.

Willeke Ros

Preliminary data has been presented at the European Society for Medical Oncology (ESMO) Annual Congress 2017:

Melero I, Segal NH, Saro Suarez JM, **Ros W**, Martinez Garcia M, Calvo E, Moreno V, Ponce Aix S, Marabelle A, Cleary JM, Hurwitz H, Eder JP, Jamois C, Belousov A, Bouseida S, Sandoval F, Bacac M, Nayak TK, Karanikas V, Argiles G. Pharmacokinetics (PK) and pharmacodynamics (PD) of a novel carcinoembryonic antigen (CEA) T-cell bispecific antibody (CEA CD3 TCB) for the treatment of CEA-expressing solid tumors.
Journal of Clinical Oncology 2017;35:2549.

Segal NH, Saro J, Melero I, **Ros W**, Argiles G, Marabelle A, Rodriguez Ruiz ME, Albanell J, Calvo E, Moreno V, Cleary JM, Eder JP, Karanikas V, Bouseida S, Sandoval F, Sabanes D, Sreckovic S, Hurwitz HI, Paz-Ares L, Tabernero J. Phase I Studies of the Novel Carcinoembryonic Antigen CD3 T-Cell Bispecific (CEA-CD3 TCB) Antibody as a Single Agent and in Combination With Atezolizumab: Preliminary Efficacy and Safety in Patients With Metastatic Colorectal Cancer (mCRC).
Annals of Oncology 2017;28:10.

ABSTRACT

Background: Cibisatamab is a novel bi-specific monoclonal antibody which binds bivalently to CEA and monovalently to CD3. Simultaneous binding of cibisatamab to CEA and CD3 leads to T-cell activation and tumor cell lysis.

Methods: BP29541 (ClinicalTrials.gov identifier NCT02324257) and WP29945 (NCT02650713) are open-label, non-randomized multicenter studies designed to evaluate the safety, tolerability, pharmacokinetics, pharmacodynamics and preliminary clinical activity of cibisatamab as a single agent (BP29541) and in combination with atezolizumab (WP29945) in CEA+ tumors. In this chapter, we describe the preliminary safety, efficacy, pharmacokinetics (PK) and pharmacodynamics (PD) of cibisatamab of which the results have been published on previous European Society for Medical Oncology (ESMO) congresses. Safety analysis was performed on all dose levels in all tumor types. Efficacy analysis was performed in colorectal cancer (CRC) patients on dose levels ≥ 60 mg for monotherapy, and dose levels ≥ 80 mg for combination therapy.

Results: Between December 2014 and March 2017, 80 patients were enrolled in BP29541, and 45 patients were enrolled in WP29945. The most common adverse events (all grades, all dose levels) related to treatment were infusion related reactions (IRRs) (55%; 40%), diarrhea (40%; 56%), and pyrexia (58%; 71%) for single agent and combination therapy respectively. The maximal tolerated dose (MTD) was 400 mg cibisatamab as a single agent. The MTD was not defined for the combination therapy. Observed dose limiting toxicities included G3 dyspnea, G3 hypoxia, G3 diarrhea, G4 colitis and G5 respiratory failure (all cibisatamab monotherapy), and G3 maculopapular rash and G3 transient increase of ALT (cibisatamab + atezolizumab). Two (6%) out of 31 CRC patients receiving ≥ 60 mg cibisatamab showed a confirmed partial response in BP29541. Both responses were seen in microsatellite stable (MSS) CRC patients. Two (18%) out of 11 MSS CRC patients receiving ≥ 80 mg cibisatamab showed a confirmed partial response in WP29945. Data suggests a linear PK profile in doses ≥ 20 mg. PD-analysis of tumor biopsies revealed T-cell proliferation, increase of PD-(L)1 expression and a decrease of CEA-expressing tumor cells upon treatment.

Conclusions: Safety profile of cibisatamab was manageable at doses up to 160 mg, both with monotherapy and in combination with atezolizumab. Cibisatamab shows encouraging anti-tumor activity in heavily pre-treated CRC patients, including patients with MSS tumors.

INTRODUCTION

Bispecific antibodies are emerging as a novel class of immunotherapies to combat cancer. As the name implies, these antibodies are capable of binding two different epitopes simultaneously. The two epitopes can either be a combination of two immunomodulators, a tumor-associated antigen and an immunomodulator, or a tumor-associated antigen and the T-cell receptor/CD3 complex[1]. The latter ones are the majority of bispecific antibodies and are known as cytotoxic effector cell redirectors. The concept of these cytotoxic effector cell redirectors is that T-cells are activated by the antibody via CD3, and redirected to the tumor area via the tumor antigen binding property.

An example of a suitable tumor-associated antigen for targeting by bispecific antibodies is carcinoembryonic antigen (CEA). CEA plays an important role in cell adhesion, invasion, and metastasis of cancer cells[2]. It is often highly expressed in various tumors including colorectal cancer (CRC), pancreatic cancer, gastric cancer, non-small cell lung cancer (NSCLC), and breast cancer. CEA inhibits anoikis, which is a process whereby cells that are no longer attached to the extracellular matrix undergo apoptosis. In healthy tissue, the highest level of expression of CEA is found in the colon. However, CEA expression is restricted to the luminal side of the gastro-intestinal tract, and therefore unreachable for CEA-targeting monoclonal antibodies.

Cibisatamab (also known as CEA-TCB) is a T-cell bispecific antibody targeting CEA expressed on tumor cells, and the CD3 epsilon chain (CD3e) on T-cells[3]. It has a human IgG1 framework and a 2:1 format, with one arm binding to CEA, and one arm binding to CEA and CD3 (Figure 1). As the CD3e binding is monovalent, activation of T-cells is prevented in the absence of simultaneous binding to CEA on tumor cells. The binding affinity is low for CD3e (80 nM), and high for CEA (0.2 nM). This differential binding affinity may lead to better targeting of cibisatamab to tumors overexpressing CEA. The Fc region of cibisatamab contains a point mutation which makes it unable to bind to the complement system and to Fc receptors, thus preventing antigen dependent cell mediated cytotoxicity[4]. Cytotoxicity assays using human peripheral blood mononuclear cells and human tumor cells showed that incubation with cibisatamab led to T-cell activation, secretion of cytotoxic granules, and induction of tumor cell lysis[5]. In vivo experiments with mice xenograft tumor models treated with cibisatamab showed regression of CEA-expressing tumors, formation of immune cell infiltrates, increased frequency of activated T-cells and, most interestingly, conversion of PD-L1 negative tumors into PD-L1 positive ones.[5]

Cibisatamab is currently being tested in study BP29541, a First Time in Human phase I open label study; WP29945, in which it is combined with atezolizumab (anti-PD-L1); and CO40939, in which colorectal patients are pretreated with obinituzumab prior to receiving atezolizumab and cibisatamab. Here is presented a summary of published data from early analysis of both BP29541 and WP29945. The data cutoff for safety and efficacy was 3rd of March 2017. The data cutoff for pharmacokinetic (PK)/ pharmacodynamic (PD) analysis was 24th of July 2017.

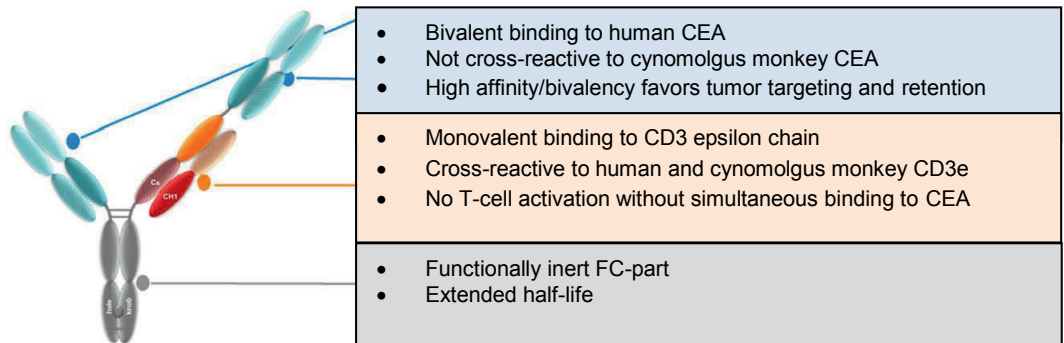


Figure 1. Design of cibusatamab. From Segal et al.[6]

METHODS

Study design

Studies BP29541 (ClinicalTrials.gov identifier NCT02324257) and WP29945 (NCT02650713) were designed to examine the safety, tolerability and maximal tolerated dose of cibusatamab alone or in combination with atezolizumab in patients with advanced CEA-positive solid tumors.

Figure 2 describes the design of both studies. BP29541 consisted of two parts (Figure 2A). Part I consisted of single patient dose escalation cohorts with doses given which were expected to be below relevant biological effects. Part II consisted of multiple patient dose escalation cohorts and an expansion cohort. WP29945 consisted of a multiple patient dose escalation part, and an expansion cohort (Figure 2B). In both studies, cibusatamab was given qW. In WP29945, atezolizumab was given as a fixed dose of 1200mg q3W.

Dose escalation was guided with a modified continual reassessment method (mCRM) - escalation with overdose control (EWOC). After each cohort of patients, the model was updated and the proposed dose was based on the logistic regression model.

Patient population

Key eligibility requirements included having locally advanced/metastatic CEA+ solid tumors, with ≥ 1 tumor lesion able to be biopsied, who progressed on or are intolerant of a standard therapy, ≥ 18 years of age, radiologically measurable disease (Response Evaluation Criteria In Solid Tumors [RECIST] v1.1), Eastern Cooperative Oncology Group performance status (ECOG PS) 0-1, adequate organ function, measurable disease based on RECIST V1.1., and a life expectancy of at least 12 weeks.

Key exclusion criteria included: prior approved anti-cancer therapy (including chemotherapy, hormonal therapy or radiotherapy) within 2 weeks prior to initiation of study treatment; prior biologic, systemic immunostimulatory, radiation or investigational therapy within 4 weeks prior to initiation of study treatment; treatment with systemic immunosuppressive medications within 2 weeks prior to initiation of study treatment; active

or untreated central nervous system metastases; uncontrolled hypertension; patients with paraspinal, paratracheal and mediastinal pathological lesions larger than 2 cm unless previously radiated; patients with bilateral lung lesions and dyspnea and/or SaOX₂ <92 at rest or patients with lobectomy or pneumonectomy with lung metastases in the remaining lung and either dyspnea and/or SaOX₂ <92 at rest ; allergy or hypersensitivity to components of cibisatamab, obinituzumab or atezolizumab; history of autoimmune diseases.

The study was conducted according to protocol, Good Clinical Practice standards, and provisions outlined in the Declaration of Helsinki. The study protocol and all amendments were approved by the appropriate institutional review board and ethics committees.

Treatment and assessments

For BP29541, a cycle consisted of one week. Cibisatamab was given intravenously (IV). For WP29945, a cycle consisted of three weeks. Patients received atezolizumab 1200mg fixed dose IV on day one of every cycle, followed by cibisatamab given IV on day 1, day 8 and day 15 of each cycle. For both studies, tumor assessments were performed during screening, every eight weeks during the first year, and every 12 weeks thereafter. Tumor response was evaluated according to RECIST v1.1 and irRC[7] using computed tomography (CT) scan or magnetic resonance imaging (MRI). Additionally, FDG-PET based tumor assessment was performed at baseline and at week six.

Outcomes

Safety outcome measures

Safety outcome measures included incidence and nature of DLTs, and incidence and severity of adverse events. The National Cancer Institute Common Terminology Criteria for Adverse Events v4.03 was used to evaluate the safety of the treatment.

Efficacy outcome measures

Efficacy/activity outcome measures described in this analysis included change in target lesion from baseline, and confirmed best overall response to treatment.

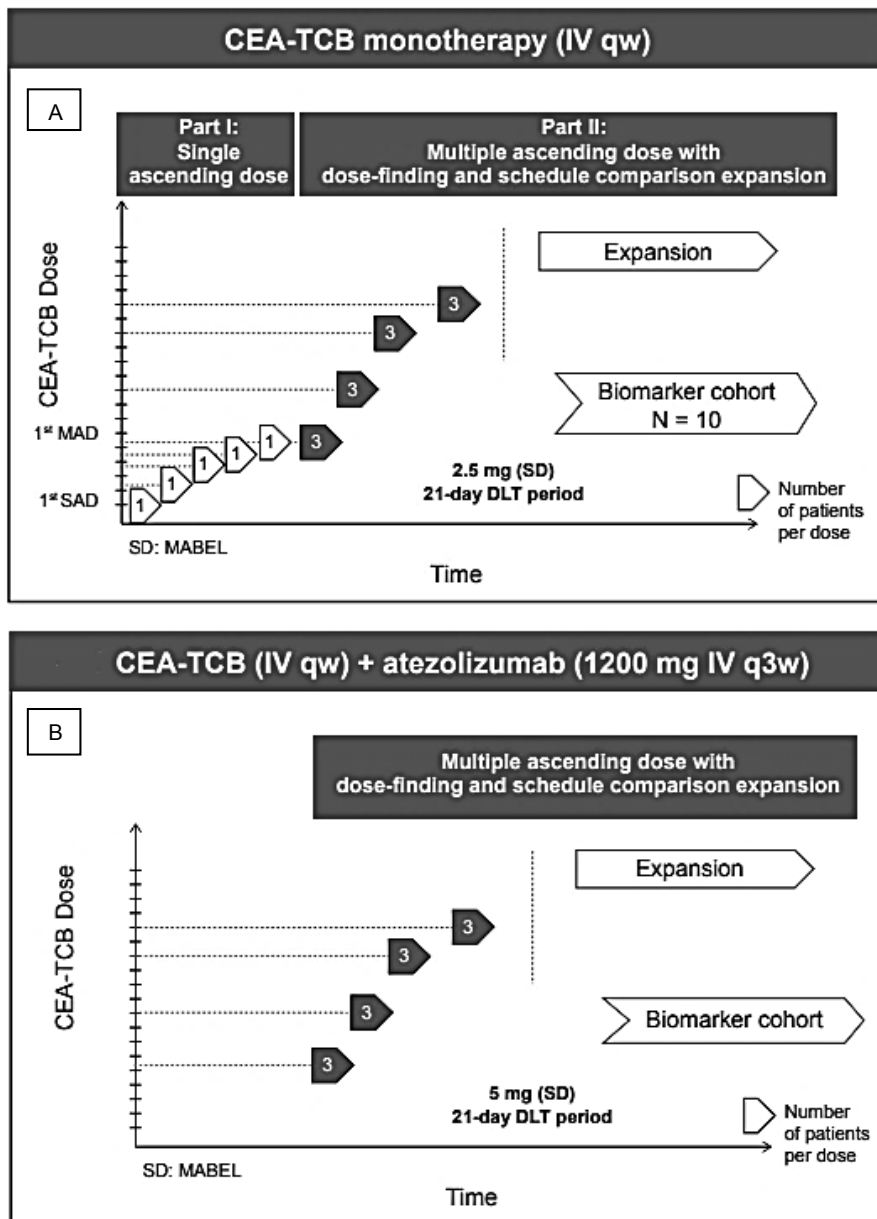
Pharmacokinetic outcome measures

Pharmacokinetic (PK) samples were drawn at every cycle in both studies. A target binding competent PK assay was used to measure serum cibisatamab concentrations. PK was analyzed with NONMEM software, version 7.3.0 (Icon Development Solutions).

Pharmacodynamic outcome measures

Plasma samples were used to measure IL-6 levels. Paired tumor biopsies were used for flow cytometry analysis and immunohistochemistry analysis. In biopsies, changes in characteristics, activation and differentiation of CD4⁺ T cells, CD8⁺ T cells, NK cells, monocytes, regulatory T-cells, and B cells were assessed.

Figure 2. Study schedule for BP29541 and WP29945. (A) Study schedule for BP29541. During the dose escalation phase, part I included single patient cohorts, whereas part II included at least 3 patients within a cohort (with and without obinutuzumab pre-treatment). (B) Study schedule for WP29945. MTD = maximal tolerated dose; DLT = dose limiting toxicity; MABEL = minimum anticipated biological effect level; SAD = single ascending dose; MAD = multiple ascending dose; SD = starting dose. From Segal et al.[6]



RESULTS

Patient inclusion

At the data cut-off point of 3rd of March 2017, 80 patients were enrolled in BP29541, of which 70 had CRC. In WP29945, 45 patients were included, of which 35 had CRC. Other included cancer types in these studies were non-small cell lung cancer (n = 6), pancreatic cancer (n = 6), gastric/esophageal cancer (n = 5) and a small number of patients had a different cancer type (n = 3).

Safety

A summary of treatment-related adverse events (AEs) is shown in Table 1. Nearly all patients experienced treatment related AEs: 95% of patients treated in the monotherapy (100% in dose levels \geq 40mg), and 91% in the combination treatment (94% in dose levels \geq 40mg). The most common adverse events (AEs) related to treatment (all grades) were infusion related reactions (IRRs) (55%; 40%), diarrhea (40%; 56%), and pyrexia (58%; 71%) for single agent and combination therapy respectively. The most common \geq Grade (G) 3 AEs related to treatment were IRRs (18%; 11%) and diarrhea (5%; 13%) for single agent and combination therapy respectively. Twenty-eight percent (monotherapy) and 31% (combination therapy) of all patients experienced a \geq G3 AE.

More than 60% of all IRRs occurred during the first two drug administrations. $G \geq 2$ IRRs correlated with post-infusion IL-6 peaks following the first infusion in the monotherapy study (Figure 3). For patients experiencing IRRs, measures were taken including premedication consisting of paracetamol, anti-histamines, corticosteroids, and slowing the infusion rate.

In BP29541, a total of five DLTs occurred at different dose levels. The first DLT was G3 dyspnea in a patient who received 40mg cibisatamab. The second DLT was G3 hypoxia, seen at the 60 mg dose level. The third DLT occurred at the 300mg dose level, which was G3 diarrhea. In the 600 mg cohort, two DLTs occurred: G4 colitis, and a fatal G5 respiratory failure. The maximum tolerated dose was established as 400 mg for monotherapy.

Two DLTs occurred in WP29945, both at the 160 mg dose level. One patient demonstrated a transient G3 alanine aminotransferase (ALAT) increase and another patient experienced G3 maculopapular rash. The MTD was not defined in the combination trial.

Table 1. Treatment related adverse events. From Segal et al.[6]. ^aSome patients were pre-treated with obinituzumab. ^bDue to DLT at 40 mg in monotherapy in a patient with NSCLC, safety data cutoff is ≥ 40 mg. ^cBased on all patients treated with monotherapy. ^dDose exceeded cycle 1 and 2 MTD (400 mg).

Safety – all patients and tumor types, %	Cibisatamab monotherapy ^a		Cibisatamab + atezolizumab	
	All (N=80)	≥ 40 mg (n = 59) ^b	All (N = 45)	≥ 40 mg (n = 33) ^b
Most common related AEs, all grades				
Any	95%	100%	91%	94%
Pyrexia	58%	56%	71%	70%
IRR	55%	64%	40%	49%
Diarrhea	40%	46%	56%	61%
Most common related AEs, grade ≥ 3^c				
Any	28%	37%	31%	39%
IRR	18%	24%	11%	12%
Diarrhea	5%	7%	13%	18%
DLTs	5 patients experienced DLTs: G3 dyspnea (40 mg); G3 hypoxia (60 mg); G3 diarrhea (300 mg); G4 colitis (600 mg) ^d ; G5 respiratory failure (600 mg) ^d		2 patients experienced DLTs: G3 transient increase of ALT (160 mg); G3 rash (160 mg)	

Clinical Activity

Patients included in the efficacy analysis for this preliminary analysis included CRC patients who received ≥ 60 mg cibisatamab for monotherapy, and CRC patients receiving ≥ 80 mg cibisatamab for combination therapy. The patients were heavily pretreated, and the majority of patients had metastases in ≥ 3 organs (Table 2). Ninety percent of patients had a confirmed microsatellite stable (MSS) status in BP29541, and for the remaining 10% the status was unknown. For WP29945, 92% of patients were MSS, and the remaining 8% (2 patients) had a MSI-H tumor.

Cibisatamab at doses of ≥ 60 mg showed promising clinical activity in CRC (Table 3). For the monotherapy, two out of 31 patients (6%) receiving ≥ 60 mg cibisatamab obtained a partial response (PR). Both patients had confirmed MSS status. 12/31 patients had a confirmed stable disease, and 16/31 patients had progressive disease (PD) as best response. One patient was not evaluable. No clear correlation was seen between dose and response for the monotherapy (data not shown). For combination treatment, a correlation was seen between dose and response, with all partial responses seen at the highest dose level of 160 mg (Figure 4). Three out of 25 patients receiving 5 – 160mg showed a confirmed PR. Two out of three patients showing a response had MSS disease; one patient showed a MSI-H tumor Two out of 11 MSS patients receiving ≥ 80 mg (18%) showed a confirmed PR. In 7/11 (64%) of MSS patients receiving ≥ 80 mg, confirmed SD was the observed best response, and in 2/11 patients (18%), PD was the best response. All patients were evaluable in the combination study.

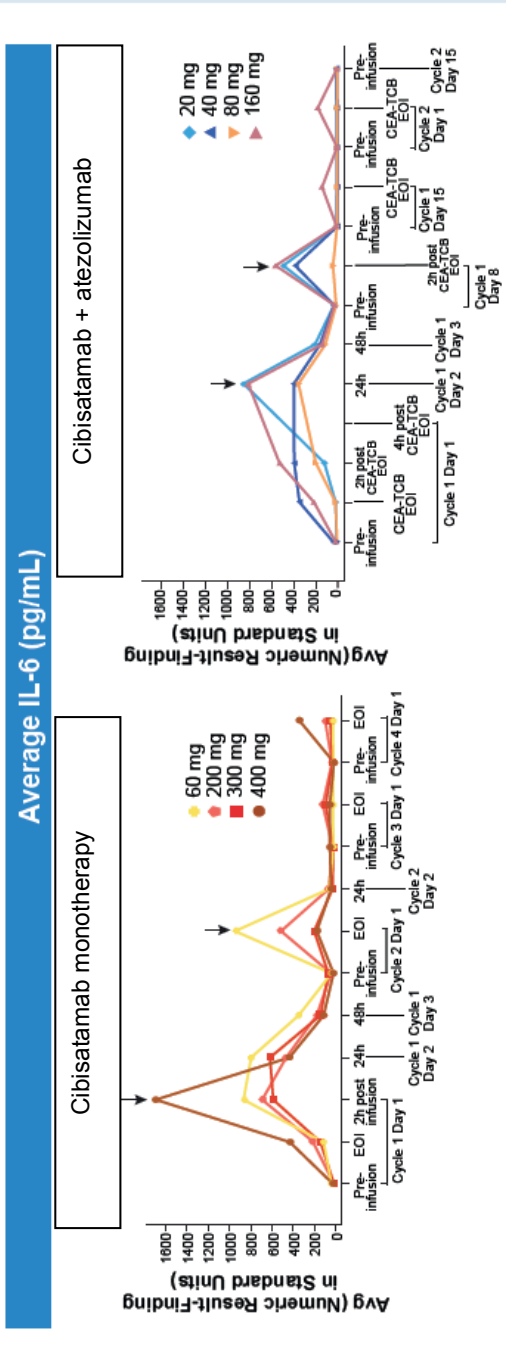


Figure 3. Average IL-6 plasma concentrations in BP29541 (left) and WP29945 (right). IL-6 peaks were observed shortly after the end of infusion of the first two administrations. EOI, end of infusion; IL-6, interleukin 6. From Segal et al. 2017[6]

Table 2. Patient demographics and baseline clinical characteristics of patients included in efficacy analysis. ^a MMR status as reported by investigators. From Segal et al. 2017[6].

Baseline characteristics	Cibisatamab monotherapy	Cibisatamab + atezolizumab	
	n = 31	n = 25 (5-160 mg)	n = 11 (80 or 160 mg)
Median age, years	60	55	53
Sex, male, n (%)	19 (61%)	13 (52%)	5 (45%)
ECOG PS 0/1, n (%)	19 (61%)/12 (39%)	13 (52%)/12(48%)	6 (55%)/5 (45%)
MSS/MSI/Unknown, n(%)^a	28 (90%)/0/3 (10%)	23 (92%)/2 (8%)/0	11 (100%)/0/0
Metastatic sites, n (%)			
Lung	21 (68%)	18 (72%)	8 (73%)
Liver	26 (84%)	18 (72%)	5 (45%)
Peritoneal carcinomatosis	7 (23%)	9 (36%)	5 (45%)
1-2 organs involved	6 (19%)	8 (32%)	5 (45%)
≥ 3 organs involved	25 (81%)	17 (68%)	6 (55%)
Prior adjuvant therapy, n (%)	12 (39%)	12 (48%)	5 (45%)
No. of prior regimens (metastatic), n (%)			
2	8 (26%)	6 (24%)	5 (45%)
≥ 3	19 (61%)	17 (68%)	6 (55%)

Table 3. Overview of confirmed best overall response to cibisatamab monotherapy and in combination with atezolizumab (RECIST v1.1). Mismatch repair status was unknown for 3 patients; two patients had MSI-high disease, sub-group of the column to the left (25 patients in combination study treated with cibisatamab at doses of 5 mg to 160 mg). From Segal et al. [6]

Confirmed best overall response (RECIST v1.1), n (%)	Cibisatamab monotherapy	Cibisatamab + atezolizumab	
	n = 31, 60 – 600 mg; MSS, n = 28, (90%) ^a	n = 25, 5 – 600 mg; MSS, n = 23, (92%) ^b	n = 11, 80 or 160 mg ^c ; MSS, n = 11, (100%)
Partial response	2 (6%)	3 (12%)	2 (18%)
Stable disease	12 (39%)	10 (40%)	7 (64%)
Disease control	14 (45%)	13 (52%)	9 (82%)
Progressive disease	16 (52%)	12 (48%)	2 (18%)
Non-evaluable	1 (3%)	-	-

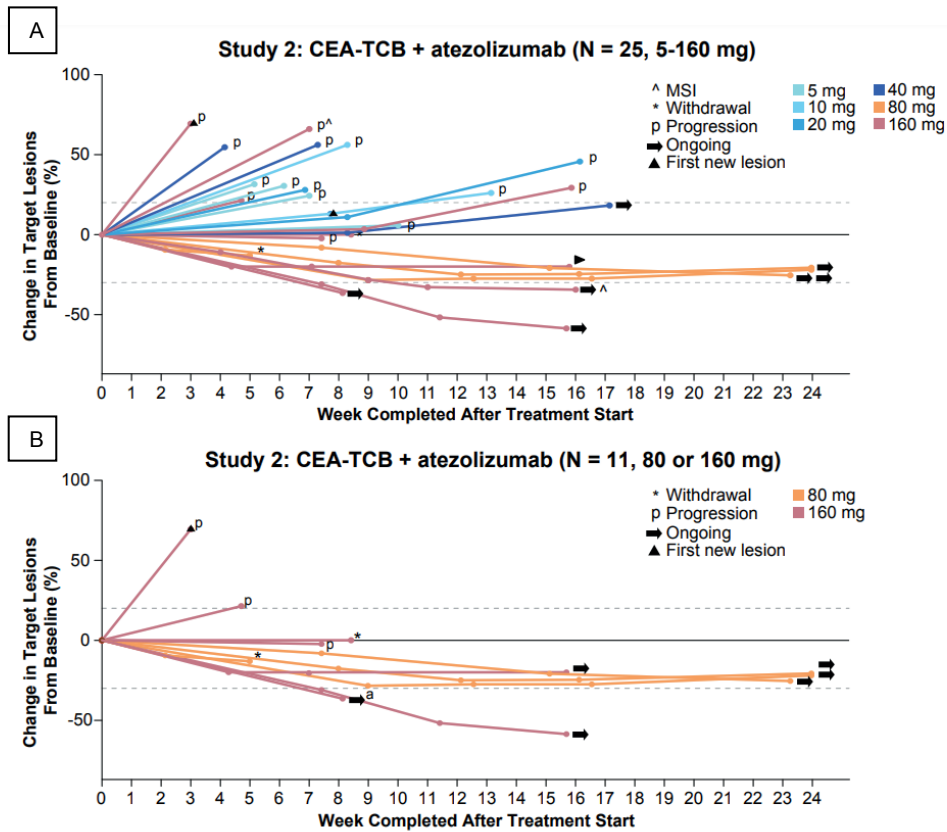


Figure 4. Spider plot of patients treated in WP29945 in all dose levels (A), and patients receiving ≥ 80 mg cibisatamab (B). From Segal et al.2017 [6]

Pharmacokinetics

In patients without anti-drug antibodies (ADA), PK was found to be near linear, with a proportional increase of serum concentrations with doses (Figure 5). Serum exposure was maintained after multiple doses. In BP29541, ADAs were detected in >50% of patients. At cibisatamab doses of 60 to 200 mg, 42% of patients lost exposure. At the higher dose levels (≥ 300 mg), only 13% of patients lost exposure). In WP29945, exposure below limit of detection was observed in 21% of patients in dose levels 80 – 160 mg. Interestingly, at similar dose levels, the percentage of patients losing exposure appeared lower with combination with atezolizumab compared to cibisatamab alone.

Pharmacodynamics

Paired biopsy sample analysis revealed pharmacodynamic (PD) changes upon cibusatamab treatment which were in concordance with the mode of action of the molecule. Cibusatamab appeared to induce T-cell proliferation, as shown by immunohistochemistry analysis using proliferation marker Ki67 (Figure 6). In BP29541, at dose levels ≥ 60 mg, a 6-fold increase of Ki67 was observed in CD3+ T-cells after seven weeks of treatment, as compared to baseline.

Both PD-1 and PD-L1 expression are shown to be increased in tumor-infiltrating immune cells upon treatment (Figure 7 and 8), suggesting T-cell engagement and activation. Furthermore, a correlation is seen between response and increase of PD-1 expression (Figure 7). In both the monotherapy and combination therapy studies, patients who showed shrinkage of target lesions subsequently demonstrated increased PD-1 expression on on-treatment tumor biopsies, whereas for patients showing SD, the percentage of PD-1 positive T-cells did not change upon treatment.

On-treatment biopsies show a reduction in CEA expression in comparison to baseline (Figure 9). This indicates that cibusatamab treatment leads to effective killing of CEA+ tumor cells by T-cells through delivery of cytotoxic granules. In addition, patients who show tumor reduction on the CT scan show a greater decrease of CEA expression on treatment biopsies as compared to non-responders.

DISCUSSION AND CONCLUSION

Here, we present analysis summary of published data from early analysis of BP29541 and WP29945 of patients. Safety profile was manageable, and both studies showed promising anti-tumor effects in MSS CRC patients.

To our knowledge, this is the first bispecific monoclonal antibody which targets CD3, that shows clinical efficacy in solid tumors. Cibusatamab showed promising anti-tumor activity both as a single agent and in combination with atezolizumab. Checkpoint blockade as monotherapy is thought to be inefficient in MSS CRC, likely due to lower numbers of neo-antigens and decreased levels of PD-(L)1 expression[8,9]. However, treatment with cibusatamab alone and in combination with atezolizumab demonstrated tumor reduction in this tumor type, as well as increase of PD-(L)1 expression in the tumor micro-environment. A higher response rate was seen in the combination therapy versus monotherapy, suggesting that the two drugs may work synergistically.

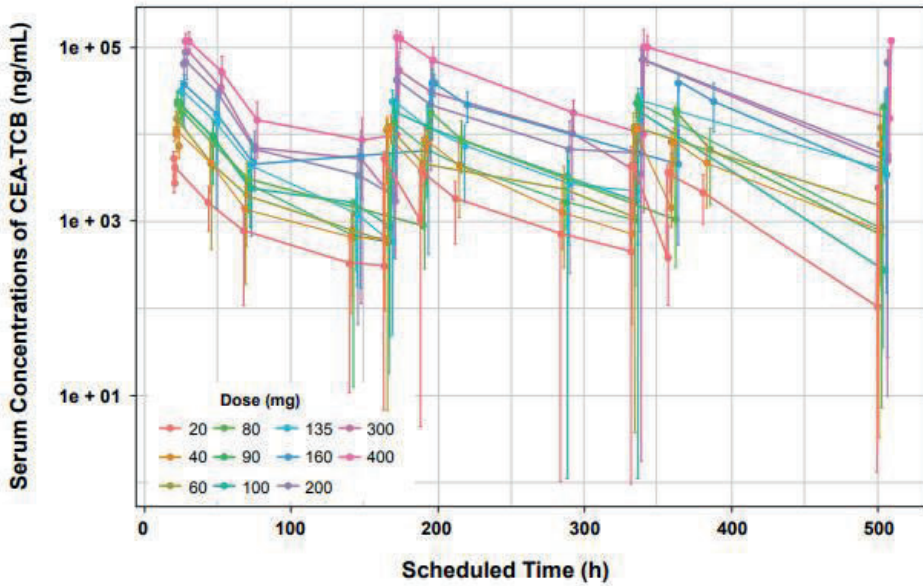


Figure 5. Pharmacokinetics: Mean (\pm SD) cibisatamab concentrations by dose in BP29541 and WP29945. From Melero et al.[10]

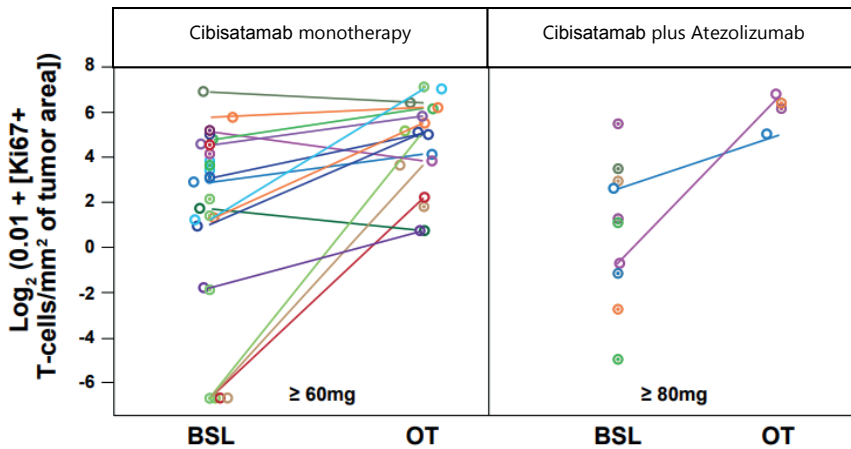


Figure 6. Proliferation rate of T-cells upon treatment with cibisatamab, as measured with Ki67. Each dot represents one patient, and paired biopsies are connected. Left: BP29541 (monotherapy), right: WP29945 (combination therapy). From Melero et al. [10]

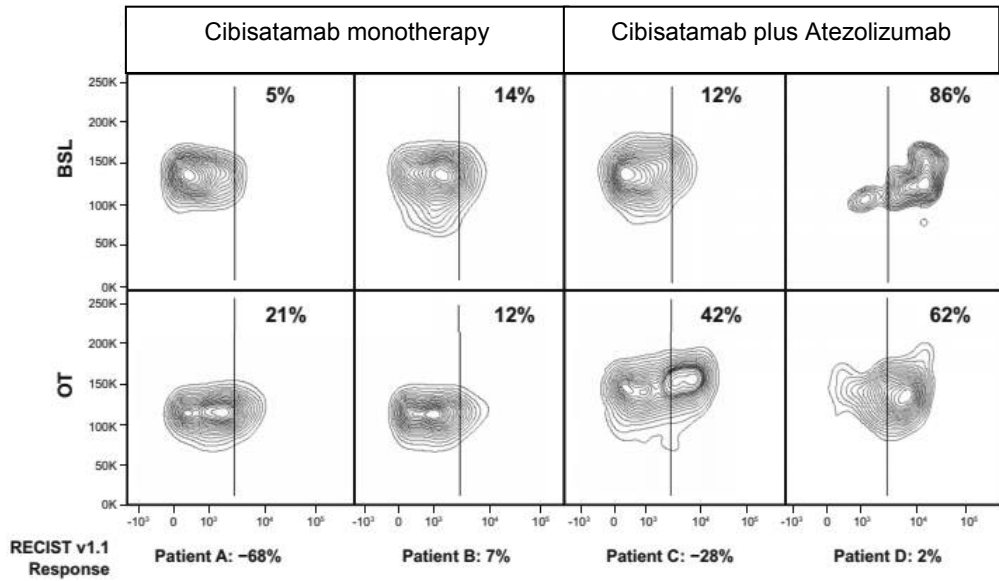


Figure 7. Representative examples showing change in PD-1 expression in tumor biopsies upon treatment with cibisatamab. BL = Baseline OT= on treatment, at week 7. From Melero et al. [10]

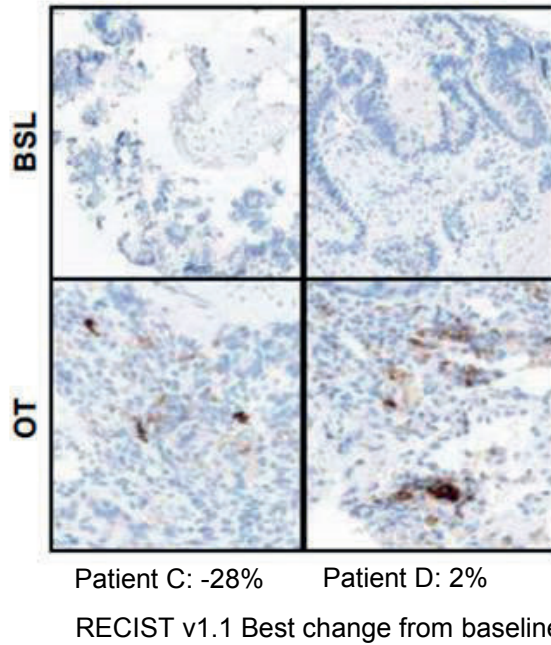


Figure 8. Increase in PD-L1 expression in tumor biopsies upon treatment with cibisatamab. BSL= baseline, OT = On treatment, week 7. From Melero et al. [10]

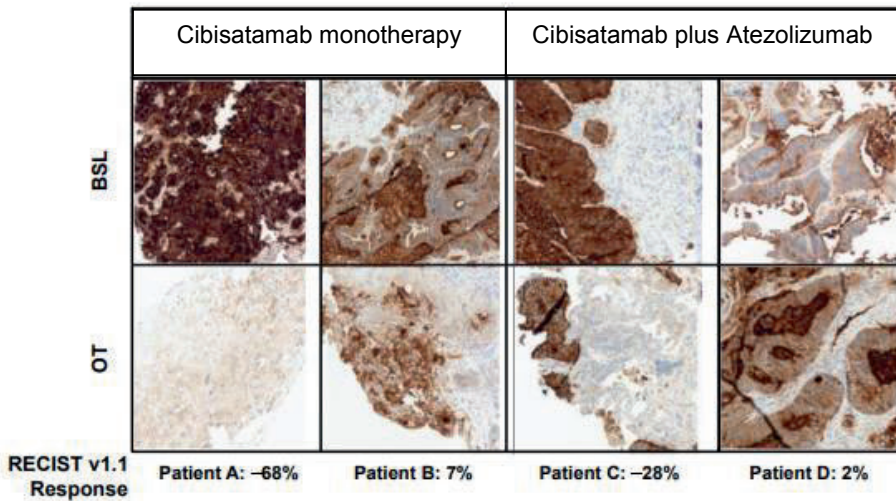


Figure 9. Representative examples from four patients showing a decrease in CEA expression in tumor biopsies upon treatment with cibisatamab. BSL = baseline, OT = on treatment, wk 7. From Melero et al. [10]

ACKNOWLEDGEMENTS

We thank all patients and their families for participating; F. Hoffman-La Roche for sponsoring; and the Clinical Pharmacology Department of The Netherlands Cancer Institute for conducting this trial.

REFERENCES

1. Dahlén E, Veitonmäki N, Norlén P. Bispecific antibodies in cancer immunotherapy. *Ther. Adv. vaccines Immunother.* 2018; 6:3–17.
2. Ordoñez C, Screaton RA, Ilantzis C, Stanners CP. Human carcinoembryonic antigen functions as a general inhibitor of anoikis. *Cancer Res.* 2000; 60:3419–3424.
3. Bacac M, Klein C, Umana P. CEA TCB: A novel head-to-tail 2:1 T cell bispecific antibody for treatment of CEA-positive solid tumors. *Oncoimmunology* 2016; 5:1203498.
4. Stewart R, Hammond SA, Oberst M, Wilkinson RW. The role of Fc gamma receptors in the activity of immunomodulatory antibodies for cancer. *J. Immunother. Cancer* 2014; 2:29.
5. Bacac M, Fauti T, Sam J et al. A novel carcinoembryonic antigen T-cell bispecific antibody (CEA TCB) for the treatment of solid tumors. *Clin. Cancer Res.* 2016; 22:3286–3297.
6. Segal NH, Saro J, Melero I et al. Phase I Studies of the Novel Carcinoembryonic Antigen CD3 T-Cell Bispecific (CEA-CD3 TCB) Antibody as a Single Agent and in Combination With Atezolizumab: Preliminary Efficacy and Safety in Patients With Metastatic Colorectal Cancer (mCRC). *Annals of Oncology* (2017) 28 (suppl_5): 122-141.
7. Hodi FS, Hwu W-J, Kefford R et al. Evaluation of Immune-Related Response Criteria and RECIST v1.1 in Patients With Advanced Melanoma Treated With Pembrolizumab. *J. Clin. Oncol.* 2016; 34:1510–1517.
8. Le DT, Uram JN, Wang H et al. PD-1 Blockade in Tumors with Mismatch-Repair Deficiency. *N. Engl. J. Med.* 2015; 372:2509–2520.
9. Passardi A, Canale M, Valgiusti M, Ulivi P. Immune Checkpoints as a Target for Colorectal Cancer Treatment. *Int. J. Mol. Sci.* 2017; 18:1324.
10. Melero I, Segal NH, Saro Suarez JM et al. Pharmacokinetics (PK) and pharmacodynamics (PD) of a novel carcinoembryonic antigen (CEA) T-cell bispecific antibody (CEA CD3 TCB) for the treatment of CEA-expressing solid tumors. *J. Clin. Oncol.* 2017; 35:2549.

Chapter 1.2

Preliminary efficacy and safety of the novel tumor targeting immunocytokines CEA-IL2v (in combination with atezolizumab) and FAP-IL2v, which contain a variant of interleukin-2.

An interim analysis of BP29435 and BP29842 of patients treated at the Netherlands Cancer Institute

Willeke Ros

Preliminary data of study BP29842 has also been presented at the European Society for Medical Oncology (ESMO) Annual Congress 2018:

Soerensen MM, **Ros W**, Rodriguez-Ruiz ME, Robbrecht D, Rohrberg KS, Martin-Liberal J, Lassen UN, Melero Bermejo I, Lolkema MP, Tabernero J, Boetsch C, Piper-Lepoutre H, Waldhauer I, Charo J, Evers S, Teichgräber V, Schellens JHM. Safety, PK/PD, and anti-tumor activity of RO6874281, an engineered variant of interleukin-2 (IL-2v) targeted to tumor-associated fibroblasts via binding to fibroblast activation protein (FAP).

Journal of Clinical Oncology 2018;36:e15155

Melero I, Castanon Alvarez E, Mau Sorensen M, Lassen U, Lolkema M, G Robbrecht D, A Gomez-Roca C, Martin-Liberal J, Tabernero J, **Ros W**, Ahmed S, Isambert N, Piper Lepoutre H, Boetsch C, Charo J, Evers S, Teichgräber V, H M Schellens J. Clinical activity, safety, and PK/PD from a phase I study of RO6874281, a fibroblast activation protein (FAP) targeted interleukin-2 variant (IL-2v).

Annals of Oncology 2018;29: viii133-viii148.

ABSTRACT

Background: Although IL-2 treatment has shown some benefit in cancer patients, its clinical use has thus far been limited due to high incidence of severe side effects. Currently, attempts of improving IL-2 treatment are made which include better targeting of IL-2. This may lead to reduced systemic toxic effects, which allow for higher dosing of the drug. Here, we report the interim analysis of clinical trials investigating two novel immunocytokines. These antibodies consist of an IL-2 variant fused with antibodies targeting the tumor site. FAP-IL-2v targets fibroblast activating protein in the tumor micro-environment. CEA-IL2v targets carcinoembryonic antigen on the tumor cells.

Methods: BP29435 (NCT02350673) investigated CEA-IL2v in combination with atezolizumab. BP29842 (NCT02627274) investigated FAP-IL2v as monotherapy. Both studies were open-label, non-randomized multicenter phase I dose escalation studies designed to evaluate the safety, tolerability, pharmacokinetics, pharmacodynamics and therapeutic activity. Here, we present interim results of patients treated at the Netherlands Cancer Institute.

Results: Between June 2015 and October 2018, six patients were enrolled in BP29435, and ten patients were enrolled in BP29842. The maximal tolerated dose for BP29435 was 15 mg qW. For BP29842, the maximal tolerated dose was 20 mg, using one-step intrapatient dose escalation (15 mg followed by 20 mg). Dose limiting toxicities observed in this interim analysis included G3 gamma-glutamyltransferase increase (BP29435), G3 hepatitis and G3 fatigue (both BP29842). All patients (100%) experienced treatment related adverse events. Common toxicities (all grades) for BP29435 included infusion related reactions (IRRs) (67%), fatigue (50%) and pyrexia (50%). Common toxicities observed in BP29842 were IRRs (90%), pyrexia (80%) and diarrhea (50%). For BP29435, the best response was SD (n = 1) lasting > 11 weeks. Anti-tumor activity was seen in BP29842, with one patient (10%) obtaining a CR, and two patients (20%) showing a PR.

Conclusions and discussions: The maximal tolerated dose for both CEA-IL2v in combination with atezolizumab, and FAP-IL2v monotherapy has been established. FAP-IL2v showed promising anti-tumor activity and will continue development as monotherapy and in combination.

INTRODUCTION

Interleukin-2 (IL-2) is an important cytokine which exerts pleiotropic effects on the immune system. It is mainly produced by antigen-stimulated CD4⁺ cells, as well as CD8⁺ cells, natural killer (NK) cells and dendritic cells (DCs)[1, 2]. Its receptor is the IL-2 receptor (IL2-R), a heterotrimeric protein which consists of an α chain (IL-2R α , CD25), a β chain (IL-2R β , CD122), and a γ chain (IL-2R γ , CD132). IL-2 is thought to fulfill both regulatory and stimulatory roles. When stimulated by an antigen, IL-2 promotes the differentiation of T-cells into effector and memory T-cells, and stimulates the cytotoxic activity of CD8⁺ and NK cells. However, IL-2 may also stimulate regulatory T-cell development and proliferation[3]. Due to its ability to stimulate CD8⁺ and NK cell activity, IL-2 was considered one of the first candidates for cancer immunotherapy. Aldesleukin is a recombinant form of human IL-2, and has been approved by the FDA for treatment of metastatic renal cell carcinoma (1992) and metastatic melanoma (1998)[4]. The usefulness of this therapy was mainly limited due to toxicity. For this reason, several attempts have been made to improve the IL-2 formulation[5–7]. This may allow for higher dosing while reducing the chance of side effects. One potential method to improve safety and efficacy is better targeting of IL-2 to the tumor site is by fusing IL-2 with a monoclonal antibody. The result is a so-called immunocytokine, in which the binding part of the monoclonal antibody targets a tumors-specific antigen.

Two tumor targeting immunocytokines containing a variant of IL-2 are under development by Roche. The two immunocytokines are CEA-IL2v (RO6895882, also recently named cergutuzumab amunaleukin), and FAP-IL2v (RO6874281). Both immunocytokines have been modified in such a way that they are not able to bind to the α chain of the IL-2R. As a result, these immunocytokines have a longer half-life compared to wild-type IL-2 based immunocytokines, and do not preferentially activate Treg cells[8]. Furthermore, the chances of developing capillary leak syndrome (CLS) may be reduced, as IL-2R α on pulmonary vascular endothelium is thought to be a main mediator of CLS[9, 10]. Both CEA-IL2v and FAP-IL2v activate and expand NK, CD4⁺ and CD8⁺ T cells in the peripheral blood, lymphoid tissues and tumor *in vivo*[8]. Furthermore, both immunocytokines showed improved safety compared to the wildtype immunocytokine, despite having a higher exposure and half-life.

CEA-IL2v targets a membrane-proximal epitope of carcinoembryonic antigen (CEA), a glycoprotein involved in cell adhesion. CEA is highly expressed in colorectal cancers (CRC) (91%), pancreatic cancers (74%), gastric cancers (64%), and nonsquamous non-small cell lung cancer (NSCLC) (64%)[11]. Study BP29820 previously investigated CEA-IL2v as monotherapy. In this study, the maximal tolerated dose was established as 30 mg q2W. The most frequently reported serious adverse events or \geq G3 AEs were pyrexia, infusion related reaction (IRR), dyspnea, capillary leak syndrome, pyrexia, hypophosphatemia, fatigue, decreased lymphocyte count, and decreased platelet count. The best reported response was stable disease. A substudy investigated the biodistribution and tumor accumulation of ⁸⁹Zirconium labeled CEA-IL2v using PET-imaging[12]. The substudy supported the therapeutic concept, and drug accumulation was seen in CEA⁺ tumors, as well as in lymphoid tissue. In the current study BP29435, CEA-IL2v is combined with the humanized aPD-L1 inhibitor atezolizumab. PD-L1 blockade has been shown to synergize with IL-2

therapy to boost exhausted T-cells[13]. In addition, IL-2 treatment may further enhance the efficacy of atezolizumab, as it expands the pool of CD8+ T-cells and NK cells. Furthermore, it prevents apoptosis and promotes the long-term survival of these cells[14]. The expansion of immune cells induces IFN- γ , which triggers a negative feedback loop by upregulating PD-L1. This feedback loop will be inhibited by blocking PD-L1 using atezolizumab.

The other tumor targeting immunocytokine, FAP-IL2v, targets fibroblast activating protein (FAP) in the tumor stroma[15]. FAP is highly expressed in squamous NSCLC (95%), head and neck squamous cell carcinoma (HNSCC) (90%), pancreatic cancer (78%), and colorectal cancer (74%)[11]. The current study investigates FAP-IL2v as monotherapy.

In this interim analysis, we describe the clinical safety and efficacy of CEA-IL2v in combination with atezolizumab (BP29435, NCT02350673) and FAP-IL2v as monotherapy (BP29842, NCT02627274). We discuss the patients treated at the Netherlands Cancer Institute/Antoni Van Leeuwenhoek Ziekenhuis (NKI/AvL) between April 2016 and August 2018.

METHODS

Study design

BP29435 investigated CEA-IL2v in combination with atezolizumab, and BP29842 investigated FAP-IL2v as a single agent. Both studies were open-label, non-randomized multicenter dose escalation phase I studies. Here, we describe the dose escalation parts of both studies of patients treated at the Netherlands Cancer Institute. The primary objectives were to describe the safety and tolerability, to determine the maximum tolerated dose (MTD), and to identify a recommended phase II dose and schedule. Secondary objectives were to assess preliminary anti-tumor activity, and to describe the pharmacodynamics effects and pharmacokinetics.

The starting dose for BP29435 was 6 mg CEA-IL2v. Atezolizumab was given as a fixed flat dose at 840 mg (q2W) or 1200 mg (q3W). For BP29842, the starting dose was 5 mg FAP-IL2v. All drugs were given as intravenous infusions. Dose escalation was carried out according to a modified Continual Reassessment Method with Overdose Control (mCRM with EWOC). A dose limiting toxicity (DLT) was defined as one of the following toxicities: grade ≥ 4 neutropenia, grade ≥ 3 febrile neutropenia, grade ≥ 4 thrombocytopenia, non-hematological toxicities \geq grade 3, failure to recover from any toxicity that results in a dose delay of the next scheduled administration of > 14 days for any regimen, elevated ALT or AST ($> 3 \times$ ULN) with elevated total bilirubin or clinical jaundice.

Patients

The key eligibility requirements included having a locally advanced/metastatic (*for BP29435 only: CEA+*) solid tumor, ≥ 1 tumor lesion amenable to biopsy, progression on or intolerance for standard therapy, ≥ 18 years of age, radiologically measurable disease (Response Evaluation Criteria in Solid Tumors [RECIST] v1.1), Eastern Cooperative Oncology Group performance status (ECOG PS) 0-1, adequate organ function, and a life expectancy of at least 12 weeks.

Key exclusion criteria included: treatment with systemic immunosuppressive medications within 2 weeks prior to initiation of study treatment; uncontrolled pleural effusion, pericardial effusion, or ascites; uncontrolled hypertension; known clinically significant cardiovascular or cerebrovascular disease; severe dyspnea at rest or requiring supplementary oxygen therapy; history of autoimmune diseases.

Outcomes

Safety Assessments

The safety outcome measures for both studies included the incidence of DLTs, incidence and severity of adverse events, and incidence of anti-drug antibodies (ADAs). The National Cancer Institute Common Terminology Criteria for Adverse Events (NCI CTCAE), Version 4.03 were used for clinical safety evaluation.

Efficacy assessments

The efficacy outcomes included confirmed best overall response; progression free survival (PFS), and overall survival (OS). Patients who were not evaluable for efficacy analysis were analyzed as non-responders. Tumor response was evaluated according to RECIST v1.1. For BP29435, tumor assessment was performed during screening, at week 8, week 12, and every 8 weeks thereafter. After the first year, tumor assessments were done every 12 weeks. For BP29842, tumor assessment was performed prior to screening, every 8 weeks for the first year, and then every 12 weeks thereafter until disease progression.

Pharmacokinetic outcome measures

Pharmacokinetic (PK) outcomes are not discussed in this interim analysis but are performed in both studies. PK outcome measures included the area under the curve (AUC), C_{max}, C_{min}, T_{max}, clearance (CL), volume of distribution (V_d), and elimination half-life (t_{1/2}) of the immunocytokines.

Pharmacodynamic outcome measures

Pharmacodynamic (PD) outcomes are not discussed in this interim analysis but are performed in both studies. The pharmacodynamic outcome measures included number of wholeblood CD4⁺ T cells, CD8⁺ T cells, NK cells, monocytes, regulatory T cells, and B cells. For BP29842, wholeblood samples were also used to evaluate the potential of inducing antigen-dependent cell mediated toxicity (ADCC) of FAP-IL2v. Plasma and serum samples were used to assess immune biomarkers such as cytokines and inflammation markers. Fresh pre- and on treatment tumor biopsy samples were analyzed for immune cell infiltration and activation by flow cytometry and immunohistochemical analysis. For BP29842, FAP content and pattern distribution were also assessed. Archival tumor was used to identify potential prognostic biomarkers.

Statistical analysis

Safety was assessed in patients who received ≥ 1 dose of FAP-IL2v (BP29842), or CEA-IL2v plus atezolizumab (BP29435) and were summarized using descriptive statistics. The Kaplan–Meier method was used to estimate PFS, OS, and DOR. The data cutoff date for this report was 16th of October 2018.

Table 1. Patient characteristics. WHO = World Health Organisation.

Demographic characteristic		CEA-IL2v atezolizumab Total (n=6)	plus FAP-IL2v Total (n=10)
Age (Years)		66.5 [50 – 73]	54 [38 – 77]
Gender (n,%)			
Male		1 (17%)	7 (70%)
Female		5 (83%)	3 (30%)
WHO PS (%)			
0		5 (83%)	4 (40%)
1		1 (17%)	6 (60%)
Tumor Type (n)			
Melanoma			4 (40%)
H&N	Squamous cell carcinoma		1 (10%)
	Adenocarcinoma		1 (10%)
CRC		4 (67%)	1 (10%)
NSCLC		2 (33%)	
Pseudomyxoma peritonei			1 (10%)
Prostate cancer			1 (10%)
Sarcoma			1 (10%)
Prior lines of therapy for advanced disease		3 [2 - 5]	3 [1-6]

RESULTS

Baseline patient characteristics

Between June 2015 and October 2018, six patients were enrolled in BP29435, and ten patients were enrolled in BP29842 (Table 1 & 2). Included tumor types for BP29435 were colorectal cancer (CRC) (67%) and non-small cell lung cancer (NSCLC) (33%). For BP29842, included tumor types were melanoma (40%), head and neck squamous cell carcinoma (HNSCC) (10%), adenocarcinoma of the head and neck (10%), CRC (10%), pseudomyxoma peritonei (10%), prostate cancer (10%), and chondrosarcoma (10%). Mean age was 67 years [50 – 73] for BP29435, and 54 years [38 – 77] for BP29842. For BP29435, the majority of patients was female (n = 5, 83%). For BP29842, the majority of patients was male (n = 7, 70%). The median prior lines for advanced disease was 3 [range 2- 5] for BP29435. The median prior lines for advanced disease was 3 [range 1 – 6] for BP29842.

Table 2. Overview of tumor type and treatment per individual patient in (A) BP29435 and (B) BP29842.

A. CEA-IL2v plus Atezolizumab			
Pt No.	Tumor Type	Dose/regimen CEA-IL2v (mg)	Dose/regimen atezolizumab
3001	CRC	6mg (q2W)	800mg q2W
3002	NSCLC	6mg (q2W)	800mg q2W
3003	CRC	20mg (q2W)	800mg q2W
3004	CRC	20mg at C1, 25mg C2 onwards (q2W)	800mg q2W
3005	CRC	10mg qW	1200mg q3W
3006	NSCLC	15mg qW	1200mg q3W
B. FAP-IL2v			
Pt No.	Tumor Type	Dose / regimen FAP-IL2v (mg)	
1112	HNSCC	5mg qW	
1123	Sarcoma	10mg qW	
1133	CRC	20 mg qW	
1151	Melanoma	20mg cycle 1 and 2, 35mg cycle 3 onwards qW	
1152	Melanoma	20mg cycle 1 and 2, 35mg cycle 3 onwards qW	
1155	Pseudomyxoma peritonei	20mg cycle 1 and 2, 35mg cycle 3 onwards qW	
1173	Prostate	20mg cycle 1, 25mg cycle 2 onwards qW	
1176	Head and neck adenocarcinoma	20 mg cycle 1, 25 mg cycle 2 onwards qW	
1183	Melanoma	15 mg cycle 1, 20 mg cycle 2 onwards qW	
1191	Melanoma	15 mg cycle 1, 20 mg cycle 2 onwards qW	

Treatment and doses

Explored dose levels for BP29435 included in this interim analysis were 6 mg q2W, 20 mg (C1); 25 mg (C2 onwards q2W, 10 mg qW, 15 mg qW, all in combination with fixed dose atezolizumab as described in the methods section (Table 2). The maximal tolerated dose was 15 mg CEA-IL2v qW in combination with 1200 mg atezolizumab q3W.

Explored dose levels for BP29842 included in this interim analysis were 5 mg, 10 mg, 20 mg, 20 mg (first two administrations) and 35 mg (third and subsequent administrations), 20 mg (first administration) and 25 mg (second and subsequent administrations), and 15 mg (first administration) and 20 mg (second and subsequent administrations) (Table 2). The maximal tolerated dose was 20 mg, using one-step intra-patient dose escalation (15 mg followed by 20 mg).

Safety

All patients experienced treatment related adverse events (AE) (Table 3). The most common AEs related to either CEA-IL2v or atezolizumab observed in BP29435 (Table 3A) were infusion related reactions (67%), fatigue (50%), pyrexia (50%), diarrhea (33%), nausea (33%), and vomiting (33%). The most common AEs observed in BP29842 related to FAP-IL2v were IRRs (90%), pyrexia (80%), diarrhea (50%), fatigue (40%), AST (40%) and ALT (30%) increase, nausea (30%), and pruritus (30%). The only observed grade (G)3 AE for BP29435 included GGT increase (n=1). For BP29842 (Table 3B), G \geq 3 AEs included ALT increase (n=1), AST increase (n=3), drug induced liver injury (n=1), fatigue (n= 1), generalized muscle weakness (n=1), hypertension (n=1), hypophosphatemia (n=1), hypotension (n=1), IRR (n=3), liver transaminase elevation (n=1), and pyrexia (n=1).

In BP29435, one out of six patients experienced a DLT. This patient was pt 3006, a NSCLC patient with lymph node metastases. The patient received 15 mg CEA-IL2v qW and 1200 mg atezolizumab q3W. The DLT was a G3 gamma-glutamyl transferase (GGT) increase, occurring one day after the first infusion. The event was resolved 27 days later. No treatment was given for this AE, and the event was deemed clinically insignificant. After two weeks of dose delay, the patient continued treatment with a dose reduction to 10 mg CEA-IL2v qW.

In BP29842, three patients experienced DLTs. The DLTs occurred at the 10 mg dose level and at the 20 mg dose level. The DLT at the 10 mg dose level was G3 fatigue occurring in patient 1133, a 49-year-old male CRC patient with lung, liver and adrenal metastases. One day after infusion, the patient developed G3 fever, had a WHO performance status of 3, and was completely bedridden. The patient received IV paracetamol on the day of DLT until recovery. The DLTs observed at the 20 mg dose levels were immune-mediated hepatitis. Patient 1173, a 64-year-old prostate cancer patient with bone metastases, experienced G3 hepatitis two days after the first infusion (Figure 1A). The patient showed elevated alkaline phosphatase (G1), AST (G2), ALT (G3) and GGT (G2) levels, and normal bilirubin levels. The AE was resolved on the 16th day after infusion. Prior to treatment, the patient had normal baseline liver enzyme functions. Ultrasound scan showed no dilatation of the gallbladder nor any other explanation for the increased liver enzymes. The patient underwent dose reduction to 15 mg FAP-IL2v qW. This dose was well tolerated, with liver

enzyme elevations no higher than G1. The other patient experiencing hepatotoxicities was patient 1176, a 45-year-old male head and neck adenocarcinoma patient with pulmonary metastases. This patient experienced G3 hepatitis as well, consisting of G3 AST/ALT increase and blood bilirubin increase, and G2 GGT and alkaline phosphatase increase (Figure 1B). Clinically, the patient was doing well. However, due to the severity of the hepatitis, treatment was stopped after one single dose. The event was fully resolved twenty days after onset.

In BP29842, three out of ten patients developed immune-mediated hepatitis which led to either drug delay, dose reduction or withdrawal from study (Figure 1). For two of these patients, the observed hepatotoxicity was considered a DLT and were described earlier. The third patient was patient 1123, a 48-year-old male chondrosarcoma patient with lung metastases. This patient received 10 mg FAP-IL2v qW. The patient experienced recurring G2 – G3 AST/ALT elevation after every infusion (Figure 1C). Doses were delayed a total of three times due to either liver enzyme increase or increased malaise. No medication was given for these adverse events. The patient withdrew informed consent due to increased malaise and fatigue related to treatment.

For BP29435, two out of six patients withdrew consent. For BP29842, two patients stopped treatment due to treatment related adverse events, and one patient withdrew consent. The patients who withdrew consent described the reason being their quality of life deteriorating due to treatment.

Table 3A. AEs (possibly) related to treatment with CEA-IL2v + atezolizumab.

Toxicities observed in BP29435 (total n = 6)	G1 - G2			G3 - G4			G5			Total (%)
Diarrhea	2 (33%)									2 (33%)
Dry mouth	1 (17%)									1 (17%)
Dry skin	1 (17%)									1 (17%)
Fatigue	3 (50%)									3 (50%)
Pyrexia	3 (50%)									3 (50%)
GGT increase				1 (17%)						1 (17%)
Hypothyroidism	1 (17%)									1 (17%)
Hepatitis	1 (17%)									1 (17%)
IRR	4 (67%)									4 (67%)
Myalgia	1 (17%)									1 (17%)
Nausea	2 (33%)									2 (33%)
Oral pain	1 (17%)									1 (17%)
Pruritus	1 (17%)									1 (17%)
Skin disorder	1 (17%)									1 (17%)
Vomiting	2 (33%)									2 (33%)
Weight loss	1 (17%)									1 (17%)
White fingers	1 (17%)									1 (17%)

Table 3B continued. AEs (possibly) related to treatment with FAP-IL2v.

Toxicities observed in BP29842. (total n = 10)				
	G1 - G2	G3 - G4	G5	Total
Abdominal pain	2(20%)			2(20%)
ALT increase	2 (20%)			2 (20%)
Anemia	1(10%)			1(10%)
Anorexia	2 (20%)			2 (20%)
AST increase		3 (30%)		3 (30%)
Blood bilirubin increase	1(10%)			1(10%)
Capillary leak syndrome	1 (10%)			1 (10%)
Chills	1(10%)			1(10%)
Constipation	1(10%)			1(10%)
Creatinine increase	1(10%)			1(10%)
Diarrhea	5 (50%)			5 (50%)
Dizziness	1(10%)			1(10%)
Dry eyes	1(10%)			1 (10%)
Edema	1(10%)			1 (10%)
Edema face	1 (10%)			1 (10%)
Erythema multiforme	1(10%)			1(10%)
Fatigue	3 (30%)	1 (10%)		4 (40%)
Flu like symptoms	2(20%)			2(20%)
Generalized muscle weakness		1(10%)		1(10%)
Hepatitis		3(30%)		3 (30%)
Hypertension		1(10%)		1(10%)
Hypophosphatemia		1(10%)		1 (10%)
Hypotension		1 (10%)		1 (10%)
IRR	6 (60%)	3 (30%)		9 (90%)
Malaise	2 (20%)			2 (20%)
Nausea	3 (30%)			3 (30%)
Pain	2 (20%)			2 (20%)
Pain in extremity	2 (20%)			2 (20%)
Pruritus	3 (30%)			3 (30%)
Pyrexia	7 (70%)	1(10%)		8 (80%)
Rash	3(30%)			3(30%)
Skin hypopigmentation	1(10%)			1(10%)
Weight loss	2 (20%)			2 (20%)

Antitumor activity

Efficacy for BP29435

Five out of six patients were available for efficacy analysis. One patient withdrew consent prior to the first tumor assessment. Zero patients showed a response (Figure 2A-C). One CRC patient (17%) showed stable disease for > 11 weeks. This patient decided to stop treatment due to increased fatigue after 15 weeks. The mean PFS was 15 weeks [6– 34], with patients receiving a mean of 6.3 cycles [3-12] (Figure 3A). The mean OS was 45 weeks [22 – 100] (Figure 3B).

Efficacy for BP29842

Eight out of ten patients were available for efficacy analysis. Two patients discontinued before the first tumor assessment due to treatment related toxicities. One patient (10%) obtained a CR, and two patients (20%) obtained a PR (Figure 2D-F). One patient (10%) had SD as best response, and 4 patients (40%) showed progression on the first scan. The mean PFS was 25 weeks [2.8 – not reached] (Figure 3C), with a mean of 17.2 received cycles [1 - 78]. The mean OS is 61.1 [15.1 – not reached] (Figure 3D). At the time of data cut-off, one patient was still on treatment, and five patients were still alive. The patient with a complete response was a 57-year-old male HNSCC patient with lymph node metastases. The patient had received three prior lines of treatment for advanced disease, including (I) chemoradiation with cisplatin with a switch to carboplatin, (II) cetuximab, carboplatin and capecitabine, and (III) oral docetaxel. The patient started treatment with 5 mg FAP-IL2v. After two months, the dose was escalated to 10 mg qW. However, due to increased fatigue and malaise, the next month the dose was reduced to 5 mg. After approximately one year of being on study, the patient changed to a q2W regimen due to recurring G1 fatigue and malaise. Tumor reduction occurred slowly and the patient obtained a PR after being on study for 44 weeks. The CR was obtained after 88 weeks of treatment. The patient stopped treatment with a sustained response after being on treatment for over two years. Six months after stop of treatment, the CT scan showed progression.

Two melanoma patients obtained a PR. The first patient was a 53-year-old female patient with BRAF/NRAS/KIT WT malign melanoma. Prior to FAP-IL2v treatment, this patient received one cycle of ipilimumab followed by six cycles of nivolumab q2W, with no response. The patient received two cycles of 20 mg FAP-IL2v qW, followed by one cycle of 35 mg. This dose was not tolerated, with the patient developing a severe IRR with G3 fever, nausea, hypotension, vomiting and dehydration. The dose was reduced to 20 mg, however the patient again developed a IRR G2, consisting of G3 fever, chills, malaise, nausea and vomiting. Finally, the dose was reduced to 10 mg, which was well tolerated during the remainder of treatment. Despite dose reductions, decrease of all target lesions was seen already at the first tumor assessment. The duration of response was 27 weeks. The patient went off study due to increase of non-target lesions. The last patient which showed a PR was a 38-year-old female with NRAS mutated melanoma. The patient had six prior lines of treatment for advanced disease. The patient received 15 mg FAP-IL2v during cycle one, and 20 mg at cycle 2 onwards. Upon treatment, the patient showed slow tumor reduction, and a PR was reached 38 weeks after start of treatment. At the time of data cut-off, the response was still ongoing.

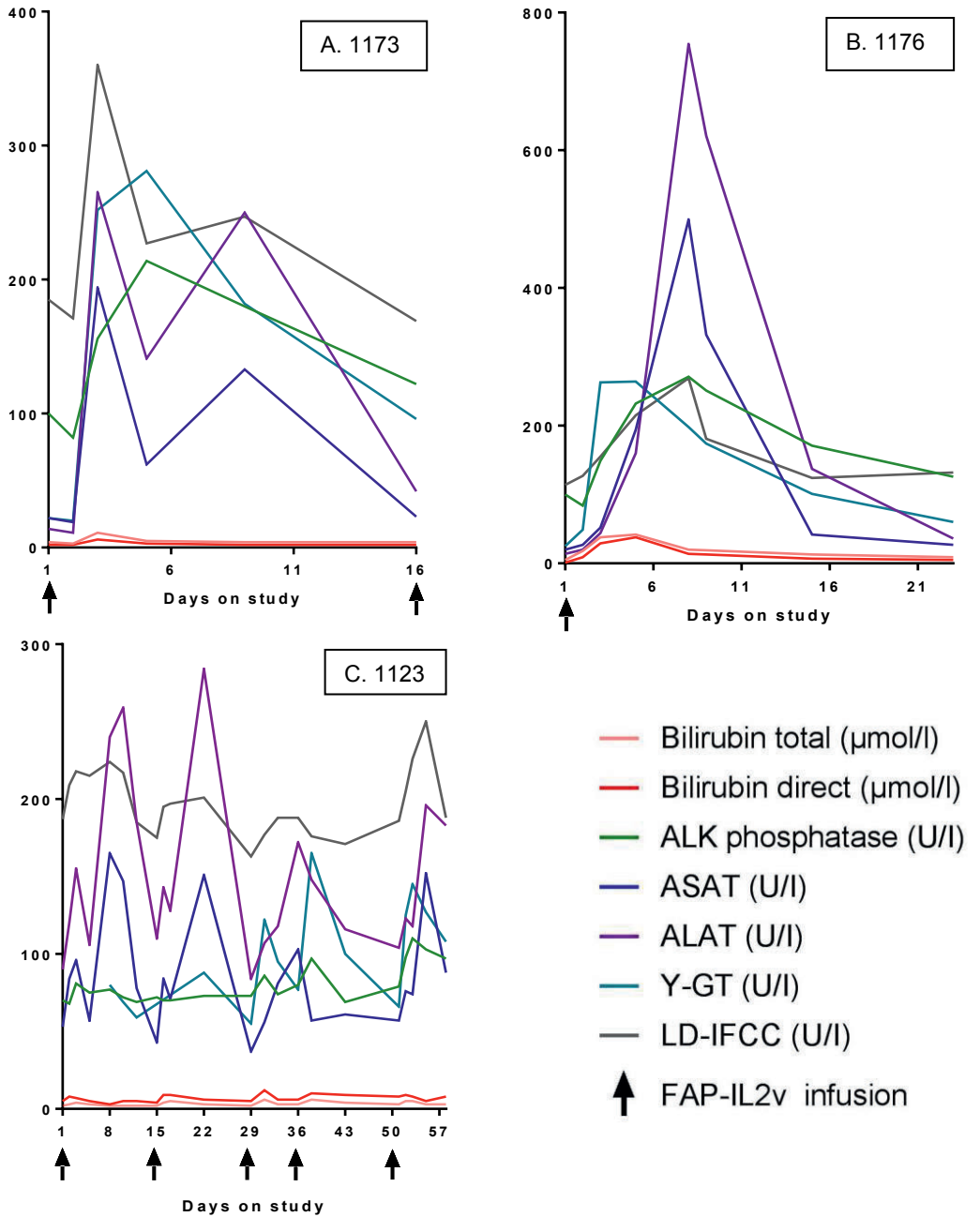


Figure 1. Overview of liver function tests of patients experiencing severe transaminase increase due to FAP-IL2v treatment. (A) Patient 1173. (B) Patient 1176. (C) Patient 1123.

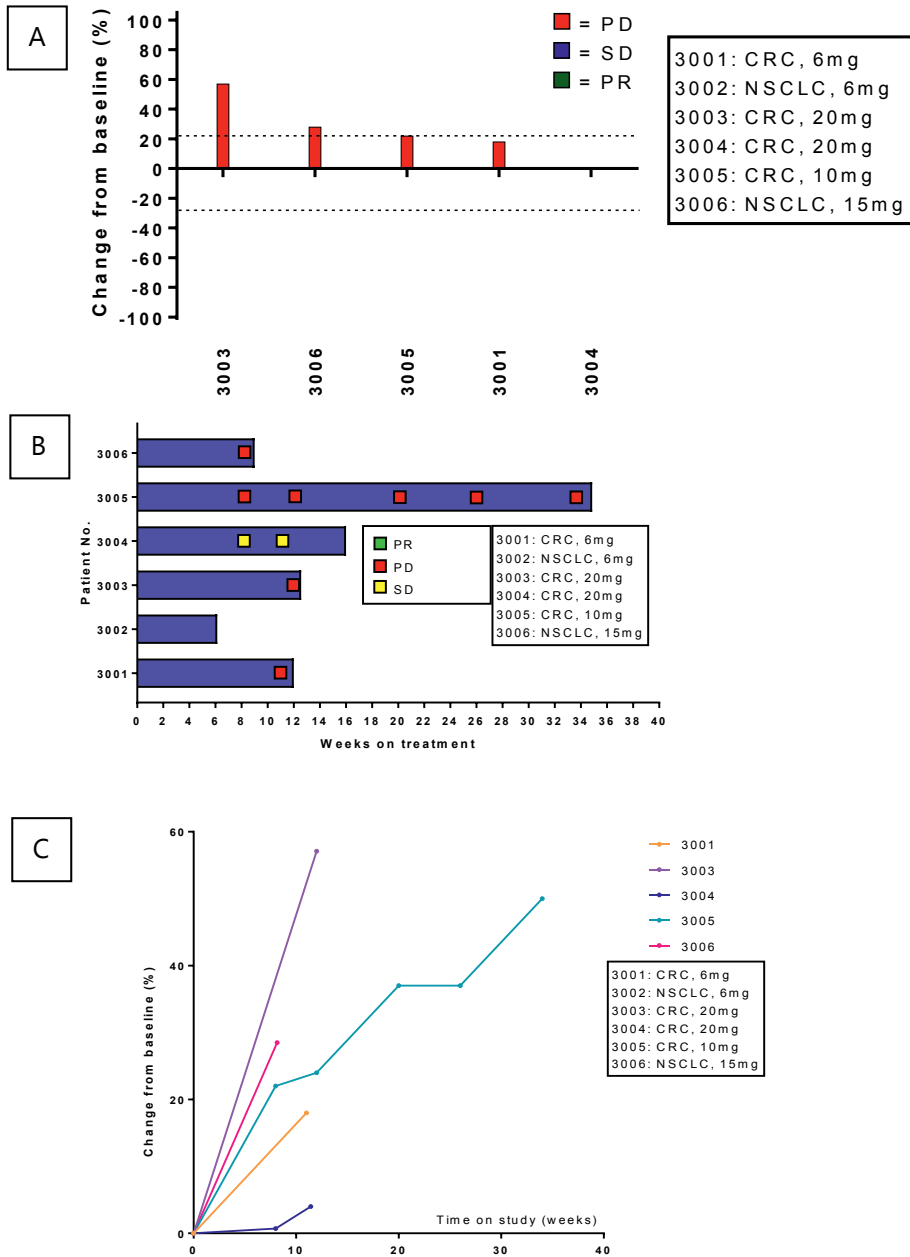


Figure 2. Efficacy analysis from BP29435(A-C) and BP29842(D-F). (A;D) Best change from baseline in tumor size. Dotted lines at 20% and -30% indicate progressive disease and partial response, respectively. (B;E) Longitudinal change from baseline in tumor size. (C;F) Longitudinal change from baseline in tumor size

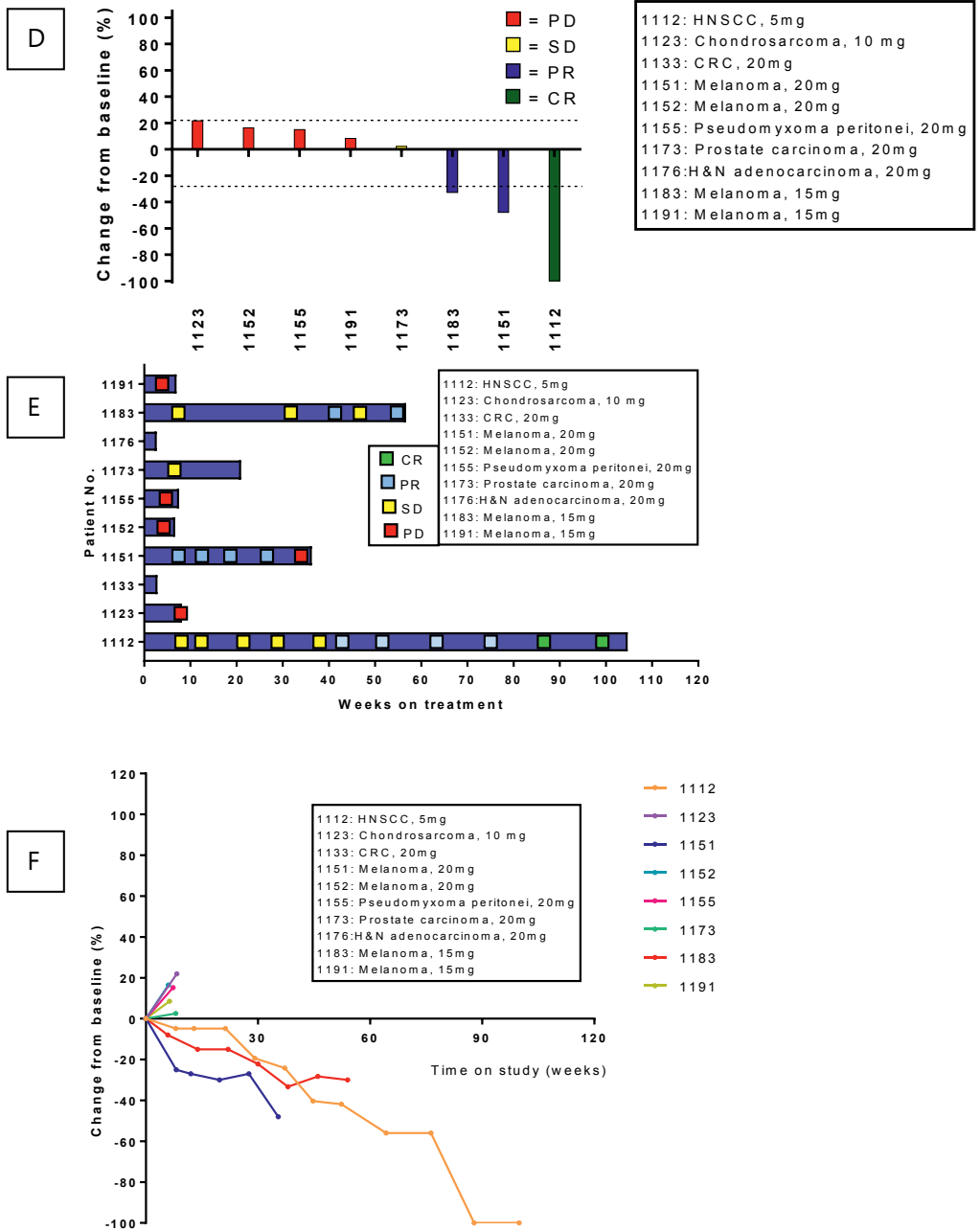
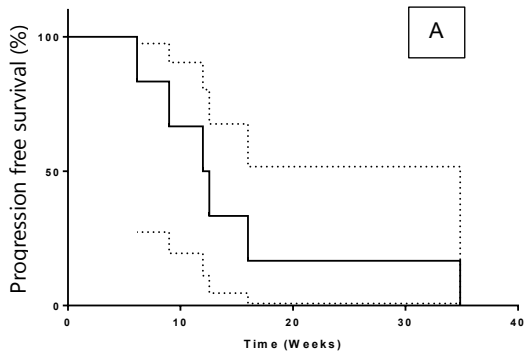
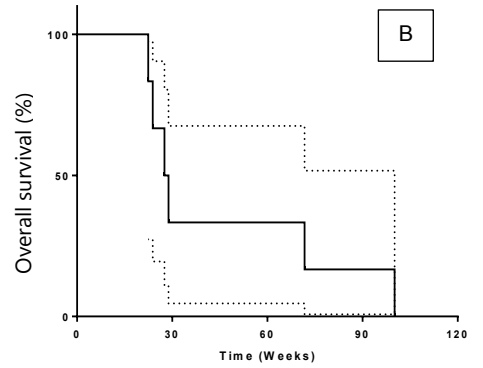


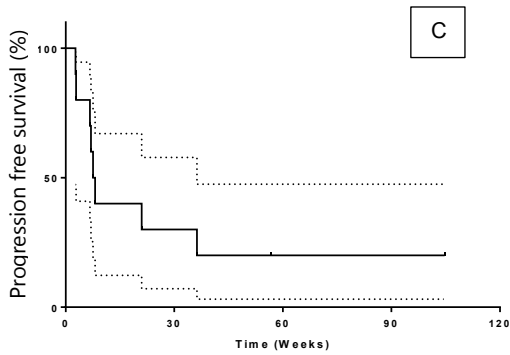
Figure 2 continued. Efficacy analysis from BP29435(A-C) and BP29842(D-F). (A;D) Best change from baseline in tumor size. Dotted lines at 20% and -30% indicate progressive disease and partial response, respectively. (B;E) Longitudinal change from baseline in tumor size. (C;F) Longitudinal change from baseline in tumor size



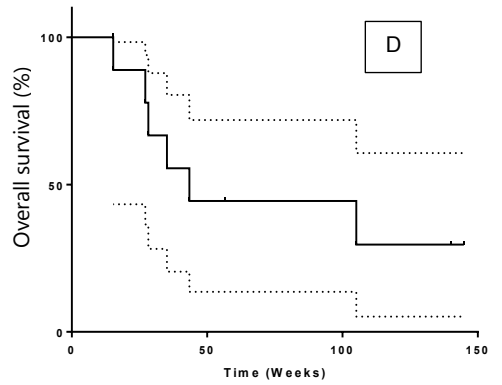
Weeks	0	5	10	15	20	25	30
No. at risk	6	6	5	2	2	2	2



Weeks	0	20	40	60	80	100
No. at risk	6	6	3	3	2	2



Weeks	0	20	40	60	80	100	120
No. at risk	10	5	3	2	2	2	1



Weeks	0	20	40	60	80	100	120	140
No. at risk	10	9	6	4	4	4	3	2

Figure 3. Kaplan-Meier estimates. (A,B) Progression-free survival and overall survival for BP29435. (C,D) Progression-free survival and overall survival for BP29842.

DISCUSSION AND CONCLUSION

We described the safety, tolerability and efficacy of two novel tumor targeting IL-2 therapies. Both FAP-IL2v and CEA-IL2v were shown to be quite toxic for patients, with two out of sixteen patients stopping treatment due to toxicity, and three patients withdrawing informed consent due to intolerability. Broad clinical implementation of these immunocytokines may prove to be challenging, as treatment requires an experienced healthcare staff that is well-trained in providing supportive and interventional management of complications, as well as being able to make rational decisions regarding further dosing.

Preliminary efficacy analysis showed promising anti-tumor activity of FAP-IL2v but not of CEA-IL2v in these small patient groups. A possible explanation for this is the difference in tumor types for which these compounds are investigated. As CEA is highly expressed in CRC, CEA-IL2v was mainly investigated in this tumor type. However, the majority of CRCs are microsatellite stable, not very immunogenic, and likely have a noninflamed tumor microenvironment, making them unlikely to respond to immunotherapy[16, 17]. In contrast, FAP-IL2v has been investigated in a wide variety of tumors, including immunogenic cancer types such as melanoma and H&N cancer[18]. In this interim analysis, two out of four melanoma patients responded to treatment. It is noteworthy to mention that one of the patients described in this interim analysis did not respond to checkpoint blockade, but did respond to IL-2 treatment.

Development of FAP-IL2v as a single agent continues in melanoma and squamous cell carcinomas expansion cohorts. Furthermore, FAP-IL2v is being further investigated as a combination partner with trastuzumab (HER2+ breast cancer), cetuximab (EGFR+ head and neck squamous cell carcinoma), and atezolizumab (solid tumors). FAP-IL2v has been shown to preferentially boost NK cells and CD8+ T cells (data not shown). For this reason it is expected that FAP-IL2v will enhance anti-tumor activity of these monoclonal antibodies: for atezolizumab through CD8+ T cells, and for cetuximab and trastuzumab through antigen-dependent cell mediated cytotoxicity of NK cells[19, 20]. For BP29435, patient recruitment has been completed and the clinical study report is in preparation.

ACKNOWLEDGEMENTS

We thank all patients and their families for participating; F. Hoffman-La Roche for sponsoring; and the Clinical Pharmacology Department of The Netherlands Cancer Institute for conducting this trial.

REFERENCES

1. Gaffen SL, Liu KD. Overview of interleukin-2 function, production and clinical applications. *Cytokine*. 2004 Nov 7;28:109-123.
2. Paliard X, de Waal Malefijt R, Yssel H et al. Simultaneous production of IL-2, IL-4, and IFN-gamma by activated human CD4+ and CD8+ T cell clones. *J. Immunol.* 1988; 141:849–855.
3. Bayer AL, Yu A, Malek TR. Function of the IL-2R for thymic and peripheral CD4+CD25+ Foxp3+ T regulatory cells. *J. Immunol.* 2007; 178:4062–4071.
4. U.S. Food and Drug Administration. Proleukin (aldesleukin) Injection label, 2012.
5. Dhupkar P, Gordon N. Interleukin-2: Old and New Approaches to Enhance Immune-Therapeutic Efficacy. *Adv. Exp. Med. Biol.*, 2017; 995:33–51.
6. Lo Re G, Lo Re F, Doretto P et al. Cyclophosphamide with or without fluorouracil followed by subcutaneous or intravenous interleukin-2 use in solid tumors: A feasibility off-label experience. *Cytokine*, 2018; 113:50-60.
7. Albertini MR, Yang RK, Ranheim EA et al. Pilot trial of the hu14.18-IL2 immunocytokine in patients with completely resectable recurrent stage III or stage IV melanoma. *Cancer Immunol. Immunother.* 2018; 67:1647–1658.
8. Waldhauer I, Nicolini V, Dunn C et al. Novel Tumor-Targeted, Engineered IL-2 Variant (IL2v)-Based Immunocytokines For Immunotherapy Of Cancer. *Blood* 2013;122:2278.
9. Krieg C, Létourneau S, Pantaleo G, Boyman O. Improved IL-2 immunotherapy by selective stimulation of IL-2 receptors on lymphocytes and endothelial cells. *Proc. Natl. Acad. Sci. U. S. A.* 2010; 107:11906–11911.
10. Hu P, Mizokami M, Ruoff G et al. Generation of low-toxicity interleukin-2 fusion proteins devoid of vasopermeability activity. *Blood* 2003; 101:4853–4861.
11. BP29842-FAP-IL2v (FAP-IL2v) Investigator/Study Coordinator Meeting. 2016.
12. van Brummelen EMJ, Huisman MC, der Veen LJ de W et al. 89Zr-labeled CEA-targeted IL-2 variant immunocytokine in patients with solid tumors: CEA-mediated tumor accumulation and role of IL-2 receptor-binding. *Oncotarget* 2018; 9:24737–24749.
13. West EE, Jin H-T, Rasheed A-U et al. PD-L1 blockade synergizes with IL-2 therapy in reinvigorating exhausted T cells. *J. Clin. Invest.* 2013; 123:2604–2615.
14. Boyman O, Cho JH, Sprent J. The role of interleukin-2 in memory CD8 cell differentiation. *Adv. Exp. Med. Biol.* 2010; 684:28–41.
15. Hamson EJ, Keane FM, Tholen S et al. Understanding fibroblast activation protein (FAP): Substrates, activities, expression and targeting for cancer therapy. *PROTEOMICS - Clin. Appl.* 2014; 8:454–463.
16. Spranger S, Luke JJ, Bao R et al. Density of immunogenic antigens does not explain the presence or absence of the T-cell-inflamed tumor microenvironment in melanoma. *Proc. Natl. Acad. Sci.* 2016; 113:7759–7768.
17. Le DT, Uram JN, Wang H et al. PD-1 Blockade in Tumors with Mismatch-Repair Deficiency. *N. Engl. J. Med.* 2015; 372:2509–2520.
18. Alexandrov LB, Nik-Zainal S, Wedge DC et al. Signatures of mutational processes in human cancer. *Nature* 2013; 500:415–421.
19. European Medicines Agency. Herceptin (trastuzumab) Eur. Public Assess. Rep., 2016.
20. European Medicines Agency. Erbitux (cetuximab) Eur. Public Assess. Rep., 2014

Chapter 2

Monoclonal antibodies targeting co-stimulatory receptor molecules

Chapter 2.1

Preliminary clinical activity and safety of OX40 agonistic monoclonal antibody GSK3174998 administered alone and in combination with pembrolizumab in selected advanced solid tumors.

A preliminary analysis of GSK201212 of patients treated at the Netherlands Cancer Institute.

Willeke Ros

Part of this study has been presented at the American Society of Clinical Oncology (ASCO) Annual Meeting 2016:

Infante JR, Ahlers CM, Hodi FS, Postel-Vinay S, Schellens JHM, Heymach J, Autio KA, Barnette MS, Struemper H, Watmuff M, Paul EM, Kaufman DR, Weber JS, Hoos A. ENGAGE-1: A first in human study of the OX40 agonist GSK3174998 alone and in combination with pembrolizumab in patients with advanced solid tumors.

Journal of Clinical Oncology 2016;34:TPS3107.

ABSTRACT

Background: OX40 is a co-stimulatory receptor molecule which is transiently expressed by activated T-cells. OX40 engagement by its ligand leads to increased proliferation, effector function and survival of T-cells, and increases anti-tumor activity. GSK3174998 is a monoclonal antibody that binds agonistically to OX40, thereby activating the OX40 pathway.

Methods: Study 201212 (clinicaltrials.gov identifier NCT02528357) is an open-label, non-randomized multicenter study designed to evaluate the safety, tolerability, pharmacokinetics, pharmacodynamics and preliminary clinical activity of GSK3174998 alone and in combination with pembrolizumab. Here, we present interim results of patients treated at the Netherlands Cancer Institute.

Results: Twenty-one patients, six males (28.6%) and 15 females (71.4%), median age 65 years [31- 77], were enrolled between May 2016 and June 2018 at the Netherlands Cancer Institute. Included tumor types were soft tissue sarcoma (STS), microsatellite instability high colorectal cancer (MSI-H CRC), head and neck squamous cell carcinoma (HNSCC), triple negative breast cancer (TNBC), bladder carcinoma, renal cell carcinoma (RCC), and non-small cell lung cancer (NSCLC). The most common adverse events (AEs) possibly related to treatment seen in the monotherapy were fatigue (31%) and pruritus (15%). For combination treatment, the most common possibly related AEs were fever (44%), fatigue (33%), nausea (22%), constipation (22%), and flushing (22%). No G3 - G4 related AEs occurred, and the maximal tolerated dose was not reached. Antitumor activity was seen in one patient with dedifferentiated liposarcoma. This patient developed a partial response after cycle 8 and lasted for 10.7 weeks.

Conclusions: GSK3174998 was well-tolerated. Preliminary clinical activity was observed in one patient with STS who received GSK3174998 monotherapy at an intermediate dose-level.

INTRODUCTION

The co-stimulatory receptor molecule OX40 (CD134) is a member of the tumor-necrosis factor (TNF) receptor superfamily. It is expressed on activated T-cells[1, 2], as well as on regulatory T cells[3]. OX40L is the only known ligand for OX40, and is expressed mainly on antigen presenting cells (APCs)[4]. The binding of OX40 with its ligand is crucial for the generation of memory T cells, as it promotes the survival of effector T cells after antigen priming. OX40 has a more prominent effect on CD4+ cells compared to CD8+ cells[5], although roles in promoting CD8+ cells have also been identified[6]. Regarding regulatory T cells, OX40 signaling appears to not only impair their function but also their development[7]. These immunomodulating effects make OX40 an attractive target for anticancer immunotherapy.

In general, immunotherapy such as OX40 treatment is thought to be most effective in inflamed tumors - tumors which are infiltrated with high densities of functional effector T cells[8]. Potential biomarkers for anti-OX40 antibodies have been identified in preclinical models[9]. Higher baseline expression of immune activation markers and lower expression of immune inhibitory and Th2 associated markers may be predictive of better outcome to anti-OX40 antibodies. Biomarkers for pharmacodynamic activity include reduced Treg cell number and function in the tumor and periphery, increased effector T cell proliferation, and increased IFN- γ , granzymes, and perforin expression in the tumor micro-environment.

GSK3174998 is a humanized IgG1 anti-OX40 agonistic monoclonal antibody. It binds to the human OX40 extracellular domain with an affinity of 4.9 nM. GSK3174998 was selected based on its ability to promote effector CD4+ T-cell proliferation, inhibit induction of immunosuppressive interleukin-10, produce CD4+ Type 1 regulatory cells, block the suppressive function of natural Treg cells, and bind to Fc receptors to augment OX40 signaling. GSK3174998 was shown to bind to human Fc γ R I, IIa R, IIa H, IIb, IIIa V158, and IIIa F158 as well as human C1q.

GSK3174998 is currently being tested in study 201212, a phase I First Time in Human (FTIH) open label study of GSK3174998 administered alone and in combination with pembrolizumab. Here, we present data from patients enrolled at the Netherlands Cancer Institute between May 2016 and June 2018.

METHODS

Study design and patient population

Study 201212 (ClinicalTrials.gov identifier NCT02528357) was designed to examine the safety, tolerability and maximal tolerated dose of GSK3174998 in patients with advanced solid tumors. Key eligibility requirements included having histologically or cytologically-documented advanced metastatic and/or unresectable solid cancer which was incurable and for which prior standard first-line treatment has failed or did not exist, progression on or intolerance to therapies that are known to provide clinical benefit, ≥ 18 years of age, adequate organ function, ≤ 5 prior lines of therapy for advanced disease, measurable disease based on response evaluation criteria in solid tumors (RECIST) V1.1., Eastern Cooperative Oncology Group (ECOG) Performance Status (PS) of 0 or 1, and a life

expectancy of at least 12 weeks. Eligible tumor types were melanoma, non-small cell lung cancer (NSCLC), renal cell carcinoma (RCC), bladder cancer, squamous cell carcinoma of the head and neck (SCCHN), soft tissue sarcoma (STS), triple-negative breast cancer (TNBC), and colorectal carcinoma displaying microsatellite instability (MSI-H CRC). The majority of these tumor types have demonstrated prior response to checkpoint inhibition therapy[10, 11]. In addition, gene expression data suggests that the selected tumor types have at least moderate OX40 expression levels[12].

Key exclusion criteria included: prior treatment with TNFR agonists (OX40, CD27, CD137, CD357); prior treatment with checkpoint inhibitors within 8 weeks (PD-1, PD-L1, CTLA-4), prior anticancer therapy within four weeks or five half-lives, whichever is shorter; prior radiation therapy within two weeks, prior investigational therapy within 30 days, prior allogeneic or autologous bone marrow transplantation or solid organ transplantation, \geq Grade (G) 3 toxicity related to prior immunotherapy leading to treatment discontinuation, major surgery or anticancer monoclonal antibody therapy within four weeks of treatment initiation, prior treatment with an anti-PD-1, anti-PD-L1, or anti-PD-L2 therapy or other immune checkpoint inhibitor, known active CNS metastases, diagnosis of immunodeficiency, autoimmune disease, interstitial lung disease, or active infection requiring systemic therapy and known severe hypersensitivity to pembrolizumab and/or any of its excipients.

A modified 3+3 design was used for dose escalation. If zero out of three patients experienced a dose limiting toxicity (DLT), escalation to the next dose level took place. If one out of three patients experienced a DLT, three additional patients would be enrolled. If two or more patients in a dosing cohort experienced a DLT, dose escalation would be stopped and at that dose level, the maximal tolerated dose (MTD) was exceeded. A DLT was defined as one of the following clinically relevant toxicities: febrile neutropenia, G4 neutropenia of >7 days duration or requiring G-CSF, G4 anemia of any duration, G4 thrombocytopenia of any duration or G3 thrombocytopenia with bleeding, G4 toxicity, G3 toxicity that does not downgrade to G1 or baseline within three days despite optimal supportive care, any G2 ocular toxicity requiring systemic steroids, or any \geq G3 ocular toxicity, toxicity that results in permanent discontinuation of GSK3174998 or pembrolizumab during the first four weeks of treatment, or any other event which in the judgment of the investigator and GSK Medical Monitor is considered to be a DLT.

The study was conducted according to protocol, Good Clinical Practice standards, and provisions outlined in the Declaration of Helsinki. The study protocol and all amendments were approved by the appropriate institutional review board and ethics committee. All patients provided written informed consent before any study related procedures were performed.

Treatment and assessments

By determining the minimum anticipated biological effect level, a dose of 0.003 mg/kg was selected as a safe starting dose for the FTIH study. GSK3174998 was dosed q3W at dose levels of 0.003, 0.01, 0.03, 0.1, 0.3, 1.0, 3.0 or 10.0 mg/kg for a maximum duration of 48 weeks, or until confirmed disease progression, death, unacceptable toxicity or withdrawal of consent. The study was a non-randomized study, and subjects were assigned to study treatment in the order in which they completed screening assessments. Patients receiving combination therapy with pembrolizumab received a flat dose of 200 mg pembrolizumab intravenously every three weeks, in addition to GSK3174998. Tumor imaging was done every 12 weeks using CT or MRI. Adverse events were monitored throughout the study period and graded according to the National Cancer Institute's Common Terminology Criteria for Adverse Events (CTCAE v4.0)

Outcomes

The primary objective of this preliminary analysis was (I) to evaluate the safety and tolerability of GSK3174998 alone and in combination with pembrolizumab, and (II) to identify the MTD or maximum administered dose (MAD). Endpoints include adverse events (AEs), serious adverse events (SAEs), withdrawals due to AEs, dose reductions or delays.

The secondary objective was to evaluate the antitumor activity of GSK3174998. Endpoints included confirmed best overall response rates, time to response (TTR), time to tumor progression (TTP), duration of response (DOR), progression free survival (PFS), and overall survival (OS). Subjects with unknown or missing response information were treated as non-responders.

Secondary and exploratory objectives will not be discussed in this interim analysis, but were investigated in the study, including (I) characterization of pharmacokinetics, (II) determination of the immunogenicity, by assessing the number and percentage of subjects who develop detectable anti-drug antibodies, (III) exploration of the relationship between antitumor activity, PK parameters, pharmacodynamic activity and other patient characteristics, and (IV) evaluation of the pharmacodynamic activity of GSK3174998 in the peripheral blood and tumor biopsies. In peripheral blood, Lymphocyte OX40 receptor membrane expression and occupancy by GSK3174998 was assessed, as well as of immune function in blood (e.g. phenotype, quantity, and activation state of T cells in the periphery, expression of circulating soluble factors such as cytokines and stress-related proteins). In tumor biopsies, the number of tumor-infiltrating lymphocytes and other immune cells expressing key phenotypic markers are assessed, as well as changes in gene expression, T-cell receptor diversity and mutational load.

Statistical analysis

Safety was assessed in patients who received ≥ 1 dose of GSK3174998 and were summarized using descriptive statistics. The Kaplan–Meier method was used to estimate PFS, OS, and DOR. The data cutoff date for this report was 19th of June 2018.

Table 1. Patient characteristics.

Demographic characteristic	Total (n=21)
Age (Years)	65 [31 – 77]
Gender (n,%)	
Male	6 (28.6%)
Female	15 (71.4%)
WHO PS (%)	
0	13 (61.9%)
1	8 (38.1%)
Tumor Type (n)	
STS	5
TNBC	4
MSI-H CRC	3
RCC	1
HNSCC	5
Bladder	1
NSCLC	2
Prior lines of therapy for advanced disease	2 [0 – 5]

RESULTS

Baseline Patient Characteristics

Twenty-one patients were enrolled between May 2016 and June 2018 (Table 1, 2). At the time of study initiation at the NKI/AvL, the dose level of 0.01 mg/kg for monotherapy was reached. Investigated dose-levels included 0.01 mg/kg, 0.03 mg/kg, 0.1 mg/kg, 0.3 mg/kg, 1 mg/kg, 3 mg/kg, and 10 mg/kg; with or without 200 mg pembrolizumab. Included tumor types were STS, MSI-H CRC, SCCHN, TNBC, bladder carcinoma, RCC, and NSCLC. The median age was 65 years [31 - 77]; the median lines of prior therapy for advanced disease was 2 [0 – 5]; 28.6% of patients were male; and 61.9% had an ECOG performance status of 0. Thirteen patients received GSK3174998 monotherapy, and nine patients received combination therapy. Out of the nine patients receiving combination therapy, one patient originally received monotherapy and switched to combination therapy after progression.

Table 2. Overview of tumor type and treatment per individual patient.

* = switched to combination therapy after initial progression on monotherapy

Pt No.	Tumor Type	Dose GSK3174998 (mg/kg)	Pembrolizumab
01	STS	0.1	No
02	STS	0.03	No
03	TNBC	0.03	No
04	STS	0.3	No
05	STS	0.3	No
06	MSI-H CRC	0.003	Yes
07	STS	0.1	No
08	RCC	0.1	No
09	MSI-H CRC	*1 ; 0.03	*Yes
10	HNSCC	0.01	Yes
11	NSCLC	0.3	No
12	NSCLC	3	No
13	TNBC	3	No
14	TNBC	3	No
15	Bladder	0.1	No
16	MSI-H CRC	1	Yes
17	HNSCC	0.3	Yes
18	HNSCC	1	Yes
19	HNSCC	10	Yes
20	HNSCC	0.1	Yes
21	TNBC	0.3	Yes

Safety

Sixteen patients (76.2%) experienced treatment-related adverse events (Table 3). The most common adverse events (AEs) possibly related to treatment were fatigue (33%), fever (23%) and nausea (14%). The most common possibly related AEs seen in the monotherapy were fatigue (31%) and pruritus (15%). For combination treatment, the most common possibly related AEs were fever (44%), fatigue (33%), nausea (22%), constipation (22%), and flushing (22%). The duration and time of onset of AEs differed amongst patients, with no apparent trend in toxicities. AEs were reversible and did not reoccur at later cycles. No grade 3 or higher treatment related AEs were observed, and no treatment related discontinuations or deaths occurred. No additional toxicities were observed in the combination therapy compared to monotherapy.

Antitumor activity

One out of 13 patients receiving monotherapy obtained a confirmed partial response, and zero out of nine patients receiving combination treatment showed a confirmed response (Figure 1). No patients showed confirmed stable disease. The median PFS was 75 days [28 – 212]; 68 days [28 – 212] for monotherapy and 75 days [28 – 94] for combination therapy. The median overall survival was 148 days [57 – 701+]; 176 days [57-701+] for monotherapy and 148 days [67 – 470+] for combination therapy (Figure 2). The median received cycles was 4 [2 - 11]; 3 [2-11] for monotherapy and 4 [2-5] for combination therapy. Eight patients

were not evaluable for efficacy analysis: six patients discontinued before the first tumor assessment due to clinical disease progression, one patient went off study prior to the first tumor assessment due to a non-related AE (hip fracture), and another patient had target lesions which were not assessable during treatment due to atelectasis and pleural effusion.

The partial response was seen in a 66-year-old female patient with dedifferentiated liposarcoma. This patient received 0.3 mg/kg GSK3174998 monotherapy. The observed partial response occurred at the third tumor assessment (Figure 3) and occurred 24 weeks after start of treatment. The patient was taken off study after the fifth tumor assessment showed progression of non-target lesions. The DOR was 10.7 weeks. The TTP was 34.7 weeks.

DISCUSSION AND CONCLUSION

We investigated the safety, maximal tolerated dose and preliminary antitumor activity of the OX40 agonistic monoclonal antibody GSK3174998. The maximal tolerated dose was not reached, and the safety profile was excellent without high-grade toxicity.

One out of 21 patients showed a partial response, which was a patient with dedifferentiated liposarcoma who received 0.3mg/kg GSK3174998 monotherapy. This is an interesting outcome, as liposarcomas generally have a low mutational burden and are not very immunogenic tumors. Rather, they are frequently driven through overexpression of MDM2 and CDK4[13]. However, dedifferentiated liposarcomas can acquire additional mutations, and can ultimately become highly mutated, making it more likely that epitopes are produced which are recognized by the immune system[14]. Another potential explanation why this patient may have responded to OX40 treatment is the prior palliative treatment with doxorubicin-based chemotherapy. Anthracyclines are capable of inducing a phenomenon known as immunogenic cell death, a form of apoptosis in which novel immunogenic antigens are released during tumor cell death. These antigens can induce an anti-tumor immune response by activating dendritic cells and subsequently activate specific T-cell responses[15, 16]. The patient received two months of weekly low-dose (15 mg) doxorubicin for palliative treatment and stopped treatment one month prior to start of OX40 treatment.

Although clinical activity has been seen in anti-OX40 monotherapy, the activity is thus far rather limiting. A possible explanation for this, is that OX40 is known to be an inducible receptor molecule. It only regulates later expansion of T-cell numbers, at the peak of the immune response[17]. This suggests that if there is no prior immune response initiated, attempting to activate the OX40 pathway may not work optimally. Indeed, it has been shown that more immunogenic tumors, which contain more activated tumor infiltrating lymphocytes, respond better to anti-OX40 therapy compared to nonimmunogenic models[18]. To fully optimize OX40 therapy, it may need to be combined with other treatment options. It can be combined with other immunotherapies, such as pembrolizumab, or even other treatment modalities such as chemotherapy. These agents may be capable of initiating an intratumoral immune response, which in return will be strengthened and sustained by anti-OX40 therapy.

Table 3. AEs at least possibly related to study treatment. AEs related to OX40 were observed in monotherapy alone, (n = 13); AEs related to OX40 or pembrolizumab were observed in the combination therapy (n = 9) and could be contributed to either drugs.

Toxicities related to GSK3174998	Grade 1, n (%)	Grade 2 n (%)	Total, n (%)
Rash	1 (8%)		1 (8%)
Pruritus	2 (15%)		2 (15%)
Urticaria	1 (8%)		1 (8%)
Fatigue	4 (31%)		4 (31%)
Fever	1 (8%)		1 (8%)
Anorexia	1 (8%)		1 (8%)
Alopecia	1 (8%)		1 (8%)
Nausea	1 (8%)		1 (8%)
Flu-like symptoms	1 (8%)		1 (8%)
Vomiting	1 (8%)		1 (8%)
Malaise	1 (8%)		1 (8%)
Dysgeusia		1 (8%)	1(8%)
Myalgia	1 (8%)		1(8%)
Toxicities related to GSK3174998 or Pembrolizumab	Grade 1, n (%)	Grade 2 n (%)	Total, n (%)
Rash	1 (11%)		1 (11%)
Fatigue	2 (22%)	1 (11%)	3 (33%)
Fever	1 (11%)	3 (33%)	4 (44%)
Nausea		1 1 (11%)	1 (11%)
Vascular disorders	1 (11%)		1 (11%)
Hyperhidrosis	1 (11%)		1 (11%)
Nausea	2 (22%)		2 (22%)
Increased throat secretion	1 (11%)		1 (11%)
Weight loss	1 (11%)		1 (11%)
Anemia		1 (11%)	1 (11%)
Flushing	2 (22%)		2 (22%)
ALAT increase	1 (11%)		1 (11%)
ASAT increase	1 (11%)		1 (11%)
Malaise	1 (11%)		1 (11%)
Constipation	2 (22%)		2 (22%)
Vomiting	1 (11%)		1 (11%)
Constipation	1 (11%)		1 (11%)
Hypothyroidism		1 (11%)	1 (11%)

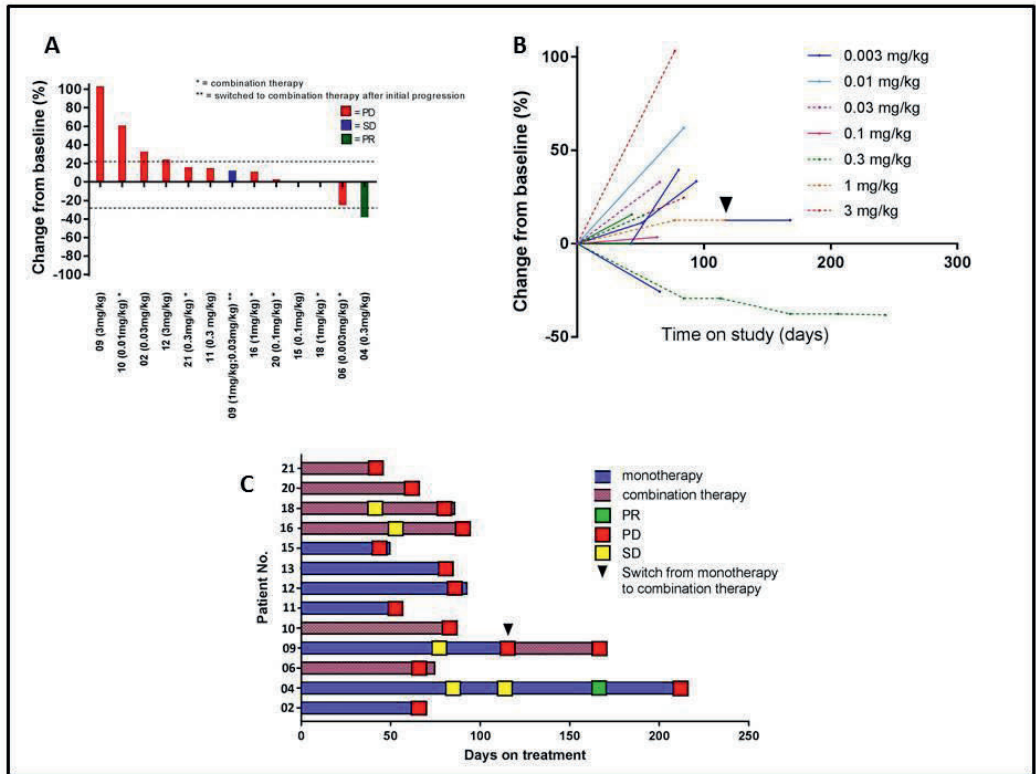


Figure 1. (A) Best change from baseline in tumor size (n=13). Dotted lines at 20% and -30% indicate progressive disease and partial response, respectively. (B) Longitudinal change from baseline in tumor size (n=13). (C) Treatment exposure and response duration. The length of each bar corresponds to the duration of treatment for each patient

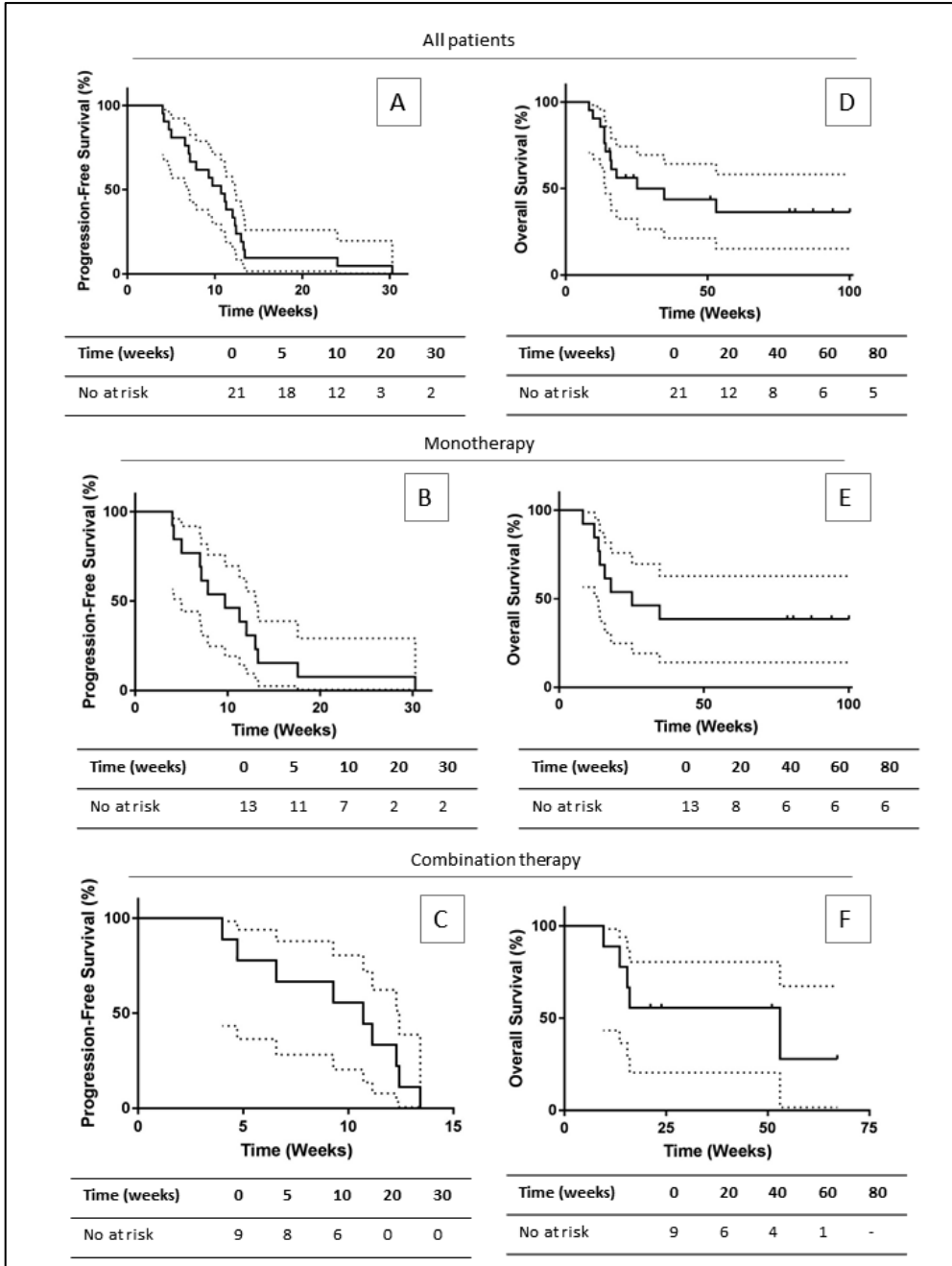


Figure 2. Kaplan-Meier estimates. (A-C) Progression-free survival of all patients (A), patients treated in monotherapy (B) and patients treated with combination therapy (C). (D) Overall survival of all patients (D), patients treated in monotherapy (E) and patients treated with combination therapy (F).

One out of nine patients receiving combination therapy showed tumor reduction of 25%. This patient received a low dose of 0.003 mg/kg GSK3174998 and 200mg pembrolizumab. This near-PR was seen in a patient with MSI-H CRC, a tumor type for which pembrolizumab monotherapy is known to be effective. Therefore, we cannot exclude that the tumor reduction was contributed solely to the pembrolizumab. Interestingly, none of the other eight patients receiving combination therapy showed even stabilization of disease, despite the majority of these patient having tumor types (three patients with MSI-H, and five patients with SCCHN) for which pembrolizumab has been approved.

To conclude, although GSK3174998 appears to be well tolerated; modest preliminary clinical activity suggests more investigation is needed in order to understand how this agonist could be further developed . Not only the correct combination partner needs to be selected, also the patient population which is most likely to respond to treatment needs to be identified. For this, we need to find biomarkers which are predictive of response. Potential biomarkers may include Treg and effector T-cell function and levels, as well as intratumoral cytotoxic immune function[9]

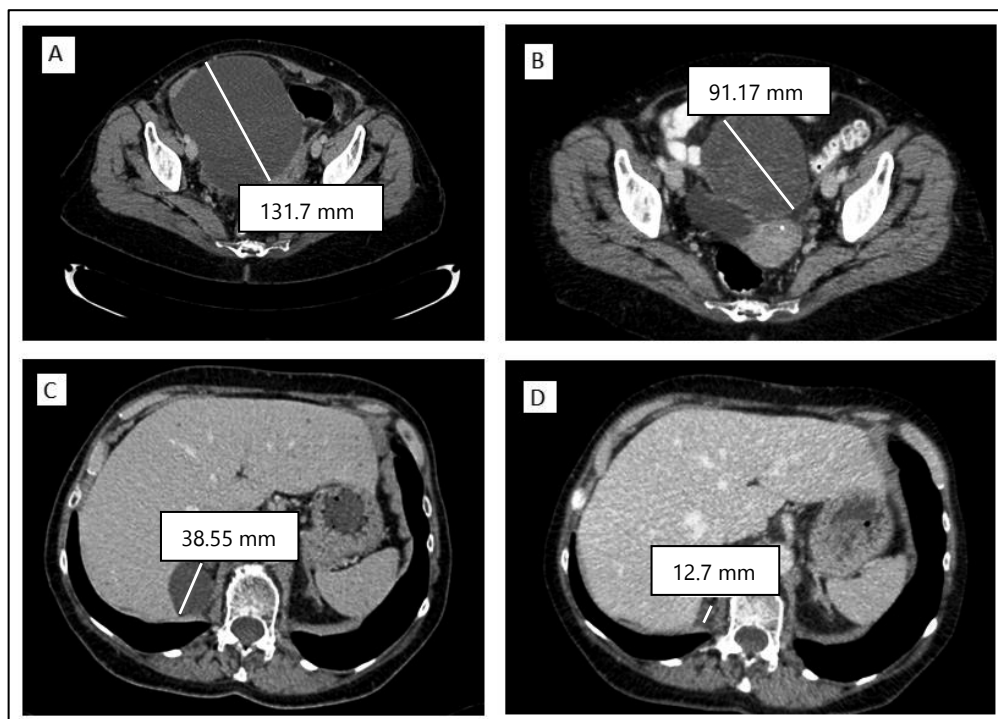


Figure 3. CT scan images of a liposarcoma patient who obtained a PR. Retroperitoneal lesion at baseline (A) and after 24 weeks of treatment (B). Liver lesion at baseline (C) and after 24 weeks of treatment (D).

ACKNOWLEDGEMENTS

We thank all patients and their families for participating; GlaxoSmithKline for sponsoring; and the Clinical Pharmacology Department of The Netherlands Cancer Institute for conducting this trial.

REFERENCES

1. Godfrey WR, Fagnoni FF, Harara MA et al. Identification of a human OX-40 ligand, a costimulator of CD4+ T cells with homology to tumor necrosis factor. *J. Exp. Med.* 1994; 180:757–762.
2. Mallett S, Fossum S, Barclay AN. Characterization of the MRC OX40 antigen of activated CD4 positive T lymphocytes—a molecule related to nerve growth factor receptor. *EMBO J.* 1990; 9(4):1063–1068.
3. Vu MD, Xiao X, Gao W et al. OX40 costimulation turns off Foxp3+ Tregs. *Blood* 2007; 110:2501–2510.
4. Chen AI, McAdam AJ, Buhlmann JE et al. Ox40-ligand has a critical costimulatory role in dendritic cell:T cell interactions. *Immunity* 1999; 11(6):689–698.
5. Godfrey WR, Fagnoni FF, Harara MA et al. Identification of a human OX-40 ligand, a costimulator of CD4+ T cells with homology to tumor necrosis factor. *J. Exp. Med.* 1994; 180:757–762.
6. Lei F, Song J, Haque R et al. Regulation of A1 by OX40 contributes to CD8(+) T cell survival and anti-tumor activity. *PLoS One* 2013; 8:70635.
7. Murata K, Satomi S, Sugamura K. Distinct Roles for the OX40-OX40 Ligand Interaction in Regulatory and Nonregulatory T Cells. *J Immunol.* 2004 Mar 15;172:3580-3589.
8. Hegde PS, Karanikas V, Evers S. The Where, the When, and the How of Immune Monitoring for Cancer Immunotherapies in the Era of Checkpoint Inhibition. *Clin. Cancer Res.* 2016; 22:1865–1874.
9. Huseni M, Totpal K, Du C et al. Anti-tumor efficacy and biomarker evaluation of agonistic anti-OX40 antibodies in preclinical models. *J. Immunother. Cancer* 2014; 2:253.
10. Opdivo (nivolumab) Prescribing information (2015) *U.S. Food and Drug Administration*.
11. Keytruda (pembrolizumab) Prescribing information (2015) *U.S. Food and Drug Administration*
12. The Cancer Genome Atlas - Cancer Genome - TCGA. Available at [<https://cancergenome.nih.gov/>].
13. Kanojia D, Nagata Y, Garg M et al. Genomic landscape of liposarcoma. *Oncotarget.* 2015;6:42429–42444.
14. Pollack SM, He Q, Yearley JH et al. T-Cell Infiltration and Clonality Correlate With Programmed Cell Death Protein 1 and Programmed Death-Ligand 1 Expression in Patients With Soft Tissue Sarcomas. *Cancer.* 2017;123:3291–3304.
15. Pol J, Vacchelli E, Aranda F et al. Trial Watch: Immunogenic cell death inducers for anticancer chemotherapy. *Oncoimmunology* 2015; 4:1008866.
16. Garg AD, Dudek-Peric AM, Romano E, Agostinis P. Immunogenic cell death. *Int. J. Dev. Biol.* 2015; 59:131–140.
17. Croft M. Co-stimulatory members of the TNFR family: keys to effective T-cell immunity? *Nat Rev Immunol.* 2003;3:609-620.
18. Weinberg AD, Rivera MM, Prell R et al. Engagement of the OX-40 receptor in vivo enhances antitumor immunity. *J. Immunol.* 2000; 164:2160–2169.

Chapter 2.2

Preliminary efficacy, safety, pharmacokinetics and pharmacodynamics data from a phase I dose-escalation study of OX40 agonistic monoclonal antibody PF-04518600 administered alone and in combination with utomilumab, a 4-1BB agonistic monoclonal antibody.

A summary of published data from early analysis of B0601002.

Willeke Ros

Preliminary data has been presented at the American Society of Clinical Oncology (ASCO) annual meeting 2017, European Society for Medical Oncology (ESMO) Annual Meeting 2017, and the American Association for Cancer Research (AACR) Annual Meeting 2018:

El-Khoueiry AB, Hamid O, Thompson J, **Ros W**, Eskens F, Doi T, Hu-Lieskovan S, Chou J, Liao K, J Ganguly B, Fleener C, Joh T, Diab A. The relationship of pharmacodynamics (PD) and pharmacokinetics (PK) to clinical outcomes in a phase I study of OX40 agonistic monoclonal antibody (mAb) PF-04518600 (PF-8600).

Journal of Clinical Oncology 2017; 35:3027

Hamid O, **Ros W**, Thompson JA, Rizvi NA, Angevin E, Chiappori A, Ott PA, Ganguly BJ, Fleener C, Liao K, Joh T, Dell V, Chou J, Hu-Lieskovan S, Eskens FALM, Diab A, Doi T, Wasser J, Spano J-P, El-Khoueiry A. Safety, pharmacokinetics (PK) and pharmacodynamics (PD) data from a phase I dose-escalation study of OX40 agonistic monoclonal antibody (mAb) PF-04518600 (PF-8600) in combination with utomilumab, a 4-1BB agonistic mAb.

Annals of Oncology 2017;28: v403-v427.

Diab A, Hamid O, Thompson JA, **Ros W**, Eskens FALM, Doi T, Hu-Lieskovan S, Long H, Joh T, Pottluri S, Wang X, Fleener C, Taylor CT, Ganguli BJ, Chou J, El-Khoueiry AB. Pharmacodynamic (PD) changes in tumor RNA expression and the peripheral blood T cell receptor (TCR) repertoire in a phase I study of OX40 agonistic monoclonal antibody (mAb) PF-04518600 (PF-8600).

Cancer Research 2018; 78:CT010

ABSTRACT

Background Stimulating effector T-cells through the co-stimulatory protein OX40 may be an effective new therapeutic strategy for eradicating cancer. Preclinical data has shown that OX40 engagement led to proliferation and activation of effector T-cells *in vitro*, and showed antitumor activity in *in vivo* models. PF-04518600 (PF-8600) is a novel fully human immunoglobulin (Ig)G2 monoclonal antibody which binds agonistically to OX40.

Methods B0601002 (ClinicalTrials.gov identifier NCT02315066) was a phase 1 open-label, dose escalation study of PF-8600 as a single agent and in combination with utomilumab (anti-4.1-BB) in patients with selected locally advanced or metastatic cancers. This thesis chapter describes the safety, efficacy, pharmacokinetics (PK), and pharmacodynamics (PD) of PF-8600 of which the results have been published on previous congresses.

Results At the data cutoff date, 51 patients were enrolled in the monotherapy part, and 42 patients were enrolled in the combination part. The most common adverse events (AEs) observed in the monotherapy were fatigue, nausea, vomiting, decreased appetite, headache, influenza like illness and pruritus. For combination treatment, the most common AEs ($\geq 5\%$) were fatigue and nausea. No dose limiting toxicities were observed, and the maximal tolerated dose was not reached. In the monotherapy, two patients obtained a partial response: a melanoma patient who was previously treated with checkpoint blockade, and a hepatocellular carcinoma patient. PK profiles exhibited a pattern consistent with target-mediated drug disposition. PD data revealed increase of proliferation and activation of peripheral CD4⁺ central memory T-cells, and upregulation of genes associated with inflammation and immune activation in the tumor tissue.

Conclusion PF-8600 alone and in combination with utomilumab was well tolerated and showed evidence of single agent efficacy as well as in combination with utomilumab. There was clear evidence of PD activity in both tumor samples and peripheral blood.

INTRODUCTION

Immunotherapy has made a large impact on anti-cancer therapy. The anti-CTLA-4 and anti-PD(L)1 antibodies have demonstrated clinical benefit in a vast amount of tumor types. The next step for immunotherapy is to develop novel strategies to improve treatment even further. One of these promising strategies is to target immunostimulatory receptor molecules, such as OX40, 4-1BB, CD27, CD40 and GITR. Targeting these receptors may reduce tumor growth by promoting immune cell proliferation and activation. OX40 is a co-stimulatory receptor molecule expressed on the surface of activated CD4+ cells and, to a lesser extent, on CD8+ T cells. It fulfills functions in memory T-cell survival, clonal expansion of naïve T-cells, generation of effective T-cell responses, suppression of regulatory T-cells, and regulation of cytokine production[1–3]. In contrast to OX40, 4-1BB is mainly expressed on activated CD8+ and NK cells. However, similar to OX40, it fulfills functions in proliferation, activation and cytokine secretion of T-cells[4]. In addition, 4-1BB also stimulates antigen-dependent cell mediated cytotoxicity of NK cells, and can induce antitumor immune responses of macrophages[4].

PF-04518600 (PF-8600) is a novel fully human IgG2 agonistic monoclonal antibody (mAb) specific for human OX40 . In vitro, PF-8600 demonstrated dose-dependent induction of cell proliferation and pro-inflammatory cytokine release. Study B0601002 investigates PF-8600 alone and in combination with the 4-1BB agonistic mAb utomilumab. By combining these two mAbs, both CD4+ and CD8+ cells are stimulated simultaneously. In vivo experiments have shown that this dual stimulation induces an enormous burst of CD8+ T cell effector function[5].

In this chapter we present the preliminary results of the dose escalation portion of the study. These results have been published previously on the American Society Clinical Oncology (ASCO) annual congress in 2017, The European Society of Medical Oncology (ESMO) annual congress in 2017 and American Association for Cancer Research (AACR) annual congress in 2018[6–8].

METHODS

Study design

Both the monotherapy and combination therapy used a modified toxicity probability interval method, targeting a dose-limiting toxicity (DLT) rate of 25% and an acceptable DLT interval of 20–30%.

Each dose level included an initial dose-escalation cohort of 2–4 patients. This cohort was expanded to ~10 patients (biopsy cohort) if the initial dose-escalation cohort blood and/or biopsy samples showed peripheral pharmacodynamic (PD) effects (Figure 1).

Patient population

Key eligibility requirements included having selected advanced malignancies. For monotherapy this included melanoma, hepatocellular carcinoma (HCC), clear-cell renal cell carcinoma (RCC), or head and neck squamous-cell carcinoma (HNSCC). For combination therapy, the included tumor types were non-small cell lung cancer (NSCLC), HNSCC, melanoma, bladder, gastric and cervical cancer. Other key eligibility requirements included: age 18 years or older; Eastern Cooperative Oncology Group (ECOG) performance status of 0 or 1; Adequate renal (creatinine $\leq 1.5\times$ upper limit of normal [ULN]), bone marrow (hemoglobin ≥ 9 g/dL), liver (bilirubin $\leq 1.5\times$ ULN), and cardiac function; measurable disease as defined by Response Evaluation Criteria in Solid Tumors (RECIST) v1.1.

Key exclusion criteria included central nervous system (CNS) primary tumors or CNS metastases; active autoimmune disorders; currently requiring systemic immune suppressive medication; solid organ or hematopoietic transplants and prior therapy with OX40 agonists.

The study was conducted according to protocol, Good Clinical Practice standards, and provisions outlined in the Declaration of Helsinki. The study protocol and all amendments were approved by the appropriate institutional review board and ethics committees.

Treatment and assessments

PF-8600 (0.01–10 mg/kg) was administered intravenously every 14 days (q2w). Utomilumab was administered intravenously every 28 days (q4w). Tumor assessment was done at baseline and every six weeks using RECIST version 1.1 and immune-related (ir)-RECIST. Imaging techniques included CT, MRI or equivalent.

Objectives

The primary objectives were to assess the safety and tolerability of PF-8600 alone and in combination with utomilumab, and to estimate the maximum tolerated dose alone and in combination with utomilumab. Secondary objectives were to assess preliminary antitumor clinical activity of PF-8600, to characterize the pharmacokinetics (PK) of PF-8600, and to assess degree of target engagement by PF-8600 by measuring unbound (free) cell surface OX40 in peripheral blood. Exploratory objectives were to assess PD activity in the blood and tumor microenvironment.

Outcomes

Safety outcome measures

Safety assessments included collection of AEs, SAEs, vital signs and physical examination, electrocardiogram (ECG [12-lead]), laboratory assessments, including pregnancy tests and verification of concomitant treatments. Assessment of adverse events (AEs) included the type, incidence, severity (graded by the National Cancer Institute Common Terminology Criteria for Adverse Events [NCI CTCAE] version 4.03) timing, seriousness, and relatedness.

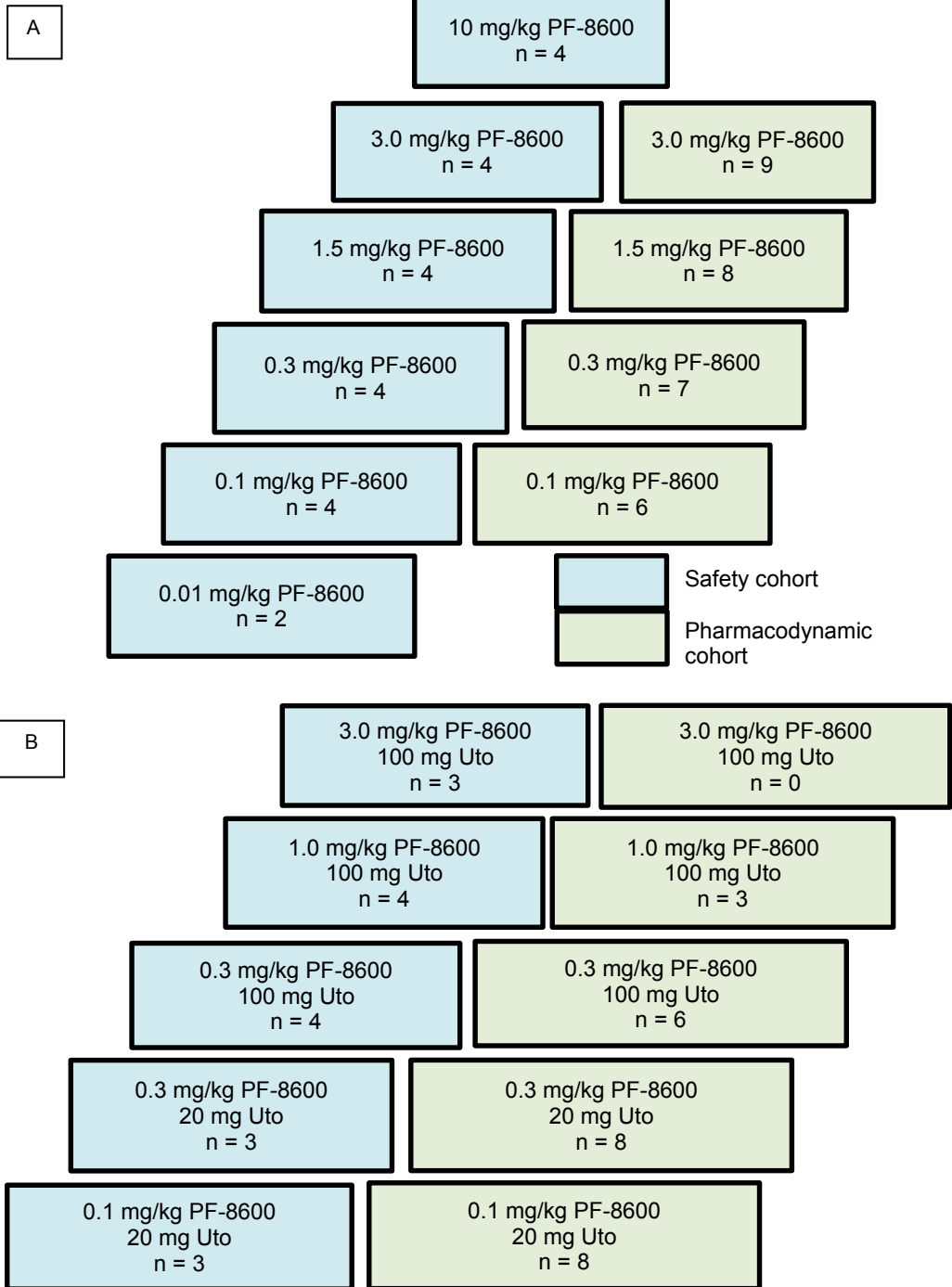


Figure 1. Study design of (A) monotherapy and (B) combination therapy. Each dose level consisted of a safety cohort (2-4 pts), and a pharmacodynamics cohort (0-9 pts).

Efficacy outcome measures

Efficacy outcome measures described in this analysis included best overall response based on investigator responses, and time to progression.

Pharmacokinetic outcome measures

Serum samples PK assessments were collected on cycle 1 (pre-dose, 1, 4, 24 hr, and day 8); cycles 2 through 6 (pre-dose and 1 hr post-dose); cycle 3 day 8, cycle 7 pre-dose; and every other cycle thereafter pre-dose. PF-8600 concentrations were analyzed using a validated electrochemiluminescence assay.

Pharmacodynamic outcome measures

Whole blood samples for immunophenotyping assessment were collected on cycles 1 through 3 on days 1 and 8, cycles 4 and 7 on day 1, and at the end of treatment. Blood samples were used to assess T-cell receptor clonality, and proliferation and activation rates of CD4+ and CD8+ central memory (CM) and effector memory (EM) T-cells.

Paired tumor biopsies were collected from a subset of patients (dosed ≥ 0.1 mg/kg) at baseline and week 6. Biopsies were used to assess mutational load and % of OX40+ cells, and to perform gene set enrichment analysis.

RESULTS

Patient characteristics

As of the data cutoff of 24th of May 2017, 52 patients were enrolled in the dose escalation phase of the monotherapy (Table 1A), and 42 patients in the combination therapy (Table 1B). For the monotherapy, HCC (37%), melanoma (29%), RCC (17%) and HNSCC (17%) patients were enrolled. Patients were heavily pretreated, with a mean prior therapies was 4.5 [1-21]. In addition, 23% of patients were treated with prior anti-CTLA-4 therapy, and 37% of patients with prior anti PD-1/PD-L1 therapy. For combination therapy, melanoma (29%), bladder (12%), gastric (14%), cervical (10%), NSCLC (10%), and HNSCC (26%) patients were included in the study. The mean prior therapies received in the combination treatment was 3.1 [range 1 – 9], and the majority received prior anti-PD-1/PD-L1 therapy (60%). 24% of patients received prior anti-CTLA-4 in the combination arm.

Safety

The investigated dose levels in this study were 0.01 (monotherapy only), 0.1, 0.3, 1.0 (combination therapy only), 1.5 (monotherapy only), 3.0, and 10.0 (monotherapy only) mg/kg PF-8600, alone or in combination with 20 or 100 mg utomilumab. 58% of patients experienced treatment related AE in the monotherapy, with no apparent relationship to dose (Table 2A). The most commonly reported treatment related AEs occurring in $\geq 5\%$ of patients were fatigue, nausea, vomiting, decreased appetite, headache, influenza like illness, and pruritis. One treatment related grade (G) 3 AE occurred in the 1.5mg/kg cohort, which was a G3 gamma glutamyl transferase elevation. In addition, one serious G2 AE occurred, which was congestive heart failure in the 0.1mg/kg cohort.

Table 1. Patient characteristics of patients treated in the monotherapy [6] (A) and combination therapy [7](B). *Some patients are still on treatment.

A.	PF-8600, mg/kg						Total (N=52)
	0.01 (n=2)	0.1 (n=10)	0.3 (n=11)	1.5 (n=12)	3.0 (n=13)	10 (n=4)	
Age, mean (range), years	52.5 (48-57)	58.2 (40- 79)	52.3 (23- 67)	67.7 (54- 78)	62.0 (45- 75)	60.0 (41-74)	60.0 (23- 79)
Baseline ECOG PS, n							
0	1	6	7	4	6	2	26
1	1	4	4	8	7	2	26
Primary diagnosis, n							
Melanoma	1	2	4	3	4	1	15
HCC	1	6	3	6	3	0	19
RCC	0	2	3	2	2	0	9
HNSCC	0	0	1	1	4	3	9
Prior therapies, mean (range), n	8.0 (2-14)	3.6 (1-14)	5.0 (1-21)	4.9 (1-10)	4.3 (1-12)	3.3 (1-12)	4.5 (1-21)
Anti-CTLA-4, n	1	2	2	3	3	1	12
Anti-PD-1/PD- L1, n	1	3	5	4	3	3	19
Median treatment duration, days (range)*	43.5 (29- 58)	71.5 (27-183)	74.0 (29-296)	50.0 (27-183)	98.0 (1 -225)	50.0 (1 -70)	70 (1-296)

Table 1 continued. Patient characteristics of patients treated in the monotherapy [6] (A) and combination therapy [7](B). ** Chemotherapy regimens excluded.

B.	PF-8600, mg/kg + Utomilumab						Total (N=52)
	0.1 +20 (n=10)	0.3 +20 (n=11)	0.3 + 100 (n=12)	1.0 + 100 (n=13)	3.0 + 100 (n=4)		
Age, mean (range), years	50.5 (22-81)	63.0 (48 -75)	60.6 (38 – 85)	57.3 (45- 70)	68.3 (61- 79)	58.6 (22- 85)	
Baseline ECOG PS, n							
0	4	6	7	3	0	20	
1	6	5	2	4	3	20	
Not reported	1	0	1	0	0	2	
Primary diagnosis, n							
Melanoma	2	4	4	1	1	12	
Bladder	2	1	1	1	0	5	
Gastric	3	1	1	1	0	6	
Cervical	1	0	0	1	0	4	
NSCLC	0	1	1	2	1	4	
HNSCC	3	4	4	1	1	11	
Prior therapies, mean (range), n	3.5 (1-6-)	2.9 (1-9)	3.3 (1-7)	2.9 (1-6)	3.0 (2-4)	3.1 (1-9)	
Anti-CTLA-4, n	2	4	1	1	2	10	
Anti-PD-1/PD-L1, n	4	9	5	4	3	25	
Median treatment duration, days (range)**	154.0 (53- 731)	219.0 (53-731)	110.5 (21- 518)	148.0 (30- 397)	274.0 (85-422)	148.0 (21-808)	

For combination treatment, 35.7% of patients experienced treatment related AEs. The most common related AEs were fatigue (9.5%), and nausea (7.1%). Treatment related AEs were all G1-G2 with the exception of one patient with asymptomatic G3 amylase and G4 lipase elevations (Table 2B). These events occurred at the 0.3mg/kg + 100mg dose level. No discontinuations due to treatment-related AEs occurred.

Overall, treatment with PF-8600 alone or in combination with utomilumab was well-tolerable, with no DLTS occurring in the study, and the maximal tolerated dose (MTD) was not established.

Table 2. AEs observed in the monotherapy (A) [6], and combination therapy [7] (B). *G3 gamma glutamyl transferase elevation. ** G2 congestive heart failure .

A. PF-8600, mg/kg	0.01 (n=2)	0.1 (n=10)	0.3 (n=11)	1.5 (n=12)	3.0 (n=13)	10 (n=4)	Total (N = 52)
All-causality, n %							
Any adverse event	2 (100)	10 (100)	11 (100)	12 (100)	13 (100)	3 (75)	51 (98)
Grade 3 -5 adverse event	1 (50)	5 (50)	2 (18)	5 (42)	9 (69)	2 (50)	24 (46)
Discontinuation due to adverse event	0	1	0	0	0	0	1
Treatment-related, n (%)							
Any adverse event	2 (100)	7 (70)	6 (55)	7 (58)	7 (54)	1 (25)	30 (58)
Grade 3 – 5 adverse event	0	0	0	1 (8)*	0	0	1 (2)
Any serious adverse event	0	1 (10)**	0	0	0	0	1 (2)
Grade 3-5 serious adverse event	0	0	0	0	0	0	0
Discontinuation due to adverse event	0	1	0	0	0	0	0
Dose-limiting toxicity	0	0	0	0	0	0	0

Table 2 Continued. AEs observed in the monotherapy (A) [6], and combination therapy [7] (B). ***G3 AE.

B. PF-8600, mg/kg + Utomilumab (mg)						
	0.1+20 (n=11)	0.3+20 (n=11)	0.3+100 (n=10)	1.0 + 100 (n=7)	3.0 +100 (n=3)	Total (N = 42)
Treatment-related, n (%)						
Any adverse event	3 (27.3)	4 (36.4)	4 (40.0)	2 (28.6)	2 (66.7)	15 (35.7)
Fatigue			2 (20.0)	1 (14.3)	1 (33.3)	4 (9.5)
Nausea	2 (18.2)		1 (10.0)			3 (7.1)
Anaemia		1 (9.1)			1 (33.3)	2 (4.8)
Decreased appetite		2 (18.2)				2 (4.8)
ALT increased		1 (9.1)				1 (2.4)
Amylase increased			1 (10.0)***			1 (2.4)
Constipation			1 (10.0)			1 (2.4)
Cough	1 (9.1)					1 (2.4)
Diarrhea	1 (9.1)					1 (2.4)
Dysgeusia		1 (9.1)				1 (2.4)
Dysphonia		1 (9.1)				1 (2.4)
Flushing	1 (9.1)					1 (2.4)
Lipase increased			1 (10.0)***			1 (2.4)
Pruritus					1 (33.3)	1 (2.4)
Pyrexia					1 (33.3)	1 (2.4)
Rash maculo- papular				1 (14.3)		1 (2.4)
Tumor pain					1 (33.3)	1 (2.4)
Vitiligo				1 (14.3)		1 (2.4)
Vomiting	1 (9.1)					1 (2.4)
Weight decreased		1 (9.1)				1 (2.4)

Clinical activity

In total, 49 patients were evaluable for assessment of best overall response in the monotherapy (Table 3A). Two out of 49 patients showed a confirmed partial response. The partial responses were observed in a melanoma patient treated at the 0.1mg/kg dose level, and a HCC patient treated at the 0.3 mg/kg dose level. Interestingly, the melanoma patient received prior ipilimumab and nivolumab, with mixed response as best response. The HCC patient received sorafenib 6 weeks prior to PF-8600 therapy. The duration of response was 10.3 weeks for the melanoma patient, and 26.1+ weeks for the HCC patient.

Twenty-eight out of 49 patients showed confirmed SD as best response, with a mean duration of stable disease of 11.8 weeks [5.1-37.4+]. Nineteen out of 49 patients showed PD as best response. The median time to tumor progression was 6.3 weeks [5.1 – 37.4+].

In the combination therapy, 37 patients were included in the efficacy analysis (Table 3B). Two patients obtained a partial response; a patient with cutaneous melanoma receiving 0.3 mg/kg PF-8600 and 20mg utomilumab, and a patient with ocular melanoma receiving 0.3mg/kg PF-8600 and 100mg utomilumab. Both patients were still on treatment during the data cutoff, with the cutaneous melanoma patient having a response of 16.1+ weeks, and the ocular melanoma pt having a response of 0.1+ weeks. Eleven (30%) out of 37 patients demonstrated SD as best response, with a duration ranging between 5.3 – 18.1+ weeks. Eighteen patients (49%) showed PD as best response, and four patients were not evaluable. The time to progression ranged from 2.4 weeks to 23.9+ weeks.

Table 3. Best overall response and time to progression for (A) monotherapy[6] and (B) combination therapy[7].

A. PF-8600, mg/kg							
	0.01 (n=2)	0.1 (n=10)	0.3 (n=11)	1.5 (n=12)	3.0 (n=11)	10 (n=3)	Total (N = 49)
Best overall response (n (%))							
Complete response	0	0	0	0	0	0	0
Partial response	0	1 (10)	1 (9)	0	0	0	2 (4)
Stable disease	0	6 (60)	6 (55)	6 (50)	8 (73)	2 (67)	28 (57)
Progressive disease	2 (100)	3 (30)	4 (36)	6 (50)	3 (27)	1 (33)	19 (39)
Duration of response, weeks*		10.3	26.1+				18.2+
Duration of stable disease, median (range), weeks*		11.7 (5.1- 24.1)	17.1 (6.1- 37.4+)	11.7 (5.4 - 37.4+)	12.1 (5.7 - 32.9+)	5.9 (5.9 - 6.0+)	11.8 (5.1 - 37.4+)
TTP, median (range), weeks*	5.8 (5.6- 6.0)	8.9 (5.1- 28.3)	7.6 (5.4- 37.4+)	6.2 (5.4- 37.4+)	11.9 (5.3- 32.9+)	5.9 (5.3- 6.0+)	6.3 (5.1- 37.4+)

Table 3 continued. Best overall response and time to progression for (A) monotherapy[6] and (B) combination therapy[7].

	Tumor type					
	Melanoma (n=10)	HNSCC (n=11)	Gastric (n=5)	Bladder (n=4)	Cervix (n=3)	NSCLC (n=4)
Best overall response (n (%))						
Complete response	0	0	0	0	0	0
Partial response	2 (20.0)	0	0	0	0	0
Stable disease	3 (30.0)	2 (18.2)	2 (40.0)	2 (50.0)	1 (33.3)	1 (25.0)
Progressive disease	4 (40.0)	7 (63.6)	1 (20.0)	2 (50.0)	1 (33.3)	3 (75.0)
Not evaluable	1 (10.0)	2 (18.2)	2 (40.0)	0	1 (33.3)	0
Duration of response, weeks*	3.1* (0.1 16.1+)	–				
Duration of stable disease, median (range), weeks*	9.5 (5.6- 18.1+)	11.7 (5.3- 18.1+)	12.0 (11.9 12.1)	– 8.5 (5.6 – 11.4+)	5.4 (5.4- 5.4)	5.9 (5.9- 5.9)
TTP, median (range), weeks*	11.6 (6.0-18.1+)	6.1 (4.0- 23.9+)	11.9 (5.4- 13.4)	9.6 (6.0- 18.1+)	6.8 (2.4- 11.1)	5.6 (3.9- 5.9+)
*At the last assessment, the max (+) patient still has response/stable disease and remains on study.						

Pharmacokinetics

Preliminary PK characterization was performed based on full cycle 1 PF-8600 concentration-time profiles of 44 patients (Figure 2). At the 0.1mg/kg dose level, PK profiles showed patterns consistent with target-mediated drug disposition, showing concentrations below predicted values. Between the doses of 0.3 and 10 mg/kg, exposure to PF-8600 increased with increasing dose in an approximately dose-proportional manner.

Pharmacodynamics

Peripheral blood

Studies have shown that treatment with immunotherapy has led to a broadening of the T cell receptor repertoire[9]. T-cell receptor sequencing analysis was performed in patients treated in the monotherapy. Clonal expansion of CD4+ and CD8+ T-cells was seen in week 6 compared to baseline (Figure 3B). Patients who achieved PR had among the lowest levels of normalized T-cell clonal expansion in the peripheral blood (Figure 3A), particularly in the CD8+ T-cell populations. Median numbers of expanded clones were similar for patients with SD or PD.

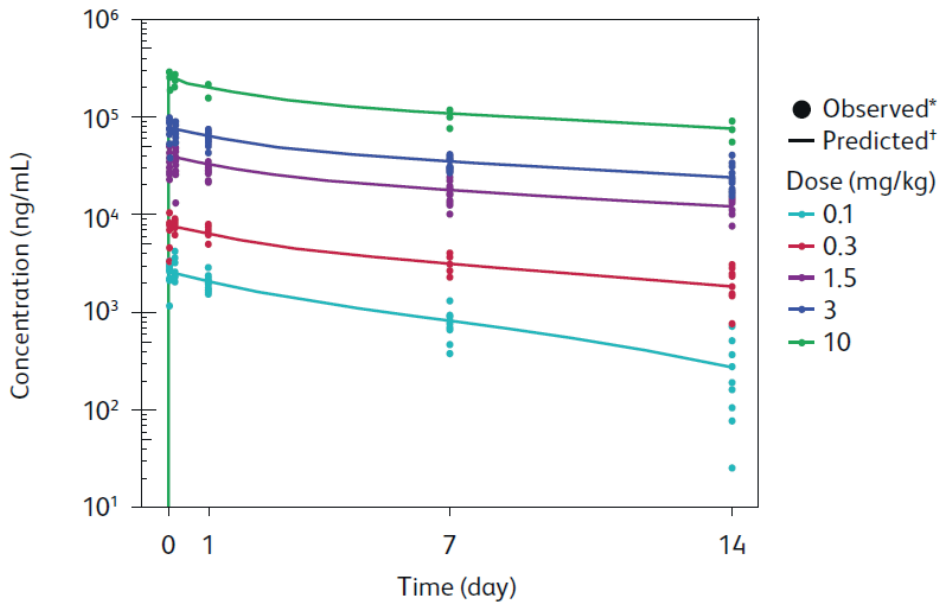


Figure 2. Predicted (lines) and observed (dots) single-dose concentration time profiles after IV infusion of PF-8600 [6].

Flow cytometry analysis using proliferation marker ki67 and activation marker HLA-DR/CD38+ revealed increase in proliferation and activation of CD4+ central memory (CM) in peripheral blood of patients treated with PF-8600 alone and in combination with utomilumab (Figure 4). Interestingly, for monotherapy, the increased proliferation and activation was observed in dose levels 0.1mg/kg, 0.3mg/kg and 3.0mg/kg but not in 1.5mg/kg and 10mg/kg cohorts (Figure 4A). More frequent and greater fold-increases of ki67 were observed in the combination therapy compared with the monotherapy (Figure 4BC). CD8+ cells were relatively unaffected (Figure 4C).

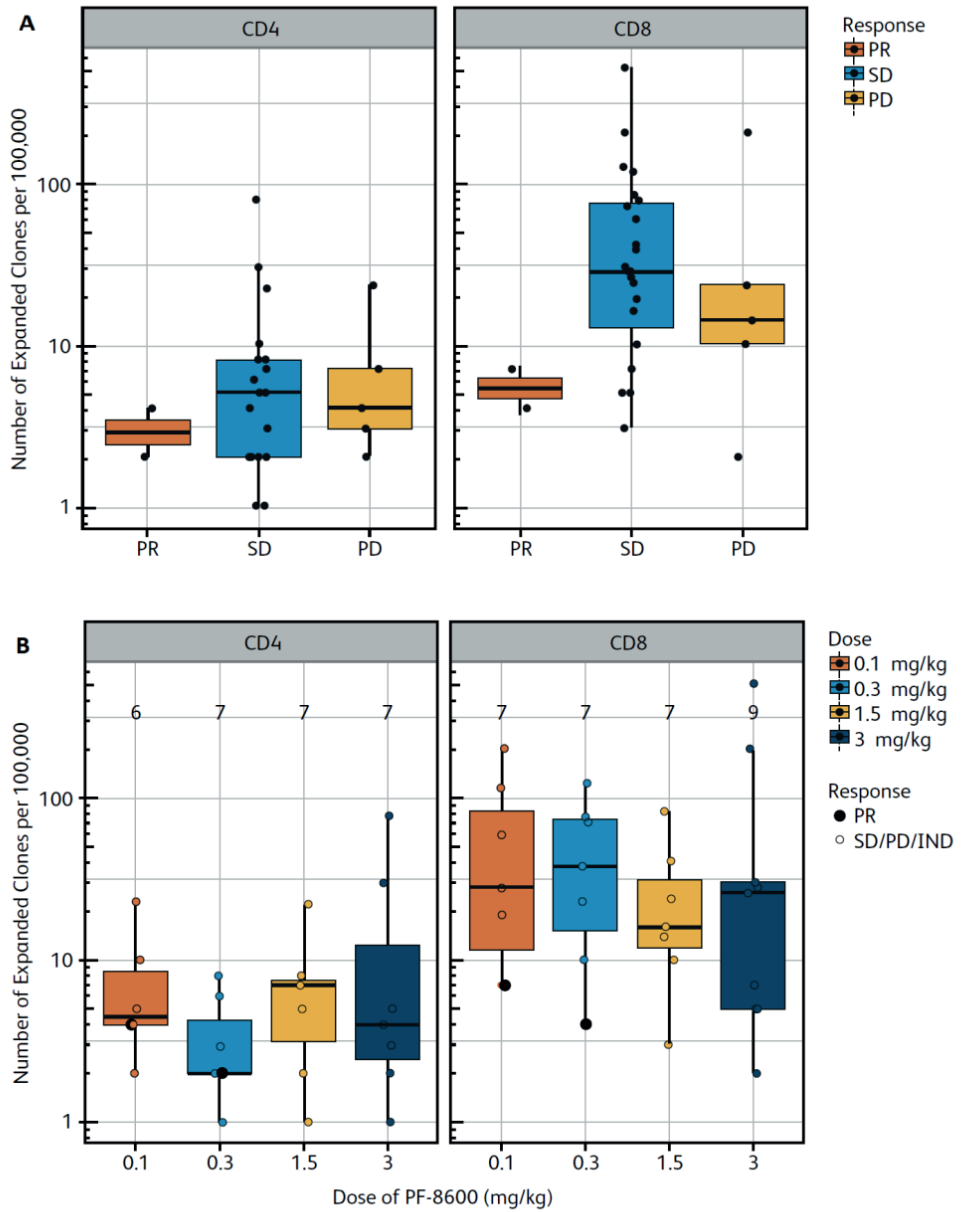


Figure 3. Expansion of peripheral blood T-cell clones, by response (A) and dose (B). Number of patients per dose group is indicated above the box plot.[6].

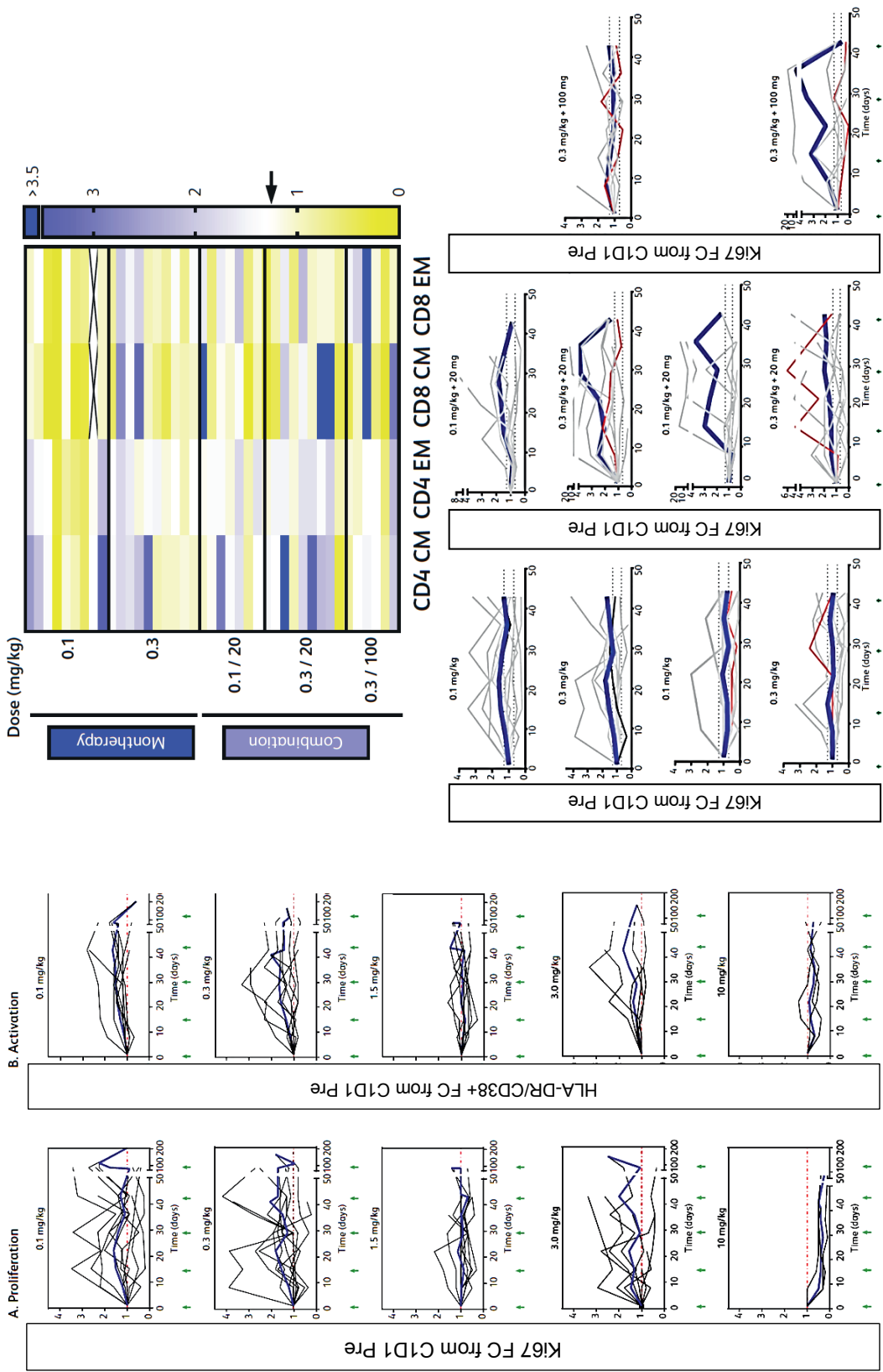


Figure 4. Peripheral changes upon treatment with PF-8600 alone and in combination. The blue line represents the average fold change observed in each cohort. Green arrows indicate dosing (A) Peripheral CD4+ CM T-cell proliferation (a) and activation (b) in the monotherapy [6]. Ki67 is represented as fold-change (FC) compared to baseline. (B) Peripheral CD4+ and CD8+ CM T-cell proliferation by dose in the monotherapy and combination therapy. Red line indicates patients with a PR [7]. (C) peripheral memory T-cell proliferation at study day 15 in the combination therapy [7].

Tumor tissue

Gene set enrichment analysis was performed to identify those pathways and individual genes that are being upregulated upon OX40 treatment (Figure 5). RNAseq data from 8 paired biopsies of patients dosed with ≥ 1.5 mg/kg PF-8600 indicated that gene sets associated with immune activation and inflammation were the most frequently upregulated (Figure 5B). These effects were not observed if samples from lower dose cohorts (0.1 and 0.3 mg/kg) were included in the analysis. Gene sets associated with cell division (mitotic spindle formation), hypoxia, epithelial to mesenchymal transition (EMT), and TGF- β signaling were among the most down-regulated in response to PF-8600 therapy in patients dosed with ≥ 1.5 mg/kg. Individual genes upregulated included markers associated with T cells, the OX40 pathway, and antigen presentation, including CD4, CD8, OX40L, and B2M. The regulatory T cell marker FOXP3 was frequently decreased or unchanged upon treatment (Figure 5A).

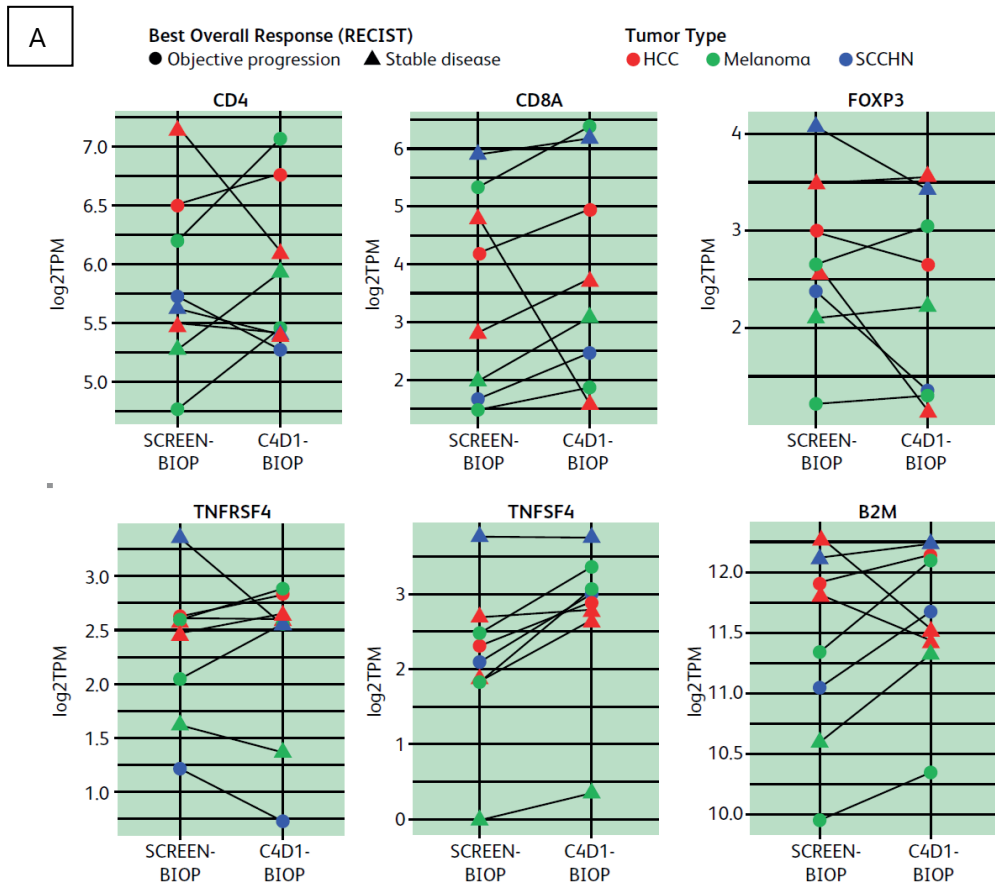


Figure 5. Gene expression changes in tumor tissue in response to PF-8600. Changes in individual genes (A), and gene sets (B)[8].

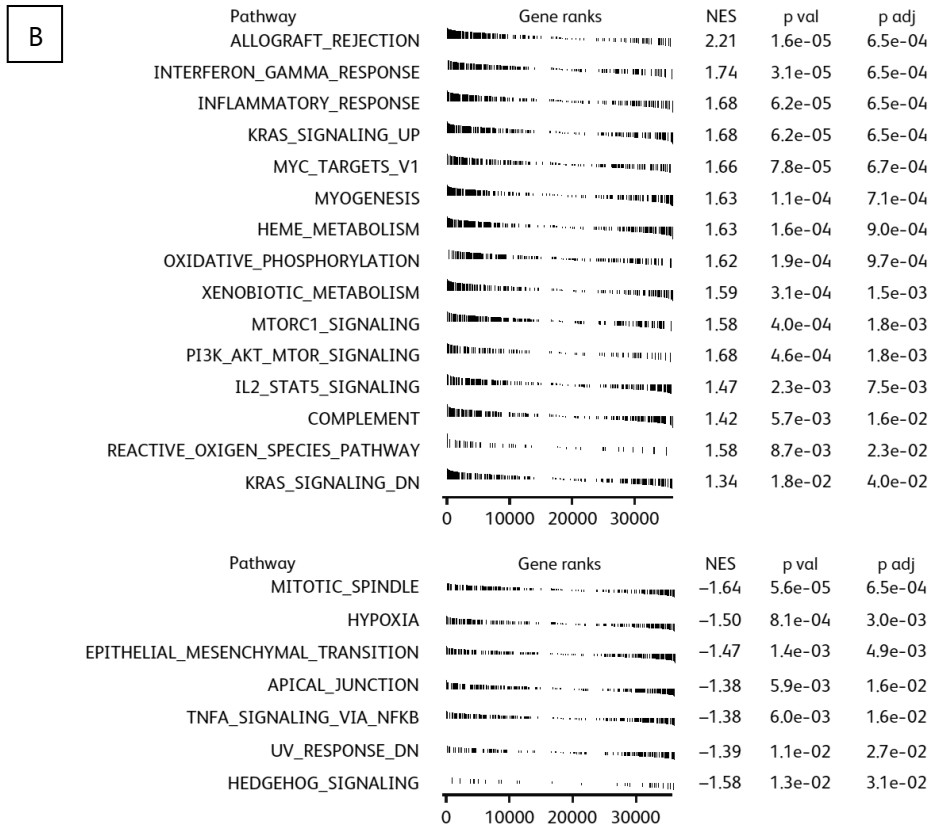


Figure 5 continued. Gene expression changes in tumor tissue in response to PF-8600. Changes in individual genes (A), and gene sets (B)[8].

Studies have shown that tumors with a high mutational burden are more likely to show a response upon treatment with immunotherapy[10]. Mutational burden was derived from tumor RNAseq analysis and revealed no difference in mutational load at baseline between patients having SD as best response and patients with PD as best response (Figure 6). However, the patient (n=1) in this analysis which had PR as best response showed a higher mutational load at baseline compared to those with SD and PD, and in addition showed decrease of mutational burden upon treatment. (Figure 6B).

An increase in percentage of OX40 positive cells is seen in a subset of patients treated with PF-8600 (Figure 7A). In addition, a positive correlation between fold-change in percent OX40-positive cells in the tumor and time to tumor progression (TTP) was observed (n=10) (Figure 7B). This correlation was not observed for CD8, CD4, or FoxP3.

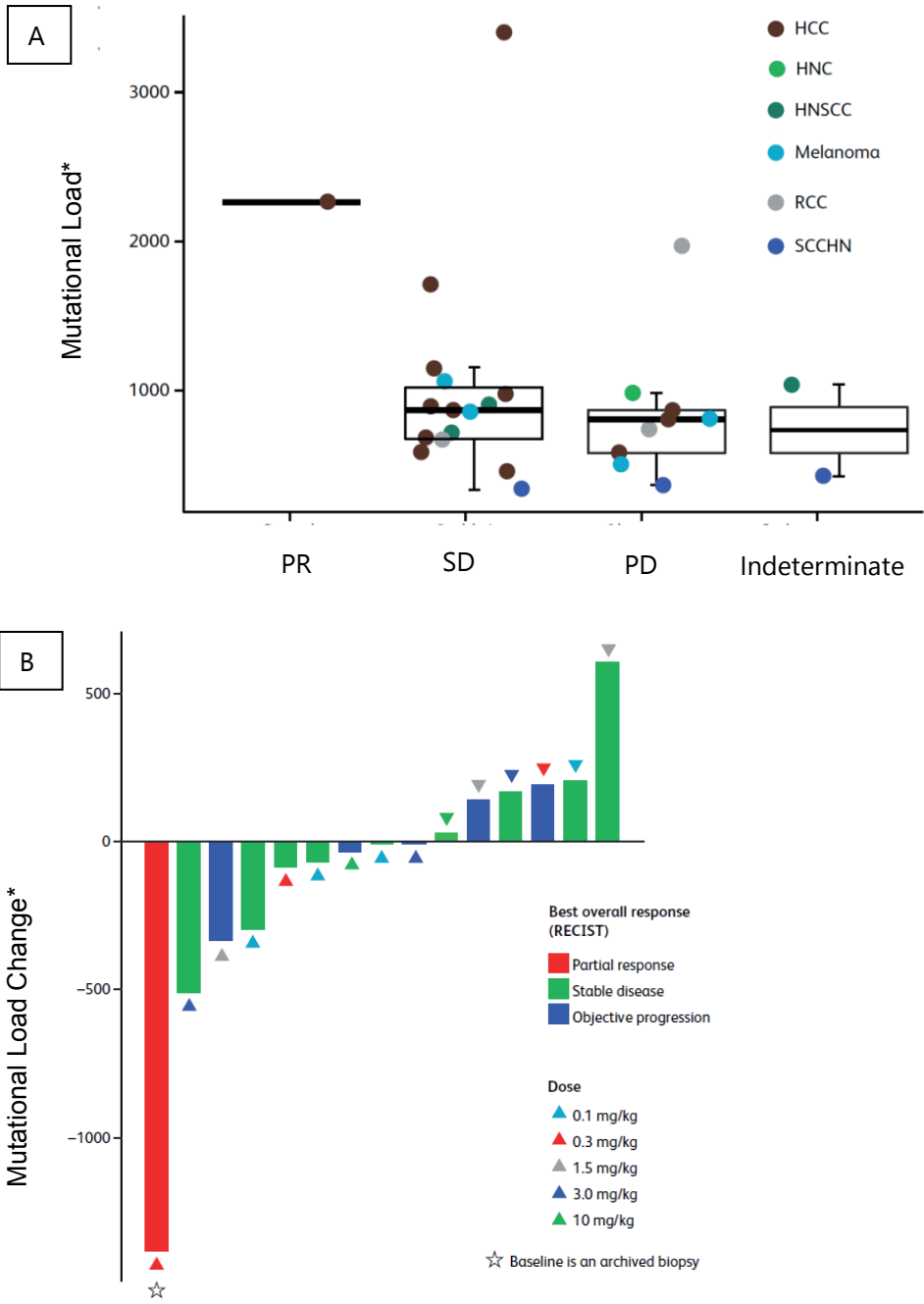


Figure 6. Mutational burden analysis. (A) Mutation burden derived from tumor RNA seq at baseline. (B) Changes in mutation burden derived from tumor RNAseq. * Number of functional mutations in transcripts normalized by library size.

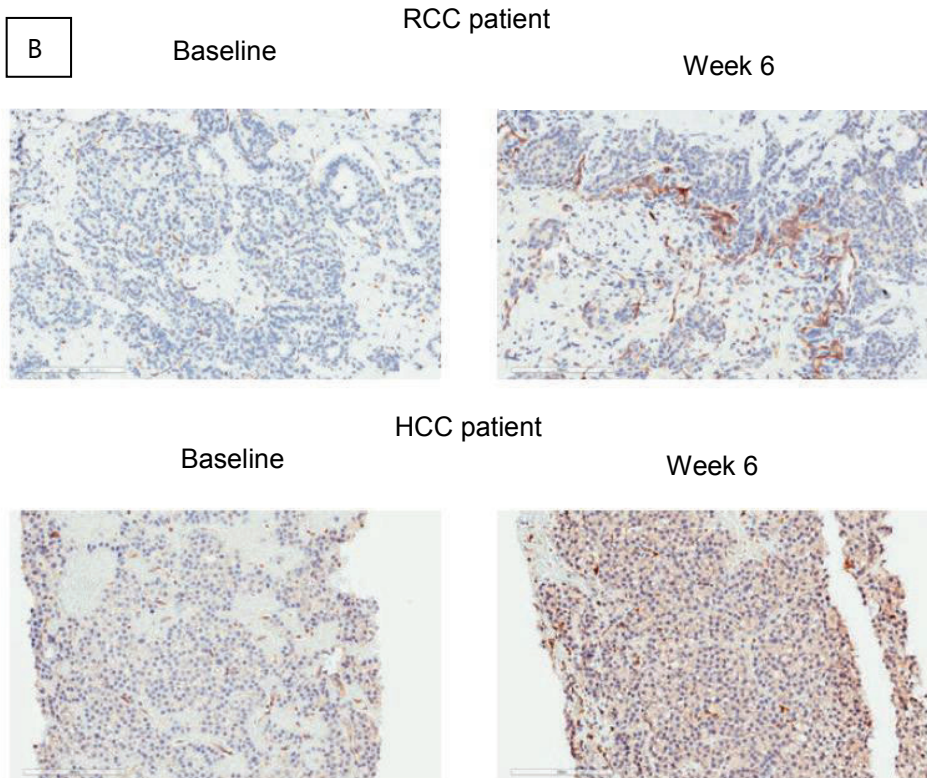
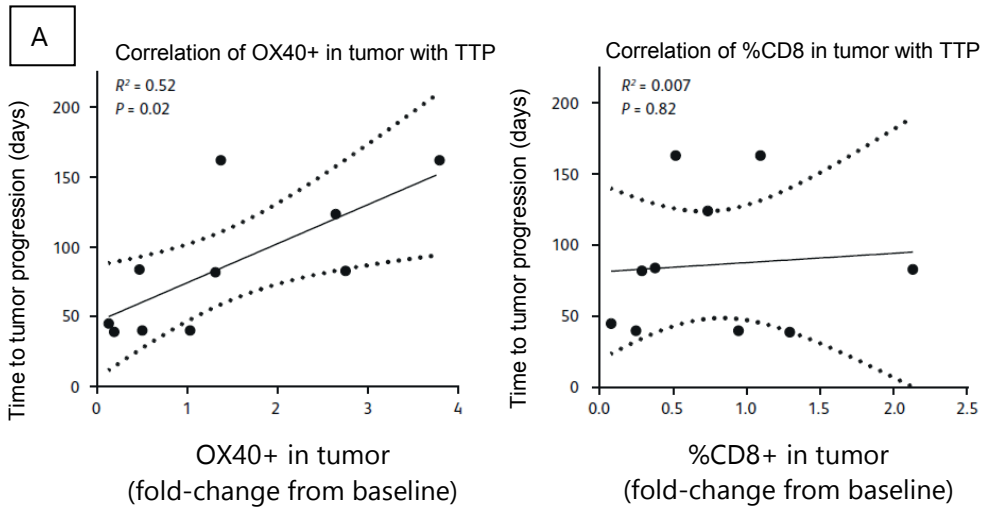


Figure 7. (A) Correlation of change in % OX40-positive cells with time to tumor progression (TTP)[8]. (B) Examples of OX40 positive staining at baseline and week 6 in a renal cell carcinoma patient and an HCC patient.

DISCUSSION AND CONCLUSION

In this chapter we presented preliminary and previously published data from study B0601002. PF-8600 demonstrated to be well-tolerable, both as a single agent and in combination with utomilumab. The MTD was not reached for both monotherapy and combination therapy. Furthermore, the vast majority of treatment-related AEs were of low grade and no dose-limiting toxicities occurred.

PF-8600 showed clinical activity, both as a single agent and in combination with utomilumab. The partial responses were seen in melanoma patients and a HCC patient. It is known that melanoma is a highly immunogenic tumor and the response rates to immunotherapy are relatively high[11–13]. Interestingly, a response to PF8600 was seen in a melanoma patient who showed at best a mixed response to checkpoint blockade therapy. It is of note that this patient received nivolumab seven weeks prior to PF-8600 therapy.

This study employed comprehensive PD analyses. As expected, PF-8600 treatment led to proliferation and activation of CD4+ cells in peripheral blood. Analysis of T-cell receptor clonality revealed that upon treatment, an increase is seen in the amount of T-cell clones. However, the patients which showed a partial response showed smaller numbers of expanded clones compared to those with a SD or PD. A possible explanation for this is that in order to have an effective immune response, it is not the quantity, but the quality of the clones that matter. An anti-tumor response may need the expansion of specific clonal populations which target specific neo-antigens.

Current PD studies are almost impossible to imagine without fresh pre- and on treatment tumor biopsy samples. In this study, tumor tissue was used to perform gene set analyses, characterization of the mutational load, characterization of immune cell subsets in the tumor, and determination of OX40 levels. Gene set enrichment analysis unsurprisingly showed upregulation of inflammatory pathways. However, the pattern of enrichment of inflammatory genes was not observed if samples from lower dose cohorts (0.1 and 0.3 mg/kg) were included in the analysis. A possible explanation for this is that biopsies were collected at least 2 weeks after the last dose. At that time, the lower doses may have not been at sufficient levels to sustain the enrichment of immune-related gene sets at a detectable level. Paradoxically, clinical responses have been observed at lower dose levels, suggesting the hypothesis that persistent enrichment of immune transcripts may not be necessary to elicit antitumor activity. These, and other PD findings will be further evaluated in the dose expansion cohorts of B0601002.

ACKNOWLEDGEMENTS

We thank all patients and their families for participating; Pfizer Incorporated for sponsoring; and the Clinical Pharmacology Department of The Netherlands Cancer Institute for conducting this trial.

REFERENCES

1. Weinberg AD. The role of OX40 (CD134) in T-cell memory generation. *Adv. Exp. Med. Biol.* 2010; 684:57–68.
2. Croft M, So T, Duan W, Soroosh P. The significance of OX40 and OX40L to T-cell biology and immune disease. *Immunol. Rev.* 2009; 229:173–191.
3. Piconese S, Valzasina B, Colombo MP. OX40 triggering blocks suppression by regulatory T cells and facilitates tumor rejection. *J. Exp. Med.* 2008; 205:825–839.
4. Chester C, Sanmamed MF, Wang J, Melero I. Immunotherapy targeting 4-1BB: mechanistic rationale, clinical results, and future strategies. *Blood* 2018; 131:49–57.
5. Lee S-J, Myers L, Muralimohan G et al. 4-1BB and OX40 dual costimulation synergistically stimulate primary specific CD8 T cells for robust effector function. *J. Immunol.* 2004; 173:3002–3012.
6. El-Khoueiry AB, Hamid O, Thompson J et al. The relationship of pharmacodynamics (PD) and pharmacokinetics (PK) to clinical outcomes in a phase I study of OX40 agonistic monoclonal antibody (mAb) PF-04518600 (PF-8600). *J. Clin. Onc.* 2017;35:3027.
7. Hamid O, Ros W, Thompson JA et al. Safety, pharmacokinetics (PK) and pharmacodynamics (PD) data from a phase I dose-escalation study of OX40 agonistic monoclonal antibody (mAb) PF-04518600 (PF-8600) in combination with utomilumab, a 4-1BB agonistic mAb. *Ann. Oncol.* 2017;28: 403-427.
8. Diab A, Hamid O, Thompson JA et al. Pharmacodynamic (PD) changes in tumor RNA expression and the peripheral blood T cell receptor (TCR) repertoire in a phase I study of OX40 agonistic monoclonal antibody (mAb) PF-04518600 (PF-8600). *Cancer Res.* 2018;78: CT010
9. Robert L, Tsoi J, Wang X et al. CTLA4 Blockade Broadens the Peripheral T-Cell Receptor Repertoire. *Clin. Cancer Res.* 2014; 20:2424–2432.
10. Rizvi NA, Hellmann MD, Snyder A et al. Mutational landscape determines sensitivity to PD-1 blockade in non-small cell lung cancer. *Science.* 2015;348:124-128
11. Spranger S, Luke JJ, Bao R et al. Density of immunogenic antigens does not explain the presence or absence of the T-cell–inflamed tumor microenvironment in melanoma. *Proc. Natl. Acad. Sci.* 2016;113:7759–7768.
12. Weber JS, D’Angelo SP, Minor D et al. Nivolumab versus chemotherapy in patients with advanced melanoma who progressed after anti-CTLA-4 treatment (CheckMate 037): a randomised, controlled, open-label, phase 3 trial. *Lancet Oncol.* 2015; 16:375–384.
13. Wolchok JD, Neyns B, Linette G et al. Ipilimumab monotherapy in patients with pretreated advanced melanoma: a randomised, double-blind, multicentre, phase 2, dose-ranging study. *Lancet Oncol.* 2010; 11:155–164.

Chapter 2.3

Preliminary efficacy and safety of CD40 agonistic monoclonal antibody selicrelumab administered in combination with atezolizumab or vanucizumab.

An interim analysis of BP29392 and BP29889 of patients treated at the Netherlands Cancer Institute.

Willeke Ros

Preliminary data of study BP29889 has been presented at the Society of Immunotherapy for Cancer (SITC) Annual Congress 2018:

Emiliano Calvo, Jan Schellens, Ignacio Matos, Elena Garralda, Morten Mau-Soerensen, Aaron Hansen, Maria Martinez-Garcia, Martijn Lolkema, Jehad Charo, Chiara Lambertini, Christoph Mancao, Katrijn Bogman, Cristiano Ferlini,, Martin Sern, **Ros W.** Combination of subcutaneous selicrelumab (CD40 agonist) and vanucizumab (anti-Ang2/VEGF) in patients with solid tumors demonstrates early clinical activity and a favorable safety profile.

Journal for ImmunoTherapy of Cancer 2018;115:386

ABSTRACT

Background: Targeting CD40 is a novel immunotherapeutic approach to combat cancer. CD40 is a co-stimulatory receptor molecule which is mainly expressed by antigen presenting cells. CD40 engagement by its ligand leads to increased proliferation, effector function and survival of T-cells, and increases anti-tumor activity. Selicrelumab is a monoclonal antibody that binds agonistically to CD40, thereby activating the CD40 pathway.

Methods: BP29392 (NCT02304393) and BP29889 (NCT02665416) investigated selicrelumab in combination with atezolizumab and vanucizumab respectively. Both studies were open-label, non-randomized multicenter phase I dose escalation studies designed to evaluate the safety, tolerability, pharmacokinetics, pharmacodynamics and therapeutic activity of selicrelumab in combination with aforementioned antibodies. Here, we present interim results of patients treated at the Netherlands Cancer Institute.

Results: Between April 2016 and August 2018, seventeen (selicrelumab plus atezolizumab) and eleven (selicrelumab plus vanucizumab) patients were enrolled. Both combinations showed a favorable safety profile, and the maximal tolerated dose was not reached. The most common adverse event (AE) related to treatment was injection site reactions (ISR) to the subcutaneous administration of selicrelumab. This toxicity was manageable when treated with topical (G2 ISR) or oral (G3 ISR) corticosteroids. Other common AEs included ASAT/ALAT increase, fatigue, fever and headache. No patient discontinued due to treatment-related AEs. One ISR was considered a dose limiting toxicity. Three (11.8%) and one (9.1%) patient showed a partial response for selicrelumab plus atezolizumab, and selicrelumab plus vanucizumab respectively. Antitumor activity was seen in a microsatellite instability-high colorectal cancer patient and a patient with squamous cell carcinoma of unknown origin (selicrelumab plus atezolizumab), and an ovarian cancer patient (selicrelumab plus vanucizumab).

Conclusions: Selicrelumab in combination with vanucizumab or atezolizumab showed a favorable safety profile and was well-tolerated. Preliminary clinical activity was observed in three out of twenty-eight patients.

INTRODUCTION

CD40 is a co-stimulatory receptor molecule belonging to the tumor necrosis factor (TNF) receptor superfamily. It is expressed on antigen presenting cells (APCs), such as dendritic cells (DCs), B-cells and monocytes, as well as on non-immune cells and a wide range of tumor cells[1–3]. Its ligand is CD154 (also known as CD40-L), and is primarily expressed by CD4+ helper T cells. Signaling through CD40 is one of the main components of T-cell help. It activates APCs and increases the expression of other co-stimulatory molecules and MHC molecules, as well as the production of pro-inflammatory cytokines[4]. Indeed, targeting CD40 has the potential to be an effective way to combat cancer. Triggering CD40 with an agonistic monoclonal antibody (mAb) can substitute for stimulation normally provided by helper T cells via CD154[5]. Although the main anti-tumor effects triggered by agonistic binding by a mAb are thought to be due to activating APCs, other immunological antitumor effects independent of T-cells have been proposed as well. For example CD40 activated macrophages can exert antitumor effects[6–8]. The exact effects of CD40 signaling differ depending on the cell type expressing CD40 and the microenvironment in which the signaling is taking place.

Due to its favorable immunological impact, CD40 has become an attractive target for cancer immunotherapy. Monoclonal antibodies targeting CD40 or its ligand are currently under development[9]. One of them is selicrelumab (RO7009789), a fully human IgG2 antibody which binds agonistically to CD40. It started its development under the name CP-870893, and has been evaluated as a single agent during a phase I clinical trial (clinicaltrials.gov identifier NCT02225002)[10]. Here, selicrelumab was given intravenously in doses ranging from 0.01 to 0.3 mg/kg and the maximal tolerated dose (MTD) was established as 0.2 mg/kg. Dose limiting toxicities included venous thromboembolism and headache. Partial responses were exclusively seen in melanoma patients (14% of all patients and 27% of melanoma patients). Selicrelumab is further being investigated as a combination partner for several other anti-cancer agents. For example, it has been combined with gemcitabine for the treatment of pancreatic ductal adenocarcinoma[11]. In this study, four out of 22 patients (19%) achieved a partial response.

Two potential candidates for combination treatment with selicrelumab are the anti-PD-L1 agent atezolizumab, and vanucizumab, a bispecific monoclonal antibody targeting ANG2 and VEGF.

Atezolizumab blocks the binding of checkpoint inhibitor PD-1 with its ligand PD-L1. CD40 activation ultimately leads to T-cell activation and subsequently PD-L1 expression[12–14]. This upregulated expression of PD-L1 may inhibit the activated T-cells and make them anergic[15]. By inhibiting PD-L1 with atezolizumab, the negative feedback loop of PD-L1 may be nullified, making T-cell responses more durable. Alternatively, atezolizumab may benefit from selicrelumab as well. Checkpoint blockade is thought to stimulate ongoing immune responses, but it is incapable of starting novel immune responses[12, 16]. Agonistic binding of CD40 may trigger novel immune responses by DC stimulation, which in return leads to priming of T-cells.

The rationale of combining selicrelumab with vanucizumab is that it may lead to novel immune cell infiltration through normalization of the tumor neovasculature[17]. CD40 signaling triggers angiogenesis by inducing the expression of both VEGF and Ang-2, two pro-angiogenic molecules produced by the endothelium, tumors and tumor-associated macrophages[18]. These proangiogenic molecules cause aberrant expression of various integrins and chemokines in the tumor microenvironment, which in return prevents proper trafficking of T-cells into tumor tissue[19, 20]. By blocking these two factors using vanucizumab, the angiogenic reaction in response to CD40 signaling is reduced. The blocking of angiogenic factors further benefits CD40 signaling, as VEGF expression is a negative feedback loop for CD40 signaling: VEGF inhibits dendritic cell maturation, and induces regulatory T-cells and checkpoint inhibitors[21–23].

In this interim analysis, we evaluated the safety, efficacy and pharmacological effects of selicrelumab in combination with atezolizumab (NCT02304393) and vanucizumab (NCT02665416). Both studies are open-label, multi-center phase I dose escalation studies. We discuss the patients treated at the Netherlands Cancer Institute/Antoni Van Leeuwenhoek Ziekenhuis (NKI/AvL) between January 2015 and August 2018.

METHODS

Study Design

BP29392 (NCT02304393) and BP29889 (NCT02665416) investigated selicrelumab in combination with atezolizumab and vanucizumab respectively. Both studies were open-label, non-randomized multicenter dose escalation phase I studies. Here, we describe the interim results of part IA, IB, and II for BP29392 and part I for BP29889. The primary objectives of part I of the studies were to evaluate the safety and tolerability of selicrelumab in combination with atezolizumab or vanucizumab, and to determine the maximal tolerated dose (MTD) or optimal biological dose (OBD) and recommended phase II dose of the combinations. The primary objectives of part II of BP29392 were to evaluate the clinical activity in head and neck squamous cell carcinoma (HNSCC), non-small cell lung cancer (NSCLC) and small and large bowel carcinoma. Secondary objectives were pharmacokinetics (PK), pharmacodynamics (PD) and immunogenicity. For BP29392, different regimens were assessed (Figure 1). For Part 1A, selicrelumab and atezolizumab were given sequentially: a single dose of selicrelumab was given on day 1 of treatment, followed by atezolizumab three weeks later. Atezolizumab was given q3W. For Part IB: selicrelumab and atezolizumab were given concomitantly: on day 1, atezolizumab was given, q3W. On day 2, a single dose of selicrelumab was given. For part II, multiple doses of selicrelumab were given. A cycle consisted of three weeks. Atezolizumab was given q3W on day 1 of every cycle. For the first four administrations, selicrelumab was given q6W, on day 2 of every odd cycle. After these administrations, selicrelumab was given q12W on day two. For BP29889, a single regimen was tested (Figure 1): vanucizumab was given on day 1 and 15, q2W, and selicrelumab was given q4W during the first eight weeks, followed by q12W administration of selicrelumab.

The starting dose of selicrelumab for both studies was 1mg. At least three patients were enrolled in each cohort. The dose limiting toxicity (DLT) assessment window was 43 days (part IA, BP29392), 22 days (part IB, BP29392), or 28 days (BP29889). Dose escalation was guided with a modified continual reassessment method (mCRM)- escalation with overdose control (EWOC). After each cohort of patients, the model was updated and the proposed dose was based on the logistic regression model.

In BP29392, a DLT was defined as one of the following toxicities: drug-related \geq grade (G) 3 febrile neutropenia, \geq G3 thrombocytopenia with G2 bleeding episodes and/or requiring at least 1 platelet transfusion, G4 neutropenia lasting \geq 7 days, Any \geq G3 hepatic toxicity with the exception if it consists of asymptomatic transaminase elevation $<8 \times$ ULN without bilirubin elevation, inability to re-treat the patient within 3 weeks of scheduled dosing because of lack of recovery to \leq G1 toxicity that is related to the study drug, and any \geq G3 non-hematologic or non-hepatic major organ adverse event excluding the following: G3 nausea or vomiting that resolves to \leq G1 within 72 hours of appropriate supportive therapy, \geq G3 fatigue that resolves to \leq G2 within 7 days, G3 arthralgia that can be adequately managed with supportive care or that resolves to \leq G2 within 7 days, G3 fever (in the absence of any clinically significant source of fever) that resolves to \leq G2 within 7 days with supportive care, \geq G3 laboratory abnormality that is asymptomatic and deemed by the investigator not to be clinically significant, G3 tumor flare defined as local pain, irritation, or rash localized at sites of known or suspected tumor, G3 infusion reaction that resolves within 12 hours to \leq G1.

In BP29889, a DLT was defined as one of the following toxicities: drug-related \geq G3 febrile neutropenia, \geq G3 thrombocytopenia with G2 bleeding episodes and/or requiring at least 1 platelet transfusion, G3 hypertension, for > 14 consecutive days, despite appropriate anti-hypertensive medication, \geq G3 thromboembolic event, \geq G2 bronchopulmonary hemorrhage, \geq G1 intracranial hemorrhage, \geq G1 reversible posterior leukoencephalopathy syndrome (RPLS), proteinuria ≥ 2 g/24 hrs for ≥ 14 days, \geq G3 proteinuria, Any \geq G1 fistula formation involving an internal organ, and any other G3 selicrelumab or vanucizumab-related toxicity which fails to revert to \leq G1 or baseline within 4 weeks despite adequate medical therapy, with the exception of \geq G3 toxicities which are judged not clinically significant by the Investigator, transient (<10 days) lymphopenia, \geq G3 skin toxicity in the absence of adequate supportive care, alopecia (any grade)

Patients

BP29392 and BP29889 were designed to examine the safety, tolerability and maximal tolerated dose of selicrelumab in combination with atezolizumab and vanucizumab respectively, in patients with advanced solid tumors. For part I in BP29392 and BP29889, all solid tumor types (with the exception of non-small cell lung cancer (NSCLC) and prostate cancer for BP29889) were eligible. Preclinical studies have shown that a wide array of tumors may respond to anti-CD40 treatment, independently of CD40 expression on tumor cells[24]. For part II in BP29392, eligible tumors types were head and neck squamous cell carcinoma (HNSCC), NSCLC, colorectal cancer (CRC) and small bowel carcinoma. These tumor types were selected based on preliminary efficacy findings in part I.

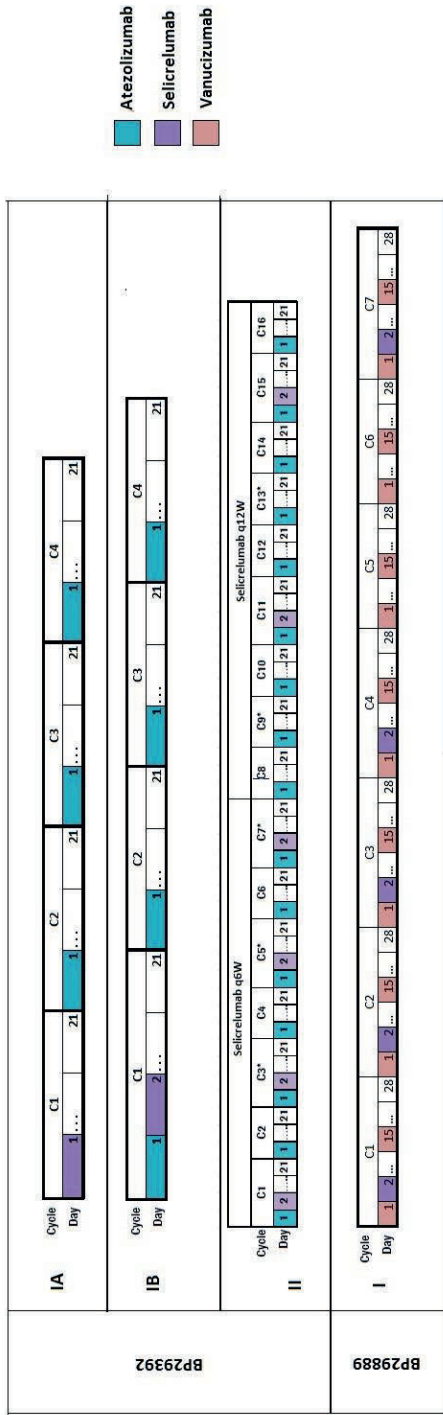


Figure 1. Dosing schema of BP29392 and BP29889.

Key eligibility requirements included having histologically or cytologically-documented advanced metastatic and/or unresectable solid cancer that was not amenable to standard therapy; for part II of BP29392 only: histologically confirmed diagnosis of advanced/metastatic small or large bowel carcinoma, HNSCC or non-squamous NSCLC previously treated with anti-PD-L1 / PD-1 inhibitor (Part II); Life expectancy \geq 16 weeks; \geq 18 years of age, adequate hematologic and organ function; for BP29889 only: adequate cardiovascular function; measurable disease based on response evaluation criteria in solid tumors (RECIST) V1.1.; Eastern Cooperative Oncology Group (ECOG) Performance Status (PS) of 0 or 1 (or 2 for BP29889 only); ability to comply with the collection of tumor biopsies.

Key exclusion criteria included: prior approved anti-cancer therapy (including chemotherapy, hormonal therapy or radiotherapy) within two weeks prior to initiation of study treatment (BP29392 only); patients who had received cyclical chemotherapy within a period of time that is shorter than the cycle length used for that treatment prior to study drug administration (BP29889 only); prior biologic, systemic immunostimulatory, or investigational therapy within four weeks prior to initiation of study treatment; patients with prostate cancer or squamous NSCLC (BP29889 only); soluble CD25 \geq 2x ULN or serum ferritin \geq 1000 ng/mL within 14 days prior to the first study treatment (BP29392 only); previous treatment with compounds targeting CD40; treatment with systemic immunosuppressive medications within two weeks prior to initiation of study treatment; uncontrolled pleural effusion, pericardial effusion, or ascites; known clinically significant liver, lung, vascular, cardiovascular or cerebrovascular disease; prior history of hypertensive crisis (BP29889 only); allergy or hypersensitivity to components of the selicrelumab, atezolizumab (BP29392) or vanucizumab (BP29889) formulation; history of autoimmune diseases.

The study was conducted according to protocol, Good Clinical Practice standards, and provisions outlined in the Declaration of Helsinki. The study protocol and all amendments were approved by the appropriate institutional review board and ethics committee. All patients provided written informed consent before any study related procedures were performed.

Treatment and assessments

Selicrelumab was administered subcutaneously (s.c.). Atezolizumab and vanucizumab were given in a fixed dose of 1200mg and 2000mg respectively. Atezolizumab was given intravenously over 60 minutes, whereas vanucizumab was given over 90 minutes.

Tumor imaging was done every six (BP29392) or eight (BP29889) weeks using CT or MRI. Adverse events were monitored throughout the study period and graded according to the National Cancer Institute's Common Terminology Criteria for Adverse Events (CTCAE v4.03)

Table 1. Patient characteristics.

Demographic characteristic	Selicrelumab plus atezolizumab Total (n=17)	Selicrelumab plus vanucizumab Total (n=11)
Age (Years)	57 [26 – 81]	56 [30 - 70]
Gender (n,%)		
Male	8 (47.1%)	4 (36.4%)
Female	9 (52.9%)	7 (63.6%)
WHO PS (%)		
0	14 (82.4%)	6 (54.5%)
1	3 (17.6%)	5 (45.5%)
Tumor Type (n)		
CRC	6	3
H&N	4	2
Ewing sarcoma	2	
Ovarian Cancer	1	3
Squamous cell carcinoma of unknown origin	1	-
Esophageal Cancer	1	-
Gallbladder Cancer	1	-
Pancreas Cancer	1	-
Cervical cancer	-	2
Urachus Cancer	-	1
Prior lines of therapy for advanced disease	2 [0 – 9]	3 [1-6]

Outcomes

The safety outcome measures for this study included the nature and frequency of DLTs, the incidence, nature and severity of adverse events graded according to the NCI CTCAE v4.03, and changes in vital signs, physical findings, ECG and clinical laboratory results during and following selicrelumab, vanucizumab, and atezolizumab administration. Safety measures not discussed in this interim analyses but were performed included incidence of ADA responses to selicrelumab, vanucizumab and atezolizumab, and possible correlation with PK, PD, safety and efficacy parameters.

Efficacy outcome measures included best confirmed; duration of objective response was defined as time from the first occurrence of a documented objective response to the time of relapse or death from any cause. Progression-free survival (PFS) was defined as the time from the first study treatment to the first occurrence of progression or death, whichever occurred first. Overall survival (OS) was defined as the time from the first study treatment to death. Patients who are not evaluable for efficacy analysis were treated as non-responders. An efficacy outcome not described in this interim analysis but was performed

included model-based estimates of tumor growth inhibition (TGI) metrics defined as deviations due to the study drugs on the kinetic curve of the tumor.

PK and PD outcomes are not discussed in this interim analysis but are performed in both studies. PK outcome measures included the area under the curve (AUC), C_{max}, C_{min}, T_{max}, clearance (CL), volume of distribution (V_d), and elimination half-life ($t_{1/2}$) of selicrelumab; AUC, C_{max}, CL, (V_d) and $t_{1/2}$ of vanucizumab; and the C_{max} and C_{min} of atezolizumab. PD outcome measures included monitoring of the number and percentage of T, B, natural killer cells, naïve and memory T cells, monocytes, activated and exhausted T cells and Treg cells in peripheral blood, *quantification of the levels of free and total soluble VEGF and Ang2 (BP29889 only)*. CD8+ cell tumor-infiltration levels in baseline and on-treatment tumor biopsy, PD-L1 expression levels on both tumor and immune-infiltrating cells in baseline and on-treatment tumor biopsy, *microvessel density, proliferation, apoptosis and hypoxia in baseline and on-treatment tumor biopsy (BP29889 only)*, monitoring of cytokines and sCD25 in the peripheral blood, identification of pro- versus anti-inflammatory immune gene expression signatures (in blood or tumor tissue), immune cell population-specific gene transcripts or T-cell receptor deep sequencing, TCR V β repertoire assessment and gene expression to define immune signature.

Statistical analysis

Safety was assessed in patients who received ≥ 1 dose of selicrelumab and were summarized using descriptive statistics. The Kaplan–Meier method was used to estimate PFS, OS, and DOR. The data cutoff date for this report was 23rd of August 2018.

RESULTS

Baseline Patient Characteristics

Between April 2016 and August 2018, seventeen patients were enrolled in BP29392 and eleven patients in BP29889 (Table 1). At the time of study initiation at the NKI/AvL, the dose level of 2mg selicrelumab was reached in BP29889, whereas for BP29392 the NKI/AvL started at the 1mg selicrelumab dose level. Included tumor types for BP29392 were colorectal cancer (CRC), HNSCC, Ewing sarcoma, gallbladder cancer, pancreatic cancer, esophageal cancer and squamous cell cancer of unknown origin (Table 2). Included tumor types for BP29889 were CRC, head and neck (H&N), ovarian cancer, cervical cancer and urachus cancer. The median age was 57 years [26- 81] and 56 years [30-70] for BP29392 and BP29889 respectively; the median lines of prior therapy for advanced disease was 2 [0 – 9] and 3 [1-6] for BP29392 and BP29889 respectively; 47.1% and 36.4% of patients were male for BP29392 and BP29889 respectively; and 82.4% and 54.5% had an ECOG performance status of 0 for BP29392 and BP29889 respectively.

Table 2 Overview of tumor type and treatment per individual patient.

	Pt No.	Tumor Type	Dose Selicrelumab (mg)	Part of study
Selicrelumab plus atezolizumab	11200	Esophageal Cancer	1	IA
	12200	CRC	2	IA
	12201	CRC	2	IA
	13200	Ewing sarcoma	16	IA
	15200	H&N	1	IB
	17200	CRC	4	IB
	19200	Gallbladder Cancer	9	IB
	20200	Pancreas Cancer	12	IB
	31200	Ewing sarcoma	21	IB
	31201	CRC	21	IB
	33200	SCC, two	36	IB
	34200	Ovarian	48	IB
	60200	CRC	16	II
	60201	CRC	16	II
	60202	H&N	16	II
60203	H&N	16	II	
60204	H&N	16	II	
	Pt No.	Tumor Type	Dose Selicrelumab (mg)	
Selicrelumab plus vanucizumab	1250	CRC	2	
	1251	Cervix	8	
	1252	H&N	12	
	1253	H&N	14	
	1254	CRC	18	
	1255	Ovary	24	
	1256	Ovary	32	
	1257	CRC	48	
	1258	Cervix	64	
	1259	Urachus	40	
	1260	Ovary	40	

Dose Escalation

The dose-levels investigated in this interim analysis included 1, 2, and 16 mg selicrelumab for BP29392 part IA; 1, 4, 9, 12, 21, 36, 48 mg selicrelumab for BP29392 part IB; 16 mg mg selicrelumab for BP29392 part II; and 2, 8, 12, 14, 18, 24, 32, 48, 64 and 40 mg selicrelumab for BP29989.

Safety

Seventeen patients (100%) experienced treatment related AEs in BP29392, and ten patients (90.1%) experienced treatment related AEs in BP29889. The most common AEs related to selicrelumab treatment were injection site reactions (ISR), which were observed in 15 (88.2%) and 10 (90.9%) patients in BP29392 and BP29889 respectively (Table 3). The injection site reaction typically consisted of redness, itching, pain, and swelling. The reaction started four to five days after the subcutaneous administration and lasted approximately a week. The reaction was manageable when treating with topical corticosteroid cream and paracetamol (for G2 ISRs), or oral prednisone (for G3 ISRs). The reaction was often recurrent but less severe in subsequent cycles. Because the administration of higher doses was divided over multiple injections, the severity of the ISR did not differ across dose levels (Supplementary Table 1 and 2).

One DLT occurred in BP29392. This DLT was a G3 ISR in a patient receiving one mg selicrelumab (Figure 2). The ISR started forming three days after the injection. Five days after the injection, the ISR was deemed a G3 reaction, due to the patient being in severe pain and the subcutaneous forming of immune infiltrates. The patient was treated with 10mg oral prednisone and fully recovered from the ISR 15 days after the injection.

Other common AEs included ASAT/ALAT increase (35.3% for BP29392 and 18.1% for BP29889), fatigue (52.9% for BP29392 and 36.4% for BP29889), fever (29.4% for BP29392 and 54.54% for BP29889) and headache (17.6% for BP29392 and 45.4% for BP29889).

G3-4 AEs observed in the studies include G3 ISR (selicrelumab; n = 1), platelet count decrease (selicrelumab; n =1), ASAT and ALAT increase (selicrelumab, vanucizumab, atezolizumab; n = 4), hypertension (selicrelumab, vanucizumab; n = 5), increased serum amylase (vanucizumab; n = 1), and increased lipase (vanucizumab; n = 1). Severity and frequency of AEs was similar across dose levels (Supplementary Table 1 and 2).

Table 3. AEs at least possibly related to study treatment (A) toxicities observed in BP29392. (B) toxicities observed in BP29989

A. Selicrelumab plus atezolizumab			
Toxicities related to Selicrelumab	G1 - 2, n (%)	G3- 4 n (%)	Total, n (%)
ALAT increase	4 (23.6%)		4 (23.6%)
ASAT increase	4 (23.6%)		4 (23.6%)
Diarrhea	2 (11.8%)		2 (11.8%)
Fatigue	2 (11.8%)		2 (11.8%)
Fever	4 (23.6%)		4 (23.6%)
Flu like symptoms	1 (5.8%)		1 (5.8%)
Hematuria	1 (5.8%)		1 (5.8%)
Injection site reaction	14 (82.4%)	1 (5.8%)	15 (88.2%)
Myalgia	1 (5.8%)		1 (5.8%)
Platelet count decrease		1 (5.8%)	1 (5.8%)
Toxicities related to Atezolizumab	G1 - 2, n (%)	G3- 4 n (%)	Total, n (%)
ALAT increase	2 (11.8%)		2 (11.8%)
ASAT increase	2 (11.8%)		1 (5.8%)
Colitis	1 (5.8%)		1 (5.8%)
Dry skin	1 (5.8%)		1 (5.8%)
Dyspnea	1 (5.8%)		2 (11.8%)
Fatigue	1 (5.8%)		2 (11.8%)
Fever	1 (5.8%)		2 (11.8%)
Flu like symptoms	3 (17.6%)		1 (5.8%)
Flushing	1 (5.8%)		1 (5.8%)
GGT increase	2 (11.8%)		1 (5.8%)
Headache	1 (5.8%)		1 (5.8%)
Infusion reaction	3 (17.6%)		3 (17.6%)
Malaise	1 (5.8%)		3 (17.6%)
Mucositis	1 (5.8%)		1 (5.8%)
Myalgia	2 (11.8%)		1 (5.8%)
Nausea	1 (5.8%)		1 (5.8%)
Neutrophil count decrease	1 (5.8%)		1 (5.8%)
Pain	1 (5.8%)		1 (5.8%)
Productive cough	1 (5.8%)		1 (5.8%)
Rash maculopapular	1 (5.8%)		1 (5.8%)
Toxicities related to either	G1 - 2, n (%)	G3- 4 n (%)	Total, n (%)
ALAT increase	1 (5.8%)	2 (11.8%)	3 (17.6%)
Alopecia	1 (5.8%)		1 (5.8%)
Anorexia	1 (5.8%)		1 (5.8%)
ASAT increase	1 (5.8%)	1 (5.8%)	2 (11.8%)
Chills	1 (5.8%)		1 (5.8%)
Diarrhea	1 (5.8%)		1 (5.8%)
Dry mouth	1 (5.8%)		1 (5.8%)
Ear pain	1 (5.8%)		1 (5.8%)
GGT increase	2 (11.8%)		2 (11.8%)
Headache	2 (11.8%)		2 (11.8%)
Nausea	3 (17.6%)		3 (17.6%)
Neutrophil count decrease	1 (5.8%)		1 (5.8%)
Pain	1 (5.8%)		1 (5.8%)
Palmar-plantar erythrodysesthesia syndrome	1 (5.8%)		1 (5.8%)

Table 3 Continued. AEs at least possibly related to study treatment. (A) Toxicities observed in BP29392. (B) Toxicities observed in BP29989.

B. Selicrelumab plus vanucizumab			
Toxicities related to Selicrelumab	G1 - 2, n (%)	G3- 4 n (%)	Total, n (%)
Fever	1 (9.1%)		1 (9.1%)
Flu-like symptoms	1 (9.1%)		1 (9.1%)
Injection related reaction	10 (90.9%)		10 (90.9%)
Papulopustular rash	1 (9.1%)		1 (9.1%)
Toxicities related to Vanucizumab	G1-2, n (%)	G3-4 n (%)	Total, n (%)
Fever	1 (9.1%)		1 (9.1%)
Hypertension		3 (27.3%)	3 (27.3%)
lipase increased		1 (9.1%)	1 (9.1%)
Localized edema	1 (9.1%)		1 (9.1%)
Pain	1 (9.1%)		1 (9.1%)
Proteinuria	1 (9.1%)		1 (9.1%)
Serum amylase increased		1 (9.1%)	1 (9.1%)
Toxicities related to either	G1-2, n (%)	G3-4 n (%)	Total, n (%)
ALAT increase	1 (9.1%)	1 (9.1%)	2 (18.2%)
Alopecia	1 (9.1%)		1 (9.1%)
Anorexia	3 (27.3%)		3 (27.3%)
Arthralgia	1 (9.1%)		1 (9.1%)
ASAT increase	2 (18.2%)		2 (18.2%)
Diarrhea	1 (9.1%)		1 (9.1%)
Dry skin	1 (9.1%)		1 (9.1%)
Dysgeusia	1 (9.1%)		1 (9.1%)
Dyspnea	1 (9.1%)		1 (9.1%)
Fatigue	4 (36.4%)		4 (36.4%)
Fever	4 (36.4%)		4 (36.4%)
Flu like symptoms	2 (18.2%)		2 (18.2%)
Flushing	1 (9.1%)		1 (9.1%)
GGT increase		1 (9.1%)	1 (9.1%)
Headache	5 (45.4%)		5 (45.4%)
Hyperhidrosis	1 (9.1%)		1 (9.1%)
Hypertension		2 (18.2%)	2 (18.2%)
Hypomagnesia		1 (9.1%)	1 (9.1%)
Nausea	3 (27.3%)		3 (27.3%)
Nightly sweating	1 (9.1%)		1 (9.1%)
Pain	3 (27.3%)		3 (27.3%)
Peripheral sensory neuropathy	1 (9.1%)		1 (9.1%)
Platelet count decreased	1 (9.1%)		1 (9.1%)
Proteinuria	1 (9.1%)		1 (9.1%)
Rash maculo-papular	1 (9.1%)		1 (9.1%)
Skin hyperpigmentation	1 (9.1%)		1 (9.1%)
Vomiting	2 (18.2%)		2 (18.2%)
ALAT increase	1 (9.1%)	1 (9.1%)	2 (18.2%)



Figure 2. G3 injection site reaction occurring in a patient five days after subcutaneous administration of 1 mg selicrelumab. Pen marks in black were used to indicate the border of the reaction site.

Antitumor activity

Efficacy for BP29392

Two out of seventeen patients (11.7%) showed a partial response (Figure 3A-C). No stable diseases ≥ 8 weeks were seen. The duration of response was not established as the patients were still on study at day of data cutoff. The time to response was 10 weeks for patient 12201, a microsatellite instability-high (MSI-H) CRC receiving 2 mg selicrelumab in part IA, and five weeks for patient 33200, a patient with squamous cell carcinoma of unknown origin receiving 36mg in part IB. Patient 12201 had a PR lasting > 110 weeks. Patient 33200 had a PR lasting >32 weeks. The latter patient showed tumor growth five weeks after establishing the PR. However, the subsequent CT scan which was taken four weeks later showed tumor reduction again. The median PFS was 10 weeks [3.29 – 110+] and the median overall survival was 24 weeks [4.57 – 113+] (Figure 4AB). Patients received a median of 4 cycles [1 – 37]. Two patients were not evaluable for efficacy: one patient showed progression prior to on treatment scan and one patient decided to stop treatment.

Efficacy for BP29889

One out of eleven patients (9.1%) demonstrated a confirmed partial response (Figure 3D-F). The PR was seen in a 67-year old female patient with ovarian cancer, who had received three prior lines of therapy. The time to response for this patient was 17 weeks. The DOR was not established (> 72 weeks) as the patient was still on study at day of data cutoff. Three patients showed a stable disease lasting > 8 weeks. The median PFS was 16 weeks [2.57 – 72.3+] and the median overall survival was 37.3 weeks [3.14 – 91.1+] (Figure 4CD). Patients received a median of 4 cycles [1 – 18]. Three patients were not evaluable for efficacy: two patients showed clinical disease progression prior to the first on treatment scan and one patient had non-reliable target lesions.

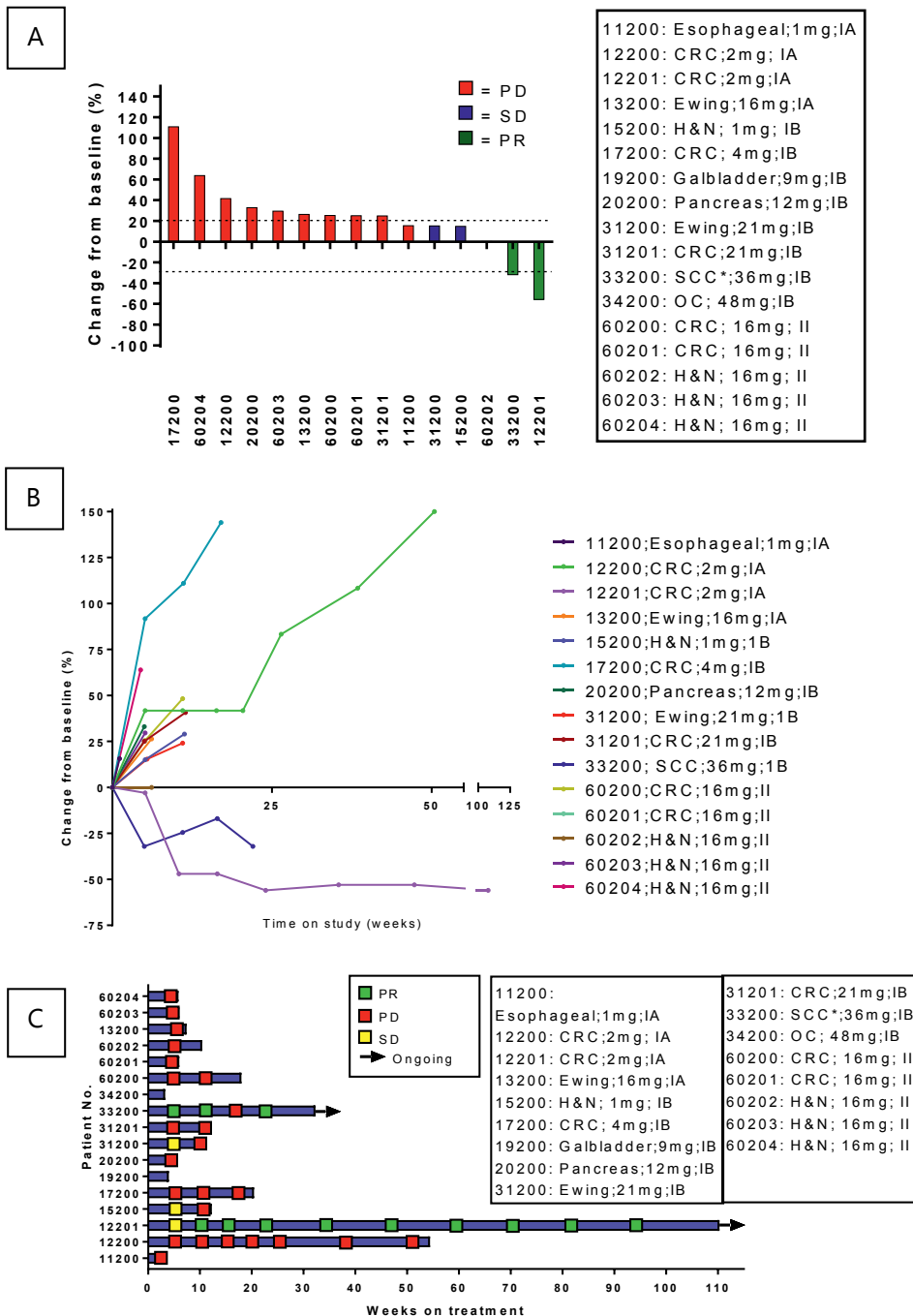


Figure 3. Efficacy analysis from BP29392(A-C) and BP29889(D-F). (A;D) Best change from baseline in tumor size. Dotted lines at 20% and -30% indicate progressive disease and partial response, respectively. (B;E) Longitudinal change from baseline in tumor size. (C;F) Longitudinal change from baseline in tumor size. CRC : Colorectal carcinoma. SCC: squamous cell carcinoma. H&N: Head and neck carcinoma. OC: Ovarian carcinoma.

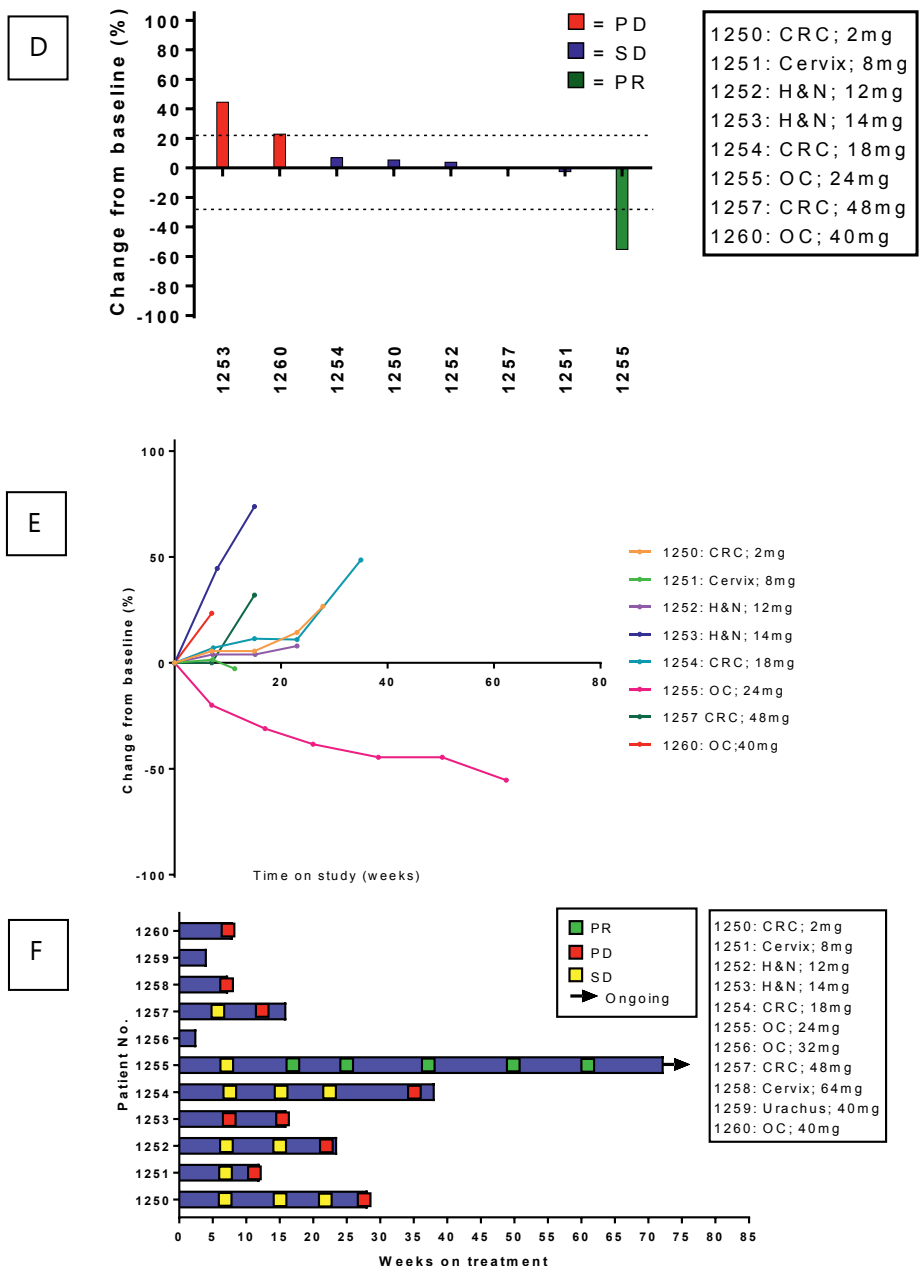


Figure 3 continued. Efficacy analysis from BP29392(A-C) and BP29889(D-F). (A;D) Best change from baseline in tumor size. Dotted lines at 20% and -30% indicate progressive disease and partial response, respectively. (B;E) Longitudinal change from baseline in tumor size. (C;F) Longitudinal change from baseline in tumor size. CRC : Colorectal carcinoma. SCC: squamous cell carcinoma. H&N: Head and neck carcinoma. OC: Ovarian carcinoma.

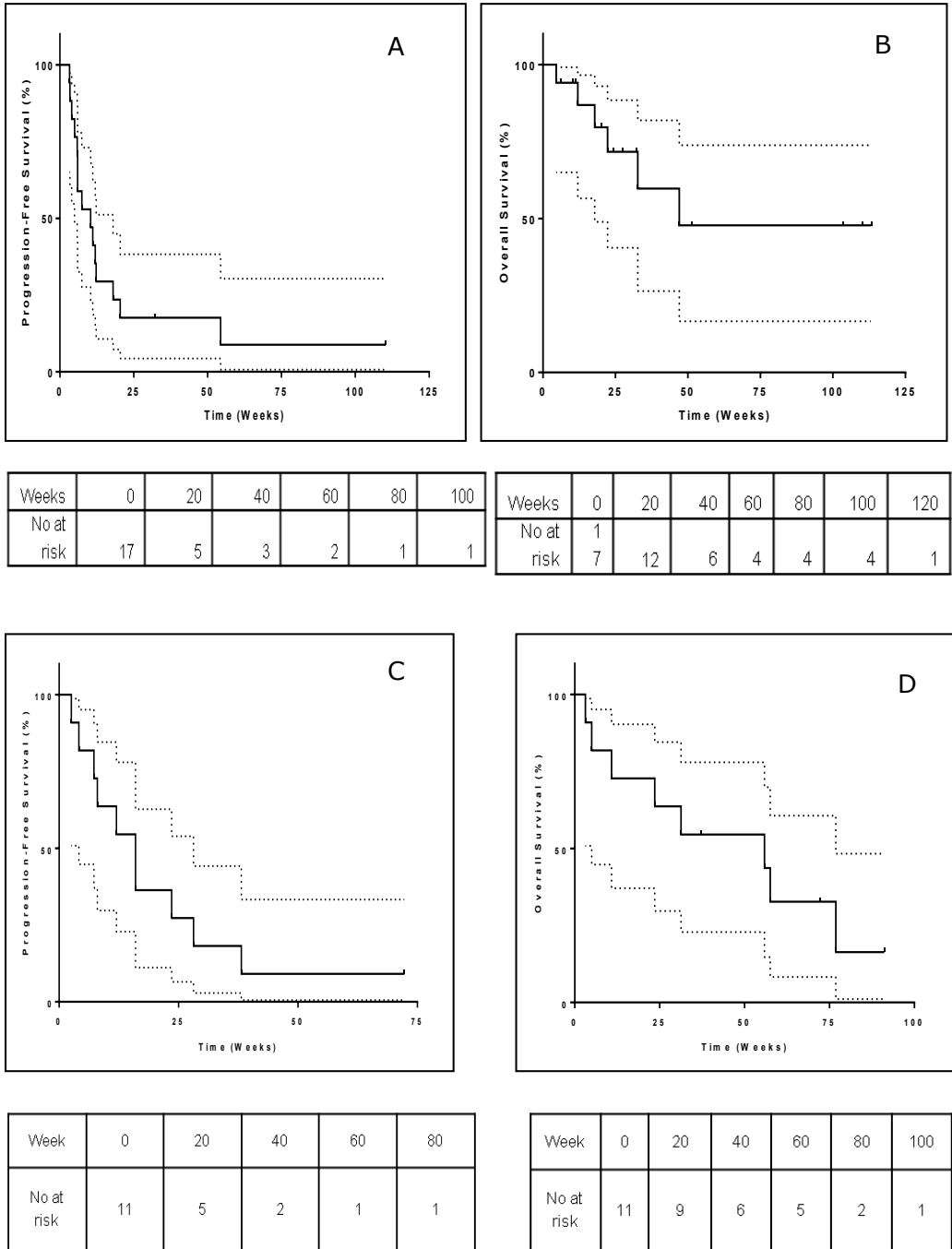


Figure 4. Kaplan-Meier estimates. (A,B) Progression-free survival and overall survival of BP29392. (C,D) Progression-free survival and overall survival of BP29889

DISCUSSION AND CONCLUSION

We present the safety, tolerability, and preliminary efficacy of selicrelumab in combination with vanucizumab or atezolizumab. Combination treatment was well tolerated, with only one DLT occurring in a patient receiving one mg selicrelumab in part IB. In both studies, the maximal tolerated dose was not reached. The main toxicity seen in the majority of patients was ISR to the subcutaneous administration of selicrelumab. Interestingly, the most severe ISR (a G3 reaction), was observed in the lowest dose-level of BP29392 part IB. Higher doses of selicrelumab were divided over multiple injections to avoid administration of high concentrations in a single injection. This, in combination with proper management with topical or oral corticosteroids made the ISR manageable. Other common AEs were ASAT/ALAT increase, fatigue, fever and headache. The administration of selicrelumab via injections may have had advantages over administration via i.v. route[26]. Reduced C_{max} levels may have led to reduced side effects, while not necessarily compromising on efficacy (data not shown). During the phase I studies of selicrelumab as a single agent, the compound was given intravenously in doses ranging from 0.01 to 0.3 mg/kg. The dose limiting toxicities at the 0.3 mg/kg dose level were venous thromboembolism and G3 headache. The most common adverse event was cytokine release syndrome (CRS), which included chills, rigors and fever. Possibly due to the fact that selicrelumab was administered s.c. rather than i.v., no CRS have occurred in patients described in this interim analysis.

The optimal biological dose, with the largest number of responses, as well as PD activity was seen at the intermediate dose levels. Peripheral B-cells have been proposed as a marker for PD activity[27]. The strongest depletion of B-cells was observed at dose levels \geq 14mg (*data not shown*). In addition, the increase in peripheral activated CD8+ T-cells was found to be optimal at the 14 mg and 18 mg cohorts (*data not shown*). For part II of both studies, 16 mg selicrelumab was estimated to be the OBD.

Clinical anti-tumor activity has been observed in both studies. Three durable partial responses were observed: in BP29392, PRs were seen in a MSI-H CRC patient and in a SCC patient, and in BP29889 the response was seen in a patient with ovarian cancer. It is uncertain to what extend the addition of selicrelumab to either vanucizumab or atezolizumab has contributed to the partial response, as checkpoint blockade has been effective in MSI-H tumors, and single agent vanucizumab has been shown to be effective in platinum-resistant recurrent ovarian cancer[28]. As the observed responses have mainly occurred in tumor types in which single agent efficacy of atezolizumab and vanucizumab has been seen, pharmacodynamic assessments are needed to conclude whether selicrelumab adds additional value to treatment. Pharmacodynamic questions that need to be answered include: (I) Do patient tumor biopsies and blood samples show that, upon selicrelumab treatment, indeed DCs are stimulated, activate tumor specific T-cells, and in return eventually lead to novel immune cell infiltration in the tumor? (II) Does vanucizumab treatment indeed lead to normalization of the tumor neovasculature, reduce inhibitory signals (such as VEGF), and subsequently lead to better immune cell infiltration in the tumor? These pharmacodynamic questions are currently being addressed in the studies. Both BP29392 and BP29889 continue with the expansion cohorts. For BP29392, enrollment is currently open for HNSCC and checkpoint-inhibitor experienced NSCLC. Colorectal

cancer cohort has been closed due to lack of efficacy. For HNSCC, three out of ten patients showed a partial response and this cohort expanded further. For NSCLC, no efficacy has been seen as of yet. For BP29889, vanucizumab has been replaced with bevacizumab, and expansion cohorts are open for platinum-resistant ovarian carcinoma, HNSCC, and checkpoint-inhibitor experienced NSCLC. The expected completions of the studies are October 2019 (BP29392) and June 2020 (BP29889).

ACKNOWLEDGEMENTS

We thank all patients and their families for participating; F. Hoffman-La Roche for sponsoring; and the Clinical Pharmacology Department of The Netherlands Cancer Institute for conducting this trial.

References

1. Tong AW, Papayoti MH, Netto G et al. Growth-inhibitory effects of CD40 ligand (CD154) and its endogenous expression in human breast cancer. *Clin. Cancer Res.* 2001; 7:691–703.
2. Kalbasi A, Fonsatti E, Natali PG et al. CD40 expression by human melanocytic lesions and melanoma cell lines and direct CD40 targeting with the therapeutic anti-CD40 antibody CP-870,893. *J. Immunother.* 2010; 33:810–816.
3. Huang Q, Qu Q-X, Xie F et al. CD40 is overexpressed by HPV16/18-E6 positive cervical carcinoma and correlated with clinical parameters and vascular density. *Cancer Epidemiol.* 2011; 35:388–392.
4. Ara A, Ahmed KA, Xiang J. Multiple effects of CD40–CD40L axis in immunity against infection and cancer. *ImmunoTargets Ther.* 2018; 7:55–61.
5. Vonderheide RH, Glennie MJ. Agonistic CD40 Antibodies and Cancer Therapy. *Clin Cancer Res* 2013; 19:1035–1043.
6. Lum HD, Buhtoiarov IN, Schmidt BE et al. In vivo CD40 ligation can induce T cell-independent antitumor effects that involve macrophages. *J. Leukoc. Biol.* 2006; 79:1181–1192.
7. Rakhmievich AL, Alderson KL, Sondel PM. T-cell-independent antitumor effects of CD40 ligation. *Int. Rev. Immunol.* 2012; 31:267–278.
8. Beatty GL, Chiorean EG, Fishman MP et al. CD40 agonists alter tumor stroma and show efficacy against pancreatic carcinoma in mice and humans. *Science* 2011; 331(6024):1612–6.
9. Hassan SB, Sørensen JF, Olsen BN, Pedersen AE. Anti-CD40-mediated cancer immunotherapy: an update of recent and ongoing clinical trials. *Immunopharmacol. Immunotoxicol.* 2014; 36:96–104.
10. Vonderheide RH, Flaherty KT, Khalil M et al. Clinical Activity and Immune Modulation in Cancer Patients Treated With CP-870,893, a Novel CD40 Agonist Monoclonal Antibody. *J. Clin. Oncol.* 2007; 25:876–883.
11. Beatty GL, Torigian DA, Chiorean EG et al. A phase I study of an agonist CD40 monoclonal antibody (CP-870,893) in combination with gemcitabine in patients with advanced pancreatic ductal adenocarcinoma. *Clin. Cancer Res.* 2013; 19:6286–6295.
12. Hegde PS, Karanikas V, Evers S. The Where, the When, and the How of Immune Monitoring for Cancer Immunotherapies in the Era of Checkpoint Inhibition. *Clin. Cancer Res.* 2016; 22:1865–1874.
13. Abiko K, Matsumura N, Hamanishi J et al. IFN- γ from lymphocytes induces PD-L1 expression and promotes progression of ovarian cancer. *Br. J. Cancer* 2015; 112:1501–1509.
14. Mimura K, Teh JL, Okayama H et al. PD-L1 expression is mainly regulated by interferon gamma associated with JAK-STAT pathway in gastric cancer. *Cancer Sci.* 2018; 109:43–53.
15. Pardoll DM. The blockade of immune checkpoints in cancer immunotherapy. *Nat. Rev. Cancer* 2012; 12:252–264.
16. Merelli B, Massi D, Cattaneo L, Mandalà M. Targeting the PD1/PD-L1 axis in melanoma: biological rationale, clinical challenges and opportunities. *Crit. Rev. Oncol. Hematol.* 2014; 89:140–165.
17. Shrimali RK, Yu Z, Theoret MR et al. Antiangiogenic Agents Can Increase Lymphocyte

- Infiltration into Tumor and Enhance the Effectiveness of Adoptive Immunotherapy of Cancer. *Cancer Res.* 2010; 70:6171–6180.
18. Selvaraj S, Raundhal M, Patidar A, Saha B. Anti-VEGF antibody enhances the antitumor effect of CD40. *Int. J. cancer* 2014; 135:1983–1988.
 19. Peske JD, Woods AB, Engelhard VH. Control of CD8 T-Cell Infiltration into Tumors by Vasculature and Microenvironment. *Adv. Cancer Res.* 2015; 128:263–307.
 20. Huang H, Langenkamp E, Georganaki M et al. VEGF suppresses T-lymphocyte infiltration in the tumor microenvironment through inhibition of NF- κ B-induced endothelial activation. *FASEB J.* 2015; 29:227–238.
 21. Voron T, Colussi O, Marcheteau E et al. VEGF-A modulates expression of inhibitory checkpoints on CD8⁺ T cells in tumors. *J. Exp. Med.* 2015; 212:139–148.
 22. Gabrilovich DI, Chen HL, Girgis KR et al. Production of vascular endothelial growth factor by human tumors inhibits the functional maturation of dendritic cells. *Nat. Med.* 1996; 2:1096–1103.
 23. Voron T, Marcheteau E, Pernot S et al. Control of the Immune Response by Pro-Angiogenic Factors. *Front. Oncol.* 2014; 4:70.
 24. Gladue RP, Cole SH, Donovan C et al. In vivo efficacy of the CD40 agonist antibody CP-870,893 against a broad range of tumor types: Impact of tumor CD40 expression, dendritic cells, and chemotherapy. *J. Clin. Oncol.* 2006; 24:2514.
 25. Hodi FS, Hwu W-J, Kefford R et al. Evaluation of Immune-Related Response Criteria and RECIST v1.1 in Patients With Advanced Melanoma Treated With Pembrolizumab. *J. Clin. Oncol.* 2016; 34:1510–1517.
 26. Fransen MF, Sluijter M, Morreau H et al. Local activation of CD8 T cells and systemic tumor eradication without toxicity via slow release and local delivery of agonistic CD40 antibody. *Clin. Cancer Res.* 2011; 17:2270–2280.
 27. Vonderheide RH, Burg JM, Mick R et al. Phase I study of the CD40 agonist antibody CP-870,893 combined with carboplatin and paclitaxel in patients with advanced solid tumors. *Oncoimmunology* 2013; 2:23033.
 28. Oaknin A, Floquet A, Le Tourneau C et al. Single agent vanucizumab (RO5520985) for platinum (Pt)-resistant recurrent ovarian cancer (OC): Results from a single arm extension phase of the phase I FIH study. *J. Clin. Oncol.* 2015; 33:5549.

Table S1. Treatment related AEs observed in BP29392 per dose level.

Part	Dose selicrelumab (mg)	Number of patients	Toxicity	G1	G2	G3
IA	1	1	Hematuria	1		
			ASAT increase		1	
			ALAT increase		1	
IA	2	2	ISR	2		
			Productive cough	1		
			Myalgia	1		
			Fatigue	2		
			Fever	1		
			Flu like symptoms	1		
			ASAT increase		1	
			ALAT increase		1	
			GGT increase		1	
			Neutrophil count decreased		1	
			Dyspnea	1		
IA	16	1	Fever		1	
			ISR	1		
			IRR		1	
IB	1	1	ISR			1
			ASAT increase		1	
			ALAT increase		1	
			Platelet count decrease			1
			Diarrhea	1		
			Fatigue	1		
			Mucositis oral	1		
			Pain in extremity		1	
			IRR	1		
			Flu like symptoms	1		
GGT increase	1					
IB	4	1	ISR		1	
			Fatigue	1		
			Ear pain	1		
			Chills	1		
			Flu like symptoms	1		
			Headache	1		
			Myalgia	1		
			Nausea	1		
			Dry skin	1		
			Malaise	1		
			Colitis	1		

Table S1 continued. Treatment related AEs observed in BP29392 per dose level.

			Diarrhea	1		
			ISR	1		
			Rash maculo papular	1		
			Anorexia		1	
			Dry mouth	1		
			Fatigue		1	
			Nausea	1		
IB	12	1	ISR	1		
			IRR		1	
			Diarrhea	1		
IB	21	2	Fatigue		1	
			ISR		2	
			ASAT increase		2	
			ALAT increase	1	1	
			Fever		1	
			Vomiting	1		
IB	36	1	ISR		1	
			Flu like symptoms	1		
			AST increase		1	
			ALT increase		1	
			GGT increase			
IB	48	1	Pneumonitis		1	
			ASAT increase			1
			ALAT increase			1
II	16	5	ISR	1	4	
			Alopecia	1		
			Fever	1		
			Pruritis		1	
			Fatigue		2	
			Palmar-plantar erythrodysesthesia syndrome	1		
			GGT increase		1	
			ASAT increase	1		
			ALAT increase	1		1
			Headache		1	

Table S2. Treatment-related AEs observed in BP29889 per dose level.

Dose selicrelumab (mg)	Number of patients	Toxicity	G1	G2	G3	G4
2	1	ISR		1		
		Flu like symptoms	1			
		Nightly sweating	1			
		Pain - Light myalgia legs	1			
		Fatigue	1			
		Vomiting	1			
		Nausea	1			
		Headache	1			
		Flank pain	1			
		Hyperhidrosis		1		
		Rash maculo-papular	1			
		Pain both shoulders	1			
		ALAT increase				1
		ASAT increase		1		
		Hypertension				1
8	1	ISR		1		
		Anorexia	1			
		Pain left abdomen	1			
		Fever	1			
		Peripheral sensory neuropathy	1			
		Headache		1		
		Bruised sensation toe left	1			
		Diarrhea	1			
		Fever	1			
		Nausea	1			
		Dyspnea	1			
12	1	ISR	1			
		Flu like symptoms	1			
		Headache	1			
14	1	ISR	1			
		Papulopustular rash	1			
		Fever	1			
		Hypertension			1	
18	1	ISR	1			
		Arthralgia	1			
		Hypertension			1	
		Arthralgia	1			
		Dry skin	1			
Skin hyperpigmentation	1					

Table S2 continued. Treatment-related AEs observed in BP29889 per dose level.

		Injection site reaction		1		
		Localized edema fingers	1			
		Proteinuria		1		
		Serum amylase increased			1	
		Lipase increased				1
		Hypertension		1		
		Fever		1		
		Alopecia	1			
		Hypomagnesia			1	
		Platelet count decreased	1			
		Fatigue	1			
		Pain left knee		1		
		Anorexia	1			
		Dysgeusia	1			
		Pain knee cavity	1			
32	1	ISR	1			
		Nausea	1			
		Fever	1			
48	1	ISR	1			
		Chills	1			
		Myalgia	1			
		Postnasal drip	1			
		Chills	1			
		Headache	1			
		Malaise	1			
		Hypertension			1	
64	1	Flu like symptoms	1			
		ISR		1		
		Pain right arm	1			
		Fatigue		1		
		Vomiting		1		
40	2	ISR		1		
		Headache	1			
		Alk. phosphatase increased		1		
		ALAT increased		1		
		GGT increased			1	
		ASAT increased	1			
		Flushing	1			
		Chills	1			

Chapter 3

Pembrolizumab in rare cancers

Chapter 3.1

Efficacy and Safety of Pembrolizumab in Previously Treated Advanced Cervical Cancer: Results From the Phase 2 KEYNOTE-158 Study.

Willeke Ros

Chung HC, **Ros W**, Delord J-P, Perets R, Italiano A, Shapira-Frommer R, Manzuk L, Piha-Paul SA, Xu L, Zeigenfuss S, Pruitt SK, Leary A. Efficacy and Safety of Pembrolizumab in Previously Treated Advanced Cervical Cancer: Results From the Phase II KEYNOTE-158 Study.

Journal of Clinical Oncology 2019; 37:1470 - 1478

ABSTRACT

Purpose: KEYNOTE-158 (ClinicalTrials.gov identifier: NCT02628067) is a phase 2 basket study investigating the antitumor activity and safety of pembrolizumab in 11 cancer types. We present interim results from patients with previously treated advanced cervical cancer.

Patients and Methods: Patients received pembrolizumab 200 mg every 3 weeks for 2 years or until progression, intolerable toxicity, or physician or patient decision. Tumor imaging was performed every 9 weeks for the first 12 months, and every 12 weeks thereafter. The primary endpoint was objective response rate (ORR) assessed per RECIST v1.1 by independent central radiologic review. Safety was a secondary endpoint.

Results: Ninety-eight patients were treated. Median age was 46.0 years (range, 24-75) and 65.3% had ECOG performance status 1. Eighty-two (83.7%) patients had PD-L1–positive tumors (combined positive score ≥ 1), 77 having previously received ≥ 1 line of chemotherapy for recurrent/metastatic disease. Median follow-up was 10.2 months (range, 0.6-22.7). ORR was 12.2% (95% CI, 6.5-20.4), with 3 complete and 9 partial responses. All 12 responses were in patients with PD-L1–positive tumors, for an ORR of 14.6% (95% CI, 7.8-24.2); 14.3% (95% CI, 7.4-24.1) in those who had received ≥ 1 line of chemotherapy for recurrent/metastatic disease. Median duration of response was not reached (range, 3.7+–18.6+ months). Treatment-related adverse events (AEs) occurred in 65.3% of patients, and the most common were hypothyroidism (10.2%), decreased appetite (9.2%), and fatigue (9.2%). Treatment-related grade 3-4 AEs occurred in 12.2% of patients.

Conclusion: Pembrolizumab monotherapy demonstrated durable antitumor activity and manageable safety in patients with advanced cervical cancer. Based on these results, the FDA granted accelerated approval of pembrolizumab for patients with advanced, PD-L1–positive cervical cancer that progressed on or after chemotherapy.

INTRODUCTION

Cervical cancer is the fourth leading cause of cancer-related mortality in women worldwide.¹ In recent years, there has been a reduced incidence of cervical cancer in developed countries related to systematic screening and we may expect the incidence and mortality rates to decline further if widespread vaccination against human papillomavirus (HPV) is adopted. Unfortunately, similar improvements have not been achieved in the developing world, where 87% of all cervical cancer-related deaths occur.¹ In contrast to patients with early-stage cervical cancer, the prognosis for patients with recurrent or metastatic disease is poor.² Following disease progression, second line and later treatment options are limited.

Cervical cancer is considered a relatively chemotherapy-resistant disease. Cisplatin, with concurrent radiation, is the primary cytotoxic agent used to treat patients with advanced cervical cancer. The objective response rate (ORR) with single-agent cisplatin ranges from 13% to 23%, and responses are often not durable.³⁻⁵ Several cisplatin-based combination regimens have been tested, and the combination with paclitaxel has shown improved ORR and progression free survival (PFS) relative to cisplatin alone, but with no significant benefit in overall survival (OS).^{6,7} The combination of cisplatin with topotecan was the first regimen to show a significant improvement in OS over cisplatin alone (9.4 versus 6.5 months, respectively; $p=0.017$).⁸ However, subsequent results from the Gynecologic Oncology Group (GOG) 204 study, comparing four platinum-based doublets (paclitaxel + cisplatin [reference arm]; vinorelbine + cisplatin; gemcitabine + cisplatin; and topotecan + cisplatin) showed no improvement in disease response in any of the experimental arms compared with paclitaxel + cisplatin.⁹ In addition, toxicity associated with cisplatin-based regimens and eventual resistance to platinum-based chemotherapy¹⁰ limit its utility.

Bevacizumab is an antiangiogenic agent with efficacy in cervical cancer, representing a shift in the treatment paradigm. The GOG 227C trial tested bevacizumab monotherapy in persistent/recurrent cervical cancer (N=46).¹¹ Compared with single-agent compounds tested in prior GOG phase 2 trials in this setting,¹²⁻¹⁷ bevacizumab showed improved PFS and OS of 3.4 months (95% CI, 2.5-4.5) and 7.3 months (95% CI, 6.1-10.4), respectively. Adverse events (AEs) included grade 3 hematologic toxicity (17.4%), hypertension (15.2%), deep venous thrombosis (10.9%), grade 4 urinary fistula (2.2%), and vaginal bleeding (2.2%). In the phase 3 GOG 240 trial of first line systemic treatment in women with metastatic or persistent/recurrent cervical cancer (N=452), the addition of bevacizumab to standard chemotherapeutic combinations (cisplatin + paclitaxel; topotecan + paclitaxel) significantly improved median OS to 16.8 months compared with 13.3 months with chemotherapy alone ($p=0.007$).¹⁸ However, increased toxicity was observed with bevacizumab in this study, with a higher incidence of grade 3 or greater thromboembolism and gastrointestinal and genitourinary fistula.¹⁸ The experience with bevacizumab demonstrates the utility of adding a non-chemotherapeutic agent to the treatment armamentarium for advanced cervical cancer, but highlights the ongoing need for novel therapies that improve clinical outcomes and are well tolerated.

In recent years, immune-checkpoint inhibitors have shown antitumor activity in multiple tumor types. Programmed death 1 (PD-1) is a T-cell coinhibitory receptor that functions in

an immunoregulatory capacity under normal conditions.¹⁹ PD-1 plays a significant role in cancer by contributing to the ability of a tumor to evade immunosurveillance.^{20,21} Given the presence of a virus leading to antigen production in the oncogenesis of cervical cancer, evaluating immune checkpoint inhibition as a treatment strategy in this setting is of great interest. Notably, PD-L1 expression has been identified in virus-induced cancers, and an upregulation of PD-1 and PD-L1 has been reported in high-risk HPV-associated cervical intraepithelial neoplasia.^{22,23}

Pembrolizumab is a highly selective, fully humanized monoclonal antibody that prevents the interaction between PD-1 and its ligands, programmed death ligand 1 (PD-L1) and programmed death ligand 2 (PD-L2).²⁴ In the multicohort phase 1b KEYNOTE-028 study, pembrolizumab monotherapy showed promising antitumor activity and manageable safety in patients with previously treated, PD-L1–positive advanced cervical cancer.²⁵ Here, we present interim results from the cohort of patients with previously treated advanced cervical cancer enrolled in the phase 2 KEYNOTE-158 basket study of pembrolizumab in 11 cancer types.

METHODS

Study Design and Patients

KEYNOTE-158 (ClinicalTrials.gov identifier: NCT02628067) is an international, open-label, multicohort, phase 2 study of pembrolizumab monotherapy in 11 advanced solid tumor types that have progressed on standard-of-care systemic therapy. Key eligibility criteria for the cervical cancer cohort included age ≥ 18 years, histologically or cytologically confirmed advanced cervical cancer, measurable disease as assessed by Response Evaluation Criteria in Advanced Solid Tumors version 1.1 (RECIST v1.1) per independent central radiologic review, progression on or intolerance to ≥ 1 line of standard therapy, Eastern Cooperative Oncology Group (ECOG) performance status 0 or 1, and adequate organ function. All patients were required to provide tumor tissue from a newly obtained core or excisional biopsy sample (preferred) or archival tumor sample of a nonirradiated lesion for PD-L1 assessment. Patients were enrolled regardless of tumor biomarker expression.

Patients were excluded from enrollment if they had active central nervous system metastases, had active autoimmune disease that required systemic treatment in the previous 2 years, had a history of noninfectious pneumonitis that required steroids or current pneumonitis, received prior therapy with an agent directed against PD-1, PD-L1, PD-L2 or another co-inhibitory T-cell receptor, received an antineoplastic monoclonal antibody in the previous 4 weeks, received chemotherapy, targeted small molecule therapy, or radiation therapy in the previous 2 weeks, or had adverse events (AEs) from previous therapy that had not resolved to grade ≤ 1 or baseline.

All patients provided written, informed consent. The study protocol was approved by the independent ethics committee or review board at each participating institution. The study was conducted in accordance with the Declaration of Helsinki and the International Conference on Harmonization Guidelines for Good Clinical Practice.

Study Treatment

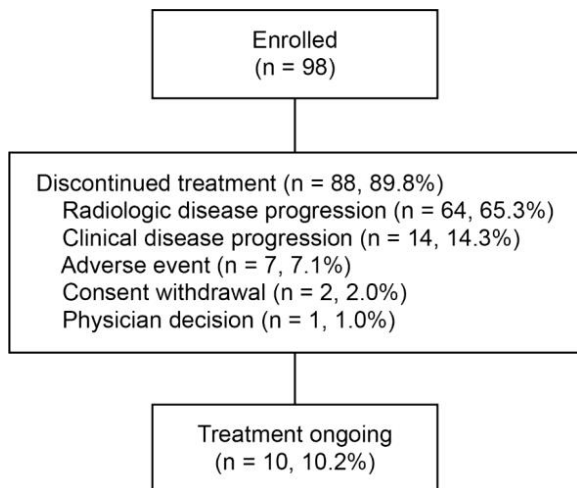
Pembrolizumab 200 mg was administered intravenously over 30 minutes every 3 weeks for up to 2 years. Treatment was discontinued upon disease progression, intolerable toxicity, physician decision, or patient withdrawal of consent. Clinically stable patients with radiologic evidence of disease progression could remain on treatment until progression was confirmed at the next imaging assessment performed ≥ 4 weeks later, or longer if approved via Sponsor consultation. Patients who discontinued treatment with stable disease (SD), partial response (PR), or complete response (CR) who exhibited subsequent disease progression were eligible for an additional 1 year of pembrolizumab.

Assessments

Tumor PD-L1 expression was analyzed using the PD-L1 IHC 22C3 pharmDx assay (Agilent Technologies, Carpinteria, CA, USA) at the Neogenomics Laboratories, Inc. testing laboratory. The measure of expression was the combined positive score (CPS), defined as the ratio of PD-L1–positive cells (tumor cells, lymphocytes, and macrophages) out of the total number of tumor cells $\times 100$. PD-L1 positivity was defined as CPS ≥ 1 . Tumor imaging was performed by computed tomography (preferred) or magnetic resonance imaging at baseline, at week 9, and every 9 weeks thereafter through 12 months, then every 12 weeks. Physical examination and laboratory tests were performed and vital signs were assessed at baseline and regularly throughout study treatment. AEs were monitored throughout treatment and for 30 days thereafter (90 days for serious AEs) and graded according to the National Cancer Institute Common Terminology Criteria for Adverse Events, version 4.0.

Statistical Analysis

The primary endpoint was ORR, defined as the proportion of patients with CR or PR, assessed by RECIST v1.1 per independent central radiologic review. Secondary endpoints included duration of response, defined as the time from first CR or PR to disease progression as assessed by RECIST v1.1 per independent central review or death, whichever occurred first; PFS, defined as the time from first dose of pembrolizumab to disease progression as assessed by RECIST v1.1 per independent central review or death, whichever occurred first; and OS, defined as the time from first dose of pembrolizumab to death. Primary and secondary endpoints were evaluated in the total and the PD-L1–positive populations. An additional efficacy analysis was conducted in the subset of patients with PD-L1–positive tumors who had previously received at least one line of chemotherapy in the recurrent/metastatic setting.

Figure 1. Patient disposition.

Efficacy was assessed in all patients who received ≥ 1 dose of pembrolizumab. ORR point estimates were accompanied by 95% confidence intervals (CIs) using the Clopper-Pearson exact method²⁶ based on binomial distribution; patients without response data were considered nonresponders. Duration of response, PFS, and OS were estimated using the Kaplan-Meier method.²⁷ Safety was assessed in all patients who received ≥ 1 dose of pembrolizumab. Summary statistics were provided for baseline demographics and disease characteristics and AEs. Results are based on an interim analysis of data, with a cutoff date of January 15, 2018; the patients continue to be followed for long-term outcomes.

RESULTS

Patients

From January 27, 2016 to August 18, 2016, 98 patients were enrolled at 42 sites in 17 countries (Table S1). Eighty-two (83.7%) patients had PD-L1–positive tumors (CPS ≥ 1), 77 of whom had received ≥ 1 line of chemotherapy for recurrent/metastatic disease. The 5 adenocarcinomas and the single adenosquamous cell carcinoma were all PD-L1–positive. All patients received ≥ 1 dose of pembrolizumab. As of the January 15, 2018 data cutoff, the median follow-up duration was 10.2 months (range, 0.6-22.7). Eighty-eight (89.8%) patients discontinued pembrolizumab, most commonly for disease progression (n=64 [65.3%]) (Figure 1). Median duration of pembrolizumab treatment was 2.9 months (range, 1 day-22.1), and the median number of pembrolizumab doses was 5 (range, 1-33). Baseline characteristics are shown in Table 1. The median age was 46.0 years (range, 24-75), 65.3% had ECOG PS 1, and 93.9% had FIGO stage IVB disease. Overall, 21.4% had previously received adjuvant and/or neoadjuvant therapy, including 4.1% whose only prior therapy was adjuvant and/or neoadjuvant therapy, and 30.6% received ≥ 3 previous lines of therapy. Most patients (86.7%) received previous radiation therapy.

Antitumor Activity

In the total population (n=98), 3 patients had a CR and 9 patients had a PR as assessed by RECIST v1.1 per independent central review, resulting in an ORR of 12.2% (95% CI, 6.5-20.4) (Table 2). A summary of previous therapies and localization of target lesions in patients whose best overall response was CR or PR is shown in Table S2. Eleven of the patients who responded were FIGO stage IVB and 1 was FIGO stage IIIB at study entry. All 12 responses were in patients with PD-L1–positive tumors, which included 1 patient with adenocarcinoma. As such, in the population of patients with PD-L1–positive tumors, the ORR was 14.6% (95% CI, 7.8-24.2); 14.3% (95% CI, 7.4-24.1) in those who had previously received ≥1 line of chemotherapy for recurrent/metastatic disease (Table 2). Nine of 12 responses were ongoing after ≥9 months follow-up (Figure 2A). Median time to response was 2.1 months (range, 1.6-4.1) and median duration of response had not been reached (range, 3.7+ to 18.6+ months) (Table 2). Eighteen patients, 15 of whom had PD-L1–positive tumors, had SD, leading to a DCR of 30.6% (95% CI, 21.7-40.7) in the total population and 32.9% (95% CI, 22.9-44.2) in the PD-L1–positive tumor population (Table 2). Best percentage change from baseline in target lesion size for the 86 patients who had ≥1 evaluable postbaseline imaging assessment is shown in Figure 2B.

Table 1. Baseline Demographics and Disease Characteristics

Characteristic	N=98
Age, years, median (range)	46.0 (24 to 75)
ECOG performance status	
0	34 (34.7)
1	64 (65.3)
FIGO stage^a	
II	1 (1.0)
IIIB	4 (4.1)
IVA	1 (1.0)
IVB	92 (93.9)
PD-L1 expression status	
Positive	82 (83.7)
Negative	15 (15.3)
Unknown	1 (1.0)
Target lesion size,^T mm, median (range)	58.4 (10.2-305.1)

Table 1 continued. Baseline Demographics and Disease Characteristics

Characteristic	N=98
Histology of current diagnosis	
Adenocarcinoma	5 (5.1)
Adenosquamous	1 (1.0)
Squamous Cell Carcinoma	92 (93.9)
Previous radiation therapy	85 (86.7)
Previous antineoplastic agents	98 (100)
Paclitaxel	85 (86.7)
Cisplatin	79 (80.6)
Carboplatin	66 (67.3)
Bevacizumab	41 (41.8)
Topotecan	17 (17.3)
Previous adjuvant and/or neoadjuvant therapy	21 (21.4)
Number of previous lines of therapy	
Adjuvant and/or neoadjuvant [‡]	4 (4.1)
1 [§]	30 (30.6)
2	34 (34.7)
3	16 (16.3)
4	10 (10.2)
≥5	4 (4.1)

Data are presented as n (%) unless otherwise noted. Abbreviations: ECOG, Eastern Cooperative Oncology Group; ULN, upper limit of normal. *FIGO (International Federation of Gynecology and Obstetrics) stages were derived from the American Joint Committee on Cancer TNM staging system.

[†]Defined as the sum of the longest diameters of target lesions measurable by central radiology review.

[‡]Protocol allowed enrollment if recurrence occurred <12 months after completion of therapy. [§]Includes 2 patients who only received systemic therapy categorized as definitive therapy (i.e., given as primary treatment for localized disease) and failed (i.e., developed recurrent/metastatic disease) in <12 months.

At the time of data cutoff, 84 (85.7%) patients in the total population experienced disease progression or death. Median PFS was 2.1 months (95% CI, 2.0-2.2), and the estimated PFS rate at 6 months was 25.0% (Figure 3A). In the PD-L1–positive tumor population, with 68 (82.9%) events, median PFS was 2.1 months (95% CI, 2.1-2.3) (Figure S1A). A total of 68 (69.4%) patients in the total population and 53 (64.6%) in the PD-L1–positive tumor population had died. Median OS was 9.4 months (95% CI, 7.7-13.1) in the total population (Figure 3B) and 11 months (95% CI, 9.1-14.1) in the PD-L1–positive tumor population (Figure S1B). In the total and PD-L1–positive tumor populations, 6-month estimates of OS were 75.2% and 80.2%, and 12-month estimates were 41.4% and 47.3%, respectively. One of the 12 responders had died as of the data cutoff date.

Safety

Sixty-four (65.3%) patients experienced ≥ 1 treatment-related AE, including 12 (12.2%) who experienced ≥ 1 grade 3 or 4 event (Table 3). There were no treatment-related AEs that led to death. Four (4.1%) patients discontinued pembrolizumab because of treatment-related AEs. The most common treatment-related AEs were hypothyroidism (10.2%), decreased appetite (9.2%), fatigue (9.2%), and diarrhea (8.2%). The only treatment-related AEs of grade 3 or 4 severity that occurred in ≥ 2 patients were increased alanine aminotransferase (n=3 [3.1%]) and increased aspartate aminotransferase (n=2 [2.0%]).

Figure 2. Antitumor Activity of Pembrolizumab in the Total Population. A. Time to and duration of response assessed by RECIST v1.1 per independent central review in patients whose best overall response was complete or partial response (n=12). The length of the bars represents the time to the last imaging assessment. B. Best change from baseline in target lesion size assessed by RECIST v1.1 per independent central review in patients with ≥ 1 evaluable postbaseline imaging assessment (n=86). RECIST, Response Evaluation Criteria in Solid Tumors.

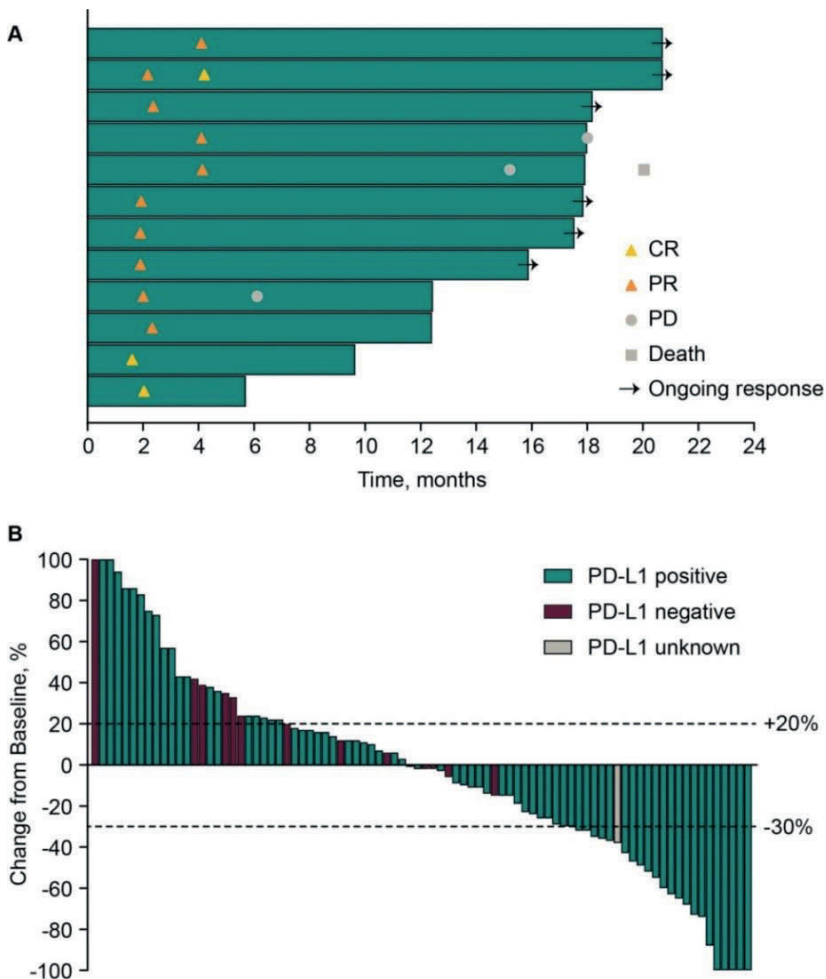
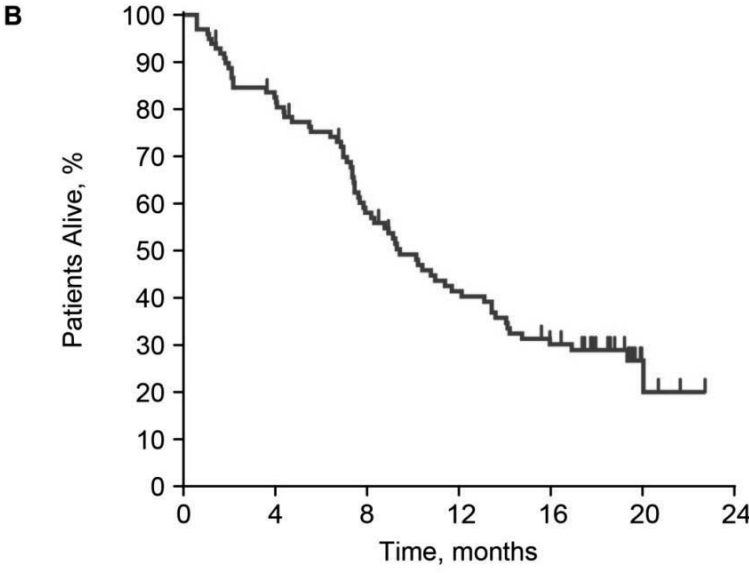
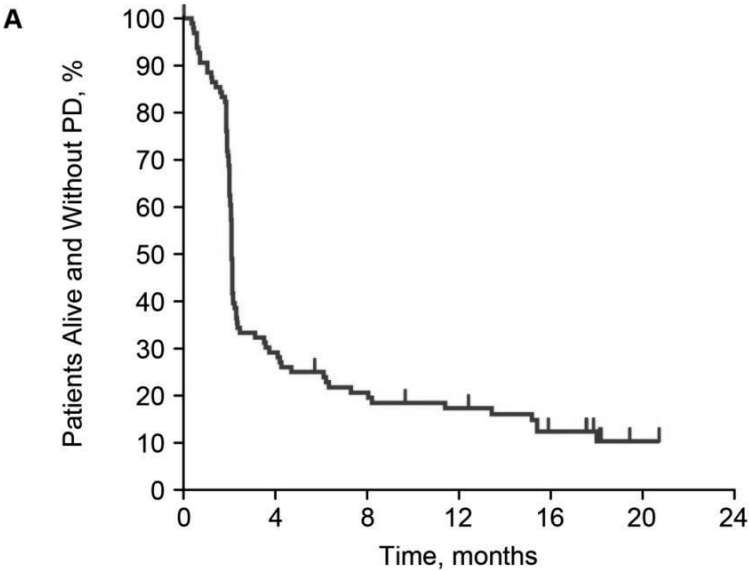


Figure 3. Kaplan-Meier estimates of survival in the efficacy population (N=98). A. Progression-free survival assessed by RECIST v1.1 per independent central review. B. Overall survival. RECIST, Response Evaluation Criteria in Solid Tumors. PD, progressive disease.



Immune-mediated AEs, which were based on a list of terms specified by the sponsor and considered regardless of attribution to study treatment or immune relatedness by the investigator, occurred in 25 (25.5%) patients, including 5 (5.1%) who experienced ≥ 1 grade 3 or 4 event. There were no immune-mediated AEs that led to death. The most common immune-mediated AEs were hypothyroidism (11.2%) and hyperthyroidism (9.2%) (Table 3). The only immune-mediated AEs of grade 3 or 4 severity were 2 cases (2.0%) of hepatitis, 2 cases (2.0%) of severe skin reactions, and 1 case (1.0%) of adrenal insufficiency.

Discussion

The present results from an interim analysis of data from the phase 2 KEYNOTE-158 clinical trial show that pembrolizumab has promising antitumor activity in patients with previously treated advanced cervical cancer. The ORR in the total population was 12.2%, with 3 patients achieving a CR and 9 patients achieving a PR. These response rates are similar or superior to those observed with other treatment options in this setting.⁵ Responses typically occurred within 2.1 months and were durable, with a median duration of response that had not been reached after a median follow-up of 10.2 months, and an estimated 90.9% of responses ongoing at 6 months. Response duration is a key consideration when assessing the clinical value of cancer therapies, and durability of response with pembrolizumab exceeded that observed with other agents available for the second-line or greater treatment of cervical cancer.⁵ In addition, reductions in tumor size were observed in more than half of the patients who had at least one evaluable post-baseline imaging assessment (n=86).

The favorable response rate and duration of response in this second-line or greater study are further supported by promising OS data (median, 9.4 months for the entire study population and 11.0 months for the PD-L1–positive population). By comparison, the reported post-progression OS following first-line chemotherapy or chemotherapy plus bevacizumab was 7.1 months and 8.4 months, respectively.²⁸ For pembrolizumab treatment in this study, the estimated 12-month OS of 41.4% for the entire study population and 47.3% for the PD-L1–positive population compare favorably to the 12-month OS rate of 37.5% reported for treatment with axalimogene filolisbac in the second-line or greater setting (NCT01266460).

Table 2. Antitumor Activity Assessed by RECIST v1.1 per Independent Central Review

Antitumor Activity	Total Population n=98	PD-L1–Positive Population		PD-L1–Negative Population n=15
		Total n=82	Previously Treated [†] n=77	
ORR, n (%) [95% CI]	12 (12.2) [6.5-20.4]	12 (14.6) [7.8-24.2]	11 (14.3) [7.4-24.1]	0 (0.0) [0.0-21.8]
DCR, n (%) [95% CI]	30 (30.6) [21.7-40.7]	27 (32.9) [22.9-44.2]	24 (31.2) [21.2-42.7]	3 (20.0) [4.3-48.1]
Best overall response, n (%)				
Complete response	3 (3.1)	3 (3.7)	2 (2.6)	0 (0.0)
Partial response	9 (9.2)	9 (11.0)	9 (11.7)	0 (0.0)
Stable disease	18 (18.4)	15 (18.3)	13 (16.9)	3 (20.0)
Progressive disease	55 (56.1)	44 (53.7)	42 (54.5)	10 (66.7)
Not able to be evaluated ^{**}	5 (5.1)	4 (4.9)	4 (5.2)	1 (6.7)
Not able to be assessed [†]	8 (8.2)	7 (8.5)	7 (9.1)	1 (6.7)
Time to response, [‡] months, median (range)	2.1 (1.6-4.1)	2.1 (1.6-4.1)	2.2 (1.6-4.1)	—
Duration of response, ^{‡§} months, median (range)	NR (3.7+ to 18.6+)	NR (3.7+ to 18.6+)	NR (4.1 to 18.6+)	—
Estimated rate of response duration ≥6 months, ^{‡§} %	10 (90.9)	10 (90.9)	10 (90.9)	—
Estimated rate of response duration ≥9 months, ^{‡§} %	9 (90.9)	9 (90.9)	9 (90.9)	—
Estimated rate of response duration ≥12 months, ^{‡§} %	7 (79.5)	7 (79.5)	7 (79.5)	—

Total population includes the 1 patient who had disease that was not evaluable for PD-L1 expression. NR, not reached; RECIST, Response Evaluation Criteria in Solid Tumors. ^{*}Patients who had received ≥1 line of chemotherapy for recurrent or metastatic disease. ^{**}Patients who had ≥1 postbaseline tumor assessment, none of which were evaluable. [†]Patients who had no postbaseline tumor assessment because of death, withdrawal of consent, loss to follow-up, or start of new anticancer therapy. [‡]Evaluated in patients who had a complete or partial response (n=12 for the total population, n=12 for the PD-L1–positive population). [§]Estimated using the Kaplan-Meier method.

The safety profile for pembrolizumab was consistent with that seen in other tumor types;²⁴ only four patients (4.1%) discontinued treatment because of treatment-related AEs, and no treatment-related mortality occurred.

In our study, patients were enrolled regardless of tumor PD-L1 expression; however, the majority of patients (83.7%) had tumors that expressed PD-L1. The ORR was higher in patients with PD-L1–positive tumors (CPS ≥ 1) relative to the overall population (14.6% versus 12.2%, respectively). No responses were observed in patients with PD-L1–negative tumors; however, because of the small number of patients with PD-L1–negative tumors who were enrolled, this study lacks the power to reliably distinguish response rates between patients with PD-L1–positive and PD-L1–negative tumors.

The present results are consistent with those from the earlier phase 1b KEYNOTE-028 trial of pembrolizumab in previously treated patients with PD-L1–positive advanced cervical cancer (n=24).²⁵ In that study, pembrolizumab was associated with a 17% ORR, as assessed by investigator, with four patients achieving PR and three patients achieving SD, and the median duration of response was 5.4 months.²⁵ Several other studies have also evaluated immunotherapies in the setting of advanced cervical cancer. A phase 1/2 trial of ipilimumab in patients with recurrent and metastatic cervical cancer (n=42) showed that of the 34 patients evaluated for best response, one patient had a PR and 10 had SD.²⁹ The median PFS and OS were 2.5 months (95% CI, 2.1-3.2) and 8.5 months (95% CI, 3.6-not reached), respectively.²⁹ The phase 1/2 CheckMate 358 trial of nivolumab reported an ORR of 26% in a cohort of 19 patients with recurrent or metastatic cervical cancer.³⁰ Compared to the current study of pembrolizumab in which 65% of patients received two or more prior lines of treatment, the patient population in CheckMate 358 was less heavily pretreated, with 30% of patients receiving nivolumab as first-line treatment for advanced disease, and only 29% of patients having received two or more prior lines of treatment.³⁰ Studies of additional single-agent immunotherapies, combinations of different immunotherapies, and combinations of immunotherapies with other classes of agents, including chemoradiation and anti-angiogenics, for the treatment of advanced cervical cancer are currently underway.³¹⁻³³

Table 3. Adverse Events in the Total Treated Population (N=98). Data are presented as n (%), where n is the number of patients who experienced ≥ 1 episode of a given event. Relatedness to treatment was determined by the investigator. Immune-mediated events were based on a list of terms specified by the sponsor and considered regardless of attribution to treatment or immune relatedness by the investigator; related terms were included. ALT, alanine aminotransferase; AST, aspartate aminotransferase.

Adverse Event	Any Grade	Grade 3-4
Treatment-related AEs of any grade that occurred in ≥ 5 patients or of grade 3-4 that occurred in ≥ 2 patients		
Any	64 (65.3)	12 (12.2)
Hypothyroidism	10 (10.2)	0
Decreased appetite	9 (9.2)	0
Fatigue	9 (9.2)	0
Diarrhea	8 (8.2)	1 (1.0)
AST increased	7 (7.1)	2 (2.0)
Asthenia	7 (7.1)	1 (1.0)
Pyrexia	7 (7.1)	1 (1.0)
Hyperthyroidism	7 (7.1)	0
Arthralgia	6 (6.1)	1 (1.0)
Nausea	6 (6.1)	0
Pruritus	6 (6.1)	0
Rash	6 (6.1)	0
Vomiting	6 (6.1)	0
Abdominal pain	5 (5.1)	0
ALT increased	3 (3.1)	3 (3.1)
Immune mediated AEs and infusion reactions that occurred in ≥ 1 patient		
Hypothyroidism	11 (11.2)	0
Hyperthyroidism	9 (9.2)	0
Infusion-related reaction	3 (3.1)	0
Colitis	2 (2.0)	0
Hepatitis	2 (2.0)	2 (2.0)
Severe skin reactions	2 (2.0)	2 (2.0)
Adrenal insufficiency	1 (1.0)	1 (1.0)
Myositis	1 (1.0)	0
Pneumonitis	1 (1.0)	0
Uveitis	1 (1.0)	0

In summary, interim results from all 98 patients with previously treated, advanced cervical cancer enrolled in the KEYNOTE-158 study and treated with pembrolizumab showed an ORR of 12.2%, including 3 patients with a CR. For the 82 patients with PD-L1–positive tumors, the ORR was 14.6%, with an ORR of 14.3% in patients who had previously received ≥ 1 line of chemotherapy for recurrent or metastatic disease. No responses were observed in patients with PD-L1–negative tumors. Responses were durable, with a median duration of response that had not been reached, and 50.0% of responses ongoing at the time of data cutoff. The safety profile was consistent with that previously observed for pembrolizumab in patients with advanced cancer, and no new safety signals were noted.²⁴ These results show that treatment with pembrolizumab offers a clinically meaningful therapeutic option for a subset of patients with previously treated advanced cervical cancer. Given these results, the FDA has granted accelerated approval of pembrolizumab for the treatment of patients with advanced, PD-L1–positive cervical cancer with disease progression on or after chemotherapy, making pembrolizumab the first immunotherapy approved for the treatment of an advanced gynecologic malignancy. Pembrolizumab is currently being tested in combination with concurrent chemoradiotherapy (NCT03144466) and with concurrent versus sequential chemoradiotherapy (NCT02635360) for patients with locally advanced cervical cancer, and with chemotherapy and bevacizumab (NCT03367871) for patients with recurrent, persistent, or metastatic cervical cancer.

ACKNOWLEDGEMENTS

We thank the patients and their families and caregivers for participating in this study, as well as all site personnel and the Merck & Co., Inc. study team; NeoGenomics Laboratories, Inc. for performing tumor PD-L1 assessment; Jan Schellens for collection of the data and provision of study materials and patients; and Aurelien Marabelle for collection of the data, provision of study materials and patients, and supervision of research. Medical writing and editorial assistance was provided by Christine McCrary Sisk and Michele McColgan, both of Merck & Co., Inc., Kenilworth, NJ, USA.

REFERENCES

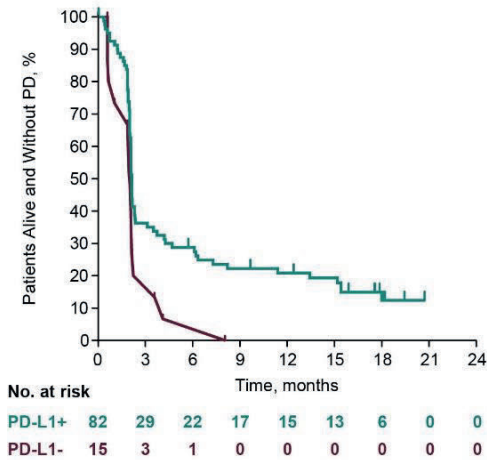
1. Torre LA, Bray F, Siegel RL, et al: Global cancer statistics, 2012. *CA Cancer J Clin* 65:87-108, 2015
2. Pfaendler KS, Tewari KS: Changing paradigms in the systemic treatment of advanced cervical cancer. *Am J Obstet Gynecol* 214:22-30, 2016
3. Thigpen T, Shingleton H, Homesley H, et al: *Cis-Dichlorodiammineplatinum(II)* in the Treatment of Gynecologic Malignancies - phase-II trials by the Gynecologic Oncology Group. *Cancer Treatment Reports* 63:1549-55, 1979
4. Bonomi P, Blessing JA, Stehman FB, et al: Randomized trial of three cisplatin dose schedules in squamous-cell carcinoma of the cervix: a Gynecologic Oncology Group study. *J Clin Oncol* 3:1079-85, 1985
5. Boussios S, Seraj E, Zarkavelis G, et al: Management of patients with recurrent/advanced cervical cancer beyond first line platinum regimens: where do we stand? A literature review. *Crit Rev Oncol Hematol* 108:164-174, 2016
6. Omura GA, Blessing JA, Vaccarello L, et al: Randomized trial of cisplatin versus cisplatin plus mitolactol versus cisplatin plus ifosfamide in advanced squamous carcinoma of the cervix: a Gynecologic Oncology Group study. *J Clin Oncol* 15:165-71, 1997
7. Moore DH, Blessing JA, McQuellon RP, et al: Phase III study of cisplatin with or without paclitaxel in stage IVB, recurrent, or persistent squamous cell carcinoma of the cervix: a Gynecologic Oncology Group study. *J Clin Oncol* 22:3113-9, 2004
8. Long HJ, Bundy BN, Jr ECG, et al: Randomized Phase III trial of cisplatin with or without topotecan in carcinoma of the uterine cervix: a Gynecologic Oncology Group Study. *J Clin Oncol* 23:4626-33, 2005
9. Monk BJ, Sill MW, McMeekin DS, et al: Phase III trial of four cisplatin-containing doublet combinations in stage IVB, recurrent, or persistent cervical carcinoma: a Gynecologic Oncology Group study. *J Clin Oncol* 27:4649-55, 2009
10. Zhu HY, Luo H, Zhang WW, et al: Molecular mechanisms of cisplatin resistance in cervical cancer. *Drug Des Dev Ther* 10:1885-95, 2016
11. Monk BJ, Sill MW, Burger RA, et al: Phase II Trial of bevacizumab in the treatment of persistent or recurrent squamous cell carcinoma of the cervix: a Gynecologic Oncology Group Study. *J Clin Oncol* 27:1069-74, 2009
12. Look KY, Blessing JA, Nelson BE, et al: A phase II trial of isotretinoin and alpha interferon in patients with recurrent squamous cell carcinoma of the cervix: a Gynecologic Oncology Group study. *Am J Clin Oncol* 21:591-4, 1998
13. Mannel RS, Blessing JA, Boike G: Cisplatin and pentoxifylline in advanced or recurrent squamous cell carcinoma of the cervix: a phase II trial of the Gynecologic Oncology Group. *Gynecol Oncol* 79:64-6, 2000
14. Rose PG, Blessing JA, Arseneau J: Phase II evaluation of altretamine for advanced or recurrent squamous cell carcinoma of the cervix: a Gynecologic Oncology Group Study. *Gynecol Oncol* 62:100-2, 1996
15. Bookman MA, Blessing JA, Hanjani P, et al: Topotecan in squamous cell carcinoma of the cervix: a phase II study of the Gynecologic Oncology Group. *Gynecol Oncol* 77:446-9, 2000
16. Rose PG, Blessing JA, Van Le L, et al: Prolonged oral etoposide in recurrent or advanced squamous cell carcinoma of the cervix: a gynecologic oncology group study. *Gynecol Oncol* 70:263-6, 1998
17. Schilder RJ, Blessing JA, Morgan M, et al: Evaluation of gemcitabine in patients with squamous cell carcinoma of the cervix: a phase II study of the Gynecologic Oncology Group. *Gynecol Oncol* 76:204-7, 2000
18. Tewari KS, Sill MW, Long HJ, et al: Improved survival with bevacizumab in advanced cervical cancer. *New Engl J Med* 370:734-743, 2014

19. Okazaki T, Chikuma S, Iwai Y, et al: A rheostat for immune responses: the unique properties of PD-1 and their advantages for clinical application. *Nat Immunol* 14:1212-8, 2013
20. Iwai Y, Ishida M, Tanaka Y, et al: Involvement of PD-L1 on tumor cells in the escape from host immune system and tumor immunotherapy by PD-L1 blockade. *Proc Natl Acad Sci USA* 99:12293-7, 2002
21. Dong H, Strome SE, Salomao DR, et al: Tumor-associated B7-H1 promotes T-cell apoptosis: a potential mechanism of immune evasion. *Nat Med* 8:793-800, 2002
22. Heeren AM, Punt S, Bleeker MC, et al: Prognostic effect of different PD-L1 expression patterns in squamous cell carcinoma and adenocarcinoma of the cervix. *Mod Pathol* 29:753-63, 2016
23. Mezache L, Paniccia B, Nyinawabera A, et al: Enhanced expression of PD L1 in cervical intraepithelial neoplasia and cervical cancers. *Mod Pathol* 28:1594-602, 2015
24. Khoja L, Butler MO, Kang SP, et al: Pembrolizumab. *J Immunother Cancer* 3:36, 2015
25. Frenel JS, Le Tourneau C, O'Neil B, et al: Safety and efficacy of pembrolizumab in advanced, programmed death ligand 1-positive cervical cancer: results from the phase Ib KEYNOTE-028 trial. *J Clin Oncol* 35:4035-41, 2017
26. Clopper C, Pearson S: The use of confidence or fiducial limits illustrated in the case of the binomial. *Biometrika* 26:404-13, 1934
27. Kaplan EL, Meier P: Nonparametric estimation from incomplete observations. *J Amer Statist Assoc* 53:457-81, 1958
28. Tewari KS, Sill MW, Penson RT, et al: Bevacizumab for advanced cervical cancer: final overall survival and adverse event analysis of a randomised, controlled, open-label, phase 3 trial (Gynecologic Oncology Group 240). *Lancet* 390:1654-63, 2017
29. Lheureux S, Butler MO, Clarke B, et al: Association of ipilimumab with safety and antitumor activity in women with metastatic or recurrent human papillomavirus-related cervical carcinoma. *JAMA Oncol* 4:e173776, 2018
30. Hollebecque A, Meyer T, Nadine Moore K, et al: An open-label, multicohort, phase 1/2 study of nivolumab in patients with virus-associated tumors (CheckMate 358): efficacy and safety in recurrent or metastatic cervical, vaginal, and vulvar cancers. Presented at American Society of Clinical Oncology Annual Meeting, Chicago, IL, June 2-6, 2017 (abstr 5504).
31. De Felice F, Marchetti C, Palaia I, et al: Immune check-point in cervical cancer. *Crit Rev Oncol Hematol* 129:40-3, 2018
32. Minion LE, Tewari KS: Cervical cancer - state of the science: from angiogenesis blockade to checkpoint inhibition. *Gynecol Oncol* 148:609-21, 2018
33. Chauhan SR, Bharadwaj M: Gearing up T-cell immunotherapy in cervical cancer. *Curr Probl Cancer* 42:175-88, 2018

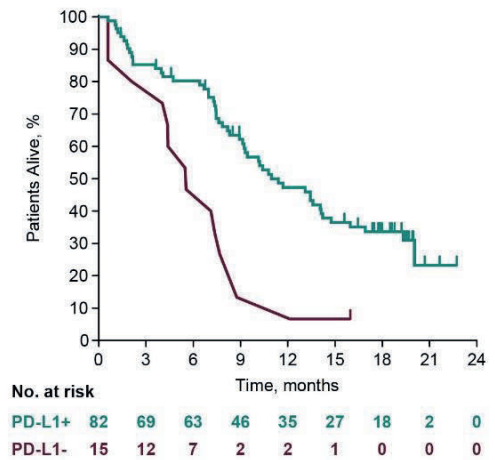
Supplementary Materials

Figure S1. Kaplan-Meier estimates of survival. A. Progression-free survival by baseline PD-L1 status assessed by RECIST v1.1 per independent central review. B. Progression-free survival in the PD-L1-positive tumor population who had previously received ≥ 1 line of chemotherapy for recurrent or metastatic disease (N=77) assessed by RECIST v1.1 per independent central review. C. Overall survival by baseline PD-L1 status. D. Overall survival in the PD-L1-positive tumor population who had previously received ≥ 1 line of chemotherapy for recurrent or metastatic disease (N=77). RECIST, Response Evaluation Criteria in Solid Tumors. PD, progressive disease.

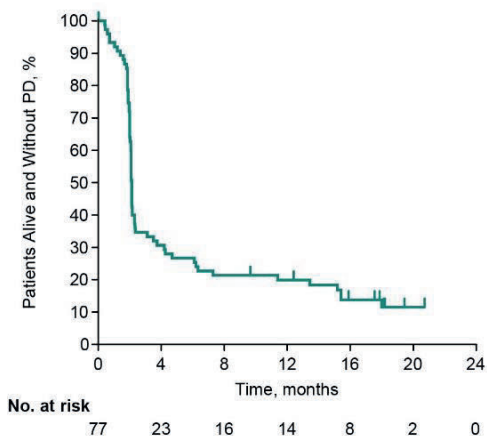
A. PFS by baseline PD-L1 status



C. OS by baseline PD-L1 status



B. PFS in the PD-L1-positive tumor population who had previously received ≥ 1 line of chemotherapy for recurrent or metastatic disease (N = 77)



D. OS in the PD-L1-positive tumor population who had previously received ≥ 1 line of chemotherapy for recurrent or metastatic disease (N = 77)

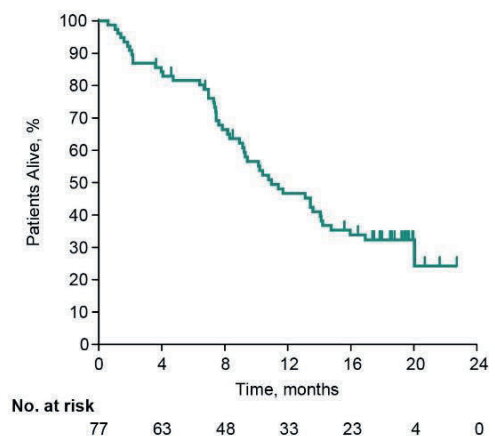


Table S1. Study Sites and Investigators Who Participated in KEYNOTE-158 Cervical Cohort

Country	Site Name	Principal Investigator
Australia	Royal Brisbane & Women's Hospital	Burge, Matthew
	Western Sydney Local Health District	Gao, Bo
	Peter MacCallum Cancer Institute	Mileshkin, Linda
Brazil	Instituto do Cancer de Sao Paulo - ICESP	Bariani, Giovanni Mendonca
Canada	Princess Margaret Cancer Centre	Hansen, Aaron
	Jewish General Hospital	Miller, Wilson
Denmark	Odense Universitetshospital	Pfeiffer, Per
	Herlev og Gentofte Hospital.	Soerensen, Peter
France	Centre Leon Berard	Cassier, Philippe
	Institut Claudius Regaud IUCT-Oncopole	Delord, Jean-Pierre
	Institut Bergonie	Italiano, Antoine
	Institut Gustave Roussy	Marabelle, Aurelien
	Centre Oscar Lambret	Penel, Nicolas
Germany	Klinikum Rechts der Isar	Kiechle, Marion
Israel	Sourasky Medical Center	Geva, Ravit
	Rambam Health Care Campus	Perets, Ruth
	Sheba Medical Center	Shapira Frommer, Ronnie
	Rabin Medical Center	Stemmer, Salomon
Italy	Istituto Nazionale Tumori Fondazione Pascale	Ascierto, Paolo
	Policlinico Le Scotte - A.O. Senese	Maio, Michele
	Istituto Clinico Humanitas	Santoro, Armando
Japan	National Cancer Center Hospital East	Doi, Toshihiko
	Kinki University Hospital	Nakagawa, Kazuhiko
	National Cancer Center Hospital	Tamura, Kenji
Netherlands	Erasmus MC	Lolkema, Martijn
	Antoni van Leeuwenhoek Ziekenhuis	Schellens, J.H.M.
Norway	Oslo Universitetssykehus Radiumhospitalet	Guren, Tormod
	Helse Bergen HF - Haukeland univeritetssykehus	Jebsen, Nina
Russia	Medical Rehabilitation Center	Arkipov, Alexander
	Evimed LLC	Gladkov, Oleg
	Russian Oncological Research Center A	Manzuk, Lyudmila
South Korea	Seoul National University Hospital	Bang, Yung-Jue
	Yonsei University Severance Hospital	Chung, Hyun Cheol
Spain	Hospital General Universitari Vall d'Hebron	Elez, Elena
	Hospital Universitario 12 de Octubre	Lopez Martin, Jose
Taiwan	Koo Foundation Sun Yat-Sen Cancer Center	Liu, Mei-Ching
UK	Royal Marsden NHS Foundation Trust	Lopez, Juanita
USA	University of California - San Francisco	Bergsland, Emily
	Mayo Clinic, Rochester, MN	McWilliams, Robert
	MD Anderson Cancer Center	Piha-Paul, Sarina
	Ohio State University Comprehensive Cancer Center	Shah, Manisha
	Maryland Oncology Hematology, Inc	Wallmark, John

Table S2. Previous therapies and localization of target lesions in patients whose best overall response was complete or partial response (n=12)

Responder Number	Chemotherapy Type(s)	Number of Lines	Previous Radiation Therapy	Previous Bevacizumab	Localization of Target Lesions
1	Cisplatin, Carboplatin, Paclitaxel	2	Y	Y	Periaortic node
2	Carboplatin, Paclitaxel	1	Y	N	Cervix, multiple intra- and extra-abdominal nodes, skin
3	Cisplatin, Vincristine, Carboplatin, Paclitaxel, Topotecan hydrochloride	2	Y	N	Lung
4	Cisplatin, Topotecan	4	Y	N	Lung
5	Cisplatin, Carboplatin, Paclitaxel	1	Y	N	Thoracic and supraclavicular nodes
6	Capecitabine, Cisplatin, Carboplatin, Paclitaxel, Irinotecan hydrochloride, Gemcitabine, Topotecan	5+	Y	Y	Lung, thoracic and intraabdominal nodes
7	Cisplatin	Neo djuvant	Y	N	Cervix
8	Cisplatin, Fluorouracil, Topotecan	1	N	N	Pulmonary node
9	Carboplatin, Paclitaxel	1	Y	N	Multiple intraabdominal lesions
10	Cisplatin, Carboplatin, Fluorouracil, Paclitaxel	2	Y	N	Lung
11	Cisplatin, Carboplatin, Paclitaxel	2	Y	N	Intra- and extra-abdominal nodes
12	Irinotecan hydrochloride, Nedaplatin	1	N	N	Cervix

Chapter 3.2

Preliminary efficacy and safety of pembrolizumab in selected advanced solid tumors.

An interim analysis of study KEYNOTE-158 of patients treated at the Netherlands Cancer Institute.

Willeke Ros

Preliminary results of KEYNOTE-158 have been presented at the American Society of Clinical Oncology (ASCO) annual congress 2018:

Chung HC, Schellens JHM, Delord J-P, Perets R, Italiano A, Shapira-Frommer R, Manzuk L, Piha-Paul SA, Wang J, Zeigenfuss S, Pruitt SK, Marabelle A. Pembrolizumab treatment of advanced cervical cancer: Updated results from the phase 2 KEYNOTE-158 study.

Journal of Clinical Oncology 2018;36:5522

Chung HC, Lopez-Martin JA, Kao SC-H, Miller WH, **Ros W**, Gao B, Marabelle A, Gottfried M, Zer A, Delord J-P, Penel N, Jalal SI, Xu L, Zeigenfuss S, Pruitt SK, Piha-Paul SA. Phase 2 study of pembrolizumab in advanced small-cell lung cancer (SCLC): KEYNOTE-158.

Journal of Clinical Oncology 2018;36:8506.

ABSTRACT

Objectives: In study KEYNOTE-158, the safety and efficacy of pembrolizumab in advanced rare cancers was assessed. A total of ten rare cancers were selected, as well as microsatellite instability high (MSI-H) tumors. Here, we present preliminary results from patients treated at the Netherlands Cancer institute.

Methods: KEYNOTE-158 was a non-randomized, single arm, multi-center, open-label trial with various tumor cohorts. Patients were treated with 200 mg pembrolizumab every 3 weeks. Response was assessed every 9 weeks for the first 12 months and every 12 weeks thereafter, according to RECIST version 1.1. Adverse events (AEs) were assessed using CTCAE version 4.0.

Results: At the Netherlands Cancer Institute, twenty-eight patients were enrolled in the cohorts small cell lung cancer, mesothelioma, cervical carcinoma, biliary carcinoma, thyroid carcinoma, vulvar carcinoma, anal carcinoma, neuro-endocrine tumors and microsatellite instability-high (MSI-H) tumors. At the data cut-off of 8 March 2018, eight patients were still on treatment. Objective response rate was 25.0% (95% CI, 10.7%, 44.9%); two patients achieved a confirmed complete response, five patients achieved a confirmed partial response and four patients had confirmed stable disease. Adverse events (AEs) possibly related to treatment were experienced by 24 patients (85.7%). The most common related AEs were diarrhea (18%), nausea (14%), pruritus (14%), and fatigue (11%). Four patients (14%) experienced grade 3-4 AEs. One AE, G4 subdural hematoma, led to study discontinuation.

Conclusion: Pembrolizumab was well-tolerated and demonstrated promising durable anti-tumor responses in various tumor types.

INTRODUCTION

Pembrolizumab is a humanized monoclonal antibody that blocks the interaction between programmed cell death protein 1 (PD-1) and its ligands, programmed death-ligand 1 (PD-L1) and programmed death-ligand 2. The PD-1 pathway plays an important role in the downregulation of the immune system and avoids autoimmunity[1]. Tumors exploit this pathway by upregulating PD-L1 on their surface, thereby preventing the immune system from eradicating the tumor cells[2]. By blocking the PD-1 pathway, the immunomodulatory signal is inhibited and this allows the T-cells to continue their cytotoxic activity against the tumor.

Pembrolizumab has been approved for a wide variety of tumors, including non-small cell lung cancer, melanoma, classical Hodgkin's lymphoma, advanced gastric cancer, microsatellite instability-high (MSI-H) cancer, cervical cancer, head and neck squamous cell cancer, hepatocellular carcinoma, primary mediastinal B-cell lymphoma, merkel cell carcinoma, and urothelial carcinoma. Study KEYNOTE-158 (KN158) aims to further explore pembrolizumab treatment across tumor types. KN158 focusses on rare malignant diseases with a high unmet medical need. Ten rare malignancies are investigated in this trial, including anal, endometrial, cervical, vulvar, thyroid, biliary and salivary gland carcinoma, neuroendocrine tumors, small cell lung cancer, mesothelioma, and non-colorectal cancer (CRC) MSI-H tumors. In these rare malignancies, response rates in the second-line setting are either low or, due to the inability to conduct large trials, uncertain at this time. In the KEYNOTE-028 (KN028) study, the efficacy and safety of pembrolizumab was studied in twenty different cancers, including the cancers included in the current study. The initial results of KN028 indicate good tolerability of pembrolizumab and promising antitumor activity[3–8].

KN158 (ClinicalTrials.gov identifier NCT02628067) is a non-randomized, multi-center, open label phase II study designed to evaluate the safety and preliminary anti-tumor activity of pembrolizumab in ten selected tumor types and non-colorectal cancer (CRC) microsatellite instability-high (MSI-H) tumors. The trial further assesses the anti-tumor effects of pembrolizumab in a selection of the tumor types of KN028. Here, we report the results of the patients enrolled in KN158 who were treated at the Netherlands Cancer Institute between 01 March 2016 and 08 March 2018. In total, 28 patients were enrolled in the cohorts anal carcinoma, biliary adenocarcinoma, neuroendocrine tumors, cervical carcinoma, vulvar carcinoma, small cell lung carcinoma, mesothelioma, thyroid carcinoma, and MSI-H Cancers.

METHODS

Patient population

Key eligibility requirements included presence of histologically or cytologically-documented advanced metastatic and/or unresectable solid cancer incurable and for which prior standard treatment was failed or did not exist, progression on or intolerance to therapies known to provide clinical benefit, ≥ 18 years of age, adequate bone marrow, renal and hepatic function, life expectancy of at least three months, measurable disease based on RECIST V1.1., ECOG PS of 0 or 1, and availability of an evaluable tumor sample for

biomarker assessments. Key exclusion criteria included prior anticancer monoclonal antibody therapy within 4 weeks of treatment initiation, prior chemotherapy, targeted small-molecule therapy, or radiation therapy within 2 weeks of treatment initiation, prior treatment with an anti-PD-1, anti-PD-L1, or anti-PD-L2 therapy or other immune checkpoint inhibitor, known active CNS metastases, diagnosis of immunodeficiency, autoimmune disease, interstitial lung disease, or active infection requiring systemic therapy, and known severe hypersensitivity to pembrolizumab and/or any of its excipients.

The study was conducted according to Good Clinical Practice standards and provisions outlined in the Declaration of Helsinki. The study protocol and all amendments were approved by the appropriate institutional review boards and ethics committees of the participating institutions. All patients provided written informed consent to participate.

Treatment and assessments

Patients received a flat dose of 200 mg pembrolizumab intravenously every three weeks until confirmed disease progression, death, unacceptable toxicity or withdrawal of consent. Tumor imaging was performed every 9 weeks for the first 12 months and every 12 weeks thereafter using CT or MRI. Adverse events were monitored throughout the study period and graded according to the National Cancer Institute's Common Terminology Criteria for Adverse Events (CTCAE v4.0)

Table 1. Patient characteristics. Continuous values are reported as median [range].

Demographic characteristic	Total (n=28)
Age (Years)	58 [31 – 77]
Gender (n, %)	
Male	11 (39.3%)
Female	17 (60.7%)
WHO PS (%)	
0	12 (42.9%)
1	16 (57.1%)
Tumor Type (n)	
Anal Squamous Cell Carcinoma	4
Biliary Adenocarcinoma	4
Neuroendocrine Tumors	1
Cervical Squamous Cell Carcinoma	6
Vulvar Squamous Cell Carcinoma	2
Small Cell Lung Carcinoma	5
Mesothelioma	1
Thyroid Carcinoma	2
MSI High solid tumor (non-colorectal)	3
Prior lines of therapy for advanced disease (median)	1 [0-4]

Outcomes

The primary efficacy endpoint is objective response rate (ORR), defined as the percentage of patients with confirmed complete response and partial response according to RECIST v.1.1 by blinded independent central review. Subjects with unknown or missing response information were to be considered as non-responders. Secondary efficacy endpoints include progression-free survival (PFS), overall survival (OS), and duration of response (DOR). PFS was defined as time from allocation to the first documented disease progression according to RECIST v1.1 or death due to any cause, whichever occurred first. OS was defined as time from allocation to death due to any cause. DOR was defined as time from first evidence of response per RECIST to disease progression in patients who achieved a confirmed partial response or better.

Safety was monitored by collection of adverse events (AEs) graded according to CTCAE V4.0, laboratory evaluation and assessment of ECOG performance status, vital signs and physical examinations.

Statistical analysis

The efficacy population included all patients with at least one radiological assessment after start of treatment. The safety population included all patients who received ≥ 1 dose of pembrolizumab. Results were summarized using descriptive statistics. The Kaplan–Meier method was used to estimate PFS, OS, and DOR. The data cutoff date for this report was 8 March 2018.

RESULTS

Baseline Patient Characteristics

Twenty-eight patients were enrolled between 01 March 2016 and 08 March 2018 (Table 1). Patients were enrolled in the cohorts anal squamous cell carcinoma ($n = 4$), biliary adenocarcinoma ($n = 4$), neuroendocrine tumors ($n = 1$), cervical squamous cell carcinoma ($n = 6$), vulvar squamous cell carcinoma ($n = 2$), small cell lung carcinoma ($n = 5$), mesothelioma ($n = 1$), thyroid carcinoma ($n = 2$), and MSI-H solid tumors ($n = 3$). The median age was 58 years (range 31-77 years), 17 patients (60.7%) were women, and 42.9% had a ECOG performance of 0. The median number of prior lines for advance disease was 1. At the time of data cut-off of 08 March 2018, eight patients were still on-study, being on treatment for at least 8 months.

Antitumor Activity

Seven out of twenty-eight patients (25.0%; 95% CI, 10.7%, 44.9%) showed a confirmed objective response according to RECIST v1.1 (Figure 1 and Table 2). Complete and partial responses were seen in anal, cervical, small cell lung cancer (SCLC), and MSI-H tumors. Median DOR was not reached, as all seven patients who showed a confirmed response were still on study with ongoing response at time of data cutoff [5.8+ – 20.4+ months]. At the time of data cutoff, 85% of responses were ongoing for 6+ months, and 71% were ongoing for 12+ months. The disease control rate was 39.3% (95% CI, 21.5%, 59.4%).

Confirmed complete responses were seen in two patients: a patient with poorly differentiated squamous cell carcinoma of the anal canal, and a patient with MSI-H small bowel adenocarcinoma. The patient with anal carcinoma had intracerebral metastases and lung metastases. This patient had received one prior line of treatment consisting of mitomycin-C and capecitabine. The patient with MSI-H small bowel carcinoma had peritoneal metastases. This patient had no prior lines of therapy for metastatic disease. Both patients remained on treatment as of the data cutoff date and were on study for 21+ (anal canal carcinoma) and 8+ (MSI-H small bowel carcinoma) months.

Confirmed partial responses were seen in five patients in total (17.9%; 95% CI, 6.1%, 36.9%): two cervical cancer patients both showing a reduction of target lesions of 74% , one SCLC patient showing a reduction of 79%, one patient with anal canal carcinoma showing a reduction of 34%, and one patient with MSI-H adenocarcinoma of the cardia showing a reduction of 48%. In addition, one cervical cancer patient had a non-confirmed PR.

Four patients had confirmed stable disease as best response (14.3%; 95% CI, 4.0%, 32.7%). The median duration of SD was 8.1 months [4.2 – 11.3]. Thirteen patients had progressive disease (46.4%; 95% CI, 27.5%, 66.1%). Four patients were not evaluable for efficacy: three patients discontinued before the first tumor assessment due to clinical disease progression or death, and another patient had target lesions which were unreliable to radiological evaluation.

Overall, the median PFS was 3.6 months [0.6 - > 21 months] and the median overall survival was 8.7 months [0.6 -> 21 months] (Figure 2). Patients received a median of 8 [4-35] cycles.

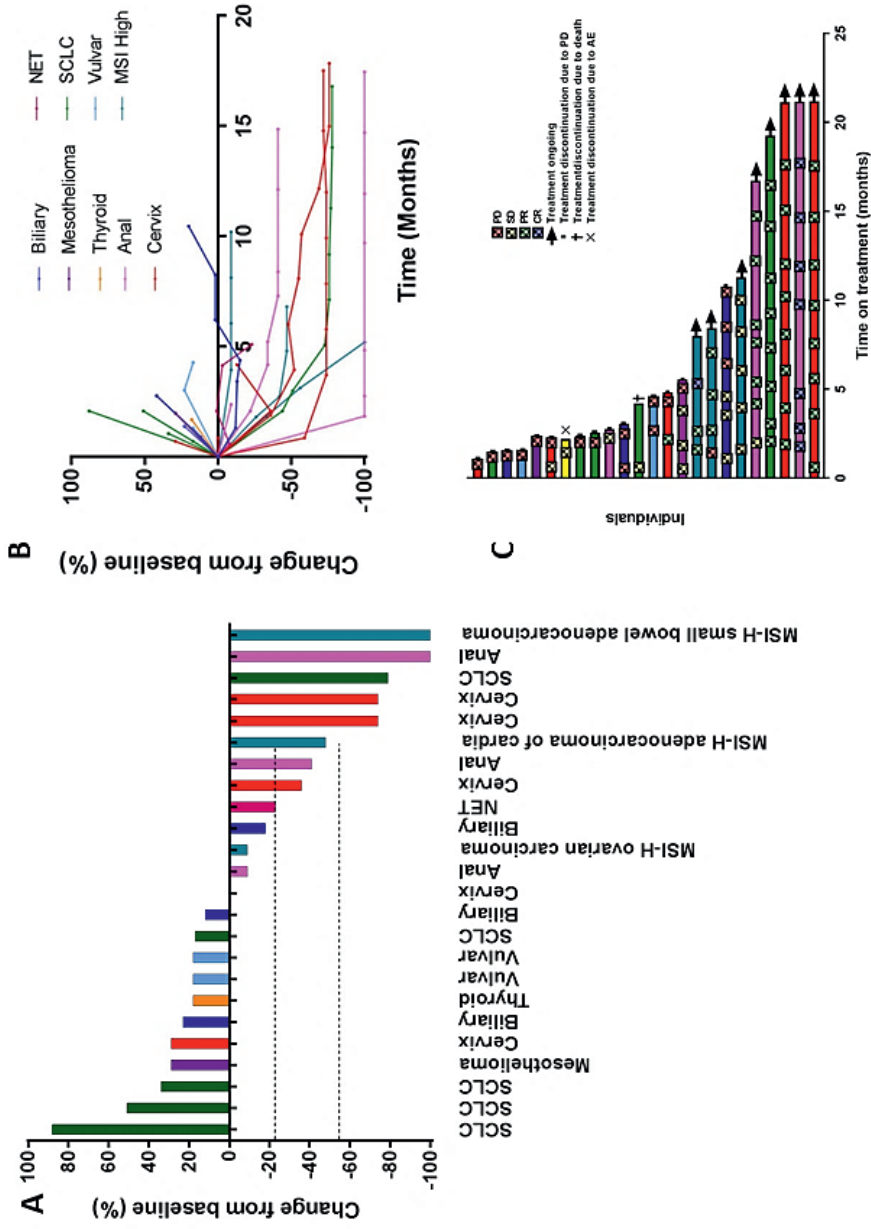
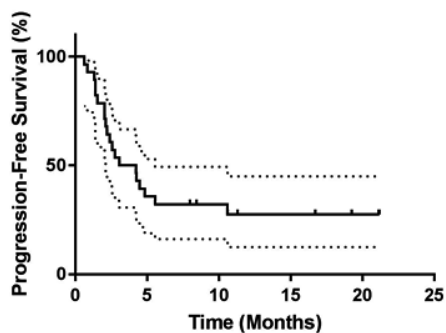


Figure 1. (A) Best change from baseline in tumor size (n=24). Dotted lines at 20% and -30% indicate progressive disease and partial response, respectively. (B) Longitudinal change from baseline in tumor size (n=24). (C) Treatment exposure and duration of response (n = 24). The length of the bars corresponds with time to the last tumor assessment.

Table 2. Best Objective Response Assessed by RECIST (version 1.1.) (n=28). Only confirmed responses are reported

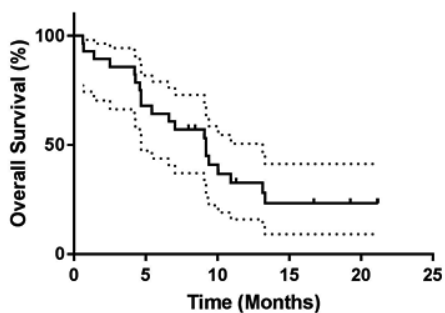
Best Objective Response	No.	%	95% CI
Objective response rate	7	25.0%	10.7% - 44.9%
Complete response	2	7.1%	0.9% - 23.5%
Partial response	5	17.9%	6.1% - 36.9%
Stable disease	4	14.3%	4.0% - 32.7%
Progressive Disease	13	46.4%	27.5% - 66.1%
Non evaluable	4	14.3%	4.0% - 32.7%

A



Month	0	5	10	15	20
No. at risk	28	11	8	6	4

B



Month	0	5	10	15	20
No. at risk	28	21	11	6	4

Figure 2. Kaplan-Meier estimates. (A) Progression-free survival. (B) Overall survival.

Safety

Twenty-four patients (85.7%) experienced adverse events at least possibly related to study drug (Table 3). The most common AEs at least possibly related to treatment include diarrhea (18%, n=5), nausea (14%, n=4), pruritus (14%, n=4), and fatigue (11%, n=3). Six grade 3-4 AEs at least possibly related to treatment were observed, including ALAT increase (n=2), ASAT increase (n=1), fever (n=1), subdural hematoma (n=1) and worsening of anemia (n=1). Immune-related events include G1 hypothyroidism (n=2), G1 pruritus (n=4) and G3 ASAT (n=2)/ALAT(n=1) increase. The G3 ASAT and ALAT increase occurred in a patient with gallbladder carcinoma with liver metastases. Elevation of liver enzymes was measured three weeks after the first pembrolizumab administration. Abdominal ultrasound was performed and showed no progression of liver metastases, no portal vein thrombosis and no cholestasis. The patient developed hepatitis, and showed reactivation of cytomegalovirus. This reactivation was considered likely related to study medication, and valganciclovir was given. ASAT and ALAT restored to baseline values approximately eight weeks after pembrolizumab administration and treatment was continued. No elevation of ASAT and ALAT was observed during subsequent cycles.

A patient with thyroid cancer developed subdural hematoma. This patient had no known history of head trauma or hypertension. The grade 4 subdural hematoma occurred after four cycles of pembrolizumab. No signs of brain metastases were detected by MRI. The event was considered possibly related to study treatment and led to study drug discontinuation. There were no treatment related deaths as of the data cutoff date.

Table 3. Adverse events at least possibly related to pembrolizumab.* Immune-related toxicities of special interest.**Led to study discontinuation.

Any-grade adverse events occurring in ≥ 2 patients , n (%)	N
Abdominal pain	2 (7%)
Anemia	2 (7%)
Arthralgia	2 (7%)
Creatinine increase	2 (7%)
Diarrhea	5 (18%)
Fatigue	3 (11%)
Hypothyroidism*	2 (7%)
Maculopapular rash	2 (7%)
Myalgia	2 (7%)
Nausea	4 (14%)
Pruritus*	4 (14%)
Weight loss	2 (7%)
Grade 3-4 adverse events occurring in ≥ 1 patient, n (%)	
ASAT increase (Grade 3)*	2 (7%)
ALAT increase (Grade 3)*	1 (4%)
Fever (Grade 3)	1 (4%)
Subdural hematoma** (Grade 4)	1 (4%)
Worsening of anemia (Grade 3)	1 (4%)

DISCUSSION AND CONCLUSION

We investigated the safety and efficacy of pembrolizumab in selected advanced tumor types, as well as in MSI-H tumors enrolled in the KN158 study at the Netherlands Cancer Institute. Treatment was well-tolerated, and tumor responses were seen across various tumor types, in particular in anal carcinoma, cervical carcinoma, SCLC and MSI-H tumors.

Two out of the four patients with anal canal carcinoma showed a tumor response. One patient obtained a complete response and one patient obtained a durable partial response (>16 months) with a tumor reduction up to 40.4%. The efficacy of pembrolizumab in anal canal carcinoma has previously been investigated in the KN028 study[7]. Among 24 patients with PD-L1 positive tumors, four patients had confirmed partial responses, for an overall response rate of 17%. PD-L1 positivity was used as a selection criteria in this study. During screening, PD-L1 positivity (defined as $\geq 1\%$ of cells expressing PD-L1) was found to be high (74%) in anal carcinoma.

Two out of six patients with cervical cancer enrolled in the KN158 study at the Netherlands Cancer Institute showed a durable partial response. Both patients showed a tumor reduction of 74% and were still ongoing for >21 months at the data cut off. Interestingly, preliminary results of the 47 patients with cervical cancer (including the six above mentioned patients treated at the Netherlands Cancer Institute) enrolled in the KN158 study showed an ORR of 17% with three confirmed responses and one unconfirmed response[9]. Forty-one (87%) patients had PD-L1 positive tumors (defined as $\geq 1\%$ of cells expressing PD-L1) and ORR appeared to be independent of PD-L1 status. In KN028, the ORR among 24 PD-L1 positive patients was 17%[5].

One out of five SCLC patients (20%) treated at the Netherlands Cancer Institute showed a durable (>19 months) partial response. The interim results of SCLC patients enrolled at the Netherlands Cancer Institute are in line with the preliminary results reported in the overall SCLC cohort of the KN158 study (i.e., including other study sites) where an ORR of 18.7% was observed at the interim analysis[10]. Responses were predominantly seen in patients who were positive for PD-L1 (35.7% compared to 6% for PD-L1 negative). However, PD-L1 negativity did not rule out the possibility of tumor response, as a CR was reported in a PD-L1 negative patient. In KN028, 31.7% of patients were positive for PD-L1 expression. In these PD-L1 positive SCLC patients, the ORR was 33%[11].

Responses were seen in two out of three patients with MSI-H tumors. One patient with small bowel carcinoma obtained a CR, one patient with adenocarcinoma of the gastroesophageal junction obtained a PR (tumor reduction up to 48%), and one patient with ovarian carcinoma obtained stable disease of > 11 months (tumor reduction up to 8%). All these patients were still on treatment at the time of data cut-off. Of note, interim results of the 21 patients with MSI-H non-CRC tumor types (including the 3 above mentioned patients treated at the Netherlands Cancer Institute) enrolled in the KN158 study showed an ORR of 42.9%, with eight confirmed and one unconfirmed response[12].

Pembrolizumab is thought to be most effective in tumors that are inflamed, i.e. are infiltrated by tumor infiltrating lymphocytes, contain active CD8+ T cells, express PD-L1, and show genomic instability[13]. The tumor types in which anti-tumor responses are observed in this

interim analysis of the 28 patients enrolled at the Netherlands Cancer Institute present these characteristics.

Both cervical and anal cancers show high rates of PD-L1 positivity in the tumor, suggesting that these tumors are immunologically active[13]. The high rate of PD-L1 positivity might be correlated with the high incidence of human papillomavirus (HPV) infection in these cancer types. HPV has been detected in >70% of cervical and anal cancers[14, 15]. HPV-induced cancers are characterized by an active immune response against HPV, and a high incidence of lymphocyte infiltration in the tumor[16]. Furthermore, HPV infection may lead to the production of neo-antigens[17]. Neo-antigens have the potential to be recognized by the immune system and may trigger an anti-tumor immune response[18].

SCLC is one of the most immunogenic tumor types, as it is often caused by carcinogenic external factors, such as smoking and asbestos. These external factors increase the mutational burden which, similarly to HPV infection, may lead to production of neo-antigens. Notably, response rates for SCLC have been shown to be higher in smokers compared to non-smokers[19].

MSI-H and dMMR tumors show genomic instability and harbor a high number of mutations which have the potential to stimulate the immune system through production of neo-peptides which, when presented by MHC-proteins, may be immunogenic[20]. Pembrolizumab has been recently approved by the US FDA for MSI-H and dMMR tumors, independently of tumor type[21].

Biomarker analysis has not been described in this interim analysis, but it is being performed. Indeed, a tumor specimen has been collected in all patients before inclusion for assessment of MSI status, gene expression profiling, and PD-L1 expression.

In conclusion, the interim/preliminary results of pembrolizumab monotherapy in the 28 patients enrolled in the KN158 study at the Netherlands Cancer Institute show promising antitumor activity and a manageable safety profile. The study is still currently ongoing, with the large majority of cohorts having completed inclusion. Study completion is expected to be finished in August 2023.

ACKNOWLEDGEMENTS

We thank all patients and their families for participating; Merck Sharp & Dohme Corp., a subsidiary of Merck & Co., Inc., Kenilworth, NJ, USA for sponsoring; and the Clinical Pharmacology Department of The Netherlands Cancer Institute for conducting this trial.

REFERENCES

1. Dai S, Jia R, Zhang X et al. The PD-1/PD-Ls pathway and autoimmune diseases. *Cell. Immunol.* 2014; 290:72–79.
2. Iwai Y, Ishida M, Tanaka Y et al. Involvement of PD-L1 on tumor cells in the escape from host immune system and tumor immunotherapy by PD-L1 blockade. *Proc. Natl. Acad. Sci. U. S. A.* 2002; 99:12293–12297.
3. Cohen RB, Delord J-P, Doi T et al. Pembrolizumab for the Treatment of Advanced Salivary Gland Carcinoma. *Am. J. Clin. Oncol.* 2018; 41:1083–1088.
4. Ott PA, Elez E, Hirt S et al. Pembrolizumab in Patients With Extensive-Stage Small-Cell Lung Cancer: Results From the Phase Ib KEYNOTE-028 Study. *J. Clin. Oncol.* 2017; 35:3823–3829.
5. Frenel J-S, Le Tourneau C, O'Neil B et al. Safety and Efficacy of Pembrolizumab in Advanced, Programmed Death Ligand 1–Positive Cervical Cancer: Results From the Phase Ib KEYNOTE-028 Trial. *J. Clin. Oncol.* 2017; 35:4035–4041.
6. Alley EW, Lopez J, Santoro A et al. Clinical safety and activity of pembrolizumab in patients with malignant pleural mesothelioma (KEYNOTE-028): preliminary results from a non-randomised, open-label, phase 1b trial. *Lancet Oncol.* 2017; 18:623–630.
7. Ott PA, Piha-Paul SA, Munster P et al. Safety and antitumor activity of the anti-PD-1 antibody pembrolizumab in patients with recurrent carcinoma of the anal canal. *Ann. Oncol.* 2017; 28:1036–1041.
8. Ott PA, Bang Y-J, Berton-Rigaud D et al. Safety and Antitumor Activity of Pembrolizumab in Advanced Programmed Death Ligand 1–Positive Endometrial Cancer: Results From the KEYNOTE-028 Study. *J. Clin. Oncol.* 2017; 35:2535–2541.
9. Schellens JHM, Marabelle A, Zeigenfuss S et al. Pembrolizumab for previously treated advanced cervical squamous cell cancer: Preliminary results from the phase 2 KEYNOTE-158 study. *J. Clin. Oncol.* 2017; 35:5514.
10. Chung HC, Lopez-Martin JA, Kao SC-H et al. Phase 2 study of pembrolizumab in advanced small-cell lung cancer (SCLC): KEYNOTE-158. *J. Clin. Oncol.* 2018; 36:8506.
11. Ott PA, Elez E, Hirt S et al. Pembrolizumab in Patients With Extensive-Stage Small-Cell Lung Cancer: Results From the Phase Ib KEYNOTE-028 Study. *J. Clin. Oncol.* 2017; 35:3823–3829.
12. Diaz LA, Marabelle A, Delord J-P et al. Pembrolizumab therapy for microsatellite instability high (MSI-H) colorectal cancer (CRC) and non-CRC. *J. Clin. Oncol.* 2017; 35:3071.
13. Hegde PS, Karanikas V, Evers S. The Where, the When, and the How of Immune Monitoring for Cancer Immunotherapies in the Era of Checkpoint Inhibition. *Clin. Cancer Res.* 2016; 22:1865–1874.
14. De Vuyst H, Clifford GM, Nascimento MC et al. Prevalence and type distribution of human papillomavirus in carcinoma and intraepithelial neoplasia of the vulva, vagina and anus: a meta-analysis. *Int. J. cancer* 2009; 124:1626–1636.
15. Pirog EC, Lloveras B, Molijn A et al. HPV prevalence and genotypes in different histological subtypes of cervical adenocarcinoma, a worldwide analysis of 760 cases. *Mod. Pathol.* 2014; 27:1559–1567.
16. Piersma SJ, Welters MJP, van der Hulst JM et al. Human papilloma virus specific T cells infiltrating cervical cancer and draining lymph nodes show remarkably frequent use of HLA-DQ and -DP as a restriction element. *Int. J. cancer* 2008; 122:486–494.
17. Qin Y, Ekmekcioglu S, Forget M-A et al. Cervical Cancer Neoantigen Landscape and Immune Activity is Associated with Human Papillomavirus Master Regulators. *Front. Immunol.* 2017; 8:689.
18. Schumacher TN, Schreiber RD. Neoantigens in cancer immunotherapy. *Science* 2015; 348:69–74.
19. Farago A. Immunotherapy in small cell lung cancer. *J. Thorac. Oncol.* 2016; 11:3–4.
20. Nebot-Bral L, Brandao D, Verlingue L et al. Hypermutated tumours in the era of immunotherapy: The paradigm of personalised medicine. *Eur. J. Cancer* 2017; 84:290–303.
21. Keytruda (pembrolizumab) Prescribing information. U.S. Food and Drug Administration (2015).

Chapter 4

Development of assays for immunotherapy

Chapter 4.1

Enzyme linked immunosorbent assay for the quantification of nivolumab and pembrolizumab in human serum and cerebrospinal fluid

Willeke Ros*, **Dick Pluim***

**Authors contributed equally*

Pluim D*, **Ros W***, van Bussel MTJ, Brandsma D, Beijnen JH, Schellens JHM. Enzyme linked immunosorbent assay for the quantification of nivolumab and pembrolizumab in human serum and cerebrospinal fluid.

Journal of Pharmaceutical and Biomedical Analysis 2019; 164:128–134.

ABSTRACT

Immunotherapy with monoclonal antibodies targeting the programmed-death-1 (PD-1) receptor has become standard of care for an increasing number of tumor types. Pharmacokinetic studies may help to optimize anti-PD-1 therapy. Therefore, accurate and sensitive determination of antibody concentrations is essential. Here we report an enzyme linked immunosorbent assay (ELISA) capable of measuring nivolumab and pembrolizumab concentrations in serum and cerebrospinal fluid (CSF) with high sensitivity and specificity. The assay was developed and validated based on the specific capture of nivolumab and pembrolizumab by immobilized PD-1, with subsequent enzymatic chemiluminescent detection by anti-IgG4 coupled with horse radish peroxidase (HRP). The lower limit of quantification for serum and CSF was 2 ng/mL for both anti-PD-1 agents. The ELISA method was validated and showed long term sample stability of >1 year. This method is reliable, relatively inexpensive and can be used in serum and CSF from pembrolizumab and nivolumab treated patients.

INTRODUCTION

Nivolumab and pembrolizumab are both monoclonal antibodies against Programmed-Death-1 (PD-1), which received FDA and EMA approval for immunotherapeutic treatment of a wide range of tumors including non-small cell lung cancer (NSCLC), melanoma, renal cell, urothelial, and microsatellite instability (MSI) high colorectal cancer. In the phase III trials both compounds showed better response rates with increased overall and progression free survival compared to standard chemotherapy.^{1,2} Furthermore, nivolumab and pembrolizumab were associated with fewer high-grade treatment-related adverse events than other second-line therapy.³ Little is known, however, about the impact of immunotherapy in patients with metastatic disease to the central nervous system. Clinical trials of immunotherapy excluded patients with active brain metastases due to a poor prognosis and uncertainty about the ability of the drugs to cross the blood brain barrier (BBB). However, current studies suggest that systemically administered immunotherapeutic antibodies demonstrate a similar durable response in the brain as in extra-cerebral sites.⁴ Studies with other monoclonal antibodies indicate that median concentrations of monoclonal antibodies may be up to 400-fold lower in the central nervous system (CNS) than in serum, due to the BBB limiting penetration of molecules with molecular weights up to 200 kDa (nivolumab 144 kDa, pembrolizumab 146 kDa).⁴⁻⁶ To the best of our knowledge no data has been published of nivolumab and pembrolizumab levels in cerebrospinal fluid (CSF). CSF is relatively easily accessible, and clinical studies suggest that drug concentrations in CSF are reasonably accurate in predicting CNS exposure.⁷ Therefore, CSF may be used as a surrogate for the interstitial fluid (ISF) in the CNS and may be used for assessing CNS exposure because tumor biopsies are considered unethical to collect for pharmacokinetic purposes.

Monitoring of nivolumab and pembrolizumab concentrations in serum and CSF may enable individualized treatment strategies and lead to a better understanding of pharmacokinetic (PK) –pharmacodynamic (PD) effect relationships of these agents. Puszkiel et al. recently reported the development and validation of an ELISA for the quantification of nivolumab in plasma from NSCLC patients.⁸ This assay has a lower limit of quantification (LLQ) of 5 µg/mL. Although this is sensitive enough for the quantification of trough plasma levels, a more sensitive assay is needed for the quantification in CSF. A five-fold more sensitive Liquid Chromatography–Mass Spectrometry (LC/MS) method has been developed that shows a LLQ of 0.977 µg/mL.⁹ Although this method is more sensitive, it may still be not possible to accurately determine trough concentrations in CSF. In addition, LC/MS is unable to show if the measured antibodies are functionally active. Furthermore, this assay relies on costly lab equipment that is not readily available at standard clinical laboratories. When properly optimized, chemiluminescent ELISA is one of the most sensitive immunoassays available with typical detection ranges of 0.01–0.04 fmole per mL.¹⁰ Here, we report the successful development and validation of an ELISA with a lower limit of quantification of 2 ng/mL, which enables the accurate quantification of both nivolumab and pembrolizumab in serum and CSF. The applicability of the presented assay is demonstrated with the analysis of serum and CSF samples from cancer patients treated with these drugs.

MATERIALS AND METHODS

Reagents and chemicals

BD Vacutainer® SST II 5 mL tubes were obtained from Becton Dickinson (Franklin lakes, NJ, USA). Ficoll-paque™ PLUS was obtained from General Electric Healthcare (Little Chalfont, UK). Nunc MaxiSorp™ white 96-well plates were purchased from VWR (Amsterdam, the Netherlands). Phosphate buffered saline (PBS) was purchased from GIBCO BRL (Gaithersburg, MD, USA). Protifar Plus low fat milk powder (ELK) was from Danone (Amsterdam, the Netherlands). Eppendorf® LoBind micro-centrifuge 2.0 mL tubes, bovine serum albumin (BSA), fetal calf serum (FCS), glycerol, thimerosal, and Tween-20 were purchased from Sigma (St. Louis, MO, USA). PBSTF consisted of PBS with 0.1% (v/v) Tween-20 and 1% (v/v) Ficoll. Ipilimumab, nivolumab and pembrolizumab were a kind gift from the Antoni van Leeuwenhoek hospital pharmacy. Mouse anti-human IgG4 Fc antibody-HRP conjugate originated from Thermo Fisher (Landsmeer, the Netherlands) as 200 µg lyophilized powder per vial, which was stored at -20 °C after reconstitution with 200 µl of 50% (v/v) glycerol, 0.05% (w/v) thimerosal, and 1% (w/v) BSA. Recombinant human PD-1 (His Tag) protein was purchased from Sino Biological Inc. (Beijing, China) as 100 µg of lyophilized powder, which was stored at -80 °C in small aliquots after reconstitution with 5.0 mL PBS. Pierce™ standard Electro Chemical Luminescence (ECL) western blotting substrate was from Pierce (Waltham, MA, USA). The ECL reagent PeroxyGlow™ was from Trevigen (Gaithersburg, MD, US). Biorad Clarity ECL was from Biorad (Veenendaal, the Netherlands). Unless stated otherwise, serum used was pooled from 6 healthy human volunteers.

Nivolumab and pembrolizumab concentrations in the clinical stocks

The concentrations of nivolumab and pembrolizumab in the clinical stock vials were determined spectrophotometrically at 280 nm with a DS-11 (DeNovix, Wilmington, DE, USA) using the following formula:

$$C_{Ab} = 10 \cdot A_{280 \text{ nm}} / (\epsilon_{Ab} \cdot L)$$

A_{280} = measured absorbance of nivolumab and pembrolizumab solution at 280 nm

C_{Ab} = concentration of nivolumab and pembrolizumab (mg/mL)

ϵ_{Ab} = extinction coefficient of human IgG₄ ($13.6 A^{280 \text{ nm}} \cdot 1\%^{-1} \cdot \text{cm}^{-1}$)¹¹

L = optical path length DS-11 (1 cm)

Serum preparation

Blood was collected in 5 mL BD Vacutainer® SST II tubes. Tubes were immediately inverted 5 times. After 30 min of coagulation at room temperature (RT), tubes were centrifuged at 1200 g for 10 min in a swing-out rotor. Next, serum was snap-frozen in liquid nitrogen in 2.0 mL vials before storage at -80 °C.

ELISA

Nunc MaxiSorp™ white 96-well flat-bottom plates were coated overnight at 4 °C with 50 µl of 2 µg/mL PD-1. The next day, wells were emptied and washed 4 times with 300 µl of PBSTF. Standard curves were prepared in 2 mL Eppendorf® LoBind vials on the day of analysis by serial dilution of a 11.0 mg/mL nivolumab clinical stock solution to 100, 50, 20, 10, 5, 2, and 0 ng/mL in ice-cold 10% (v/v) serum in PBSTF. Quality controls (QCs) were prepared from different nivolumab and pembrolizumab stock solutions, independently from the standard curves, at 5, 20, and 160 µg/mL in serum, and stored at -80 °C. On the day of analysis, patient serum and QCs were diluted 10-fold with PBSTF, and CSF was diluted 2-fold with 20% serum (v/v) in PBSTF, in order to have the same 10% serum (v/v) in PBSTF final matrix. If necessary, CSF and serum were additionally diluted 2- and 100-fold, respectively, with 10% (v/v) serum in PBSTF. The 10-fold diluted QCs were additionally diluted 100-fold to 5, 20, and 160 ng/mL with 10% (v/v) serum in PBSTF. Next, QC160 was further diluted 2-fold to 80 ng/mL with 10% serum (v/v) in PBSTF. Patient serum, CSF, and QCs were analyzed as 50 µl duplicates per plate. Samples were added as 50 µl triplicates per plate, which was subsequently sealed and incubated for 2 h at RT. Then, the plate was emptied and washed 4 times with 300 µl of PBSTF. After addition of 50 µl of 1 µg/mL anti-human IgG4-HRP in PBSTF, plates were sealed and incubated for 1 h at RT. Next, plates were emptied and washed 4 times with 300 µl of PBSTF. Subsequently, 100 µl of Pierce standard ECL was added and luminescence was measured within 15 min using a Tecan Infinite 200 Pro plate reader at 1 s per well of read time.

Optimization of anti-human IgG4-HRP concentration

Nivolumab standard curves were prepared at concentrations of 100, 50, 20, 10, 5, 2, and 0 ng/mL in ice-cold 10% (v/v) serum in PBSTF. In triplicate 50 µl of each standard was incubated for 2 h at RT on plate. After 3 washes with 300 µl of PBSTF, 50 µl of 1:500, 1:1000, and 1:2000 in PBSTF diluted anti-human IgG4-HRP was added and incubated for 1 h at RT. Subsequently, the plate was washed and luminescence was measured after addition of ECL, as described in the ELISA section.

Serum matrix effect

The effect of different concentrations of serum on the quantification of nivolumab was determined in triplicate in standard curves prepared in 2 mL Eppendorf® LoBind vials on the day of analysis by serial dilution of 11.0 mg/mL nivolumab clinical stock solution to 100, 50, 20, 10, 5, and 2 ng/mL in ice-cold PBSTF containing 0, 10%, and 20% (v/v) serum. To assess the dilution integrity, nivolumab was spiked in triplicate at 1000 µg/mL in serum and 2 µg/mL in CSF. Next, serum and CSF were diluted 1000 and 2-fold to 1 µg/mL, respectively, as described in ELISA. Further 2-fold serial dilutions with 10% serum (v/v) in PBSTF were then applied to serum and CSF to a final nominal nivolumab concentration of 62.5 ng/mL. The accuracies of the back-calculated nivolumab concentrations relative to the nominal spike concentrations at each serial dilution level were determined.

Specificity and limit of detection

Wells coated with and without PD-1 were incubated in triplicate with 100 μl of 0 and 100 ng/mL nivolumab in PBSTF. Next, plates were washed and incubated with secondary antibody as described under ELISA. After 4 washes, 100 μl of Pierce standard, Biorad Clarity, and Trevigen Peroxyglow™ ECL were added and luminescence was measured. The effect of three of the most commonly used blocking agents was tested. Wells coated with PD-1 were incubated for 3 h at RT with 300 μl of 2% and 5% (w/v) BSA in PBS, 2% and 5% (w/v) ELK in PBS, 40% and 100% (v/v) FCS in PBS, and PBS as negative control. Next, wells were emptied and incubated for 2 h with 50 μl of 10% (v/v) serum in PBSTF. Treatment of nivolumab is sometimes combined with ipilimumab, which is a fully human monoclonal antibody against cytotoxic T-lymphocyte-associated antigen-4 (CTLA-4). Although its target is different, a possible analytical interference cannot be ruled out. Therefore, we spiked 0, 20, and 80 ng/mL of nivolumab in 10% (v/v) serum in PBSTF and 50% (v/v) CSF containing 10% (v/v) serum in PBSTF. After addition of 0, 100, 200, and 500 ng/mL of ipilimumab, these samples were analyzed by ELISA, as described. The limit of detection (LOD) was defined as the average background level plus 5 times the standard deviation and was determined in serum from 10 healthy volunteers and in CSF from 10 immunotherapy naïve cancer patients.

Standard curve fitting

Calibration curves are commonly fit using polynomial or logistic models.¹² We compared the goodness of fit of a quadratic and 4-parameter logistic model on 21 standard curves using Graphpad Prism 6. Net luminescence was calculated as the luminescence of samples minus the average luminescence of the duplicate blank samples. Net luminescence of standards 2–100 ng/mL was plotted against the nominal nivolumab concentration. Curve fits were not forced through 0, and back-calculated concentrations had to be within 15% of the nominal concentrations for all 7 calibration standards.

Lower limit of quantification

The lower limit of quantification (LLQ) was determined in triplicate in ice-cold PBSTF, containing 10% (v/v) serum from 7 different volunteers, spiked with 1, 2, 3, 4, 5 ng/mL of nivolumab or pembrolizumab. CSF from 6 immunotherapy naïve patients was diluted 2-fold with ice-cold PBSTF containing 20% (v/v) serum, which was spiked with 1, 2, 3, 4, and 5 ng/mL of nivolumab or pembrolizumab. The LLQ was defined as the nominal input level at which the nivolumab and pembrolizumab concentrations could be determined with a precision $\leq 20\%$ and an accuracy of 80–120%. Furthermore, the analyte response at the LLQ should be at least five times the response compared to the blank response.

Between- and within-day precision and accuracy

Samples containing 5, 20 or 80 ng/mL nivolumab in 10% (v/v) serum in PBSTF were measured in triplicate on six consecutive days. The between-day (BDP) and within-day precision (WDP) were calculated by one-way analysis of variance (ANOVA) for each spike level using the run day as classification variable using the software package SPSS v15.0 for windows (SPSS, Chicago, USA). The day mean square (DayMS), error mean square (ErrMS) and the grand mean (GM) of the observed concentrations across run days were used.

The WDP% and BDP% for each spike level were calculated using the formulas:

$$\text{WDP}\% = (\text{ErrMS})^{0.5}/\text{GM} \times 100\%$$

$$\text{BDP}\% = [(\text{DayMS} - \text{ErrMS})/n]^{0.5}/\text{GM} \times 100\%$$

With n being the number of replicates within each run.

Accuracy was determined as the relative difference between the nominal input concentration and measured concentration. Imprecisions $\leq 15\%$ and accuracy between 85–115% were considered acceptable.

Pembrolizumab quantification

Standard curves were prepared in 2 mL Eppendorf® LoBind vials on the day of analysis by serial dilution of 11.0 mg/mL nivolumab and 27.8 mg/mL pembrolizumab clinical stock solutions to 100, 50, 20, 10, 5, and 2 ng/mL in ice-cold 10% (v/v) serum in PBSTF. These standards were analyzed in triplicate on three consecutive days. The concentrations of the pembrolizumab standards (Mw = 146,286 Da) were back-calculated from the nivolumab (Mw = 143,597 Da) standard curves. After correction for the 1.87% difference in molecular weight, the back-calculated pembrolizumab concentrations had to be within 15% of the nominal pembrolizumab concentrations.

Stability

To assess the long-term storage stability, nivolumab and pembrolizumab were spiked at 0.1, 1, 10, and 100 $\mu\text{g/mL}$ in serum. This largely covers the whole range of concentrations found in patient serum along the PK curve. Aliquots of 50 μl of spiked serum were snap-frozen in liquid nitrogen and stored for 0, 7, 120, 360, and 480 days at -80°C . At these time points nivolumab and pembrolizumab concentrations were determined in triplicate, after dilution to 50 ng/mL in ice-cold 10% (v/v) serum in PBSTF.

Stability of nivolumab and pembrolizumab at 10 and 50 ng/mL, diluted in ice-cold 10% (v/v) serum in PBSTF, was tested after 0, 6, and 24 h on ice, using freshly prepared nivolumab standard curves.

Freeze-thaw stability was tested for nivolumab and pembrolizumab spiked at 10 and 100 $\mu\text{g/mL}$ in serum. Nivolumab and pembrolizumab concentrations were determined after 0, 1, 2, and 3 snap-freeze/thaw cycles, after dilution to 100 ng/mL with 10% (v/v) serum in PBSTF. Nivolumab and pembrolizumab concentrations were considered stable if the determined concentrations were within 15% of the nominal concentrations.

Clinical applicability

The clinical application of the ELISA method was demonstrated in serum from seven patients treated once every 2 weeks with nivolumab (n = 4) or once every 3 weeks with pembrolizumab (n = 3). Patient 1 received concomitantly ipilimumab at 3.3 mg/kg (Table 3). Blood was drawn from these patients at day 0 (predose + end of infusion), and predose at cycle 2. To demonstrate clinical applicability of the ELISA for determination of nivolumab in CSF, CSF was collected from 15 patients with a solid tumor and a clinical suspicion of leptomeningeal metastases but a normal or equivocal MRI who underwent a diagnostic lumbar puncture (LP). All patients have been included in a diagnostic CSF study at the NKI comparing the sensitivity and specificity of immunoflowcytometry assays for circulating

tumor cells (CTC) detection with CSF cytology. Five patients were treated with nivolumab. Three out of these five patients had melanoma and concomitantly received ipilimumab at 3 mg/kg (Table 4). The other 10 patients had not received any immunotherapy prior to sampling and served as a negative control group. An aliquot of 1–2 mL of CSF was collected in 2.0 mL vials and stored at -80°C .

Both clinical studies have been approved by the Ethics Committee of the Netherlands Cancer Institute and subjects provided whole blood and CSF samples after written informed consent.

Statistical analysis

Statistical evaluation was performed using the unpaired two-tailed student *t*-test in Excel, unless indicated otherwise. Matrix effects were analyzed using the paired two-tailed *t*-test in Excel. The slopes and intercept of nivolumab and pembrolizumab standard curves were compared using linear regression analysis in Graphpad Prism 6. *P*-values of ≤ 0.05 were considered to be significant.

Method validation

Validation of the ELISA method was performed based on the guidelines for bioanalytical assays provided by the FDA.¹³

RESULTS

Optimization of anti-human IgG4-HRP concentration

We tested anti-human IgG4-HRP at dilutions of 1:500, 1:1000, and 1:2000 in PBSTF. The 1:1000 dilution resulted in a significantly higher ($P < 0.001$) signal to noise ratio, as compared to the other dilutions, over the whole range of spiked nivolumab concentrations from 2 to 100 ng/ml (Supplementary Table 1).

Serum matrix effect

We found that addition of 10% and 20% (v/v) serum to PBSTF had a significant effect on the accuracy of nivolumab quantification over the whole standard curve concentration range with an average of decrease in nivolumab concentration of 14.1% at 10% (v/v) serum to PBSTF ($P < 0.001$) and 21.4% at 20% serum to PBSTF ($P < 0.001$) (Supplementary Table 2). Therefore, we used 10% (v/v) serum in PBSTF, for both serum and CSF samples, as well as for the standard curves and quality controls (QCs), to assure accurate quantification of nivolumab. Next, dilution integrity was assessed in triplicate in quality controls, spiked with nivolumab at 160 $\mu\text{g}/\text{mL}$, after a standard 1000-fold dilution followed by an additional 2-fold dilution. The back-calculated nivolumab concentration did not deviate more than 15% from the nominal spike concentration, which indicates good dilution integrity. Furthermore, samples spiked with nivolumab at 1000 and 2 $\mu\text{g}/\text{mL}$ in serum and CSF, respectively, which required an additional 16-fold dilution after the standard 1000-fold dilution, also showed adequate dilution integrity (Table 1).

Specificity

The signal to noise ratios of nivolumab using Pierce standard ECL, Biorad Clarity, and Trevigen Peroxyglow were 363, 100, and 2000, respectively. Although, Peroxyglow showed superior signal to noise ratio, we chose to develop the ELISA with about 10-fold less expensive Pierce standard ECL. The detection of nivolumab was very specific: wells coated with PD-1 showed luminescence of 5762 ± 182 , which was not significantly higher than the luminescence of 5439 ± 454 for wells not coated with PD-1. This ensures the absence of any meaningful interaction between the secondary antibody and PD-1, and indicates that net luminescence, defined as measured luminescence minus background signal from ECL, originates only from the reaction of the secondary antibody with nivolumab. There was a large difference in background signal after blocking with different agents (PBS only, BSA, FCS, ELK). The lowest background of $10.2 \times 10^3 \pm 552$ arbitrary luminescent units (ALU) was obtained without blocking, which are the wells incubated with PBS only. In sequence of increasing background signal, 2% BSA, 40 and 100% FCS, 5% BSA, and 2 and 5% ELK, resulted in significant ($P < 0.001$) higher backgrounds of 270×10^3 , 338×10^3 , 363×10^3 , 423×10^3 , 823×10^4 , and 842×10^4 ALU, respectively (Figure 1). To put this in perspective, 100 ng/mL nivolumab resulted on average in net luminescence of 240×10^4 ALU. Based on these results, we concluded, that blocking should be omitted in this ELISA.

Table 1. Dilution integrity was assessed, after indicated number of serial 2-fold dilutions with 10% (v/v) serum in PBSTF, for serum spiked at 160 (Quality Control) and 1000 $\mu\text{g/mL}$, and CSF spiked at 2 $\mu\text{g/mL}$ nivolumab. Results are the average of three replicate measurements. PBSTF = phosphate buffered saline supplemented with 0.1% Tween-20 and 1% Ficoll.

Nivolumab spiked	Total dilution factor	Number of 2-fold serial dilutions	Nominal conc. ng/mL	Determined conc. \pm SD $\mu\text{g/mL}$	Accuracy \pm SD (%)
QC at 160 $\mu\text{g/mL}$	2000	1	80	153 ± 9.6	95.6 ± 6.0
Serum at 1000 $\mu\text{g/mL}$	1000	1	1000	129 ± 5.7	13.4 ± 1.7
	2000	2	500	251 ± 14.9	25.5 ± 5.3
	4000	4	250	483 ± 21.7	48.2 ± 3.2
	8000	8	125	880 ± 21.4	87.9 ± 3.4
	16000	16	62.5	921 ± 44.4	94.9 ± 9.0
CSF at 2 $\mu\text{g/mL}$	2	1	1000	0.26 ± 0.011	12.9 ± 4.4
	4	2	500	0.50 ± 0.030	25.1 ± 5.9
	8	4	250	0.97 ± 0.043	48.3 ± 4.5
	16	8	125	1.75 ± 0.085	87.2 ± 4.9
	32	16	62.5	1.84 ± 0.089	96.3 ± 3.2

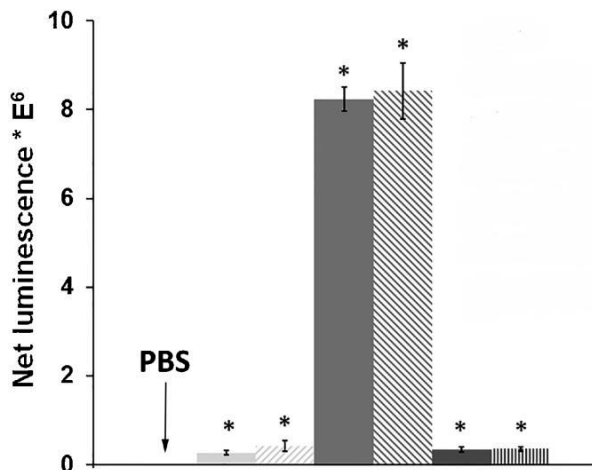


Figure 1. Background signal after 3 h of incubation with 300 μ l of the following blocking solutions in phosphate buffered saline (PBS): PBS as control \blacksquare ; 2% \square and 5% ▨ bovine serum albumin (BSA); 2% \blacksquare and 5% ▨ low fat milk powder; 40% \blacksquare and 100% ▨ fetal calf serum (FCS). Results \pm SD of 3 different samples are shown. * Indicates significant $P < 0.05$ higher background relative to PBS.

Addition of ipilimumab had no significant effect on the quantification of nivolumab in both serum and CSF (Supplementary Table 3). Furthermore, the background level was not significantly increased by 500 ng/mL of ipilimumab (data not shown).

The mean background level of 10% (v/v) serum from 10 different volunteers in PBSTF was 0.22 ± 0.039 (range 0.089–0.37) ng/mL. The mean background of 50% (v/v) CSF in PBSTF containing 10% (v/v) serum from 10 patients was 0.31 ± 0.011 (range 0.21–0.45) ng/mL. From these backgrounds, limits of detection (LOD) for nivolumab in serum and CSF of 0.65 ng/mL, and 0.75 ng/mL, respectively, were calculated.

Lower limit of quantification (LLQ)

The LLQ of nivolumab and pembrolizumab in serum and CSF was 2 ng/mL. In serum, nivolumab was determined at the LLQ with a mean accuracy of 101% (range 97.4%–110%, $n = 7$), and mean precision of 3% (range 0%–9.5%). Pembrolizumab was determined at LLQ with a mean accuracy of 100% (range 91.4%–105%, $n = 7$), and mean precision of 3.9% (range 1.6%–5.8%). In CSF, nivolumab was determined at LLQ with a mean accuracy of 103% (range 101%–106%, $n = 6$) and mean precision of 2.2% (range 0.4%–4.2%). Pembrolizumab was determined at LLQ with mean accuracy of 102% (range 98.9%–105%, $n = 6$), and mean precision of 3.4% (range 0.4%–4.2%).

Between- and within-day precision

Nivolumab was measured at 6 consecutive days in triplicate at 5, 20, 80 ng/mL spiked in 10% (v/v) serum in PBSTF. The mean within- and between day imprecisions, and the nivolumab quantification accuracy at these nominal input levels were within 15%, and 85–115%, respectively (Table 2).

Table 2. Imprecisions and accuracy at indicated nivolumab and pembrolizumab nominal input levels after dilution of quality control samples prepared in 100% serum to a final matrix composition of 10% (v/v) serum in PBSTF. Imprecisions were calculated from triplicate measurements on three consecutive days by one-way analysis of variance (ANOVA) for each spike level using the run day as classification variable. Accuracy is determined as the ratio between the measured and nominal concentration. WDP = within-day precision; BDP = between-day precision.

Nominal input ng/mL	Nivolumab			Pembrolizumab		
	WDP %	BDP %	accuracy %	WDP %	BDP %	accuracy %
5	3.3	4.1	102.5	6.1	5.3	98.1
20	3.4	4.1	99.5	6.5	6.6	101.9
80	4.2	4.6	100.8	5.1	0.6	105.7

Pembrolizumab quantification

Concentrations of nivolumab and pembrolizumab, back-calculated from nivolumab standard curves, were compared by linear regression analysis. No significant differences in slope and intercept were found, which indicates that assay response over the investigated standard curve concentration range is the same for both antibodies (Supplementary Table 4). In addition, the Pearson correlation coefficient (*r*) of 1.00 indicates good correlation between the quantification of both antibodies. Therefore, we conclude that pembrolizumab can be accurately quantified against standard curves prepared from nivolumab if the 1.87% molecular weight difference is taken into account.

Stability

Nivolumab and pembrolizumab were stable at 0.1, 1, 10, and 100 µg/mL spiked in PBSTF containing serum, in storage at -80 °C for at least 480 days. Furthermore, samples containing nivolumab and pembrolizumab, at 10 and 50 ng/mL in 10% (v/v) serum in PBSTF, could be stored on ice for 6 h without significant decrease in concentration of both antibodies. However, after 24 h of storage on ice nivolumab and pembrolizumab concentrations decreased significantly by 13% (*P*=0.026) and 19% (*P*=0.005), respectively. Samples containing 10 and 100 µg/mL of nivolumab and pembrolizumab spiked in 10% (v/v) serum in PBSTF were subjected to 3 freeze-thaw cycles. The measured drug concentrations, after 1000-fold dilution of samples in 10% (v/v) serum in PBSTF, did not differ significantly from the spiked concentrations (Supplementary Table 5).

Table 3. Patients and treatment characteristics used to demonstrate applicability of the ELISA in serum. Patients received indicated dose of nivolumab at day 1 of every course. In addition, melanoma patients received 3 mg/kg ipilimumab; NSCLC = non-small cell lung cancer; q2w and q3w = administration every 2 and 3 weeks, respectively.

Patient #	Tumor type	Therapeutic antibody	Dosing regime	Dose mg/kg	Dose mg
1	Melanoma	Nivolumab	q2w	1.3	100
2	Melanoma	Pembrolizumab	q3w	2.1	200
3	NSCLC	Nivolumab	q2w	2.8	140
4	NSCLC	Nivolumab	q2w	5.7	240
5	NSCLC	Pembrolizumab	q3w	3.0	200
6	Melanoma	Pembrolizumab	q3w	2.5	150
7	NSCLC	Nivolumab	q2w	2.6	240

Clinical applicability

Nivolumab (n = 4 patients) and pembrolizumab (n = 3 patients) serum concentrations were determined in seven patients treated with different doses of nivolumab and pembrolizumab (Figure 2). Predose nivolumab and pembrolizumab serum concentrations for all seven patients were below the limit of detection. At end of infusion, we found nivolumab C_{max} concentrations of 43.9–65.1 µg/mL for two patients treated with nivolumab at 2.6 and 2.8 mg/kg, which is within the concentration range reported by EMA of 61.3 ± 26.4 µg/mL for patients treated with nivolumab at 3 mg/kg (n = 13 patients).¹⁴ Patients 1 and 4 were treated with nivolumab doses that were about a factor 2 below and above this 3 mg/kg level, which resulted in nivolumab serum concentrations of 19.6 and 107 µg/mL, respectively. Trough nivolumab serum concentrations ranged from 3.1 for patient 1 (1.3 mg/kg) to 56.2 µg/mL for patient 4 (5.7 mg/kg). Pembrolizumab serum concentrations at end of infusion were 43.9, 46.5, and 65.1 µg/mL for the three patients treated with a 200 mg dose of pembrolizumab, which is within the range reported by EMA of 67.5 ± 23 µg/mL (n = 150) for patients treated at this dose.¹⁵ Trough pembrolizumab concentrations ranged from 8.01 to 22.8 µg/mL. The concentrations of nivolumab in CSF of five patients treated with 1 or 3 mg/kg nivolumab ranged from 14.5 to 304 ng/mL and levels of nivolumab in concomitantly drawn serum ranged from 1.8 to 33.5 µg/mL (Table 4). The serum/CSF ratios of nivolumab ranged from 52–299. Although, the sample size is small and inter-patient variability in nivolumab levels in CSF is substantial, these data indicate that there is a low penetration of nivolumab in the brain.

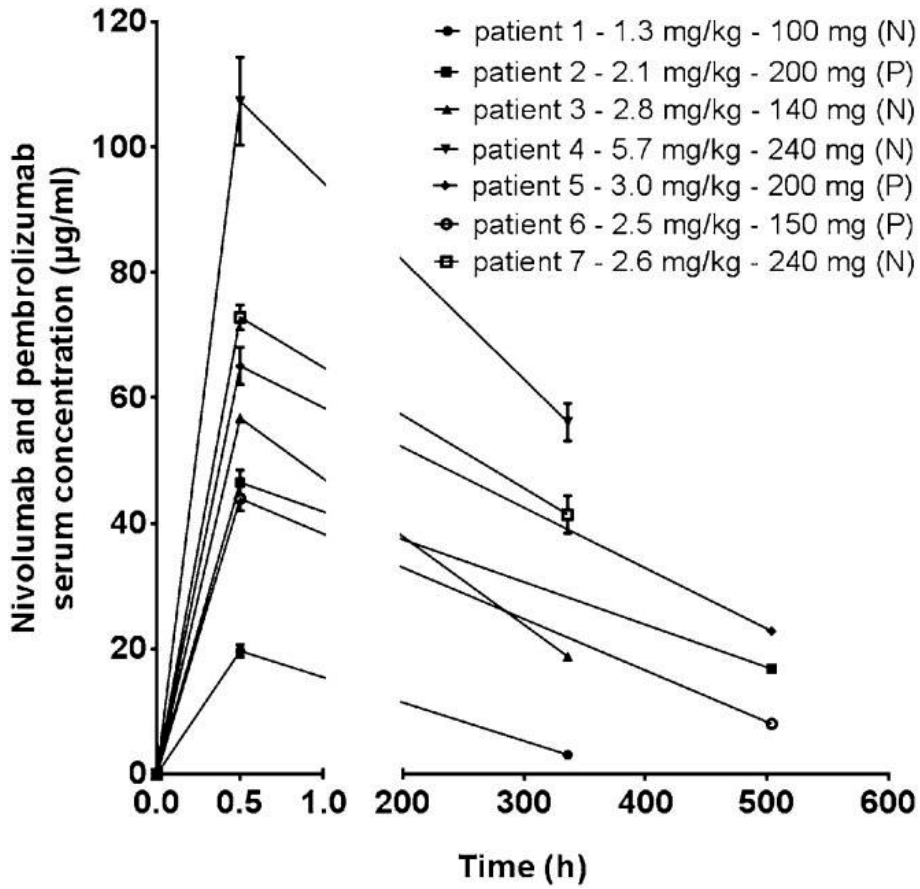


Figure 2. Pharmacokinetics of nivolumab (N; n=4) and pembrolizumab (P; n=3) in serum from 7 patients treated with indicated doses (mg/kg). Blood was drawn at baseline (0 min), end of infusion (30 min), and predose course 2 (336 and 504 h). Results are expressed as the means \pm SD of 3 different samples.

Table 4. Measured nivolumab concentrations in serum and CSF from 5 patients receiving the indicated dose of nivolumab at day 1 of every course. In addition, melanoma patients received 3 mg/kg ipilimumab. Results are the average of three replicate measurements \pm SD. CSF = cerebrospinal fluid; NSCLC = non-small cell lung cancer; PK = pharmacokinetics; C = course; D = day; q2w and q3w = administration of nivolumab every 2 and 3 weeks, respectively.

Pt #	Tumor type	Nivo-lumab dosing regimen	PK sample	Dose mg/kg	Dose mg	Measured nivolumab concentration \pm SD in ng/mL		Ratio serum/CSF
						serum	CSF	
137	Breast cancer	q3w	C1D16	1	61	4481 \pm 287	15 \pm 0.9	299
123	Melanoma	q3w	C1D21	1	80	1831 \pm 138	35 \pm 0.9	52
113	Melanoma	q3w	C1D21	1	77	4410 \pm 324	39 \pm 1.9	113
135	Melanoma	q2w	C1D12	3	245	13,759 \pm 311	150 \pm 2.5	92
114	NSCLC	q3w	C3D14	3	240	33,454 \pm 705	304 \pm 11	110

DISCUSSION

Pembrolizumab and nivolumab are both anti-PD-1 monoclonal IgG4 antibodies, which have been approved for various advanced cancers, showing improved overall and progression free survival compared to standard-of-care in phase III trials.^{16–20} Intracranial activity of these agents has been observed in progressing brain metastases in patients with melanoma and NSCLC.^{21,22} Studies show a rapid and durable brain metastasis response rate of 22% in 18 melanoma patients and 33% in 18 NSCLC patients. Despite these encouraging data, many patients fail to respond to anti-PD-1 treatment in the brain or on extra-cerebral sites. Additional combination therapies and biomarker development will be important, particularly in patients with brain metastases who may have a different disease biology than patients with extra-cerebral disease. It is unclear whether the effect of anti-PD-1 agents in brain metastases is due to systematically activated T-cells that cross the blood-brain barrier or whether the anti-PD-1 agent actually has its action mechanism in the brain itself and therefore has to cross the BBB.²¹ Our data now show that only minimal nivolumab concentrations reach the brain/CSF with serum to CSF ratios of 52–299. Recently, Puszkiel et al. reported the first ELISA for the determination of nivolumab in plasma.⁸ Puszkiel et al. have demonstrated that their ELISA is sensitive enough to measure trough nivolumab levels in patients receiving nivolumab at 3 mg/kg. However, our results indicate that treatment of patients with nivolumab at 1–1.3 mg/kg can result in trough levels below the 5000 ng/mL lower quantification limit of their ELISA (Figure 2 and Table 4).

Here, we report the development and validation of a sensitive, quick and inexpensive ELISA which can be used to measure both nivolumab and pembrolizumab concentrations in biological fluids. Most ELISAs describe the use of time consuming blocking steps with BSA, FCS, and ELK-based protein solutions to prevent nonspecific binding of antibodies.⁸ These blocking agents, however, prevented the sensitive detection of nivolumab in our ELISA due to an increase of background signal that originates from nonspecific binding of the secondary anti-IgG4-HRP antibody. Therefore, we tried the highly branched hydrophilic polysaccharide Ficoll as an alternative blocking agent, as suggested by Huber et al.²³ Furthermore, the original developers of the ELISA described that addition of Tween-20 in the antibody and washing solutions is sufficient to reduce nonspecific binding.²⁴ Based on these findings, we omitted a separate blocking step and combined both the Ficoll and Tween-20 in the antibody and washing solutions. Further enhancement in sensitivity was obtained through chemiluminescent detection of the anti-IgG4-HRP. An advantage of this assay is a 100-fold reduction in the amount of recombinant PD-1 used for coating the ELISA plates, which significantly reduces the cost of the assay. The method has a LLQ of 2 ng/mL for both nivolumab and pembrolizumab, which will most likely be sensitive enough to allow quantification of both peak and trough levels of nivolumab and pembrolizumab in serum and CSF from most patients.

Clinical trials are showing promising results from the combination of nivolumab and pembrolizumab with ipilimumab.^{25,26} We showed that quantification of nivolumab with our ELISA was not affected by analytical interference from an 25-fold excess of ipilimumab. Moreover, the background of the assay was not significantly increased by 500 ng/mL of ipilimumab. Therefore, our ELISA can be used to accurately quantify nivolumab and pembrolizumab in plasma and CSF from patients receiving combination therapy.

CONCLUSIONS

We developed and validated a sensitive ELISA for the quantitative determination of nivolumab and pembrolizumab in serum and CSF. The ELISA has a LLQ of 2 ng/mL, which enables accurate quantification of the low levels of these anti-PD-1 antibodies found in CSF. To our knowledge, this is the first evaluation of nivolumab concentration levels in CSF. The concentrations of nivolumab in CSF ranged from 14.5 to 304 ng/mL, at trough nivolumab serum levels in 5 patients receiving nivolumab at 1 and 3 mg/kg, respectively. The method is accurate, precise, and shows good long-term sample storage stability using standard laboratory equipment and techniques. This quantitative ELISA for nivolumab and pembrolizumab can be used in future clinical trials.

REFERENCES

1. Larkin J, Minor D, D'Angelo S, et al. Overall Survival in Patients With Advanced Melanoma Who Received Nivolumab Versus Investigator's Choice Chemotherapy in CheckMate 037: A Randomized, Controlled, Open-Label Phase III Trial. *J Clin Oncol*. 2018; 36:383-390.
2. Sul J, Blumenthal GM, Jiang X, He K, Keegan P, Pazdur R. FDA Approval Summary: Pembrolizumab for the Treatment of Patients With Metastatic Non-Small Cell Lung Cancer Whose Tumors Express Programmed Death-Ligand 1. *Oncologist*. 2016;21:643-650.
3. Shu CA, Rizvi NA. Into the Clinic With Nivolumab and Pembrolizumab. *Oncologist*. 2016;21:527-528.
4. Yushak ML, Chiang VL, Kluger HM. Clinical trials in melanoma patients with brain metastases. *Pigment Cell Melanoma Res*. 2015;28:741-743.
5. Stemmler H-J, Schmitt M, Willems A, Bernhard H, Harbeck N, Heinemann V. Ratio of trastuzumab levels in serum and cerebrospinal fluid is altered in HER2-positive breast cancer patients with brain metastases and impairment of blood-brain barrier. *Anticancer Drugs*. 2007;18:23-28.
6. Pestalozzi BC, Brignoli S. Trastuzumab in CSF. *J Clin Oncol*. 2000;18:2349-2351.
7. Lin J. CSF as a Surrogate for Assessing CNS Exposure: An Industrial Perspective. *Curr Drug Metab*. 2008;9:46-59.
8. Puszkiel A, Noé G, Boudou-Rouquette P, et al. Development and validation of an ELISA method for the quantification of nivolumab in plasma from non-small-cell lung cancer patients. *J Pharm Biomed Anal*. 2017;139:30-36.
9. Iwamoto N, Shimada T, Terakado H, Hamada A. Validated LC-MS/MS analysis of immune checkpoint inhibitor Nivolumab in human plasma using a Fab peptide-selective quantitation method: nano-surface and molecular-orientation limited (nSMOL) proteolysis. *J Chromatogr B*. 2016;1023-1024:9-16.
10. Zhang S, Garcia-D'Angeli A, Brennan JP, Huo Q. Predicting detection limits of enzyme-linked immunosorbent assay (ELISA) and bioanalytical techniques in general. *Analyst*. 2014;139:439-445.
11. Nikolayenko I V, Galkin OY, Grabchenko NI, Spivak MY. Preparation of highly purified human IgG , IgM , and IgA for immunization and immunoanalysis. *Ukr Bioorganica Acta*. 2005;2:3-11.
12. Herman RA, Scherer PN, Shan G. Evaluation of logistic and polynomial models for fitting sandwich-ELISA calibration curves. *J Immunol Methods*. 2008;339:245-258.
13. FDA, Food and Drug Administration, Guidance for Industry: Bioanalytical method validation. 2001.
14. Sancho-Lopez A, de Graeff P, European Medicines Agency, Assessment report nivolumab EMA/CHMP/76688/2015.
15. Melchiorri D, Mueller-Berghaus J. European Medicines Agency. Assessment report pembrolizumab EMA/CHMP/16441/2017.
16. Robert C, Schachter J, Long G V, et al. Pembrolizumab versus Ipilimumab in Advanced Melanoma. *N Engl J Med*. 2015;372:2521-2532.
17. Robert C, Long G V, Brady B, et al. Nivolumab in previously untreated melanoma without BRAF mutation. *N Engl J Med*. 2015;372:320-330.
18. Brahmer J, Reckamp KL, Baas P, et al. Nivolumab versus Docetaxel in Advanced Squamous-Cell Non-Small-Cell Lung Cancer. *N Engl J Med*. 2015;373:123-135.
19. Borghaei H, Paz-Ares L, Horn L, et al. Nivolumab versus Docetaxel in Advanced Nonsquamous Non-Small-Cell Lung Cancer. *N Engl J Med*. 2015;373:1627-1639.
20. Garon EB, Rizvi NA, Hui R, et al. Pembrolizumab for the Treatment of Non-Small-Cell Lung Cancer. *N Engl J Med*. 2015;372:2018-2028.
21. Dudnik E, Yust-Katz S, Nechushtan H, et al. Intracranial response to nivolumab in NSCLC patients with untreated or progressing CNS metastases. *Lung Cancer*. 2016;98:114-117.

22. Goldberg SB, Gettinger SN, Mahajan A, et al. Pembrolizumab for patients with melanoma or non-small-cell lung cancer and untreated brain metastases: early analysis of a non-randomised, open-label, phase 2 trial. *Lancet Oncol.* 2016;17:976-983.
23. Huber D, Rudolf J, Ansari P, et al. Effectiveness of natural and synthetic blocking reagents and their application for detecting food allergens in enzyme-linked immunosorbent assays. *Anal Bioanal Chem.* 2009;394:539-548.
24. Engvall E, Perlmann P. Enzyme-linked immunosorbent assay, Elisa. 3. Quantitation of specific antibodies by enzyme-labeled anti-immunoglobulin in antigen-coated tubes. *J Immunol.* 1972;109:129-135.
25. Kirchberger MC, Hauschild A, Schuler G, Heinzerling L. Combined low-dose ipilimumab and pembrolizumab after sequential ipilimumab and pembrolizumab failure in advanced melanoma. *Eur J Cancer.* 2016;65:182-184.
26. Hodi FS, Chesney J, Pavlick AC, et al. Combined nivolumab and ipilimumab versus ipilimumab alone in patients with advanced melanoma: 2-year overall survival outcomes in a multicentre, randomised, controlled, phase 2 trial. *Lancet Oncol.* 2016;17:1558-1568.

SUPPLEMENTARY DATA

Supplementary table 1. Effect of indicated secondary antibody dilutions on the signal to noise ratio of the mean luminescence at different spiked (nominal) nivolumab concentrations in 10% (v/v) serum in PBSTF. Results are the average of three replicate measurements \pm SD, * indicates a significant difference. ALU = arbitrary luminescence unit; S/N = signal to noise ratio i.e. ALU of nivolumab standard : ALU of standard 0.

Nominal nivolumab conc. ng/mL	Secondary antibody dilutions					
	1:500		1:1000		1:2000	
	ALU	S/N	ALU	S/N	ALU	S/N
100	3026518	348 \pm 5.05	2460188	452 \pm 5.23*	1165947	202 \pm 2.28
50	1382593	159 \pm 6.46	1277491	235 \pm 20.0*	609230	106 \pm 0.58
20	496599	57.1 \pm 0.96	429751	79.0 \pm 0.93*	305220	53.0 \pm 0.01
10	249029	28.6 \pm 0.22	213621	39.3 \pm 0.17*	153399	26.6 \pm 0.26
5	128316	14.7 \pm 0.09	106484	19.6 \pm 0.08*	74215	12.9 \pm 0.14
2	55591	6.4 \pm 0.05	45401	8.3 \pm 0.09*	35591	6.2 \pm 0.05
0	8701		5442		5764	

Supplementary table 2. Effect of 0, 10, and 20% serum on the measured concentrations of nivolumab relative to the spiked (nominal) concentrations of nivolumab in PBSTF (* indicates a significant difference). Results are the average of three replicate measurements \pm SD. PBSTF = phosphate buffered saline supplemented with 0.1% Tween-20 and 1% Ficoll.

Nominal	Measured nivolumab concentrations \pm SD in ng/mL in PBSTF + serum		
	0% serum	10% serum	20% serum
100	98.8 \pm 4.05	87.5 \pm 1.89 *	78.8 \pm 3.57 *
50	52.3 \pm 0.59	46.6 \pm 0.70 *	43.6 \pm 0.68 *
20	18.8 \pm 0.02	15.9 \pm 0.45 *	14.6 \pm 0.25 *
10	10.1 \pm 0.46	8.6 \pm 0.07 *	7.9 \pm 0.08 *
5	5.1 \pm 0.06	4.1 \pm 0.03 *	3.8 \pm 0.02 *
2	2.0 \pm 0.03	1.8 \pm 0.03 *	1.6 \pm 0.01 *
1	1.0 \pm 0.03	0.8 \pm 0.03 *	0.7 \pm 0.04 *

Supplementary table 3. Influence of indicated nominal concentrations of ipilimumab on the quantification of nivolumab spiked at 20 and 80 ng/mL in 10% (v/v) serum, and 50% (v/v) cerebrospinal fluid (CSF) in PBSTF containing 10% (v/v) serum. Results are the average of three replicate measurements \pm SD. PBSTF = phosphate buffered saline supplemented with 0.1% Tween-20 and 1% Ficoll.

Nominal ipilimumab conc. ng/mL	Measured nivolumab concentrations \pm SD in ng/mL at 20 and 80 ng/ml nivolumab spike level			
	10% serum		50% CSF	
	20	80	20	80
0	18.5 \pm 1.5	87.2 \pm 2.5	20.4 \pm 0.8	79.1 \pm 2.5
100	18.5 \pm 2.6	79.3 \pm 4.1	20.6 \pm 1.4	79.1 \pm 3.9
200	19.4 \pm 1.3	82.8 \pm 3.9	20.2 \pm 1.6	76.5 \pm 5.5
500	18.9 \pm 1.1	77.8 \pm 3.3	20.9 \pm 2.7	76.5 \pm 2.6

Supplementary table 4. Comparison of assay response for nivolumab and pembrolizumab. Standard curves containing 2, 5, 10, 20, 50, and 100 ng/mL nivolumab and pembrolizumab were measured in triplicate on three consecutive days. Concentrations, expressed in pM \pm between day standard deviation, of both antibodies were back-calculated from the nivolumab standard curves. Subsequently, pembrolizumab concentrations were corrected by 1.87% to adjust for its higher molecular weight in comparison with nivolumab.

Nominal input concentration		Back-calculated concentrations (n = 3)			
Nivolumab	Pembrolizumab	Nivolumab		Pembrolizumab	
pM	pM	pM \pm SD	Accuracy %	pM \pm SD	Accuracy %
696	684	675 \pm 9.0	-3.1	672 \pm 16.6	-1.7
348	342	361 \pm 15	3.7	361 \pm 20.7	5.7
139	137	143 \pm 5.0	2.5	141 \pm 8.7	3.3
69.6	68.4	68.5 \pm 3.7	-1.7	68.4 \pm 5.0	0.1
34.8	34.2	34.3 \pm 1.8	-1.6	34.5 \pm 2.2	0.9
13.9	13.7	14.1 \pm 0.1	0.9	14.0 \pm 0.3	2.6

Supplementary table 5. Effect of indicated number of freeze-thaw cycles on the measured concentrations of nivolumab and pembrolizumab spiked at 10 and 100 μ g/mL in 10% (v/v) serum in PBSTF. Samples were measured after 1000-fold dilution in 10% (v/v) serum in PBSTF. Results are the average of three replicate measurements \pm SD.

Freeze-thaw cycle	Spike concentration in μ g/mL of			
	Nivolumab		Pembrolizumab	
	10	100	10	100
	Measured concentrations \pm SD in ng/mL			
0	9.57 \pm 0.52	99.5 \pm 5.6	9.64 \pm 0.33	98.0 \pm 2.4
1	10.3 \pm 0.22	99.4 \pm 2.4	9.68 \pm 0.35	97.9 \pm 5.5
2	9.64 \pm 0.58	98.5 \pm 7.8	9.39 \pm 0.75	104 \pm 4.1
3	9.87 \pm 0.47	95.2 \pm 7.7	9.51 \pm 0.53	99.5 \pm 3.2

Chapter 4.2

Multiparameter flow cytometry assay for quantification of immune cell subsets, PD-1 expression levels and PD-1 receptor occupancy by nivolumab and pembrolizumab

Willeke Ros*, Dick Pluim*

**Authors contributed equally*

Pluim D*, **Ros W***, Miedema IHC, Beijnen JH, Schellens JHM. Multiparameter flow cytometry assay for quantification of immune cell subsets, PD-1 expression levels and PD-1 receptor occupancy by nivolumab and pembrolizumab. *Cytometry Part A [In press.]*

ABSTRACT

We report the development and validation of a twelve parameter immunofluorescence flow cytometry method for the sensitive determination of cell concentrations, their expression of PD-1, and PD-1 receptor occupancy. Cell subsets include CD4⁺ and CD8⁺-T-cells, B-cells, natural killer cells, classical-, intermediate- and non-classical monocytes, and myeloid- and plasmacytoid dendritic cells. Cells were isolated from peripheral blood by density gradient centrifugation. The validation parameters included specificity, linearity, limit of quantification, precision, biological within- and between subject variation. The lower limit of quantification was 5.0% of PD-1⁺ cells. Samples were stable for at least 153 days of storage at - 80°C. The clinical applicability of the method was demonstrated in 11 advanced cancer patients by the successful determination of immune cell concentrations, relative number of PD-1⁺ immune cells, and number of PD-1 molecules per immune cell. Shortly after infusion of nivolumab, receptor occupancy on CD8⁺-T-cells was 98%. Similar values were found during predose cycle 2, suggesting receptor occupancy remained high throughout the entire cycle.

INTRODUCTION

Checkpoint blockade therapy has demonstrated remarkable efficacy against numerous cancer types. The monoclonal antibodies nivolumab and pembrolizumab have shown anti-tumor activity in melanoma, non-small cell lung cancer (NSCLC), urothelial cancer, head and neck cancer, gastric cancer, renal cell carcinoma (RCC), Hodgkin's Lymphoma, cervical cancer and mismatch repair deficient tumors (dMMR) [1–9]. Overall response rates have been up to 30 - 40% for melanoma, up to 20% for NSCLC, and up to 25% in RCC treated with programmed cell death protein 1 (PD-1) inhibitor monotherapy [3, 4, 10].

Both nivolumab and pembrolizumab block PD-1, a protein on the surface of immune cells acting as a receptor checkpoint molecule. Upon binding of PD-1 to its ligand PD-L1, expressed on tumor cells, activated T-cells become anergic, which makes them unable to eradicate cancer cells. The therapeutic anti-PD-1 IgG₄ antibodies nivolumab and pembrolizumab can block this interaction, thereby preventing T-cell inhibition and allowing effective anti-tumor immune responses. Whereas pembrolizumab is a humanized antibody, nivolumab is a fully human antibody. Pembrolizumab and nivolumab bind at partly overlapping sites of the extracellular domain of PD-1. Nivolumab binding is dominated by interactions with the PD-1 N-loop, whereas for pembrolizumab this is with the PD-1 CD loop [11]. Both antibodies bind PD-1 with high affinity: Nivolumab binds PD-1 with a half maximal effective concentration (EC₅₀) of 3.06 pM, and pembrolizumab with 29 pM [12, 13].

Much effort has been put into identifying biomarkers which help select those patients who are likely to respond to treatment. Approved biomarkers include PD-L1 expression and mismatch repair deficient/microsatellite instability high tumors [14, 15]. Other biomarkers correlating to response include tumor infiltrating lymphocytes, number of CD8⁺-T-cells, T-cell receptor clonality, and IFN- γ signature expression [16–20]. Furthermore, absolute lymphocyte and monocyte counts have shown to predict time to response, time to progression, overall survival, and immune related adverse effects of immunotherapy [21, 22].

Potential other pharmacodynamic biomarkers which may require further investigation are the receptor occupancy (RO) of PD-1 upon treatment with anti-PD-1 immunotherapeutic antibodies, and PD-1 expression on immune cell subtypes other than T-cells [23]. PD-1 RO has been described during the phase I study of nivolumab [24]. RO was determined on CD3⁺-peripheral blood mononuclear cells (PBMCs) from patients receiving 0.3, 1, 3 or 10 mg/kg. In this study, the mean RO was 85% (70 - 97%) at the end of infusion (EOI), and 72% (59 - 81%) after 57 days of infusion. RO was dose-independent and the half-life was 150 days. The method which was used to assess RO is in brief: PBMCs were incubated with either an isotype control or nivolumab, followed by incubation with a murine biotin-labelled anti-human-IgG₄. RO was estimated as the ratio of the percent of CD3⁺-cells stained with isotype control to that stained with nivolumab.

Thus far, the main focus of PD-1 expression in relationship to anti-PD-1 treatment has been on CD4⁺ and CD8⁺-T-cells [25]. In cancer patients, naïve T-cells show low (~1%)

percentages of PD-1 expression, whereas for central memory and effector memory T-cells this percentage lies substantially higher (40 - 60%) [26–28]. However, PD-1 is not solely expressed on T-cells. PD-1 also appears to play roles on B-cells, natural killer (NK)-cells, monocytes and dendritic cells [29–33]. Approximately 25% (5 – 45%) of B-cells, and up to 8% (2 – 13%) of NK-cells express PD-1 [33–35]. PD-1 expression on monocytes and dendritic cells has been described as well, but results are inconsistent [30, 31].

A high variability is seen across studies regarding PD-1 expression on immune cell subsets. This variability may have been caused by clinical factors such as disease status and disease type [26, 31]. Another possible source of variability could have been the use of methods that were not robust or thoroughly validated.

Here, we report the development and validation of a sensitive pharmacodynamic assay for the determination of the concentration of CD4⁺ and CD8⁺-T-cells, B-cells, NK-cells, classical monocytes (CM), intermediate monocytes (IM), non-classical monocytes (NCM), myeloid dendritic cells (mDC), and plasmacytoid dendritic cells (pDC) in blood, number of PD-1⁺ immune cells, and number of PD-1 molecules per immune cell. Our method does not rely on isotype controls, which can result in an erroneous estimation of the background level [36]. Within- and between subject biological variation in the relative number of PD-1⁺ cells and PD-1 expression were determined in 10 healthy volunteers. Clinical applicability was demonstrated in 11 advanced cancer patients who were treated with nivolumab (n = 6) or pembrolizumab (n = 5).

MATERIAL AND METHODS

Reagents and chemicals

The water used was of Milli-Q grade (Millipore, USA). Ficoll-paque[™]PLUS was obtained from General Electric Healthcare (Little Chalfont, UK). Phosphate buffered saline (PBS) was purchased from GIBCO BRL (Gaithersburg, MD, USA). Eppendorf[®] LoBind micro-centrifuge 2.0 mL tubes, bovine serum albumin (BSA), fetal calf serum (FCS), and human IgG1k were purchased from Sigma (St. Louis, MO, USA). Beads buffer (BB) and BB-5%BSA consisted of PBS with 2 mM EDTA, and respectively 0.5% and 5% (w/v%) BSA. All buffers were filtered through 0.22 µm filters. PBS and buffers were chilled on ice before use. Neutral methanol-free 40% (w/v%) formaldehyde in physiological salt was prepared from paraformaldehyde purchased from Merck (Darmstadt, Germany). Live/Dead[™] Fixable Violet Dead Cell Stain and Spherotech rainbow beads were purchased from ThermoFisher (Landsmeer, the Netherlands). Live-dead stain was diluted 500-fold in PBS immediately before use. Ionomycin, phorbol-12-myristate-13-acetate, and Cryosofree[™] were from Sigma (St. Louis, USA). Quantum[™] Simply Cellular[®] mouse IgG (QSC) beads were from Bio-Rad (Veenendaal, the Netherlands).

Antibody cocktail consisted of 8 µl of human IgG1k from Sigma and the following anti-human antibodies: 0.5 µl of CD3-APC-Cy7 (clone Hit3a), 1 µl of CD8-PerCP-Cy5.5 (clone SK1), 2 µl of CD14-BV510 (clone M5E2) and 0.5 µl of CD16-AF700 (clone 3G8) from ITK (Uithoorn, the Netherlands), 1 µl of CD4-APC (clone VIT4) from Miltenyi (Leiden, the

Netherlands), 0.5 μ l of CD11c-BV650 (B-Ly6), 2 μ l of CD19-BV711 (clone SJ25C1), 0.5 μ l of CD56-FITC (clone TULY56), 0.5 μ l of CD123-BV605 (clone 7G3), and 0.5 μ l of HLA-DR-BV786 (clone G46-6) from Becton Dickinson (Heidelberg, Germany). PD-L2 was from Sino Biological (Beijing, China). Anti-human PD-1 (clone PD1.3.1.3) was from Miltenyi. Anti-human IgG₄-PE (clone HP6025) was from ITK (Uithoorn, the Netherlands). Ipilimumab (Yervoy[®]), nivolumab (Opdivo[®]) and pembrolizumab (Keytruda[®]) were a kind gift from the Antoni van Leeuwenhoek hospital pharmacy. To remove protein aggregates all antibodies were centrifuged at 10,000g for 8 min, after which the supernatant was used.

Subjects and sample collection

Subjects asked for study participation included 10 healthy volunteers not known with cancer, and 11 patients with advanced cancer. Blood samples from healthy volunteers were used to assess number and variability of immune cells and their PD-1 expression, and blood samples from patients were used for demonstrating the clinical applicability of the method. From each subject 10 mL of blood was collected in a heparin tube. Blood was kept at room temperature (RT) and within 30 min, 7.0 mL of blood was transferred to a CPT[™]-citrate vacutainer tube (BD). Total volume was adjusted to 8 mL with PBS. All study participants had given written informed consent in accordance with institutional and national guidelines. The study protocol was approved by the ethical committee of the Netherlands Cancer Institute.

Centrifugation

Unless stated otherwise, all centrifugations were performed in 2 mL Lo-bind eppendorf tubes in a centrifuge equipped with a swing-out rotor at 500g for 4 min at 4°C. After centrifugation the supernatant was removed by aspiration, leaving 100 μ L on the pellet.

PBMC pre-processing

Unless stated otherwise, the assay development and validation were performed with unstimulated PBMCs, which may provide a good representation of the actual in vivo patient PD-1 levels on these immune cells at the time of blood sampling. Each CPT tube, containing 7.0 mL whole blood, was centrifuged in a swing-out rotor at 1,500g for 25 min at RT. Next, the layer of plasma was aspirated and the layer of PBMCs was poured into a 15 mL tube on ice. The CPT tube was washed with 5 mL of ice-cold BB, which was pooled with the PBMCs in the 15 mL tube. The sample volume was adjusted to 15 mL with ice-cold BB and inverted 5 times before centrifugation. The supernatant was aspirated and the pellet was resuspended in 1 mL of BB, which was completely transferred to a 2 mL tube using a second wash with 0.5 mL of BB. After centrifugation, the supernatant was aspirated and the pellet washed twice with 1 mL of PBS. Samples were again centrifuged, after which the total volume was adjusted to 690 μ L. After addition of 10 μ L of 500-fold diluted Live-Dead marker, samples were incubated on ice for 15 min. Next, aliquots of 25 μ L of cell suspension were transferred in triplicate, unless otherwise specified, to 2 mL tubes on ice, containing 54 μ L of BB-5%BSA and 16 μ L of antibody cocktail and samples were incubated vertically for 1 h on ice at 300 rpm using a Heidolph Vibramax[™] 100. After that, samples were incubated for an additional 1 h with 10 μ g/mL nivolumab or pembrolizumab, washed three times with 1 mL of BB, and centrifuged. Subsequently, samples were fixed for 15 min at RT by addition of 1 mL 2% (w/v) of formaldehyde. After centrifugation, pellets were

washed with 1 mL BB and aspirated to leave 50 μ L on the pellets. For cryopreservation, 500 μ L of Cryosofree™ was added before samples were snap-frozen in liquid nitrogen and stored at -80°C .

Detection of PD-1

Samples were defrosted in a 37°C water bath until the remaining volume of ice was about half the initial sample volume. After almost complete defrosting under constant manual shaking at RT, samples were put on ice for complete defrosting. Samples were washed once with 1 mL BB, and once with BB-5%BSA, respectively. After centrifugation, 8 $\mu\text{g}/\text{mL}$ of anti-IgG4-PE in BB-5%BSA was added and vials were incubated standing upright in an ice box at 300 rpm using a Heidolph Vibramax 100 plate mixer (Essex, UK). Next, samples were washed twice with 1 mL BB, centrifuged, and kept on ice until analysis by flow cytometry.

Fluorescent-activated cell sorting and PD-1 determination

Samples were measured using twelve-color flow cytometry on a Becton Dickinson Fortessa LSR2. Sequential gating (Figure 1) was applied for the enumeration of 9 immune cell subsets with subsequent quantification of their PD-1 expression using FlowJo v10.0.7 software (Ashland, USA). The threshold for qualifying cells as PD-1⁺ was set at 5.0% of the cells with the highest median fluorescent intensity (MFI) of PE in background control samples. The used fluorochrome, voltage, laser, filter, and compensation settings for each detection antibody are listed in supplementary Table 1.

Optimization of PD-1 signal to noise ratio

Samples containing 400k PBMCs were incubated for 1 h in BB-5%BSA with or without 10 $\mu\text{g}/\text{mL}$ nivolumab, washed extensively with BB, and incubated at RT for 1 h with 8 $\mu\text{g}/\text{mL}$ of anti-IgG4-PE in BB containing 0.5, 2.0, and 5% BSA, and at 0°C with BB-5%BSA (supplementary Figure 1).

Effect of formaldehyde and cryopreservation

Samples containing 400k PBMCs from a healthy volunteer were incubated without (negative control, NC) or with 10 $\mu\text{g}/\text{mL}$ of nivolumab or pembrolizumab for 1 h on ice, after which they were washed three times with 1 mL BB. Next, samples were left unfixed (NC) on ice, or fixed with 4% (w/v%) formaldehyde for 15 min at RT, washed with 1 mL BB, centrifuged, and snap-frozen in liquid nitrogen after addition of 500 μ L of Cryosofree™. Same day, snap-frozen samples were defrosted and washed twice with 1 mL BB, centrifuged, and incubated for 1 h at 0°C with 8 $\mu\text{g}/\text{mL}$ of anti-IgG4-PE. Different samples containing 400k PBMCs were similarly incubated with nivolumab or pembrolizumab, washed, and left unfixed on ice (0%) or fixed with 1, 2 and 4% (w/v%) formaldehyde for 15 min at RT. After 1 wash with 1 mL BB, samples were incubated for 1 h at 0°C with 8 $\mu\text{g}/\text{mL}$ of anti-IgG4-PE. Cells were kept on ice and PD-1 on CD8⁺T-cells was analyzed the same day by flow cytometry.

Antibody target saturation curves

In order to determine PD-1 target saturation, samples containing 400k PBMCs from a healthy volunteer were incubated for 1 h with 0, 0.02, 0.05, 0.1, 0.2, 0.5, 1, 2, 5, 10, and 20 $\mu\text{g}/\text{mL}$ nivolumab or pembrolizumab in BB-5%BSA. Subsequently, PD-1 was detected using

8 µg/mL of anti-IgG₄-PE, as described previously. Growth stimulated PBMCs, which were cultured as described in the specificity section, were used for this nivolumab experiment. PBMCs from another healthy volunteer were pre-incubated for 1 h with 10 µg/mL nivolumab to saturate the PD-1 targets, followed by detection with 0, 0.67, 1, 1.3, 2, 2.7, 4, 5.3, 6.7, 13.3, 20 µg/mL of anti-IgG₄-PE.

Next, the effect of different amounts of PBMC input per sample on PD-1 staining and cell recovery was assessed in samples containing 100k, 200k, 300k, 400k, and 500k PBMC. These samples were incubated for 1 h on ice without (background controls) and with 10 µg/mL nivolumab. After extensive washing, PD-1 was detected with 8 µg/mL of anti-IgG₄-PE as described for our pre-processing and PD-1 detection method.

Quantification of the number of PD-1 molecules per cell

The threshold for qualifying cells as PD-1⁺ was set at 5.0% of the cells with the highest median fluorescent intensity (MFI) of PE in background control samples. The negative contribution of these 5.0% background cells to the MFI of nivolumab or pembrolizumab treated cells (supplementary Figure 2), was corrected for according to the following formula:

$$\text{Corrected net MFI} = \text{MFI}_{\text{niv}} + (\text{MFI}_{\text{niv}} - \text{MFI}_{\text{bckg}}) * \frac{\%_{\text{bckg}}}{(\%_{\text{PD1niv}} - \%_{\text{bckg}})}$$

MFI_{niv} = MFI of nivolumab or pembrolizumab treated cells

MFI_{bckg} = MFI of the 5.0% most PE positive background cells

%_{bckg} = background threshold level = 5.0%

%PD1_{niv} = percentage of PD-1⁺ cells in nivolumab or pembrolizumab treated samples

A mix of five different QSC beads, each with a manufacturer determined known amount of anti-mouse IgG₁ binding sites (ABS), was incubated in triplicate for 1 h on ice with 8.0 µg/mL of anti-IgG₄-PE in BB-BB-5%BB. After two washes with 1 mL BB, samples were centrifuged and measured by FACS using the same settings as used for PD-1 detection in cells. Log(ABS) against log(net MFI-PE) linear regression analysis was used, according to the manufacturer's instructions, for samples incubated with 8 µg/mL of anti-IgG₄-PE, in order to calculate the number of anti-IgG₄-PE per cell from the corrected net MFI of PE in samples. Next, the number of PE bound per anti-IgG₄ antibody (PE labeling ratio) was determined spectrophotometrically using the following formula:

$$\text{PE labeling ratio} = \frac{\epsilon_{\text{IgG4}}}{\epsilon_{\text{PE}}} * \frac{\text{Abs}_{566}}{(\text{Abs}_{280} - \text{CF} * \text{Abs}_{566})}$$

ε_{IgG4} = molar extinction coefficient of IgG₄ = 210.000

ε_{PE} = molar extinction coefficient of PE = 1.863.000

Abs₂₈₀ = Absorbance of total protein at 280nm

Abs₅₆₆ = Absorbance of PE at 566nm

CF = Correction factor of PE contribution to Abs₂₈₀ = 0.17

The number of PD-1 per cell was calculated by dividing the number of anti-IgG₄-PE per cell by the PE labeling ratio.

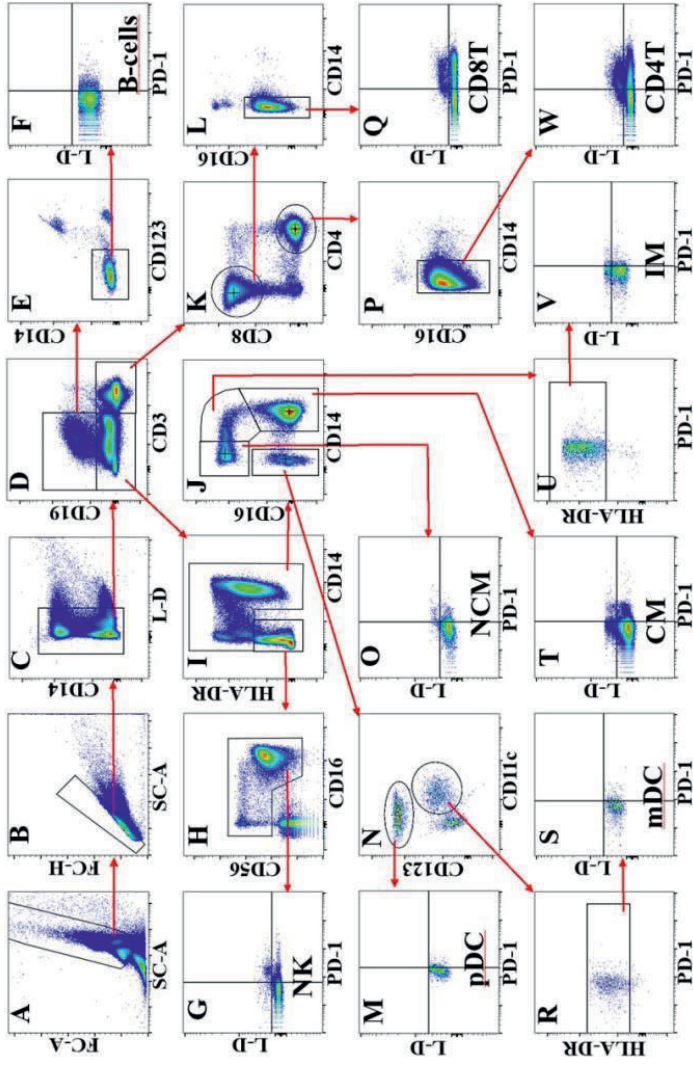


Figure 1. Gating strategy to discriminate nine immune cell populations. Red arrows indicate the gating direction. Peripheral blood mononuclear cells are gated (A) using forward (FS) and sideward scatter (SC), with subsequent elimination of doublets by FS-height (FS-H) against FS-area (FS-A) gating (B). After rough elimination of dead cells (C) by live-dead protein stain (L-D), the negative dendritic-monocyte-natural killer cells (NK) are separated (D) from B-cells (CD19⁺) and T-cells (CD3⁺). CD3⁺ T-cells were further differentiated into CD4⁺ and CD8⁺ T-cells (K). NK-cells differentiated from dendritic cells and monocytes as HLA^{DR}, CD14⁺, CD16⁺, CD56^{+/±} (H, I). Dendritic cells are identified in plots J and N as CD14⁺, CD16⁺, CD123⁺, CD11c⁺ myeloid dendritic cells, and CD14⁺, CD16⁺, CD123⁺, CD11c⁺ plasmacytoid

dendritic cells (pDC). Monocytes are divided into classical, non-classical and intermediate monocytes (J) based on their relative amount of CD14 and 16 expression. After removal of the last remaining contaminating cells (E, L, P, R, U), PD-1 is detected in the final plots (F, G, M, O, Q, S, T, V, W) using quadrant gating to eliminate remaining dead cells. Background samples that have not been treated with nivolumab or pembrolizumab were used to set the position of the quadrant gate at exactly 5.0% PD-1⁺ cells for each of the viable immune cell populations.

Specificity of PD-1 detection

In order to determine PD-1 target saturation, samples containing 400k PBMCs from a healthy volunteer were incubated for 1 h with 0, 0.02, 0.05, 0.1, 0.2, 0.5, 1, 2, 5, 10, and 20 µg/mL nivolumab or pembrolizumab in BB-5%BSA. Subsequently, PD-1 was detected using 8 µg/mL of anti-IgG₄-PE, as described previously. Growth stimulated PBMCs, which were cultured as described in the specificity section, were used for this nivolumab experiment. PBMCs from another healthy volunteer were pre-incubated for 1 h with 10 µg/mL nivolumab to saturate the PD-1 targets, followed by detection with 0, 0.67, 1, 1.3, 2, 2.7, 4, 5.3, 6.7, 13.3, 20 µg/mL of anti-IgG₄-PE.

Next, the effect of different amounts of PBMC input per sample on PD-1 staining and cell recovery was assessed in samples containing 100k, 200k, 300k, 400k, and 500k PBMC. These samples were incubated for 1 h on ice without (background controls) and with 10 µg/mL nivolumab. After extensive washing, PD-1 was detected with 8 µg/mL of anti-IgG₄-PE as described for our pre-processing and PD-1 detection method.

Storage stability

Stability of PD-1 and cell numbers was assessed in blood from a healthy volunteer stored for 0, 0.5, 1, 2, and 4 h at room temperature in heparin tubes. After isolation PBMCs were spiked at 250k cells per sample and incubated with nivolumab or pembrolizumab, as described for sample pre-processing.

To assess the stability of cell numbers and PD-1 detection during long term storage at -80°C, PBMCs from a healthy volunteer were spiked at 200k cells per sample. After incubation with nivolumab or pembrolizumab, samples were processed, snap-frozen in liquid nitrogen and stored at -80°C, as described for our pre-processing method. After 0, 53, and 153 days of storage, samples were, in triplicate, defrosted and incubated with anti-IgG₄-PE for detection of PD-1 by flow cytometry, as described for our PD-1 detection method.

Healthy volunteer study

Peripheral blood from 10 different healthy volunteers (5 male, 5 female, age range 25 - 48) was collected between 9:00 and 10:00 AM on three different days with weekly intervals. PBMCs were isolated from 7.0 mL of blood, and incubated, in triplicate, with 10 µg/mL of nivolumab or pembrolizumab, and further processed as described in PBMC pre-processing and PD-1 detection. In order to determine the cell recovery of our method, total initial PBMC cell concentrations were measured using a Roche Innovatis Casy™ Coulter counter.

Clinical applicability

In order to determine the clinical applicability of our method, blood was drawn from advanced cancer patients (supplementary Table 6) who received nivolumab (n = 6) or pembrolizumab (n = 5) in 2, 3 or 4 weekly course intervals (q2W, q3W, or q4W). Blood was drawn at baseline, at the end of the first infusion (EOI), and predose of cycle 2. PBMCs were isolated from 7.0 ml of blood and incubated with 10 µg/mL of nivolumab or pembrolizumab, i.e. the same antibody as administered to the respective patient. Samples were further processed as described in PBMC pre-processing and PD-1 detection.

Statistical Analysis

Specificity of PD-1 detection was defined as the difference in PD-1 signal between background control samples and samples incubated with PD-1 blocking agents before incubation with nivolumab and pembrolizumab. Linearity of PD-1⁺ cell recovery of immune cell subsets, and between MFI and number of PD-1 per QSC bead were tested using linear regression analysis in Graphpad Prism 6.01. The lower limit of quantification (LLOQ) of the percentage of PD-1⁺-cells was defined as the percentage of PE positive background cells \pm 5 times standard deviation (SD).

For determination of assay precision and biological variation, data from the volunteer study was checked for normal distribution using the Shapiro-Wilk test. The assay within- and between day precision (WDP and BDP) were determined using one-way analysis of variance (ANOVA) using the run day as classification variable, using Excel, and should not exceed 15% of the coefficient of variation (CV). Within subject biological variation (WSBV) was defined as the coefficient of variation between three independent weekly results for each subject. Between subject biological variation (BSBV) was defined as coefficient of variation between the mean within subject results. Statistical evaluation using Student's *t*-test, and Quartile analysis was performed in Excel. Differences in biomarker levels between patient sampling points were evaluated using Wilcoxon matched pair signed rank tests in Graphpad Prism 6.01. *P*-values smaller than 0.05 were considered to be significant.

RESULTS

Optimization of PD-1 signal to noise ratio

The signal to noise ratio (S/N) of PD-1 detection on PD-1⁺CD8⁺-T-cells at RT in BB with 0.5% (w/v%) BSA was 2.9 ± 0.1 . S/N ratios significantly increased to 3.1 ± 0.1 (*P* = 0.04) and 3.7 ± 0.1 (*P* = 0.002) if BB with 2.0% and 5.0% (w/v%) BSA was used, respectively. Incubation at 0°C with 5% BSA resulted in a significant additional increase of the S/N ratio to 4.1 ± 0.1 (supplementary Figure 1, *P* = 0.0001).

Effect of formaldehyde and cryopreservation

In comparison with unfixed cells, fixation with 4% formaldehyde followed by cryopreservation had a negative effect on the percentage of PD1⁺-cells of $-11.8\% \pm 5.2\%$ (*P* = 0.025) in samples treated with nivolumab (supplementary Figure 3A). Fixation with 2% formaldehyde resulted in an increase of the PD-1 signal on CD8⁺ T-cells by $15.0\% \pm 1.8\%$ (*P* = 0.023) for nivolumab and $21.2\% \pm 1.3\%$ (*P* = 0.006) for pembrolizumab treated samples. In nivolumab treated samples, the percentage of PD-1⁺-cells was significantly higher after fixation with 2% formaldehyde (*P* = 0.048). In pembrolizumab treated samples no significant change was detected (supplementary Figure 3B).

Linearity of PD-1 detection

Flow cytometer PE MFI signals were linearly correlated to the number of PE molecules per QSC bead (*r* = 0.999). Antibody target saturation was assessed from curves of nivolumab, pembrolizumab, and anti-IgG₄-PE (supplementary Figure 4), using Eadie Hofstee plots constructed by linear regression. The Km-values were respectively 0.127, 0.117, and 0.317 $\mu\text{g/mL}$ for nivolumab, pembrolizumab, and anti-IgG₄-PE as determined from the slopes.

The concentrations used in our PD-1 detection method are 10 µg/ml nivolumab and pembrolizumab, and 8 µg/ml anti-IgG₄-PE. These concentrations resulted in PD-1 detection at, respectively 98.9%, 101.3%, and 96.9% of the maximum possible MFI signal strength calculated from the intercept of the Eadie Hofstee plots. The lowest antibody concentrations that did not result in significant lower PD-1 MFI, as compared to the concentrations chosen for our method, were 2 µg/ml nivolumab, 0.5 µg/ml pembrolizumab, and 2 µg/ml anti-IgG₄-PE.

The number of PD-1⁺ cells recovered for the immune cell subsets correlated linearly over the tested spike range from 100k – 500k PBMCs input per sample ($r > 0.997$). The slopes of these curves did not significantly differ from 1 indicating complete cell recovery over the tested concentration range. Furthermore, the difference in percentage of PD1⁺ and number of PD-1 per CD4⁺ and CD8⁺-T-cell was less than 6.9% between the 100k and 500k PBMC spike levels (supplementary Table 4A).

Specificity of PD-1 detection

For determination of assay specificity, using PBMCs isolated from a healthy volunteer, it is necessary to *ex vivo* growth stimulate these cells to ensure detectable levels of PD-1 on all immune cell subsets. The average percentages of PD-1⁺ found on the subset was as follows: 38% for CD4⁺-T-cells, 41% for CD8⁺-T-cells, 21% for B-cells, 1% for NK-cells, 67% for CM, 18% for IM, 10% for NCM, 40% for mDC and 15% for pDC. In samples that were pre-incubated with anti-PD-1 clone PD1313 in combination with PD-L2, the percentage of PD-1⁺ cells was significantly decreased by more than $97.0 \pm 1.8\%$, and the number of PD-1⁺-CD4⁺ and CD8⁺-T-cells by more than $99.5\% \pm 0.4\%$ (Figure 2 and supplementary Table 2). The MFI of PD-1 in all PD-1 blocked samples was not significantly different from the background control samples, which indicates highly specific detection of PD-1. Furthermore, the background signal, number of detected PD-1 per cell and percentage of PD-1⁺-CD4⁺ and CD8⁺-T-cells did not significantly change due to exposure to 10 and 50 µg/mL of ipilimumab before incubation with 10 µg/mL of nivolumab or pembrolizumab (supplementary Table 3). This indicates no significant interference from ipilimumab with the detection of PD-1.

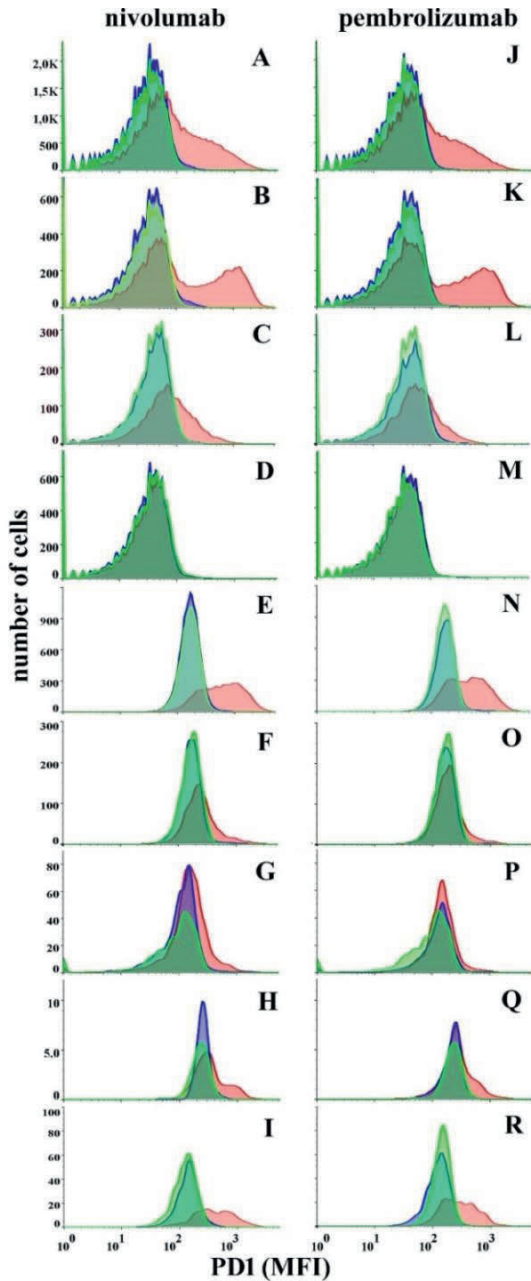


Figure 2. Specificity of PD-1 detection in immune cells. Cells were cultured in RPMI medium under growth stimulating conditions. Background samples were not treated with nivolumab and pembrolizumab (green histograms = background). Cells were incubated with (blue histograms) or without (red histograms) PD-L2 and PD1313, followed by incubation with nivolumab (A – I) and pembrolizumab (J - R). PD-1 was detected by anti-IgG₄-PE, which is expressed as median fluorescence intensity (MFI). Shown are CD4⁺-T-cells (A ; J), CD8⁺-T-cells (B ; K), B-cells (C ; L), natural killer cells (D ; M), classical monocytes (E ; N), intermediate monocytes (F ; O), non-classical monocytes (G ; P), myeloid dendritic cells (H ; Q), and plasmacytoid dendritic cells (I ; R).

Storage stability

PD-1 expression and immune cell numbers were stable for 0.5 h in blood stored in heparin tubes. After 1, 2, and 4 h of storage both PD-1 expression and cell numbers were significantly decreased ($P < 0.02$, Figure 3). The difference in the number of cells between samples stored for 0 and 153 days was 14.1% or less (supplementary Table 5A). In addition, the percentage of PD-1⁺ cells and number of PD-1⁺ per cell were not significantly lower, and showed a decrease of 6.8% after 153 days of storage (supplementary Table 5BC). Therefore, we concluded that the number of immune subset cells, percentage of PD-1⁺ cells and number of PD-1 per cell are at least stable for 153 days of storage at -80°C. The between day precision (BDP) was better than 9.0% for the determination of the number of cells, percentage of PD-1⁺ and number of PD-1 per cell.

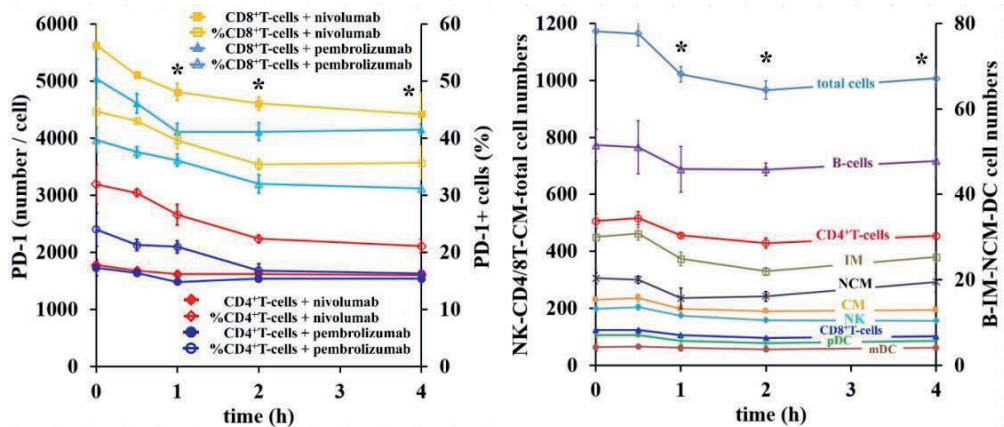


Figure 3. Stability of PD-1 in blood from a healthy volunteer stored for 0, 0.5, 1, 2 and 4 h at room temperature in heparin tubes before isolation of PBMC using cell preparation tubes. A. Shown are the results for nivolumab (—◆—, —◇—) and pembrolizumab (—●—, —○—) treated CD4⁺-T-cells for the number of PD-1 per cell and percentage of PD-1⁺ cells, respectively. Results are shown for the number of PD-1 and percentage of PD-1⁺CD8⁺-T-cells after nivolumab (—■—, —□—) and pembrolizumab (—▲—, —△—) treatment. B. The effect of storage on the total cell numbers (—◇—), CD4⁺ and CD8⁺-T-cells (CD4/8T, —○—, —▲—), B-cells (—△—), natural killer cells (NK, —◇—), classical monocytes (CM, —■—), intermediate monocytes (IM, —□—), non-classical monocytes (NCM, —×—), plasmacytoid dendritic cells (pDC, —■—), and myeloid dendritic cells (mDC, —●—). Results are the mean of three separate samples ± standard deviation (SD). * indicates a significant decrease relative to t = 0

Table 1. Biological variation of PD-1 in healthy volunteers. (1A), percentage of PD-1⁺ cells, and number of PD-1 per cell for nivolumab (1B) and pembrolizumab (1C), for CD4 and CD8 T-cells (CD4T and CD8T), B-cells (B), natural killer cells (NK), classical monocytes (CM), intermediate monocytes (IM), non-classical monocytes (NCM), plasmacytoid dendritic cells (pDC), and myeloid dendritic cells (mDC). Q1 - 4 indicates whether the measured cell concentration was within the 1st, 2nd, 3rd, or 4th quartile (= 25, 50, 75, 100 percentile, respectively) of the reference healthy volunteer population (n = 10). LLOQ = lower limit of quantification and was defined as background + 5 times SD; WDP = within day precision; WSBV = within subject biological variation; BSBV = between subject biological variation); ND = not determined. Data are the mean of indicated number of volunteers (n), each measured in triplicate, ± standard deviation (SD).

Cell type	Cells / μ L blood	Cells / μ L blood range	Q1	Q2	Q3	Q4	Background %PD-1 ⁺ cells	LLOQ net %PD-1 ⁺	WDP (%)	WSBV (%)	WSBV range (%)	BSBV (%)
CD4T	514 ± 141	242 - 832	442	528	583	832	4.92 ± 1.03	5.06	4.2 ± 1.5	11.6 ± 8.2	1.7 - 21.5	24.9
CD8T	240 ± 89.4	98.3 - 430	169	234	296	430	4.96 ± 0.93	4.61	4.0 ± 1.4	18.1 ± 20.7	5.2 - 63.4	30.8
B	86.2 ± 38.3	44.0 - 172	58.9	76.0	92.7	172	4.87 ± 0.86	4.19	6.7 ± 2.5	14.8 ± 5.0	6.9 - 25.8	42.6
NK	131 ± 53.1	42.8 - 253	85.5	120	163	253	4.94 ± 1.05	5.20	4.0 ± 1.2	19.5 ± 8.1	8.0 - 33.5	37.1
CM	240 ± 66.3	142 - 479	190	232	273	479	4.86 ± 1.19	5.79	4.4 ± 1.4	17.8 ± 11.1	9.6 - 28.7	23.3
IM	9.89 ± 4.73	2.00 - 18.7	6.54	8.84	13.8	18.7	4.94 ± 1.04	5.14	7.7 ± 4.1	22.8 ± 11.2	8.6 - 52.5	43.2
NCM	13.7 ± 6.70	1.81 - 28.8	10.4	12.7	17.4	28.8	4.91 ± 1.10	5.42	8.0 ± 2.2	18.3 ± 6.8	9.1 - 38.0	46.7
pDC	5.26 ± 2.02	2.32 - 8.49	3.31	5.04	6.78	8.88	4.91 ± 0.98	4.83	8.8 ± 2.6	16.6 ± 7.9	7.8 - 33.5	35.8
mDC	5.87 ± 3.27	1.85 - 15.6	3.92	5.05	6.60	15.6	4.88 ± 1.15	5.61	6.2 ± 2.0	18.5 ± 12.5	7.3 - 45.1	53.3
total	1513 ± 290	1086 - 2422	1315	1460	1636	2422	ND	ND	3.9 ± 1.9	9.7 ± 5.7	1.6 - 16.2	17.2

Table 1. Continued.

Cell type	net PD-1 ⁺ cells							net number of PD-1 per cell								
	n	Cells (%)	WDP (%)	WSBV (%)	WSBV range (%)	BSBV (%)	PD-1	WDP (%)	WSBV (%)	WSBV range (%)	BSBV (%)	PD-1	WDP (%)	WSBV (%)	WSBV range (%)	BSBV (%)
CD4T	10	37.0 ± 1.1	3.0 ± 1.6	6.4 ± 2.9	3.0 - 11.5	13.6	2074 ± 48.1	2.3 ± 0.8	7.7 ± 6.2	0.9 - 15.0	16.1	2074 ± 48.1	2.3 ± 0.8	7.7 ± 6.2	0.9 - 15.0	16.1
CD8T	10	36.4 ± 0.9	2.5 ± 1.1	8.2 ± 5.2	2.3 - 15.1	12.7	2867 ± 112	3.9 ± 2.3	16.0 ± 10.0	1.6 - 31.3	12.7	2867 ± 112	3.9 ± 2.3	16.0 ± 10.0	1.6 - 31.3	12.7
B	6	7.1 ± 1.2	7.0 ± 6.4	ND	ND	31.0	1167 ± 42.0	3.6 ± 2.3	ND	ND	10.2	1167 ± 42.0	3.6 ± 2.3	ND	ND	10.2
NK	0	<LLOQ	ND	ND	ND	ND	<LLOQ	ND	ND	ND	ND	<LLOQ	ND	ND	ND	ND
CM	3	10.6 ± 2.5	23.8 ± 10.7	ND	ND	73.5	1425 ± 39.3	2.8 ± 2.6	ND	ND	5.4	1425 ± 39.3	2.8 ± 2.6	ND	ND	5.4
IM	3	10.7 ± 2.1	19.6 ± 4.6	ND	ND	67.8	1730 ± 52.4	3.0 ± 1.0	ND	ND	7.3	1730 ± 52.4	3.0 ± 1.0	ND	ND	7.3
NCM	3	12.3 ± 2.5	20.7 ± 6.9	ND	ND	54.1	1748 ± 87.8	5.0 ± 3.7	ND	ND	19.1	1748 ± 87.8	5.0 ± 3.7	ND	ND	19.1
pDC	6	6.0 ± 1.2	19.5 ± 10.2	ND	ND	15.0	3111 ± 185	5.9 ± 6.0	ND	ND	11.0	3111 ± 185	5.9 ± 6.0	ND	ND	11.0
mDC	9	7.2 ± 1.6	22.7 ± 8.1	ND	ND	21.2	1482 ± 113	7.6 ± 6.5	ND	ND	14.8	1482 ± 113	7.6 ± 6.5	ND	ND	14.8

Cell type	net PD-1 ⁺ cells							net number of PD-1 per cell								
	n	Cells (%)	WDP (%)	WSBV (%)	WSBV range (%)	BSBV (%)	PD-1	WDP (%)	WSBV (%)	WSBV range (%)	BSBV (%)	PD-1	WDP (%)	WSBV (%)	WSBV range (%)	BSBV (%)
CD4T	10	29.4 ± 1.3	4.5 ± 1.8	6.9 ± 2.5	3.4 - 3.9	16.1	1933 ± 60.1	3.1 ± 2.0	8.3 ± 5.3	2.6 - 18.1	14.2	1933 ± 60.1	3.1 ± 2.0	8.3 ± 5.3	2.6 - 18.1	14.2
CD8T	10	30.1 ± 1.1	3.8 ± 1.5	9.0 ± 6.1	2.3 - 15.1	16.7	2583 ± 139	5.4 ± 7.9	16.5 ± 8.8	4.5 - 23.7	23.5	2583 ± 139	5.4 ± 7.9	16.5 ± 8.8	4.5 - 23.7	23.5
B	3	5.9 ± 1.2	20.0 ± 6.9	ND	ND	12.9	981 ± 19.6	2.0 ± 1.1	ND	ND	15.8	981 ± 19.6	2.0 ± 1.1	ND	ND	15.8
NK	0	<LLOQ	ND	ND	ND	ND	<LLOQ	ND	ND	ND	ND	<LLOQ	ND	ND	ND	ND
CM	1	13.9 ± 3.2	22.9	ND	ND	ND	1371 ± 59.7	4.4	ND	ND	ND	1371 ± 59.7	4.4	ND	ND	ND
IM	0	<LLOQ	ND	ND	ND	ND	<LLOQ	ND	ND	ND	ND	<LLOQ	ND	ND	ND	ND
NCM	2	7.6 ± 2.0	26.3 ± 13.2	ND	ND	23.5	1669 ± 56.6	3.4 ± 0.7	ND	ND	17.2	1669 ± 56.6	3.4 ± 0.7	ND	ND	17.2
pDC	0	<LLOQ	ND	ND	ND	ND	<LLOQ	ND	ND	ND	ND	<LLOQ	ND	ND	ND	ND
mDC	2	6.7 ± 1.7	26.1 ± 9.6	ND	ND	23.2	1355 ± 63.0	4.7 ± 1.5	ND	ND	5.8	1355 ± 63.0	4.7 ± 1.5	ND	ND	5.8

Healthy volunteer study

The cell recovery of single and live PBMCs by our method was $89.7\% \pm 4.3\%$ (range 85.1 – 92.6%, $n = 10$) of the total number of spiked PBMCs as determined by Coulter cell counting. Cell concentrations, percentage of PD-1⁺ cells, and number of PD-1 per cell were determined with a within day precision better than 15% (Table 1A). The standard deviation in the predefined 5.0% background level was less than 1.0% and only slightly varied between immune cell subsets, which resulted in LLOQs of 4.19 – 5.79% for the percentage of PD-1⁺ cells (Table 1A). The cell concentrations of CD8⁺-T-cells showed the highest WSBV of $18.1\% \pm 20.7\%$. The mean BSBV of the measured cell concentrations for each immune cell subset was about two-fold higher than the mean WSBV (Table 1A). The measured concentrations for each immune cell subset were divided into 4 equal 25 percentile parts by Quartile analysis (Table 1A), which enabled the use of these values as reference for measured cell concentrations in patients.

PD-1 was detected on all immune cell subsets with the exception of NK-cells. The number of volunteers with levels of PD-1⁺ cells above LLOQ was highest for CD4⁺ and CD8⁺-T-cells. In addition, the percentage of PD-1⁺ cells and number of PD-1 per cell were significantly ($P < 0.001$) higher in CD4⁺ and CD8⁺-T-cells than for the other immune cell subsets (1B and C), with the exception of pDC. The mean percentage of PD-1⁺ CD4 and CD8 T-cells in nivolumab treated samples was $37.4\% \pm 1.1\%$ and $36.4\% \pm 0.9\%$, respectively (Table 1B). In pembrolizumab treated samples, the mean percentage of PD-1⁺ CD4⁺ and CD8⁺-T-cells were significantly lower and were $29.4\% \pm 1.3\%$ and $30.1\% \pm 1.1\%$, respectively (Table 1C, $P = 0.001$). Furthermore, the mean number of detected PD-1 per CD4 and CD8 T-cell in nivolumab treated samples was 2074 ± 48.1 and 2867 ± 112 , respectively, which was significantly lower ($P = 0.001$) than in pembrolizumab treated samples at 1933 ± 60.1 and 2583 ± 139 , respectively. The same trend was observed on other immune cell subsets, although significance was not reached due to the limited number of volunteers with detectable PD-1.

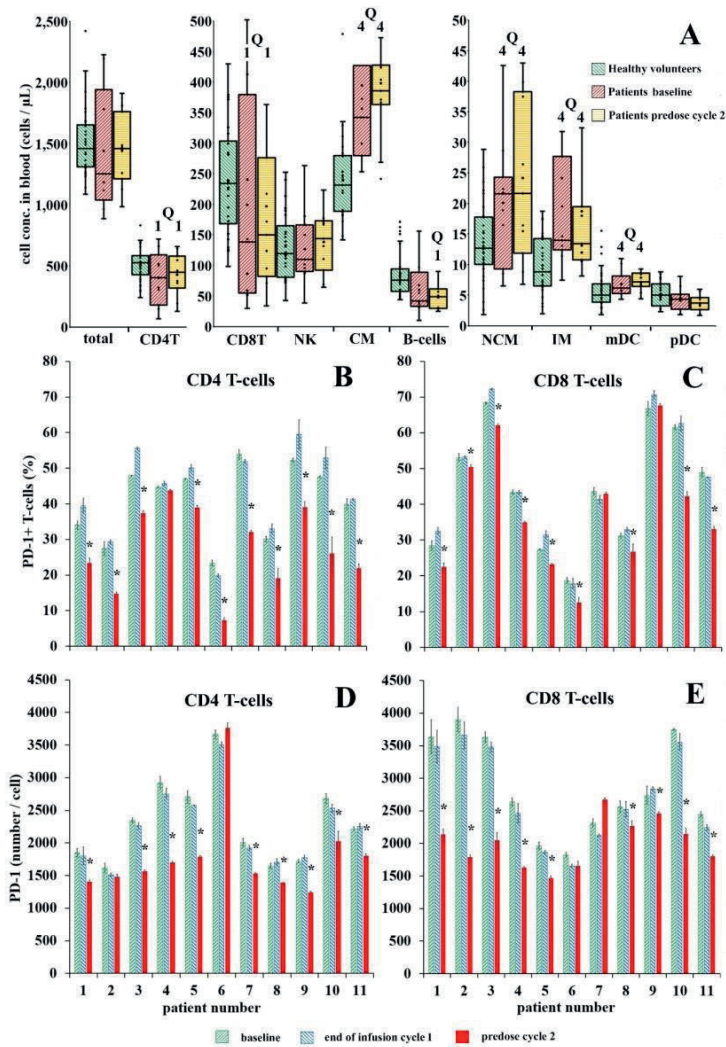


Figure 4. Clinical bio-marker monitoring. Patients (n = 11, supplementary Table 6) were administered with nivolumab (n = 6) or pembrolizumab (n = 5) in 2 – 4 weekly course intervals. Blood was drawn at baseline at the end of infusion of cycle 1 (EOI), and predose of cycle 2. Peripheral blood mononuclear cells were isolated, and ex vivo incubated with nivolumab or pembrolizumab for PD-1 saturation. A. Cell concentrations in blood of total immune cell subsets (total), CD4⁺ and CD8⁺-T-cells (CD4/8T), B-cells, natural killer cells (NK), classical monocytes (CM), non-classical monocytes (NCM), intermediate monocytes (IM), myeloid dendritic cells (mDC), and plasmacytoid dendritic cells (pDC) in patients at baseline and predose of cycle 2 (▨, ▩, respectively) in comparison with the reference healthy volunteer population (▧, n = 10). Quartile analysis was used to show whether cell concentrations were within Q1 (0 - 25 percentile) or Q4 (75 – 100 percentile) of the reference population. Percentage of PD-1⁺ cells and number of PD-1 per CD4⁺-T-cell (B and D, respectively) and CD8⁺-T-cell (C and E, respectively) at baseline (▧), EOI (▨), and predose of cycle 2 (▩). * indicates a significant reduction. Results are the mean of 10 volunteers and 11 patients ± between subject standard deviation (A) or within subject standard deviation (B – E).

Clinical applicability

The measured cell concentrations in patients were significantly ($P < 0.001$) higher by 64.9%, 46.7%, 144%, and 16.2% in CM, NCM, IM, and mDC immune cell subsets, respectively, as compared to the reference healthy volunteer population (Figure 4A). However, measured CD4⁺- and CD8⁺-T-cell, and B-cell concentrations were significantly ($P < 0.015$) lower in patients by 21.8%, 16.8%, and 30.4%, respectively. Total cell concentrations in patients at baseline and predose cycle 2 were not significantly lower than in healthy volunteers (Table 2A).

The percentage of PD-1⁺ cells and number of PD-1 per cell at baseline and EOI were not significantly different from healthy volunteers. However, at predose of cycle 2, the percentage of PD-1⁺ CD4⁺ and CD8⁺-T-cells were significantly lower by 34.5% ($n = 10$, $P = 0.001$) and 16.4% ($n = 9$, $P = 0.002$), respectively, relative to baseline (Figure 4BC, Table 2BC). Furthermore, the number of PD-1 per cell was significantly decreased by 22.6% for CD4⁺-T-cells ($n = 9$, $P = 0.003$) and 26.0% for CD8⁺-T-cells ($n = 9$, $P = 0.007$) at predose of cycle 2 relative to baseline (Figure 4DE, Table 2BC). The BSBV in the determination of percentage of PD-1⁺ cells and number of PD-1 per CD4⁺-T-cell at baseline were 25.7% and 27.7%, and for CD8⁺-T-cells BSBV was 37.7% and 26.2%, respectively. PD-1 RO on CD4⁺ and CD8⁺-T-cells of patients who were given nivolumab were $98.9\% \pm 2.5\%$ and $98.2\% \pm 2.5\%$, respectively. RO on CD4⁺-T-cells was $95.0\% \pm 1.1\%$ in patients who were given pembrolizumab. RO occupation on CD4⁺-T-cells by pembrolizumab and nivolumab showed no significant difference. However, RO on CD8⁺-T-cells was significantly lower at $91.6\% \pm 1.1\%$ ($P = 0.014$) in patients who were given pembrolizumab, as compared to nivolumab. PD-1 RO at EOI, in patients who were given nivolumab or pembrolizumab, was not significantly different from RO at predose cycle 2 (Table 2B and C).

Table 2. Clinical applicability of the assay in patients administered with nivolumab (n = 6) or pembrolizumab (n = 5). Blood was drawn during cycle 1 before administration (baseline) and immediately after end of infusion (EOI), and predose of cycle 2 (pre-C2). After isolation, peripheral blood mononuclear cells were either left on ice (background) or incubated with nivolumab or pembrolizumab, i.e. the same antibody type patients received therapeutically. Shown are the results for cell concentrations per μL blood (7A), percentage of PD-1⁺ cells, and number of PD-1 per cell for nivolumab (7B) and pembrolizumab patients (7C), for CD4 and CD8 T-cells (CD4T and CD8T), B-cells (B), natural killer cells (NK), classical monocytes (CM), intermediate monocytes (IM), non-classical monocytes (NCM), plasmacytoid dendritic cells (pDC), and myeloid dendritic cells (mDC). Δ is the relative difference as compared to the mean cell concentration found for the reference healthy volunteer population (n = 10). Q indicates the quartile (= 25 percentile) of the reference healthy volunteer population to which the measured patient cell concentration corresponds. * indicates a significant difference between baseline and predose cycle 2. Data are the mean of indicated number of patients (n), each measured in triplicate, \pm standard deviation (SD).

A Cell type	baseline					EOI					pre-C2					
	Cells / μL blood	Cells / μL blood range	Δ (%)	Q	Cells / μL blood	Cells / μL blood range	Δ (%)	Q	Cells / μL blood	Cells / μL blood range	Δ (%)	Q	Cells / μL blood	Cells / μL blood range	Δ (%)	Q
CD4T	402 \pm 12.4	69.4 - 719	-16.8%	1	425 \pm 19.2	79.5 - 727		1	429 \pm 14.9	129 - 642	-17.7%	1	129 \pm 14.9	129 - 642	-17.7%	1
CD8T	199 \pm 4.89	55.1 - 593	-21.8%	1	206 \pm 6.11	56.6 - 585		1	197 \pm 7.21	1.6 - 583	-16.5%	1	1.6 - 583	1.6 - 583	-16.5%	1
B	60.0 \pm 2.7	10.3 - 156	-30.4%	2	63.5 \pm 4.7	10.9 - 132		2	48.5 \pm 2.5	25.5 - 90.7	-43.8%	1	25.5 - 90.7	25.5 - 90.7	-43.8%	1
NK	127 \pm 41.2	38.7 - 264	-3.2%	3	115 \pm 62.3	53.0 - 233		3	138 \pm 33.8	68.8 - 223	5.5%	3	68.8 - 223	68.8 - 223	5.5%	3
CM	395 \pm 10.5	254 - 747	64.9%	4	376 \pm 18.0	202 - 727		4	398 \pm 10.2	242 - 473	66.3%	4	242 - 473	242 - 473	66.3%	4
IM	24.1 \pm 1.95	7.50 - 100	144.1%	4	24.0 \pm 1.76	10.1 - 84.6		4	18.7 \pm 1.61	10.6 - 54.5	89.4%	4	10.6 - 54.5	10.6 - 54.5	89.4%	4
NCM	20.1 \pm 1.19	6.50 - 42.6	46.7%	4	19.5 \pm 2.03	7.67 - 39.0		4	24.2 \pm 1.82	6.79 - 43.0	76.6%	4	6.79 - 43.0	6.79 - 43.0	76.6%	4
pDC	4.17 \pm 0.19	1.83 - 8.07	-20.7%	2	3.78 \pm 0.29	1.76 - 8.59		2	3.75 \pm 0.22	1.72 - 6.01	-28.7%	2	1.72 - 6.01	1.72 - 6.01	-28.7%	2
mDC	6.82 \pm 0.30	4.36 - 11.0	16.2%	4	7.36 \pm 0.52	3.51 - 13.3		4	7.87 \pm 0.37	4.44 - 14.4	34.2%	4	4.44 - 14.4	4.44 - 14.4	34.2%	4
total	1,442 \pm 42.3	887 - 2,227	-4.7%	2	1,430 \pm 58.2	814 - 2,013		2	1,448 \pm 33.6	964 - 1,911	-4.3%	2	964 - 1,911	964 - 1,911	-4.3%	2

Table 2. Continued

B

cell type	net PD-1 ⁺ cells (%)				net number of PD-1 per cell						
	n	Baseline	n	EOI	n	pre-C2	baseline	EOI	RO (%)	pre-C2	RO (%)
CD4T	6	37.4 ± 0.8	6	40.0 ± 0.8	6	27.6 ± 0.7*	2517 ± 72	2402 ± 56	98.9 ± 2.5	1949 ± 35*	100 ± 2.7
CD8T	6	39.9 ± 0.7	6	41.7 ± 0.8	6	34.3 ± 3.2*	2931 ± 113	2768 ± 122	98.2 ± 2.5	1788 ± 57*	98.5 ± 2.4
B	4	5.5 ± 1.1	4	7.4 ± 1.3	1	15.2 ± 0.7	1141 ± 76	1080 ± 33	94.3 ± 3.5	1440 ± 22	98.0 ± 2.5
NK	0	<LLOQ	2	5.6 ± 1.1	2	9.2 ± 1.5	<LLOQ	1150 ± 75	94.3 ± 2.8	1330 ± 40	94.9 ± 6.5
CM	0	<LLOQ	2	6.4 ± 1.7	3	13.0 ± 2.2	<LLOQ	2593 ± 464	86.0 ± 3.8	2188 ± 6	101 ± 3.2
IM	0	<LLOQ	1	7.6 ± 1.7	2	18.6 ± 2.7	<LLOQ	1937 ± 67	113 ± 9.1	2020 ± 25	98.4 ± 2.3
NCM	1	5.4 ± 1.4	2	5.8 ± 1.3	2	17.8 ± 2.3	1948 ± 194	1916 ± 90	96.8 ± 6.1	1980 ± 56	97.1 ± 1.0
pDC	1	6.9 ± 1.6	0	<LLOQ	4	9.5 ± 0.7	6084 ± 298	<LLOQ	ND	2591 ± 71	95.6 ± 2.6
mDC	1	5.9 ± 1.1	3	6.0 ± 1.5	1	11.3 ± 2.2	1260 ± 54	1308 ± 45	95.8 ± 7.8	1119 ± 4	101 ± 2.3

C

Cell type	net PD-1 ⁺ cells (%)				net number of PD-1 per cell						
	n	Baseline	n	EOI	n	pre-C2	baseline	EOI	RO (%)	pre-C2	RO (%)
CD4T	5	44.7 ± 0.9	5	47.7 ± 1.9	5	27.7 ± 2.1*	2053 ± 47	2037 ± 47	95.0 ± 1.1	1600 ± 43*	98.5 ± 2.2
CD8T	5	50.4 ± 1.2	5	51.0 ± 1.0	5	42.5 ± 1.0*	2761 ± 69	2656 ± 69	91.6 ± 1.1	2271 ± 48*	90.6 ± 1.2
B	2	4.9 ± 0.8	2	6.0 ± 1.1	1	4.3 ± 0.3	1053 ± 39	1091 ± 58	99.1 ± 3.9	950 ± 4	102 ± 1.2
NK	0	<LLOQ	0	<LLOQ	0	<LLOQ	<LLOQ	<LLOQ	<LLOQ	<LLOQ	<LLOQ
CM	2	7.1 ± 1.3	2	6.0 ± 2.2	1	7.0 ± 0.8	2221 ± 40	1878 ± 84	97.5 ± 6.8	1215 ± 18	95.4 ± 0.6
IM	1	6.4 ± 1.7	1	5.9 ± 0.7	1	8.9 ± 0.6	1811 ± 79	3842 ± 178	88.3 ± 6.1	1421 ± 8	97.3 ± 1.7
NCM	1	5.8 ± 0.9	2	7.2 ± 2.2	1	6.6 ± 1.8	1474 ± 18	2499 ± 123	99.2 ± 4.7	1486 ± 108	92.8 ± 0.7
pDC	0	<LLOQ	0	<LLOQ	0	<LLOQ	<LLOQ	<LLOQ	<LLOQ	<LLOQ	<LLOQ
mDC	1	6.3 ± 0.8	3	6.4 ± 1.2	0	<LLOQ	1367 ± 17	1448 ± 44	101 ± 5.3	<LLOQ	<LLOQ

DISCUSSION

We have described here a PD-1 detection method which is highly specific for PD-1. Background control samples are used for setting the gates that determine PD-1 positivity. Brahmer et al. used background controls containing human IgG₄ isotype antibody as a control for non-specific binding of nivolumab and pembrolizumab (24). Others have reported that using isotype antibodies can give erroneous results, and have shown that adequate blocking of non-specific antibody interactions and using directly conjugated antibodies can most often prevent the use of isotypes in flow cytometry (37). By using anti-PD-1 antibody clone PD1313 and PD-L2, the interaction between nivolumab / pembrolizumab and PD-1 was completely blocked. This demonstrates that our method was 100% specific for PD-1 and that the use of an IgG₄ isotype antibody was not necessary. After correction for 90% cell recovery, the average cell concentrations we found in healthy volunteers for different immune cell subsets were as follows: 1780 (1278 – 2849) PBMCs; 1156 (508 – 2013) lymphocytes; 310 (172 – 620) total monocytes; 101 (57 -202) B-cells; 154 (51 -202) NK-cells; 6.9 (2.2 – 18.4) mDCs; and 6.2 (2.7 – 10) pDCs per μ l blood. These values are in concordance with values reported by other investigators (38–40). Although the normal range for concentrations of immune cell subsets has been reported by many investigators, there is debate regarding both the percentage and the absolute numbers of cells constituting this range. Methods that depend on density gradient centrifugation rather than whole blood cell counting prior to enumeration of immune cells may lead to an underestimation of the absolute cell concentrations of (some) immune cell subsets.

Reproducibility over time and between instruments is crucial in longitudinal and multicenter studies. In flow cytometry, QSC beads allow comparison of experiments over time and between different instruments (41). We show that the use of QSC beads enabled the reproducible quantification of PD-1 levels in samples that were stored at -80°C in Cryosofree™.

To our knowledge, this is the first indirect detection method for the quantification of the number of PD-1 molecules on, and number of PD-1⁺ B-cells, monocytes, and dendritic cells in peripheral human blood. For pharmacodynamic assays, indirect detection methods rather than direct methods are preferred, as they enable the determination of RO and changes in receptor expression separately. However, direct detection may potentially be more sensitive, as their sensitivity is not affected by non-specific binding of nivolumab and pembrolizumab [41]. Other investigators reported detectable levels of PD-1⁺ for B-cells, NK-cells, monocytes, and dendritic cells in peripheral blood from cancer patients and healthy volunteers using direct detection methods. However, results were often inconsistent, which may have been caused by the use of not thoroughly validated methods e.g. methods for which important validation parameters such as specificity and lower limit of quantification were not established. Other investigators have reported percentages of 40 – 60% of PD-1⁺CD4⁺ and PD-1⁺CD8⁺-T-cells in peripheral blood from cancer patients, which is similar to our findings [25–28]. Wang et al. reported approximately 10,000 number of PD-1 receptors per growth activated human T-cell [42]. This is in good agreement with the range of 2,000 – 3,000 PD-1 receptors per T-cell we found for unstimulated PBMCs from healthy volunteers,

considering the 5-fold increase in PD-1 expression induced by anti-CD3 growth stimulation of PBMCs (supplementary Figure 3).

Thus far, receptor occupancy by nivolumab and pembrolizumab has only been described in one study [24]. PD-1 occupancy was described on CD3⁺-T-cells that were cryopreserved in DMSO, and was found to be dose-independent with maximal occupancy of 85% at the end of infusion. Nivolumab concentrations in plasma were 50 µg/mL at EOI for patients that received 3 mg/kg. The investigators hypothesized that PD-1 occupancy analyses of cryopreserved PBMCs may underestimate occupancy on fresh PBMCs. However, for batch analysis of samples from clinical studies, cryopreservation is necessary. In order to keep nivolumab and pembrolizumab attached to PD-1 during the cryopreservation and wash steps, cells were fixed with 2% formaldehyde which resulted in 15% higher PD-1 signals. Instead of DMSO we used Cryosofree™ as cryopreservative, which is far superior for retaining cell vitality [43]. Furthermore, DMSO infiltrates the cells and requires laborious removal during the slow thawing procedure, which compromises reproducibility and cell recovery. Cryosofree™ does not enter the cells and can simply be washed away after thawing, resulting in much higher vital cell recoveries with good reproducibility, as confirmed by our study. We found that the mean RO on CD8⁺-T-cells from cancer patients that were given nivolumab or pembrolizumab was 99% and 91%, respectively, after 2 – 4 weekly courses of treatment. Similar RO values were found at baseline day 1 immediately after infusion. These results are in line with our in vitro experiments, indicating > 83% PD-1 occupancy on CD8⁺-T-cells exposed for 1 h to a relatively low 0.05 µg/mL concentration of nivolumab.

The detection of PD-1 on CD4⁺ and CD8⁺-T-cells was on average 7% lower in samples incubated with pembrolizumab compared to nivolumab. This is likely caused by the difference in binding sites on PD-1 for both antibodies [44]. This may possibly explain the fact that RO of PD-1 on CD8⁺-T-cells was on average 7% lower in patients which were administered pembrolizumab, as compared to patients treated with nivolumab.

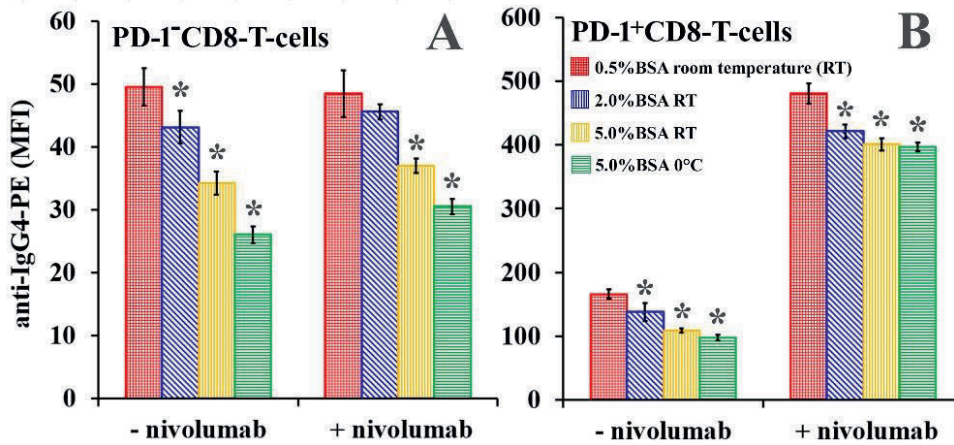
The discovery of factors that influence the clinical response to immunotherapy remains an area of active research and is important to maximize the benefit/risk ratio of these agents in clinical practice. For that purpose, we tested the clinical applicability of our method in cancer patients. We reported a significant drop in the number of PD-1⁺ T-cells and the number of PD-1 receptors per T-cell after one course of nivolumab or pembrolizumab. This may potentially be a pharmacodynamic effect, which requires further investigation regarding predictive value for nivolumab and pembrolizumab immunotherapy outcome. Compared to other methods, our method offers efficient determination of multiple biomarkers on a large panel of immune cell subsets in a single experiment.

REFERENCES

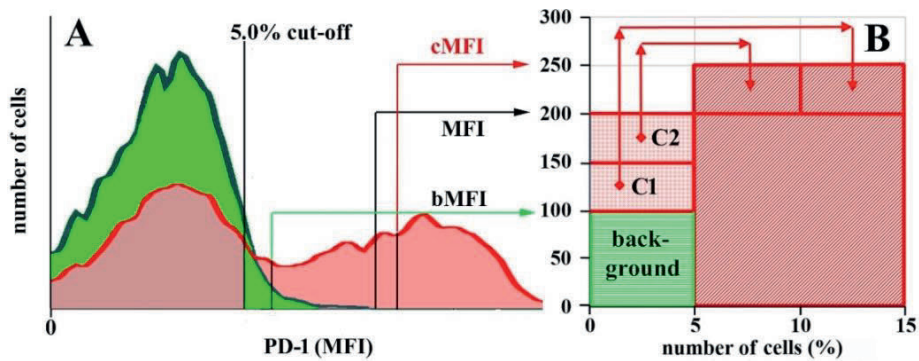
1. Le DT, Durham JN, Smith KN et al. Mismatch repair deficiency predicts response of solid tumors to PD-1 blockade. *Science* 2017; 357:409–413.
2. Larkin J, Minor D, D'Angelo S et al. Overall Survival in Patients With Advanced Melanoma Who Received Nivolumab Versus Investigator's Choice Chemotherapy in CheckMate 037: A Randomized, Controlled, Open-Label Phase III Trial. *J Clin Oncol.* 2018;36:383-390
3. Weber JS, D'Angelo SP, Minor D et al. Nivolumab versus chemotherapy in patients with advanced melanoma who progressed after anti-CTLA-4 treatment (CheckMate 037): a randomised, controlled, open-label, phase 3 trial. *Lancet Oncol.* 2015; 16:375–384.
4. Motzer RJ, Escudier B, McDermott DF et al. Nivolumab versus Everolimus in Advanced Renal-Cell Carcinoma. *N. Engl. J. Med.* 2015; 373:1803–1813.
5. Sul J, Blumenthal GM, Jiang X et al. FDA Approval Summary: Pembrolizumab for the Treatment of Patients With Metastatic Non-Small Cell Lung Cancer Whose Tumors Express Programmed Death-Ligand 1. *Oncologist* 2016; 21:643–650.
6. Kang Y-K, Boku N, Satoh T et al. Nivolumab in patients with advanced gastric or gastro-oesophageal junction cancer refractory to, or intolerant of, at least two previous chemotherapy regimens (ONO-4538-12, ATTRACTION-2): a randomised, double-blind, placebo-controlled, phase 3 trial. *Lancet* 2017; 390:2461–2471.
7. Harrington KJ, Ferris RL, Blumenschein G et al. Nivolumab versus standard, single-agent therapy of investigator's choice in recurrent or metastatic squamous cell carcinoma of the head and neck (CheckMate 141): health-related quality-of-life results from a randomised, phase 3 trial. *Lancet Oncol.* 2017; 18:1104–1115.
8. Ansell SM. Nivolumab in the Treatment of Hodgkin Lymphoma. *Clin. Cancer Res.* 2017; 23:1623–1626.
9. Sharma P, Retz M, Siefker-Radtke A et al. Nivolumab in metastatic urothelial carcinoma after platinum therapy (CheckMate 275): a multicentre, single-arm, phase 2 trial. *Lancet Oncol.* 2017; 18:312–322.
10. Garon EB, Rizvi NA, Hui R et al. Pembrolizumab for the Treatment of Non-Small-Cell Lung Cancer. *N. Engl. J. Med.* 2015; 372:2018–2028.
11. Fessas P, Lee H, Ikemizu S, Janowitz T. A molecular and preclinical comparison of the PD-1-targeted T-cell checkpoint inhibitors nivolumab and pembrolizumab. *Semin. Oncol.* 2017; 44:136–140.
12. European Medicines Agency. Keytruda (pembrolizumab) Eur. Public Assess. Rep., 2016.
13. European Medicines Agency. Opdivo (nivolumab) Eur. Public Assess. Rep., 2016.
14. U.S. Food and Drug Administration. Opdivo (nivolumab) Prescribing information. 2015
15. U.S. Food and Drug Administration. Keytruda (pembrolizumab) Prescribing information. 2015
16. Nakamura Y, Kitano S, Takahashi A, Tsutsumida A. Nivolumab for advanced melanoma: pretreatment prognostic factors and early outcome markers during therapy. *Oncotarget* 2016; 7:77404–15.
17. Loi S, Adams S, Schmid P et al. Relationship between tumor infiltrating lymphocyte

- (TIL) levels and response to pembrolizumab (pembro) in metastatic triple-negative breast cancer (mTNBC): Results from KEYNOTE-086. *Ann. Oncol.* 2017;28:605-649.
18. Tumeah PC, Harview CL, Yearley JH et al. PD-1 blockade induces responses by inhibiting adaptive immune resistance. *Nature* 2014; 515:568–571.
 19. Ribas A, Robert C, Hodi FS et al. Association of response to programmed death receptor 1 (PD-1) blockade with pembrolizumab (MK-3475) with an interferon-inflammatory immune gene signature. *J. Clin. Oncol.* 2015; 33:3001.
 20. Chow LQM, Haddad R, Gupta S et al. Antitumor Activity of Pembrolizumab in Biomarker-Unselected Patients With Recurrent and/or Metastatic Head and Neck Squamous Cell Carcinoma: Results From the Phase Ib KEYNOTE-012 Expansion Cohort. *J. Clin. Oncol.* 2016; 34:3838–3845.
 21. Diehl A, Yarchoan M, Hopkins A et al. Relationships between lymphocyte counts and treatment-related toxicities and clinical responses in patients with solid tumors treated with PD-1 checkpoint inhibitors. *Oncotarget* 2017; 8:114268–114280.
 22. Parikh K, Kumar A, Ahmed J et al. Peripheral monocytes and neutrophils predict response to immune checkpoint inhibitors in patients with metastatic non-small cell lung cancer. *Cancer Immunol. Immunother.* 2018; 67:1365–1370.
 23. Agrawal S, Feng Y, Roy A et al. Nivolumab dose selection: challenges, opportunities, and lessons learned for cancer immunotherapy. *J. Immunother. Cancer* 2016; 4:72.
 24. Brahmer JR, Drake CG, Wollner I et al. Phase I study of single-agent anti-programmed death-1 (MDX-1106) in refractory solid tumors: safety, clinical activity, pharmacodynamics, and immunologic correlates. *J. Clin. Oncol.* 2010; 28:3167–3175.
 25. Choueiri TK, Fishman MN, Escudier B et al. Immunomodulatory activity of nivolumab in metastatic renal cell carcinoma. *Clin. Cancer Res.* 2016; 22:5461–5471.
 26. Zheng H, Liu X, Zhang J et al. Expression of PD-1 on CD4+ T cells in peripheral blood associates with poor clinical outcome in non-small cell lung cancer. *Oncotarget* 2016; 7:56233–56240.
 27. Kamphorst AO, Pillai RN, Yang S et al. Proliferation of PD-1+ CD8 T cells in peripheral blood after PD-1–targeted therapy in lung cancer patients. *Proc. Natl. Acad. Sci.* 2017; 114:4993–4998.
 28. van de Ven R, Niemeijer A-LN, Stam AGM et al. High PD-1 expression on regulatory and effector T-cells in lung cancer draining lymph nodes. *ERJ Open Res.* 2017;3:00110-2016
 29. Asano T, Meguri Y, Yoshioka T et al. PD-1 modulates regulatory T-cell homeostasis during low-dose interleukin-2 therapy. *Blood* 2017; 129:2186–2197.
 30. Lim TS, Chew V, Sieow JL et al. PD-1 expression on dendritic cells suppresses CD8+T cell function and antitumor immunity. *Oncoimmunology* 2015; 5:1085146
 31. MacFarlane AW, Jillab M, Plimack ER et al. PD-1 Expression on Peripheral Blood Cells Increases with Stage in Renal Cell Carcinoma Patients and Is Rapidly Reduced after Surgical Tumor Resection. *Cancer Immunol. Res.* 2014; 2:320–331.
 32. Ren Z, Peng H, Fu Y-X. PD-1 Shapes B Cells as Evildoers in the Tumor Microenvironment. *Cancer Discov.* 2016; 6:477–478.

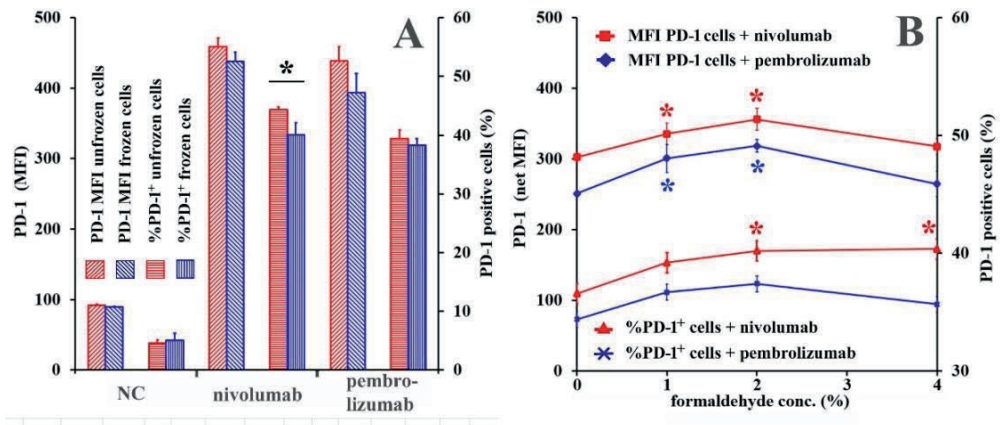
33. Thibult ML, Mamessier E, Gertner-dardenne J et al. Pd-1 is a novel regulator of human B-cell activation. *Int. Immunol.* 2013; 25:129–137.
34. Das R, Verma R, Sznol M et al. Combination Therapy with Anti–CTLA-4 and Anti–PD-1 Leads to Distinct Immunologic Changes In Vivo. *J. Immunol.* 2015; 194:950–959.
35. Liu Y, Cheng Y, Xu Y et al. Increased expression of programmed cell death protein 1 on NK cells inhibits NK-cell-mediated anti-tumor function and indicates poor prognosis in digestive cancers. *Oncogene* 2017; 36:6143–6153.
36. Keeney M, Gratama JW, Chin-Yee IH, Sutherland DR. Isotype controls in the analysis of lymphocytes and CD34+ stem and progenitor cells by flow cytometry--time to let go! *Cytometry* 1998; 34:280–283.
37. Simmons A. The establishment of normal hematology values using the hemalog. *Am. J. Med. Technol.* 1974; 40:321–325.
38. Comans-Bitter WM, de Groot R, van den Beemd R et al. Immunophenotyping of blood lymphocytes in childhoodReference values for lymphocyte subpopulations. *J. Pediatr.* 2005; 130:388–393.
39. Chen P, Sun Q, Huang Y et al. Blood dendritic cell levels associated with impaired IL-12 production and T-cell deficiency in patients with kidney disease: implications for post-transplant viral infections. *Transpl. Int.* 2014; 27:1069–1076.
40. Perfetto SP, Ambrozak D, Nguyen R et al. Quality assurance for polychromatic flow cytometry using a suite of calibration beads. *Nat. Protoc.* 2012; 7:2067–2079.
41. Sternebring O, Alifrangis L, Christensen TF et al. A weighted method for estimation of receptor occupancy for pharmacodynamic measurements in drug development. *Cytom. Part B - Clin. Cytom.* 2016; 90:220–229.
42. Wang C, Thudium KB, Han M et al. In Vitro Characterization of the Anti-PD-1 Antibody Nivolumab, BMS-936558, and In Vivo Toxicology in Non-Human Primates. *Cancer Immunol. Res.* 2014; 2:846–856.
43. Matsumura K, Bae JY, Hyon SH. Polyampholytes as cryoprotective agents for mammalian cell cryopreservation. *Cell Transplant.* 2010; 19:691–699.
44. Ghiotto M, Gauthier L, Serriari N et al. PD-L1 and PD-L2 differ in their molecular mechanisms of interaction with PD-1. *Int. Immunol.* 2010; 22:651–660.


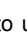








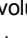
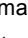






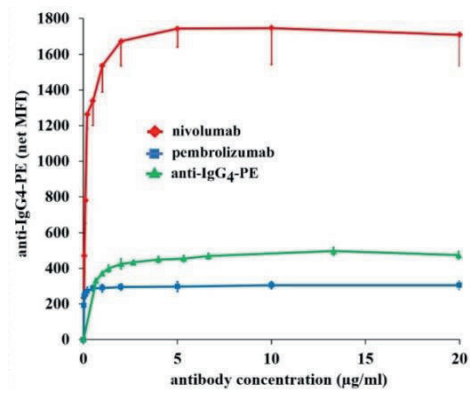
Supplementary Figure 1. Effect of different incubation conditions on the median fluorescence staining intensity (MFI) of PD-1⁺ (A) and PD-1⁺ (B) CD8⁺T-cells by anti-IgG₄-PE, after pre-incubation with (+) or without (-) 10 µg/ml nivolumab. Results are the mean of three separate samples ± SD, incubated with beads buffer containing 0.5 (red checkered), 2.0 (blue checkered), and 5.0% (yellow checkered) (w/v%) bovine serum albumin (BSA) at room temperature and beads buffer with 5% BSA at 0°C (green checkered). * indicates a significant reduction in MFI relative to 0.5%BSA.






Supplementary Figure 2. Correction method used for calculation of the specific median fluorescent intensity (MFI) of PD-1. The MFI of PD-1 in cells treated with nivolumab or pembrolizumab is negatively affected by the lower MFI of the background cells, which requires correction. A. Histograms overlays of background (green) and nivolumab (red) treated samples. Cells were qualified as PD-1⁺ using 5.0% cut-off. B. Graphical presentation of the MFI correction procedure for a sample containing 10% net PD-1⁺ cells with a PD-1 MFI of 200. The 5.0% background cells have an MFI of 100 (bMFI, green checkered). The lower MFI of the background cells results in an underestimation of the MFI of the PD-1⁺ cells, which was corrected according to our method (cMFI, red checkered).



Supplementary Figure 3. Effect of fixation and cryopreservation on PD-1 (net) median fluorescent intensity (MFI, 1st marker) and number of PD-1⁺ cells (%PD-1⁺, 2nd marker). A. Effect of snap-freezing with Cryosofree™ on the PD-1 median fluorescent intensity (MFI = ) and percentage of PD-1⁺CD8⁺-T-cells () was assessed compared to unfixed and not frozen negative controls (NC, MFI = ; %PD-1⁺ = ). PBMC from a healthy volunteer were incubated without (NC) or with 10 µg/ml nivolumab (, ) and pembrolizumab (, ). NC were kept on ice, while the other samples were fixed with 4% (w/v%) formaldehyde, followed by snap-freezing in Cryosofree™. B. Effect of fixation, with different concentrations of formaldehyde on the MFI of PD-1 (, ) and percentage of PD-1⁺ cells (, ) in samples pre-incubated with 10 µg/ml nivolumab (, ) and pembrolizumab (, ). * indicates a significant difference in %PD-1⁺ due to Cryosofree™ (A) or in MFI and %PD-1⁺ relative to unfixed samples (B).



Supplementary Figure 4. Antibody target saturation curves. *Ex vivo* growth stimulated or unstimulated peripheral blood mononuclear cells (PBMC) were incubated with indicated concentrations of nivolumab () and pembrolizumab (), respectively. Samples were incubated with 8 µg/mL of anti-IgG₄-PE. PBMC pre-incubated with nivolumab were incubated with indicated concentrations of anti-IgG₄-PE (). PBMCs used for each curve were from different healthy volunteers. Results are the mean ± standard deviation (SD) of three independent samples.

Supplementary Table 1. FACS settings for detection of indicated biomarkers by 12 parameter flow cytometry. A. Overview of used fluorochromes, lasers, filters and voltages. B. compensation settings. – indicates that the indicated percentage should be subtracted from the signal of the horizontally aligned biomarkers. L-D = Live-dead™ protein fixable marker.

A

Biomarker	Fluorochrome	Laser (nm)	Filter	Voltage
Live-dead	V450	405	450/50	400
CD14	BV525	405	530/30	444
CD123	BV605	405	610/20	600
CD11c	BV650	405	660/20	555
CD19	BV710	405	710/50	551
HLA-DR	BV786	405	780/60	629
CD56	FITC	480	530/30	400
CD8	PerCP-C5.5	480	710/50	568
PD-1	PE	561	585/15	458
CD4	APC	640	670/14	650
CD16	APC-AF700	640	730/45	650
CD3	APC-Cy7	640	780/60	650

B

Bio-marker	L-D	CD14	CD123	CD11c	CD19	HLA	CD56	CD8	PD-1	CD4	CD16	CD3
L-D	100	0	0	0	0	0	0	0	0	0	0	0
CD14	7	100	0	0	0	0	0	0	0	0	0	0
CD123	0	0	100	33	0.8	0	0	0	0	0	0	0
CD11c	0	0	25	100	17	10	0	0	0	0	0	0
CD19	0	0	0	0	100	0	0	0	0	38	80	0
HLA	0	0	0	1	2	100	0	0	0	0	0	10
CD56	0	0	0	0	0	0	100	0	0	0	0	0
CD8	0	0	0	0	60	0	0	100	0	0	90	0
PD-1	0	0	0	0	0	0	0	17	100	0	0	0
CD4	0	0	0	0	0	0	0	0	0	100	80	15
CD16	0	0	0	0	0	0	0	0	0	0.5	100	13
CD3	0	0	0	0	0	0	0	0	0	3	7	100

Supplementary Table 2. Specificity of PD-1 detection in immune cells from a healthy volunteer. Peripheral blood mononuclear cells were cultured in RPMI medium under growth stimulating conditions. Cells were incubated with PD-L2 and PD-1 blocking antibody clone PD1313, followed by incubation with nivolumab and pembrolizumab and detection with anti-IgG4-PE. Shown are the results for CD4⁺ and CD8⁺-T-cells (CD4T and CD8T), B-cells (B), natural killer cells (NK), classical monocytes (CM), intermediate monocytes (IM), non-classical monocytes (NCM), plasmacytoid dendritic cells (pDC), and myeloid dendritic cells (mDC). Data are represented as the mean percentage of PD-1 positive cells (%PD-1⁺) and the mean number of PD-1 molecules per PD-1⁺ cell of three separate samples ± standard deviation (SD). <LLOQ indicates data below the lower limit of quantification = net 5% of PD-1 positive cells.

Cell type	nivolumab				pembrolizumab			
	Net %PD1 ⁺ cells	%PD-1 inhibition	Number of PD-1 / cell	PD-1/cell inhibition	Net %PD1 ⁺ cells	%PD-1 inhibition	Number of PD-1 / cell	PD-1/cell inhibition
CD4T	37.6 ± 0.5	99.9 ± 1.9	2397 ± 94	97.0 ± 1.8	31.1 ± 0.6	97.9 ± 0.9	2290 ± 24	99.5 ± 0.4
CD8T	41.3 ± 0.8	99.0 ± 2.3	6105 ± 231	98.2 ± 1.0	36.4 ± 0.2	98.9 ± 0.9	5510 ± 133	99.6 ± 0.1
B	27.7 ± 0.5	100 ± 1.4	1753 ± 29	98.0 ± 6.2	18.6 ± 0.8	95.9 ± 4.6	1631 ± 11	100.0 ± 7.0
NK	1.2 ± 0.7	<LLOQ	<LLOQ	<LLOQ	0.0 ± 0.3	<LLOQ	<LLOQ	<LLOQ
CM	67.0 ± 0.6	100 ± 1.3	9126 ± 91	94.4 ± 1.7	56.2 ± 0.8	99.9 ± 2.1	7130 ± 98	94.4 ± 1.5
IM	18.4 ± 0.3	99.5 ± 4.0	4902 ± 116	83.6 ± 4.1	10.4 ± 0.7	86.4 ± 13.0	4677 ± 136	80.3 ± 4.1
NCM	10.1 ± 2.0	93.1 ± 16.4	2845 ± 104	80.9 ± 3.7	10.3 ± 0.8	88.1 ± 9.3	2569 ± 20	91.3 ± 17.3
pDC	39.7 ± 6.2	91.6 ± 6.0	5711 ± 314	86.3 ± 4.3	22.9 ± 1.0	101 ± 6.3	5462 ± 270	91.5 ± 8.4
mDC	15.1 ± 1.4	93.4 ± 1.6	3863 ± 283	86.1 ± 11.7	15.4 ± 1.7	84.5 ± 4.5	3866 ± 192	85.6 ± 10.0

Supplementary Table 3. Interference of ipilimumab with the detection of PD-1. Peripheral blood mononuclear cells from a healthy volunteer were incubated with 0, 10 and 50 µg/mL ipilimumab, followed by incubation with nivolumab and pembrolizumab. PD-1 was detected on CD4⁺ and CD8⁺-T-cells (CD4T and CD8T). Data are the mean of three separate samples ± standard deviation (SD) of the percentage of PD-1 positive cells (%PD-1⁺) and their median fluorescent intensity (MFI).

Ipilimumab conc. µg/mL	Background control						Nivolumab						Pembrolizumab											
	CD4T		CD8T		CD4T		CD8T		CD4T		CD8T		CD4T		CD8T									
	%PD1 ⁺	PD-1 MFI	%PD1 ⁺	PD-1 MFI	%PD1 ⁺	PD-1 MFI	%PD1 ⁺	PD-1 MFI	%PD1 ⁺	PD-1 MFI	%PD1 ⁺	PD-1 MFI	%PD1 ⁺	PD-1 MFI	%PD1 ⁺	PD-1 MFI								
0	4.8 ± 0.6	85.4 ± 0.5	5.4 ± 1.0	81.1 ± 0.0	35.9 ± 1.5	155 ± 3.5	43.6 ± 0.5	371 ± 4.6	27.7 ± 0.4	141 ± 2.0	39.3 ± 0.9	337 ± 15	4.1 ± 1.1	84.3 ± 0.9	4.3 ± 0.9	85.9 ± 0.8	34.6 ± 0.2	155 ± 1.7	44.4 ± 0.8	378 ± 7.8	26.1 ± 0.7	141 ± 2.1	38.5 ± 0.7	333 ± 12
10	4.1 ± 0.9	85.4 ± 0.5	4.6 ± 0.7	80.6 ± 0.5	33.7 ± 1.1	155 ± 0.0	44.1 ± 0.4	369 ± 17	26.2 ± 0.7	142 ± 7.1	37.7 ± 0.8	330 ± 25	4.1 ± 0.9	85.4 ± 0.5	4.6 ± 0.7	80.6 ± 0.5	33.7 ± 1.1	155 ± 0.0	44.1 ± 0.4	369 ± 17	26.2 ± 0.7	142 ± 7.1	37.7 ± 0.8	330 ± 25

Supplementary Table 4. Linearity of PD-1 detection in samples containing 100k and 500k PBMC from a healthy volunteer. Samples were incubation with nivolumab. A. Relative difference (Δ) in measured cells between samples spiked with 100k and 500k PBMC. Shown are the results for total live cells, CD4⁺ and CD8⁺-T-cells (CD4T and CD8T), B-cells (B), natural killer cells (NK), classical monocytes (CM), intermediate monocytes (IM), non-classical monocytes (NCM), plasmacytoid dendritic cells (pDC), and myeloid dendritic cells (mDC). B. Relative difference (Δ) between the percentage of PD-1⁺ and number of PD-1 per CD4⁺ and CD8⁺-T-cells in samples containing 100k and 500k PBMC. Data are represented as the mean of three separate samples \pm standard deviation (SD).

A

Cell type	Number of measured cells at input level		
	100,000	500,000	Δ (%)
Total	104865	529000	0.9
CD4T	40,179	196,494	2.2
CD8T	9,296	45,315	2.5
B	3,581	19,637	-9.7
NK	17,399	83,002	4.6
CM	18,582	94,723	-2.0
IM	2,887	14,366	0.5
NCM	1,548	8,709	-12.5
pDC	376	2,015	-7.2
mDC	604	3,389	-12.2

B

Cell type	Net number of PD1 ⁺ cells			Number of PD-1 / cell		
	100,000	500,000	Δ (%)	100,000	500,000	Δ (%)
CD4T	27.6 \pm 1.8	29.5 \pm 2.2	6.9	1814 \pm 73	1776 \pm 75	-2.1
CD8T	40.4 \pm 1.7	41.7 \pm 1.6	3.3	4708 \pm 204	4652 \pm 222	-1.2

Supplementary Table 5. Long term storage stability of PD-1 in PBMC isolated from a healthy volunteer. Samples spiked with 200k PBMC were treated with nivolumab or pembrolizumab. Cells were snap frozen in liquid nitrogen using Cryosofree™. Samples were stored for 0, 53, and 153 days, after which PD-1 was determined. 5A. Number of measured total live cells, CD4⁺ and CD8⁺-T-cells (CD4T and CD8T), B-cells (B), natural killer cells (NK), classical monocytes (CM), intermediate monocytes (IM), non-classical monocytes (NCM), plasmacytoid dendritic cells (pDC), and myeloid dendritic cells (mDC). 5B and C. Measured percentage of PD-1⁺ cells and number of PD-1 per CD4⁺ and CD8⁺-T-cells in respectively nivolumab and pembrolizumab samples. $\Delta_{0-153}\%$ = relative difference between day 0 and 153 in measured cell numbers, percentage of PD-1⁺ cells, and number of PD-1 per cell. BDP = between day precision. Data are the mean of three separate samples \pm standard deviation (SD).

Cell type	Number of measured cells at day				
	0	53	153	Δ_{0-153} (%)	BDP (%)
Total	177310	166011	166778	-5.9%	3.7%
CD4T	71380	64199	73631	3.2%	7.3%
CD8T	16155	16260	16383	1.4%	0.7%
B	4176	4376	4248	1.7%	2.4%
NK	23309	23750	23629	1.4%	1.0%
CM	23652	27097	25659	8.5%	6.8%
IM	2286	2560	2477	8.4%	5.8%
NCM	1025	1031	1066	4.0%	2.1%
pDC	686	616	590	-14.1%	7.7%
mDC	429	512	479	11.8%	9.0%

5B.

Cell type	PD1 ⁺ cells (%) at day					Number of PD-1 / cell at day				
	0	53	153	Δ_{0-153} (%)	BDP (%)	0	53	153	Δ_{0-153} (%)	BDP (%)
CD4T	25.2 \pm 1.4	27.0 \pm 1.3	24.2 \pm 2.2	-4.4	5.6	1592 \pm 92.5	1652 \pm 38.9	1624 \pm 81.5	2.0	1.9
CD8T	38.2 \pm 1.6	39.4 \pm 0.6	37.1 \pm 0.4	1.5	3.4	5194 \pm 154	4992 \pm 138	4842 \pm 143	-6.8	3.5

5C.

Cell type	PD1 ⁺ cells (%) at day					Number of PD-1 / cell at day				
	0	53	153	Δ_{0-153} (%)	BDP (%)	0	53	153	Δ_{0-153} (%)	BDP (%)
CD4T	20.6 \pm 1.1	22.0 \pm 1.8	20.9 \pm 3.3	1.5	3.4	1561 \pm 58.7	1574 \pm 70.1	1584 \pm 85.2	1.5	0.7
CD8T	34.8 \pm 1.5	34.3 \pm 1.6	34.1 \pm 1.7	-1.9	1.0	4480 \pm 347	4469 \pm 169	4761 \pm 107	6.3	3.7

Supplementary Table 6. Overview of patients included in the study. Advanced cancer patients with indicated tumor type were administered with nivolumab or pembrolizumab, based on their bodyweight (3 mg/kg), or a flat dose (mg) in two (q2w), three (q3w) or four (q4w) weekly intervals.

Patient #	Cancer type	Treatment	Dose	Schedule
1	Melanoma	Nivolumab	480 mg	q4w
2	Mesothelioma	Nivolumab	3 mg/kg	q2w
3	NSCLC	Nivolumab	3 mg/kg	q2w
4	Mesothelioma	Nivolumab	3 mg/kg	q4w
5	Renal	Nivolumab	480 mg	q4w
6	Head and neck	Nivolumab	240 mg	q4w
7	Bladder	Pembrolizumab	200 mg	q3w
8	Melanoma	Pembrolizumab	200 mg	q3w
9	Bladder	Pembrolizumab	200 mg	q3w
10	Melanoma	Pembrolizumab	150 mg	q3w
11	Melanoma	Pembrolizumab	200 mg	q3w

Chapter 5

Antidrug antibodies

CHAPTER 5.1

Antidrug Antibody Formation in Oncology: Clinical Relevance and Challenges

Willeke Ros*, Emilie van Brummelen*

**Authors contributed equally*

Van Brummelen EMJ*, **Ros W***, Wolbink G, Beijnen JH, Schellens JHM. Antidrug Antibody Formation in Oncology: Clinical Relevance and Challenges. *The Oncologist*. 2016;21: 1260 - 1268

ABSTRACT

In oncology, an increasing number of targeted anticancer agents and immunotherapies are of biological origin. These biological drugs may trigger immune responses which lead to the formation of antidrug antibodies (ADAs). ADAs are directed against immunogenic parts of the drug and may affect efficacy and safety. In other medical fields, such as rheumatology and hematology, the relevance of ADA formation is well established. However, the relevance of ADAs in oncology is just starting to be recognized and literature on this topic is scarce.

In an attempt to fill this gap in the literature, we provide an up-to-date status of ADA formation in oncology. In this focused review, data on ADAs was extracted from 81 clinical trials with biological anticancer agents. We found that most biological anticancer drugs in these trials are immunogenic and induce ADAs (63%). However, it is difficult to establish the clinical relevance of these ADAs. In order to determine this relevance, the possible effects of ADAs on pharmacokinetics, efficacy and safety parameters need to be investigated. Our data show that this was only done in fewer than 50% of the trials. In addition, we describe the incidence and consequences of ADAs for registered agents. We highlight the challenges in ADA detection and argue for the importance of validating, standardizing and describing well the used assays.

Finally, we discuss prevention strategies such as immunosuppression and regimen adaptations. We encourage the launch of clinical trials that explore these strategies in oncology.

IMPLICATIONS FOR PRACTICE

Because of the increasing use of biologicals in oncology, many patients are at risk of developing antidrug antibodies (ADA) during therapy. Although clinical consequences are uncertain, ADAs may affect pharmacokinetics, patient safety and treatment efficacy. ADA detection and reporting is currently highly inconsistent, which makes it difficult to evaluate the clinical consequences. Standardized reporting of ADA investigations in context of aforementioned parameters is critical to understanding the relevance of ADA formation for each drug. Furthermore, the development of trials that specifically aim to investigate clinical prevention strategies in oncology is needed.

INTRODUCTION

Drug-induced immunogenicity has been recognized as a major challenge in the development of biological drugs. These biological drugs, such as proteins, peptides and antibodies, consist of large and complex structures and some of these structures may not belong to the patients' self-repertoire. Drug administration to patients may induce humoral immune responses causing the formation of antidrug antibodies (ADAs). ADAs may inactivate the drug, cause loss of targeting and/or an increased clearance of ADA-drug complexes which may lead to suboptimal exposure and loss of efficacy^{1,2}. Patients who develop ADAs are also at risk for increased toxicity caused by the immune response that accompanies ADA formation, loss of drug targeting or formation of highly immunogenic complexes³⁻⁵.

Extensive research is being conducted to study the immunogenicity of biological drugs, such as anti-tumor necrosis factor α (anti-TNF- α) and factor VIII. This research is an important contribution to the current knowledge of risk factors for immunogenicity, formation and detection of ADAs, and possible strategies to prevent ADA formation. It has become clear that immunogenicity is not solely dependent on the biological drug. Emerging data indicate that the development of an immune response may be influenced by a variety of factors such as dose, administration regimen, administration route, product quality and handling, co-medication, patients' immune-status and genetic factors such as major histocompatibility genotype^{2,6}. As a result, formation of ADAs is subject to a high inter-individual variability.

Although different medical fields have shown that ADA formation may have important consequences for therapy⁵, little attention is paid to ADA formation during anticancer therapy. Importantly, the risks and consequences of ADAs in oncology may not be identical to those in other fields e.g. rheumatology and haematology. There are several factors that need to be specifically considered in oncology, such as the use of immunostimulatory compounds, the substantial number of immunocompromised patients, concomitant treatment and immunosuppressing therapies.

This paper reviews the current knowledge on ADA formation in oncology, with the purpose of raising awareness and allowing a better understanding of the potential effects of ADAs. Topics that will be discussed include the incidence and clinical consequences of ADAs, the analytical methods that are used for detection, and the challenges in interpreting these data. Finally, in the last section of this review, we discuss challenges and potential strategies to deal with ADA formation in clinical practice, such as changes in the treatment regimen, and concomitant treatment with immunosuppressive drugs.

INCIDENCE OF ADAS IN ONCOLOGY

The U.S. Food and Drug Administration (FDA) and European Medicines Agency (EMA) published guidelines to recommend evaluation of immunogenicity of therapeutic proteins at the earliest stage of drug development and every subsequent stage^{4,7}. Clinical evaluation is of high importance, since currently no tools are available to adequately predict clinical immunogenicity based on (pre-)clinical data. To study the reported immunogenicity of biological anticancer agents in clinical development, a focused PubMed literature review was performed including the keywords ‘oncology’ OR ‘cancer’ AND ‘immunogenicity OR anti-drug-antibodies’ AND ‘clinical trial’ NOT vaccine (full description of methods in Supplementary Material). Among the 81 reviewed studies with biological anticancer agents, ADAs were detected in 63%. This number indicates that the majority of compounds in oncology is immunogenic and induces ADA formation. Over the last years, the intrinsic immunogenicity of monoclonal antibodies (mAbs) has been reduced by the transition from murine to chimeric, humanized and fully human mAbs⁸. Our data support this as well for the mAbs used in oncology. The incidence of ADA formation was significantly less for human agents compared to humanized ($p=0.03$), chimeric ($p=0.007$) and murine agents ($p=0.004$) (Figure 1). However, even for human mAbs, ADAs are detected for 26.3%.

Eight studies reported the presence of pre-existing ADAs before the start of treatment^{9–15}. Although the incidence of ADAs after treatment was not significantly different between trials with and without pre-existing ADAs (75% vs. 62%, $p=0.70$) patients with pre-existing ADAs may develop ADAs faster and in higher quantities¹². However, these ADAs can also be transient and post-dose ADA status can become negative^{10,16}.

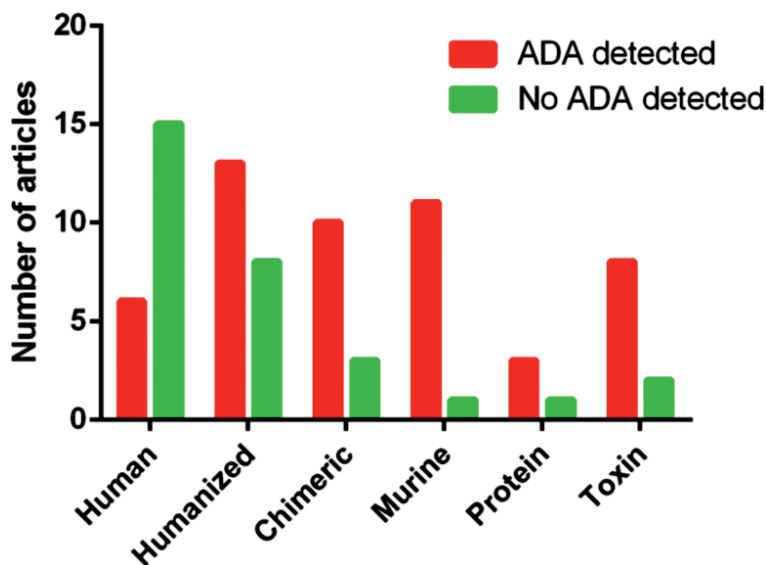


Figure 1. Detection of ADAs for murine, chimeric, humanized, human monoclonal antibodies, protein drugs, and toxins.

CLINICAL RELEVANCE

In order to understand the clinical consequences of ADA formation, it is necessary to determine the impact on pharmacokinetics (PK), efficacy and toxicity. For the majority of agents, the clinical relevance of ADA formation is not well established. In clinical trial reports, the titers and percentages of ADA positive patients are often summarized, but the consequences of ADAs are not investigated. In the following sections, we discuss the relation between ADAs and these clinical parameters.

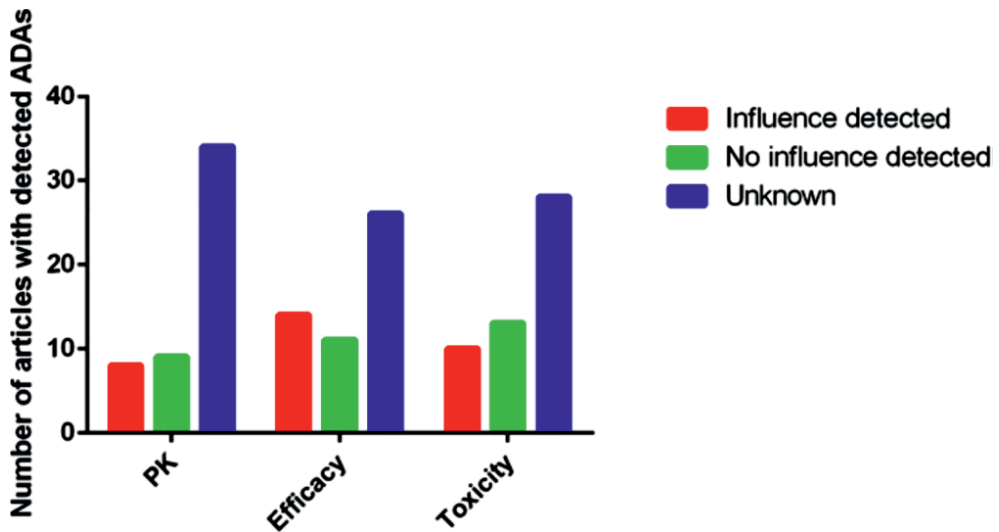


Figure 2. Influence of ADA formation on pharmacokinetics, efficacy, and toxicity.

CONSEQUENCES OF ADA FORMATION ON PHARMACOKINETICS, EFFICACY, AND TOXICITY

Pharmacokinetics

ADAs can alter the PK profile of biologicals by causing accelerated clearance of ADA-drug complexes. This can lead to a lower and even subtherapeutic exposure (area under the curve (AUC)), as well as lower maximum concentrations (C_{max}), and a shorter elimination half-life ($T_{1/2}$), which have important consequences for treatment efficacy^{9,14,17–22}. The impact of ADAs on PK is dependent on the affinity, the type of ADAs and the amount of free drug that is not bound to ADAs. To understand the relevance, comparing maximum concentration levels (C_{max}) and exposure (AUC) in both presence and absence of ADAs is essential. In the reviewed trials, data on ADAs are not routinely reported in context with PK. Among the 51 trials in which ADAs were detected, effects on PK were not explored in 67% and nine trials (18%) reported no influence of ADA formation on PK (Figure 2). Only eight trials (16%) confirmed that PK was affected by ADAs. One of these, Posey *et al.*, compared PK for cycle 1 and cycle 4 knowing that 50% of the patients had ADA titers¹⁷. All but two patients showed similar C_{max} values for both cycles. One of these patients showed a very high ADA

titer (460 ng/ml) and a 28% decrease in C_{max} . The other patient, who received a higher dose, showed a much lower ADA titer (86 ng/ml), but surprisingly showed an undetectable C_{max} during cycle 4. Possibly, more high-affinity ADAs were present in this patient. This illustrates that the relationship between ADA and PK is difficult to describe and is dependent on ADA titers and affinity. Reduced drug-levels or exposures may indeed be direct results of ADA-drug binding, but may also be a consequence of increased clearance or an increase in target-mediated drug disposition. In clinical development, the use of a PK-pharmacodynamic model can provide information on the relative contribution of ADAs²³.

Efficacy

Even though ADAs can alter PK, this does not always translate to impaired therapeutic activity. Patients are specifically at risk of reduced efficacy if high titers of high-affinity neutralizing ADAs are present during treatment. Neutralizing ADAs bind to the variable regions of the antibody to prevent targeting, thus hampering the therapeutic activity²⁰. In contrast, binding ADAs that bind to non-selective epitopes of the antibody, such as the Fc region, do not necessarily cause decreased therapeutic activity. However, both types of ADAs may lead to rapid clearance. In Yu *et al.*, neutralizing ADAs against the chimeric mAb ch14.19 were formed, which prevented binding of ch14.19 to its target disialoganglioside (GD2)²⁴. Three out of eight patients in the study showed high ADA titers, yet these patients still had partial responses. Despite high titers, these ADAs may have had low affinities, or the neutralizing ADAs were formed after treatment was completed. In our dataset, out of 51 trials that detected ADA formation, 14 articles (27%) associated this with pharmacodynamic alterations or reduced efficacy, while in the majority of trials (51%) the effects were not explored (Figure 2). Eleven trials (21%) found that ADAs had no effect on efficacy.

Toxicity

The most common toxic effects of ADAs are infusion-related reactions (IRRs)²⁵. Multiple mechanisms can underly an IRR. Hypersensitivity reactions are IgE mediated²⁶, but IRRs can also be mediated by IgG or IgM ADAs. In hypersensitivity reactions, high titers of IgE ADAs are formed after drug exposure and bind to the FcεRI on mast cells. Upon re-exposure, drug that binds to cell-bound IgE triggers degranulation of histamine which causes an allergic reaction. As a consequence, treatment may be aborted to prevent severe allergic reactions upon retreatment²⁷. In IgG-mediated reactions, binding of IgG to the drug may activate antibody-dependent cell-mediated toxicity. The Fc region of IgG ADAs binds to natural killer cells, causing a release of pro-inflammatory cytokines²⁸. Furthermore, IgG aggregates and IgM are also capable of causing an inflammatory response through activation of the complement system²⁹. Clinical manifestations of IRRs occur during or shortly after infusion of the drug and include a broad range of symptoms including fever, skin rash, hypotension, gastrointestinal symptoms and more. Since clinical symptoms are similar for each mechanism it is difficult to distinguish between different types of IRR. However, IRRs may also be independent of ADA formation and vice versa²⁷. An example of a non-ADA dependent IRR is cytokine release syndrome, in which cytokine-producing T-cells cause a systemic inflammatory response²⁶.

In the majority of studies in our dataset, the relationship between ADAs and toxicity was not investigated. For 20% of the studies, ADAs were related to IRRs such as rigors, coughing,

dyspnea, back pain, rash, chills, chest tightness, hypotension, urticaria, bone pain and fever (Figure 2). Besides inducing immune-mediated reactions, ADAs can also indirectly affect toxicity by causing a loss of targeting. If ADAs neutralize the therapeutic agent and prevent binding of the drug to its target, drug-induced toxicity may be decreased³⁰. We hypothesize that for immunotoxins and bispecific (e.g. T-cell activating) antibodies, the effect of neutralization by ADAs may be complicated: these antibodies consist of a targeting moiety and a pharmacologically active moiety. If the ADAs neutralize the targeting moiety, the drug may cause systemic toxicity due to loss of targeting.

CLINICAL RELEVANCE OF ADA FORMATION FOR MARKETED DRUGS

Among drugs investigated in the 81 reviewed trials, nine are currently marketed. To assess the relevance of ADAs for the agents used in clinical practice more thoroughly, we reviewed 26 EMA and FDA drug reports³¹⁻⁵⁶. Registered drugs have overcome many obstacles in order to be approved, including the hurdle of immunogenicity. For most registered biological anticancer drugs, only a low percentage of patients form ADAs, and these ADAs often do not have a clinical effect. This is true for commonly used drugs such as cetuximab (3.4%), trastuzumab (8%), rituximab (1 – 2%) and panitumumab (3.8%). Remarkably, for bevacizumab, ramucirumab, trastuzumab-emtansine, elotuzumab and blinatumomab, the clinical consequences of ADAs are unknown, despite relevant percentages of ADA positive patients (Table 1). The immune checkpoint inhibitors such as nivolumab, pembrolizumab, and ipilimumab have low immunogenicity (10%, 0.4% and <2% respectively) and ADAs are thought to have little impact on efficacy. Interestingly, the percentage of patients forming ADAs against nivolumab was higher when treated in combination with ipilimumab (21.9% vs. 10% in monotherapy)⁵⁷.

For ipilimumab (monotherapy), an ADA incidence of <2% was reported. However, the assay was sensitive to drug interference, leading to a potential underestimation of the number of ADA positive patients⁵⁸. Additional subset analyses indeed confirmed that the percentage of ADA positive patients may approach 7% instead. This demonstrates the importance of knowing the strengths and weaknesses of the assay in order to interpret the results correctly.

Tositumomab, catumaxomab, brentuximab-vedotin and aldesleukin are registered drugs which are highly immunogenic. These drugs either consist of a toxin conjugate, are a recombinant form of human protein, or are murine mAbs, and induce ADAs in 35% (brentuximab-vedotin) to 94% (catumaxomab) of patients. ADAs during tositumomab and brentuximab-vedotin therapies increase toxicity, whereas for aldesleukin only PK is affected. In all these cases, the relation to efficacy was not investigated. For catumaxomab, no clinical consequences were described in the drug report. Phase I data suggest that ADAs were formed mostly after the last infusion of catumaxomab, making it unlikely that these ADAs are clinically relevant⁵⁹.

Table 1. Overview of ADA relevance in registered biological anticancer agents based on European Public Assessment Reports (EPARs) unless otherwise indicated³¹⁻⁵⁰. N= neutral to immune system I = inhibits immune system S = stimulates immune system C = chimeric H = human HZ = humanized P = protein

TYPE	DRUG	TARGET	IMMUNOSTIMULATOR EFFECT	ADAS DETECTED	Frequency (%)	EFFECTS ON PK	EFFECTS ON TOXICITY	EFFECTS ON EFFICACY
H	Panitumumab	EGFR	N	yes	3.8%	no	no	no
H	Ipilimumab	CTLA4	S	yes	<2%	nd	nd	no
H	Nivolumab	PD-1	S	yes	10%	no	no	no
H	Ofatumumab	CD20	I	no	0%	na	na	na
H	Necitumumab	EGFR	N	yes	4.1% (FDA)	nd	no	nd
H	Daratumumab	CD38	I	No	0% (FDA)	na	na	na
HZ	Obinutuzumab	CD20	I	yes	6%	nd	no	no
HZ	Bevacizumab	VEGF	N	yes	0.63% (FDA)	nd	nd	nd
HZ	Trastuzumab	HER2	N	yes	8%	no	no	no
HZ	Ramucirumab	VEGFR2	N	yes	2.2%	nd	nd	nd
HZ	Pertuzumab	HER2	N	yes	3%	nd	yes	nd
HZ	Pembrolizumab	PD-1	S	yes	0.4%	no	no	no
HZ	Elotuzumab	SLAMF7	S	yes	18.5% (FDA)	nd	nd	nd
C	Rituximab	CD20	I	yes	1 % (iv) 2% (sc)	no	no	no
C	Siltuximab	IL-6	I	yes	0.2%	nd	no	no
C	Dinutuximab	GD2	N	yes	17%	yes	no	nd
C	Cetuximab	EGFR	N	yes	3.4%	no	no	no
M	Ibritumomab	CD20	I	yes	1.3% (FDA)	nd	no	nd
M	Catumaxomab	EpCAM + CD3	S	yes	94%	nd	no	nd
M	Tositumomab	CD20	I	yes	80% (FDA).	nd	yes	nd
T	Brentuximab Vedotin	CD30	I	yes	35%	no	yes	no
T	Trastuzumab - emtansine	HER2	N	yes	5.3%	nd	nd	nd
P	IFN α	IFN α -R	S	yes	2.9	nd	no	no
P/H	Aflibercept	VEGF	N	yes	3.8	no	no	no
P	Aldesleukin	IL2-R	S	yes	70.8 (FDA)	yes	nd	nd
H	Blinatumomab	CD19,CD3	S	yes	1.4%	nd	nd	nd

ASSESSMENT OF IMMUNOGENICITY

The clinical relevance can only be assessed when reliable and valid data on ADA formation are collected for the drug of interest. Whereas drug detection assays are relatively easy to develop and to interpret because the detection target is clear, this is more difficult for ADA assays because the ADA population is heterogeneous. Furthermore, it is unclear which ADAs are clinically relevant and detection is complicated by interference of the drug and ADA-drug complexes. In our dataset, the most popular method for ADA detection is Enzyme Linked Immunosorbent Assay (ELISA), including direct⁶⁰, sandwich⁶¹, bridging⁶², and competitive ELISAs¹⁶. Other methods include high-performance liquid chromatography (HPLC)⁶³, electrochemiluminescence assays (ECL)^{10,64–66}, radiometric assays^{17,67}, radioimmunoassays (RIA)^{63,68–70} and cytotoxicity assays^{71,72} (Figure 3). The results are qualitative reports of the patient's ADA status (positive/negative), often accompanied by titer levels.

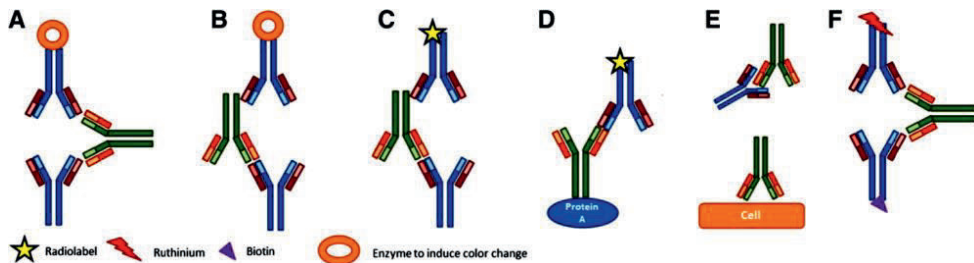


Figure 3. Schematic representation of techniques used to detect antidrug antibodies (ADAs). (A): Bridging enzyme-linked immunosorbent assay (ELISA) with drug as binding agent and enzyme-linked drug as idiotype-detecting agent. (B): Sandwich ELISA with drug as binding agent and enzyme-linked secondary antibody as isotype-detecting agent. (C): Radioimmunoassay with radiolabeled drug binding to ADAs. (D): Antigen-binding test in which IgG from serum is pulled down by protein A bound to a solid carrier, and radiolabeled drug is added and binds to ADAs. (E): Cytotoxicity assays measure ADA-induced alterations in cytotoxic effects of the drug. (F): Bridging electrochemiluminescence assays measure electrochemical signals from the ruthinium-labeled drug bound to the ADA-biotin-streptavidin complex.

For a proper understanding of assay results, it is essential to know which type of ADA is detected by the assay. ADAs may consist of multiple immunoglobulin subclasses, and are either freely circulating or drug-bound. However, most assays, including ELISAs, measure only free IgG subclasses. Drug-bound ADAs and important immunoglobulin subclasses, such as IgE, are not detected which may lead to an underestimation of the incidence and the titer of ADAs⁷³.

To manage drug interference, samples can be acidified in order to separate drug-ADA complexes⁷⁴. Samples can also be taken prior to dosing, when drug concentrations are low⁷⁴. Another option is using the antigen binding test (ABT). ABTs are less vulnerable to drug interference and can measure moderate amounts of ADA-drug immunocomplexes⁵. In this assay, ADAs of the IgG class, including those that are drug-bound, are pulled down during the first step of the assay using protein A. Then, radiolabeled drug binds to the ADA, and the radiation signal is measured (Figure 3). If the samples are acidified prior to the ABTs, the assay is even more tolerant to drug interference⁵. However, in spite of their increased resistance to drug interference, even ABTs may give an underestimation, as not all immunoglobulin subtypes are measured.

Different assays detect different subclasses and idiotypes of ADAs, and currently no assay is able to detect all ADAs. This is one of the reasons why ADA formation across different trials cannot be accurately compared. To increase sensitivity, a tiered approach can be applied, consisting of a screening assay, a confirmatory assay and finally characterization of the ADAs⁷⁵. In a number of trials, ADAs were detected already prior to treatment, and these samples were occasionally deemed false-positive¹⁵. Using the aforementioned tiered approach, these samples should be analyzed for ADA with a confirmatory assay in order to truly validate that these patients are ADA negative. An example of this approach is the phase I trial of AGS-1C4D4, a human anti-prostate stem cell antigen monoclonal antibody⁷⁶. An ECL test served as the screening test in which three patients were tested ADA positive. A second assay was performed for confirmation, which yielded negative results. Therefore, patients were considered negative for the presence of anti-AGS-1C4D4 antibodies.

Although accurately detecting the presence and incidence of ADAs is important, it may be even more crucial to characterize the effects of the detected ADAs. Assays that determine the presence of neutralizing antibodies, such as cytotoxicity assays⁷², can select for those ADAs that affect efficacy.

To summarize, ADA assays should be rationally designed to detect the most relevant range of ADAs, and results should be consistently reported to allow an understanding of the characteristics and consequences of the detected ADAs. Furthermore, standardization of assays is essential to allow comparison of results on ADA formation between different trials. For this, the recently developed guidelines for ADA assays for clinical use published by the ABIRISK consortium could be used⁷⁵.

PREVENTION STRATEGIES

Although reducing intrinsic immunogenicity of the drug is a successful approach to reduce ADA formation, clinical results show that this is not sufficient to prevent ADA formation in all patients. Several prevention strategies have been applied in clinical practice and their potential will be explored in this section.

Tolerance induction by adaptations to the treatment regimen

Several studies indicate that immunogenicity can be reduced by increasing the exposure through high-dose and high-frequency therapy^{5,27,77–80}. The effects of high-dose and high-frequency treatment were first observed in haemophilia patients treated with factor VIII after the doses were increased from normal treatment regimen to twice daily infusions⁸⁰. In patients treated with infliximab, the incidence of ADA formation was 28% after a single dose of infliximab compared to 6% after repeated doses^{81,27}. It is hypothesized that the tolerance is mediated by activation of regulatory T-cells⁸², and apoptosis of effector T-cells⁸³. However, it is unknown if this is a consequence of increased plasma concentrations (C_{max} , C_{ss}), prolonged exposure ($T_{1/2}$), higher exposure (AUC), or any combination of these.

In oncology, the effects of modifications to the treatment regimen are conflicting. Among the nine studies that reported ADA formation for different doses, the majority found that ADA formation was not dose-dependent^{21,71,84–86} and only two studies confirm a decrease in ADA formation with higher doses^{17,19}.

The main limitations of high-dose or high-frequency treatment are the therapeutic and toxic effects of the drug. One possible method to avoid these, is by administering only the immunogenic part of the molecule without the pharmacologically active moiety, as was done by Somerfield *et al.*⁷⁸. In this study, patients treated with alemtuzumab received the non-binding SM3 shortly prior to treatment. SM3 differs from alemtuzumab in only a single point mutation, which prevented binding to CD52. In this way, high doses may be administered without causing unacceptable toxicity. This strategy reduced the percentage of ADA positive patients significantly from 74 % to 21%. However, introducing this additional compound into the clinic may be very costly and time-consuming, and occupation of the target by this compound may be a problem.

In contrast to the results of high-dose and high-frequency treatment, four studies report that tolerance was induced by decreasing the exposure through lower doses, continuous infusion or subcutaneous administration^{71,87–89}. For the humanized antibody trastuzumab, ADA formation was twice as high after intravenous administration (14.6%) as after subcutaneous administration (7.1%) in equivalent doses⁸⁹. For the anti-mesothelin immunotoxin SS1P, a bolus injection administered in 3 days every other day induced ADAs in 88%, whereas an equivalent dose of a 10-day continuous infusion induced ADAs in 75%⁷².

In summary, it is clear that adaptations to the dose and treatment regimen can alter immunogenicity. Most evidence is available for tolerance induction by high-dose and high

frequency therapy but this appears not effective for all drugs. Modifications to the treatment regimen are relatively easy adjustments and should be considered based on successful cases that have been described in literature.

Immunosuppression

In rheumatology, the use of immunosuppressive agents is an effective treatment strategy that simultaneously reduces the frequency of ADA formation up to 46%⁹⁰⁻⁹⁴. Concomitant treatment with methotrexate (MTX) in low (5-10 mg), intermediate (12.5 – 20 mg), or high weekly doses (>22.5 mg) successfully led to reduction of ADA formation in adalimumab treated rheumatoid arthritis patients in a dose-dependent manner⁹⁰. A similar effect was observed in rheumatoid arthritis patients who received infliximab. After a single dose of infliximab, ADAs were formed in 53%, 21% and 7% (1, 3, and 10 mg infliximab/kg) of the patients. When combined with 7.5 mg MTX weekly, the incidence was respectively 15%, 7% and 0%⁹². Azathioprine, 6-mercaptopurine, hydrocortisone, and rituximab have also been applied in rheumatology, but results are inconclusive⁹⁴⁻⁹⁷.

In oncology, immunosuppression can be effective for the treatment of hematological malignancies, but for many solid tumors immunosuppression may be undesired. Among the articles we reviewed, only two investigated the effects of immunosuppression and showed that cyclophosphamide and cyclosporin could not prevent ADA formation^{98,99}.

Unique challenges regarding the use of immunosuppression to prevent ADA formation in oncology may be the large group of immunocompromised patients and the increasing use of immunostimulatory agents such as immunotoxins, interleukin-2, CD3-, CD19-, CD28 agonists, anti-PD1 and anti-CTLA-4. Both factors may alter the risk of ADA formation (decrease and increase, respectively) and for these patients special prevention strategies may be required. Our data showed no significant difference ($p=1.0$) in ADA formation between the trials with immunostimulatory agents (75% detected ADAs (n=20)), immunosuppressing agents (69% (n=13)) and non-immunotherapies (56% (n=48)) (Figure 4). No data were available to compare ADA formation between immunocompromised and immunocompetent patients. Although some trials investigated immunostimulatory agents combined with immunosuppression, effects on treatment efficacy and ADA formation could not be determined based on the reported data¹⁸. However, it is clear that despite immunosuppression, patients are still at risk of ADA formation^{23,100}. This is illustrated by the trial by Welt *et al.*³⁰ with the humanized antibody huA33 in which concomitantly administered chemotherapy led to bone marrow suppression in 10 of 16 patients. The majority of ADA negative patients were immunocompromised (4/6), but one patient with severe neutropenia showed high and increasing ADA titers.

A feasible prevention strategy for oncology may be targeted B-cell inhibition with anti-CD20 agents such as rituximab, veltuzumab or obinutuzumab which inhibit *de novo* humoral antibody responses. Several trials have been done with B-cell inhibiting agents but these did not detect effects on ADA formation^{61,69,72,87,101,102}. Hassan *et al.* showed that rituximab was able to induce full depletion of CD20 positive B-cells, but this did not prevent ADAs targeted towards the therapeutic drug¹⁰³. Maeada *et al.*¹⁰⁴ described a case of a rituximab

treated mantle-cell lymphoma patient, who developed high titers of anti-rituximab antibodies leading to a decreased exposure, and Sausville *et al.*⁶⁹ detected ADAs in 75% of B-cell lymphoma patients treated with the B-cell targeting anti-CD22 immunotoxin IgG-RFB4-SMPT-dgA. These trials show that ADA formation is still possible despite B-cell depletion, but it is not clear if the frequencies, titers or onset may be reduced. Taken together, immunosuppression has successfully reduced ADA formation in rheumatology but evidence for immunosuppression in oncological patients, and in combination with immunotherapies or immunocompromisation is lacking. The absence of observed effects of immunosuppression on ADAs may be explained by the fact that these clinical trials were not designed to investigate this thoroughly. Clinical trials specifically designed to determine the effect of immunosuppressive therapy, such as anti-CD20, on anti-drug antibody formation may determine whether immunosuppression is useful in oncology.

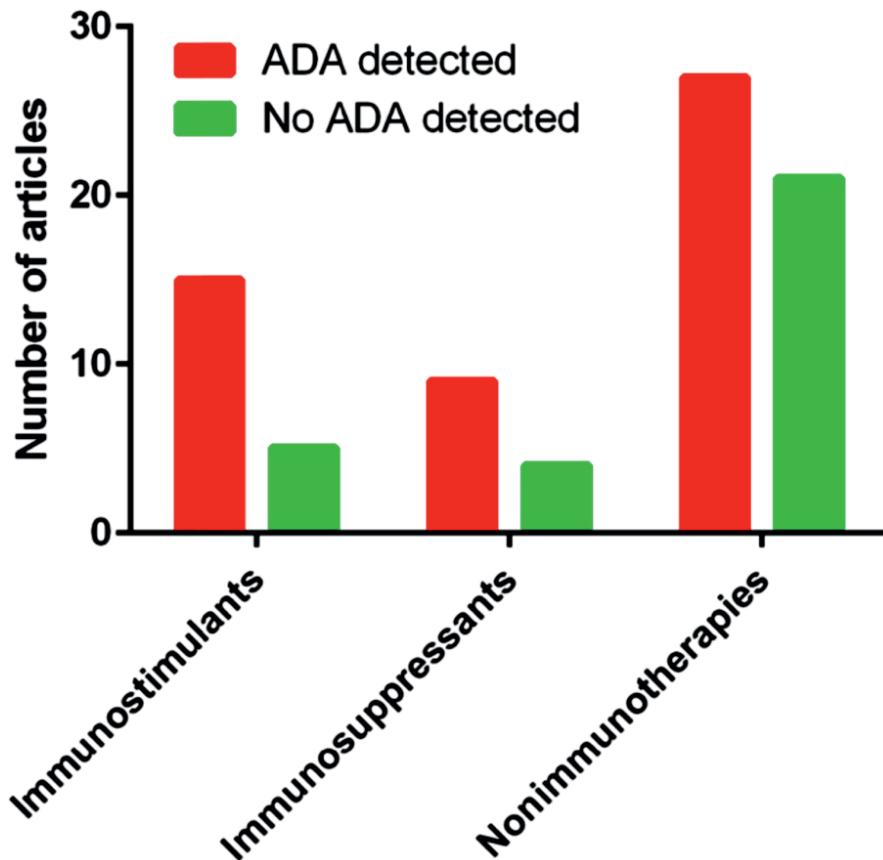


Figure 4. Detection of ADAs for immunostimulants, immunosuppressants, and nonimmunotherapies.

CONCLUSIONS

We confirmed that the majority of biological anticancer agents in clinical development induce ADA formation. For most agents that were EMA or FDA approved, ADAs have been detected but have not been an obstacle for approval. However, even among marketed agents, important gaps in the data on ADA formation exist. In most cases the consequences of ADAs for efficacy, pharmacokinetics and toxicity are not thoroughly investigated. Routine investigation of the relationship between ADAs and these parameters may help to establish the clinical relevance and explain variability in drug responses and safety.

Furthermore, inconsistent reporting and heterogeneity in detection methods complicate interpretation of the obtained results regarding ADA formation. Consistent reporting of the method of assessment, the incidence and characteristics of the detected ADAs will allow proper interpretation and comparison of the relevance of ADA formation. We would like to encourage the use of standardized terms for immunogenicity reporting as published by the ABIRISK consortium⁷⁵.

If ADAs are considered clinically relevant for a specific agent, strategies for prevention or management of the consequences may be designed. One potential method that is quick and easy to investigate is regimen adjustment. Although the mechanisms are not yet fully understood, clinically relevant effects have been observed, as we described in this review. More aggressive measures to be considered include immunosuppressive treatment with for example anti-CD20 or methotrexate, although more research is necessary to evaluate whether these methods are feasible in oncology.

REFERENCES

1. van Schie KA, Hart MH, de Groot ER, et al. The antibody response against human and chimeric anti-TNF therapeutic antibodies primarily targets the TNF binding region. *Ann Rheum Dis* 2015;74:311–314.
2. van Schouwenburg PA, van de Stadt LA, de Jong RN, et al. Adalimumab elicits a restricted anti-idiotypic antibody response in autoimmune patients resulting in functional neutralisation. *Ann Rheum Dis* 2013;72:104–109.
3. Hansel TT, Kropshofer H, Singer T, et al. The safety and side effects of monoclonal antibodies. *Nat Rev Drug Discov* 2010;9:325–338.
4. U.S. Food and Drug Administration. Guidance for industry: adaptive design clinical trials for drugs and biologics. 2010.
5. van Schouwenburg PA, Rispens T, Wolbink GJ. Immunogenicity of anti-TNF biologic therapies for rheumatoid arthritis. *Nat Rev Rheumatol* 2013;9:164–172.
6. Deehan M, Garcês S, Kramer D, et al. Managing unwanted immunogenicity of biologics. *Autoimmun Rev* 2015; 14:569-574.
7. European Medicines Agency. Guideline on immunogenicity assessment of biotechnology-derived therapeutic proteins. EMA 2007.
8. Hwang WYK, Foote J. Immunogenicity of engineered antibodies. *Methods* 2005;36:3–10.
9. Colnot DR, Quak JJ, Roos JC, et al. Phase I therapy study of 186Re-labeled chimeric monoclonal antibody U36 in patients with squamous cell carcinoma of the head and neck. *J Nucl Med* 2000;41:1999–2010.
10. Murakami H, Ikeda M, Okusaka T, et al. A Phase I study of MEDI-575, a PDGFR α monoclonal antibody, in Japanese patients with advanced solid tumors. *Cancer Chemother Pharmacol* 2015;76:631–639.
11. Hartmann F, Renner C, Jung W, et al. Anti- CD16 / CD30 Bispecific Antibodies as Possible Treatment for Refractory Hodgkin ' s Disease Anti- CD16 / CD30 Bispecific Antibodies as Possible Treatment for Refractory Hodgkin ' s Disease. *Leuk Lymphoma* 2015;8194:385–392.
12. Papadopoulos KP, Isaacs R, Bilic S, et al. Unexpected hepatotoxicity in a phase I study of TAS266, a novel tetravalent agonistic Nanobody(R) targeting the DR5 receptor. *Cancer Chemother Pharmacol* 2015;75:887–895.
13. Pietzner K, Vergote I, Santoro A, et al. Re-challenge with catumaxomab in patients with malignant ascites: results from the SECIMAS study. *Med Oncol* 2014;31:308.
14. MacDonald GC, Rasamoeliso M, Entwistle J, et al. A phase I clinical study of intratumorally administered VB4-845, an anti-epithelial cell adhesion molecule recombinant fusion protein, in patients with squamous cell carcinoma of the head and neck. *Med Oncol* 2009;26:257–264.
15. Becerra CR, Conkling P, Vogelzang N, et al. A phase I dose-escalation study of MEDI-575, a PDGFR(alpha) monoclonal antibody, in adults with advanced solid tumors. *Cancer Chemother Pharmacol* 2014;74:917–925.
16. Plumner ER, Attard G, Pacey S, et al. Phase 1 and pharmacokinetic study of lexatumumab in patients with advanced cancers. *Clin Cancer Res* 2007;13:6187–6194.
17. Posey JA, Ng TC, Yang B, et al. A Phase I Study of Anti-Kinase Insert Domain-containing Receptor Antibody , IMC-1C11 , in Patients with Liver Metastases from Colorectal Carcinoma. 2003;9:1323–1332.
18. Posey JA, Khazaeli MB, Bookman MA, et al. A phase I trial of the single-chain immunotoxin SGN-10 (BR96 sFv-PE40) in patients with advanced solid tumors. *Clin Cancer Res* 2002;8:3092–3099.
19. Scott AM, Wiseman G, Welt S, et al. A Phase I Dose-Escalation Study of Sibrotuzumab in Patients with Advanced or Metastatic Fibroblast Activation Protein-positive Cancer A Phase I Dose-Escalation Study of Sibrotuzumab in Patients with Advanced or Metastatic Fibroblast Activation. 2003;9:1639–1647.

20. Caron PC, Schwartz MA, Co MS, et al. Murine and humanized constructs of monoclonal antibody M195 (anti-CD33) for the therapy of acute myelogenous leukemia. *Cancer* 1994;73:1049–1056.
21. Hank JA, Gan J, Ryu H, et al. Immunogenicity of the Hu14.18-IL2 immunocytokine molecule in adults with melanoma and children with neuroblastoma. *Clin Cancer Res* 2009;15:5923–5930.
22. MacDonald GC, Rasamoeliso M, Entwistle J, et al. A phase I clinical study of VB4-845: weekly intratumoral administration of an anti-EpCAM recombinant fusion protein in patients with squamous cell carcinoma of the head and neck. *Drug Des Devel Ther* 2009;2:105–114.
23. Gómez-Mantilla JD, Trocóniz IF, Parra-Guillén Z, et al. Review on modeling anti-antibody responses to monoclonal antibodies. *J Pharmacokinet Pharmacodyn* 2014;41:523–536.
24. Yu AL, Uttenreuther-Fischer MM, Huang CS, et al. Phase I trial of a human-mouse chimeric anti-disialoganglioside monoclonal antibody ch14.18 in patients with refractory neuroblastoma and osteosarcoma. *J Clin Oncol* 1998;16:2169–2180.
25. Baert F, Noman M, Vermeire S, et al. Influence of immunogenicity on the long-term efficacy of infliximab in Crohn's disease. *N Engl J Med* 2003;348:601–608.
26. Vultaggio A, Nencini F, Pratesi S, et al. Manifestations of Antidrug Antibodies Response: Hypersensitivity and Infusion Reactions. *J Interferon Cytokine Res* 2014;34:946–952.
27. Cheifetz A, Mayer L. Monoclonal antibodies, immunogenicity, and associated infusion reactions. *Mt Sinai J Med* 2005;72:250–256.
28. Vidarsson G, Dekkers G, Rispens T. IgG Subclasses and Allotypes: From Structure to Effector Functions. *Front Immunol* 2014;5:520.
29. Karsten CM, Köhl J. The immunoglobulin, IgG Fc receptor and complement triangle in autoimmune diseases. *Immunobiology* 2012;217:1067–1079.
30. Welt S, Ritter G, Williams C, et al. Preliminary report of a phase I study of combination chemotherapy and humanized A33 antibody immunotherapy in patients with advanced colorectal cancer. *Clin Cancer Res* 2003;9:1347–1353.
31. European Medicines Agency. Vectibix (panitumumab) Eur. Public Assess. Rep., 2015.
32. European Medicines Agency. Opdivo (nivolumab) Eur. Public Assess. Rep., 2016.
33. European Medicines Agency. Arzerra (ofatumumab), 2016.
34. European Medicines Agency. Keytruda (pembrolizumab) Eur. Public Assess. Rep., 2016.
35. European Medicines Agency. MabThera (rituximab) Eur. Public Assess. Rep., 2016.
36. European Medicines Agency. Sylvant (siltuximab) Eur. Public Assess. Rep., 2015.
37. European Medicines Agency. Unituxin (dinutuximab) Eur. Public Assess. Rep., 2015.
38. European Medicines Agency. Erbitux (cetuximab) Eur. Public Assess. Rep., 2015.
39. European Medicines Agency. Removab (catumaxomab) Eur. Public Assess. Rep., 2014.
40. European Medicines Agency. Adcetris (brentuximab vedotin) Eur. Public Assess. Rep., 2016.
41. European Medicines Agency. Kadcyla (trastuzumab emtansine) Eur. Public Assess. Rep., 2016.
42. European Medicines Agency. IntronA (interferon alfa-2b) Eur. Public Assess. Rep., 2016.
43. European Medicines Agency. Zaltrap (affibercept) Eur. Public Assess. Rep., 2015.
44. European Medicines Agency. Blinicyto (blinatumomab) Eur. Public Assess. Rep., 2015.
45. U.S. Food and Drug Administration. Potrazza (necitumumab) Prescribing information., 2015.
46. U.S. Food and Drug Administration. Darzalex (daratumumab) Prescribing information., 2015.
47. U.S. Food and Drug Administration. Avastin (bevacizumab) Prescribing information., 2011.
48. U.S. Food and Drug Administration. Empliciti (elotuzumab) Prescribing information., 2015.
49. U.S. Food and Drug Administration. Zevalin (ibritumomab) Prescribing information., 2008.
50. U.S. Food and Drug Administration. Bexxar (Tositumomab; Iodine 131 tositumomab) approval label., 2003.
51. U.S. Food and Drug Administration. Proleukin (aldesleukin) approval label., 2012.
52. European Medicines Agency. Herceptin (trastuzumab) Eur. Public Assess. Rep., 2016.
53. European Medicines Agency. Gazyvaro (obinutuzumab) Eur. Public Assess. Rep., 2015.
54. European Medicines Agency. Yervoy (ipilimumab) Eur. Public Assess. Rep., 2016.

55. European Medicines Agency. Cyramza (ramucirumab) Eur. Public Assess. Rep., 2016.
56. European Medicines Agency. Perjeta (pertuzumab) Eur. Public Assess. Rep., 2016.
57. U.S. Food and Drug Administration. Opdivo (nivolumab) Prescribing information., 2015.
58. U.S. Food and Drug Administration. Yervoy (ipilimumab) Prescribing information., 2013.
59. Ruf P, Kluge M, Jäger M, et al. Pharmacokinetics, immunogenicity and bioactivity of the therapeutic antibody catumaxomab intraperitoneally administered to cancer patients. *Br J Clin Pharmacol* 2010;69:617–625.
60. Wakelee HA, Patnaik A, Sikic BI, et al. Phase I and pharmacokinetic study of lexatumumab (HGS-ETR2) given every 2 weeks in patients with advanced solid tumors. *Ann Oncol* 2010;21:376–381.
61. Scheinberg DA, Straus DJ, Yeh SD, et al. A phase I toxicity, pharmacology, and dosimetry trial of monoclonal antibody OKB7 in patients with non-Hodgkin's lymphoma: effects of tumor burden and antigen expression. *J Clin Oncol* 1990;8:792–803.
62. Morris MJ, Eisenberger MA, Pili R, et al. A phase I/IIA study of AGS-PSCA for castration-resistant prostate cancer. *Ann Oncol* 2012;23:2714–2719.
63. Wong JYC, Chu DZ, Yamauchi DM, et al. A phase I radioimmunotherapy trial evaluating 90Yttrium-labeled anti-carcinoembryonic antigen (CEA) chimeric T84.66 in patients with metastatic CEA-producing malignancies. *Clin Cancer Res* 2000;6:3855–3863.
64. Rasche L, Duell J, Castro IC, et al. GRP78-directed immunotherapy in relapsed or refractory multiple myeloma - results from a phase 1 trial with the monoclonal immunoglobulin M antibody PAT-SM6. *Haematologica* 2015;100:377–384.
65. von Pawel J, Harvey JH, Spigel DR, et al. Phase II trial of mapatumumab, a fully human agonist monoclonal antibody to tumor necrosis factor-related apoptosis-inducing ligand receptor 1 (TRAIL-R1), in combination with paclitaxel and carboplatin in patients with advanced non-small-cell lung cancer. *Clin Lung Cancer* 2014;15:188–196.
66. Salgia R, Patel P, Bothos J, et al. Phase I dose-escalation study of onartuzumab as a single agent and in combination with bevacizumab in patients with advanced solid malignancies. *Clin Cancer Res* 2014;20:1666–1675.
67. Forero A, Meredith RF, Khazaeli MB, et al. Phase I study of 90Y-CC49 monoclonal antibody therapy in patients with advanced non-small cell lung cancer: effect of chelating agents and paclitaxel co-administration. *Cancer Biother Radiopharm* 2005;20:467–478.
68. Chiorean EG, Hurwitz HI, Cohen RB, et al. Phase I study of every 2- or 3-week dosing of ramucirumab, a human immunoglobulin G1 monoclonal antibody targeting the vascular endothelial growth factor receptor-2 in patients with advanced solid tumors. *Ann Oncol* 2015;26:1230–1237.
69. Sausville EA, Headlee D, Stetler-Stevenson M, et al. Continuous infusion of the anti-CD22 immunotoxin IgG-RFB4-SMPT-dgA in patients with B-cell lymphoma: a phase I study. *Blood* 1995;85:3457–3465.
70. Caron PC, Jurcic JG, Scott AM, et al. A phase 1B trial of humanized monoclonal antibody M195 (anti-CD33) in myeloid leukemia: specific targeting without immunogenicity. *Blood* 1994;83:1760–8.
71. Kreitman RJ, Hassan R, Fitzgerald DJ, et al. Phase I Trial of Continuous Infusion Anti-Mesothelin Recombinant Immunotoxin SS1P. *Clin Cancer Res* 2009;15:5274–5279.
72. Kreitman RJ, Tallman MS, Robak T, et al. Phase I trial of anti-CD22 recombinant immunotoxin moxetumomab pasudotox (CAT-8015 or HA22) in patients with hairy cell leukemia. *J Clin Oncol* 2012;30:1822–1828.
73. Hart MH, de Vrieze H, Wouters D, et al. Differential effect of drug interference in immunogenicity assays. *J Immunol Methods* 2011;372:196–203.
74. Mikulskis A, Yeung D, Subramanyam M, et al. Solution ELISA as a platform of choice for development of robust, drug tolerant immunogenicity assays in support of drug development. *J Immunol Methods* 2011;365:38–49.
75. Rup B, Pallardy M, Sikkema D, et al. Standardizing terms, definitions and concepts for

- describing and interpreting unwanted immunogenicity of biopharmaceuticals: Recommendations of the innovative medicines initiative ABIRISK consortium. *Clin Exp Immunol* 2015;181:385-400.
76. Antonarakis ES, Carducci MA, Eisenberger MA, et al. Phase I rapid dose-escalation study of AGS-1C4D4, a human anti-PSCA (prostate stem cell antigen) monoclonal antibody, in patients with castration-resistant prostate cancer: a PCCTC trial. *Cancer Chemother Pharmacol* 2012;69:763-771.
 77. Michallet M-C, Saltel F, Flacher M, et al. Cathepsin-Dependent Apoptosis Triggered by Supraoptimal Activation of T Lymphocytes: A Possible Mechanism of High Dose Tolerance. *J Immunol* 2004;172:5405-5414.
 78. Somerfield J, Hill-Cawthorne GA, Lin A, et al. A novel strategy to reduce the immunogenicity of biological therapies. *J Immunol* 2010;185:763-768.
 79. Brackmann HH, Gormsen J. Massive factor-VIII infusion in haemophilic with factor-VIII inhibitor, high responder. *Lancet* 1977;2:933.
 80. Brackmann HH, Oldenburg J, Schwaab R. Immune tolerance for the treatment of factor VIII inhibitors--twenty years' "bonn protocol". *Vox Sang* 1996;70:30-35.
 81. Rutgeerts P, Feagan BG, Lichtenstein GR, et al. Comparison of Scheduled and Episodic Treatment Strategies of Infliximab in Crohn's Disease. *Gastroenterology* 2004;126:402-413.
 82. De Groot AS, Moise L, McMurry JA, et al. Activation of natural regulatory T cells by IgG Fc-derived peptide "Tregitopes." *Blood* 2008;112:3303-3311.
 83. Michallet M-C, Saltel F, Flacher M, et al. Cathepsin-dependent apoptosis triggered by supraoptimal activation of T lymphocytes: a possible mechanism of high dose tolerance. *J Immunol* (Baltimore, Md 1950) 2004;172:5405-5414.
 84. Tolcher AW, Sweeney CJ, Papadopoulos K, et al. Phase I and pharmacokinetic study of CT-322 (BMS-844203), a targeted adnectin inhibitor of VEGFR-2 based on a domain of human fibronectin. *Clin Cancer Res* 2011;17:363-371.
 85. Crombet T, Torres O, Neninger E, et al. Phase I clinical evaluation of a neutralizing monoclonal antibody against epidermal growth factor receptor. *Cancer Biother Radiopharm* 2001;16:93-102.
 86. Manzke O, Tesch H, Borchmann P, et al. Locoregional treatment of low-grade B-cell lymphoma with CD3 x CD19 bispecific antibodies and CD28 costimulation: I. Clinical phase I evaluation. *Int J Cancer* 2001;91:508-515.
 87. Forero A, Weiden PL, Vose JM, et al. Phase 1 trial of a novel anti-CD20 fusion protein in pretargeted radioimmunotherapy for B-cell non-Hodgkin lymphoma. *Blood* 2004;104:227-36.
 88. Martinsson-Niskanen T, Riisbro R, Larsson L, et al. Monoclonal antibody TB-403: a first-in-human, Phase I, double-blind, dose escalation study directed against placental growth factor in healthy male subjects. *Clin Ther* 2011;33:1142-1149.
 89. Jackisch C, Kim S-B, Semiglazov V, et al. Subcutaneous versus intravenous formulation of trastuzumab for HER2-positive early breast cancer: updated results from the phase III HannaH study. *Ann Oncol* 2015;26:320-325.
 90. Krieckaert CL, Nurmohamed MT, Wolbink GJ. Methotrexate reduces immunogenicity in adalimumab treated rheumatoid arthritis patients in a dose dependent manner. *Ann Rheum Dis* 2012;71:1914-1915.
 91. Maini R, St Clair EW, Breedveld F, et al. Infliximab (chimeric anti-tumour necrosis factor alpha monoclonal antibody) versus placebo in rheumatoid arthritis patients receiving concomitant methotrexate: a randomised phase III trial. ATTRACT Study Group. *Lancet* 1999;354:1932-1939.
 92. Maini RN, Breedveld FC, Kalden JR, et al. Therapeutic efficacy of multiple intravenous infusions of anti-tumor necrosis factor alpha monoclonal antibody combined with low-dose weekly methotrexate in rheumatoid arthritis. *Arthritis Rheum* 1998;41:1552-1563.
 93. Garman RD, Munroe K, Richards SM. Methotrexate reduces antibody responses to recombinant human alpha-galactosidase A therapy in a mouse model of Fabry disease. *Clin*

- Exp Immunol 2004;137:496–502.
94. Garces S, Demengeot J, Benito-Garcia E. The immunogenicity of anti-TNF therapy in immune-mediated inflammatory diseases: a systematic review of the literature with a meta-analysis. *Ann Rheum Dis* 2013;72:1947–1955.
 95. Farrell RJ, Alsahli M, Jeen YT, et al. Intravenous hydrocortisone premedication reduces antibodies to infliximab in Crohn's disease: A randomized controlled trial. *Gastroenterology* 2003;124:917–924.
 96. Vande Casteele N, Gils A, Singh S, et al. Antibody response to infliximab and its impact on pharmacokinetics can be transient. *Am J Gastroenterol* 2013;108:962–71.
 97. Messinger YH, Mendelsohn NJ, Rhead W, et al. Successful immune tolerance induction to enzyme replacement therapy in CRIM-negative infantile Pompe disease. *Genet Med* 2012;14:135–142.
 98. Oratz R, Speyer JL, Wernz JC, et al. Antimelanoma monoclonal antibody-ricin A chain immunoconjugate (XMMME-001-RTA) plus cyclophosphamide in the treatment of metastatic malignant melanoma: results of a phase II trial. *J Biol Response Mod* 1990;9:345–354.
 99. Selvaggi K, Saria EA, Schwartz R, et al. Phase I/II study of murine monoclonal antibody-ricin A chain (XOMAZYME-Mel) immunoconjugate plus cyclosporine A in patients with metastatic melanoma. *J Immunother Emphasis Tumor Immunol* 1993;13:201–207.
 100. Harding FA, Stickler MM, Razo J, et al. The immunogenicity of humanized and fully human antibodies: Residual immunogenicity resides in the CDR regions. *MAbs* 2010;2:256–265.
 101. Witzig TE, Tomblyn MB, Misleh JG, et al. Anti-CD22 90Y-epratuzumab tetraxetan combined with anti-CD20 veltuzumab: a phase I study in patients with relapsed/refractory, aggressive non-Hodgkin lymphoma. *Haematologica* 2014;99:1738–1745.
 102. Morschhauser F, Leonard JP, Fayad L, et al. Humanized Anti-CD20 Antibody, Veltuzumab, in Refractory/Recurrent Non-Hodgkin's Lymphoma: Phase I/II Results. *J Clin Oncol* 2009;27:3346–3353.
 103. Hassan R, Williams-gould J, Watson T, et al. Pretreatment with Rituximab Does Not Inhibit the Human Immune Response against the Immunogenic Protein LMB-1. 2004;10:16–18.
 104. Maeda T, Yamada Y, Tawara M, et al. Successful treatment with a chimeric anti-CD20 monoclonal antibody (IDEC-C2B8, rituximab) for a patient with relapsed mantle cell lymphoma who developed a human anti-chimeric antibody. *Int J Hematol* 2001;74:70–75.

Chapter 6

Combining immunotherapy with chemotherapy

Chapter 6.1

Enhancing anti-tumor response by combining immune checkpoint inhibitors with chemotherapy in solid tumors.

Willeke Ros*, Kimberley Heinhuis*

****Authors contributed equally***

Heinhuis KM*, **Ros W***, Kok M, Steeghs N, Beijnen JH, Schellens JHM. Enhancing antitumor response by combining immune checkpoint inhibitors with chemotherapy in solid tumors.

Annals of Oncology 2019;30:219–235.

ABSTRACT

Background: Cancer immunotherapy has changed the standard of care for a subgroup of patients with advanced disease. Immune checkpoint blockade (ICB) in particular has shown improved survival compared with previous standards of care for several tumor types. Although proven to be successful in more immunogenic tumors, ICB is still largely ineffective in patients with tumors that are not infiltrated by immune cells, the so-called cold tumors.

Patients and methods: This review describes the effects of different chemotherapeutic agents on the immune system and the potential value of these different types of chemotherapy as combination partners with ICB in patients with solid tumors. Both preclinical data and currently ongoing clinical trials were evaluated. In addition, we reviewed findings regarding different dosing schedules, including the effects of an induction phase and applying metronomic doses of chemotherapy.

Results: Combining ICB with other treatment modalities may lead to improved immunological conditions in the tumor microenvironment and could thereby enhance the antitumor immune response, even in tumor types that are so far unresponsive to ICB monotherapy. Chemotherapy, that was originally thought to be solely immunosuppressive, can exert immunomodulatory effects which may be beneficial in combination with immunotherapy. Each chemotherapeutic drug impacts the tumor microenvironment differently, and in order to determine the most suitable combination partners for ICB it is crucial to understand these mechanisms.

Conclusion: Preclinical studies demonstrate that the majority of chemotherapeutic drugs has been shown to exert immunostimulatory effects, either by inhibiting immunosuppressive cells and/or activating effector cells, or by increasing immunogenicity and increasing T-cell infiltration. However, for certain chemotherapeutic agents timing, dose and sequence of administration of chemotherapeutic agents and ICB is important. Further studies should focus on determining the optimal drug combinations, sequence effects and optimal concentration–time profiles in representative preclinical models.

INTRODUCTION

Drug development in oncology is shifting from targeting intrinsic properties of cancer cells to the tumor microenvironmental and the immune system of the host. Boosting T-cell memory may lead to more durable anticancer responses than seen with conventional anticancer therapy [1]. Endogenous anticancer response can be enhanced by blocking inhibitory checkpoint molecules. These checkpoint molecules function by dampening immune cells, a mechanism that prevents auto-immunity. Tumors utilize checkpoint inhibition in order to prevent T-cell-mediated tumor cell killing, by upregulating the ligands of checkpoint inhibitors, such as PD-L1. Activating checkpoint inhibition pathways turns T-cells anergic and leads to T-cell exhaustion.

Approved drugs for immune checkpoint blockade (ICB) include the anti-PD1 antibodies nivolumab and pembrolizumab, the anti-PD-L1 antibodies atezolizumab, avelumab and durvalumab, and the anti-CTLA-4 antibodies ipilimumab and tremelimumab. ICB has been approved for use in a wide range of tumors, including melanoma, non-small cell lung cancer (NSCLC), renal cell cancer, Merkel cell cancer, Hodgkin's lymphoma, urothelial cancer and mismatch repair deficient (dMMR)/ microsatellite instability high (MSI-H) tumors [1–5].

Extensive research has been carried out identifying factors contributing to response to ICB (Table 1). Currently approved biomarkers for ICB are PD-L1 expression and dMMR/MSI-H tumor status [42, 43]. In practice, lactate dehydrogenase (LDH) and tumor mutational burden are also commonly used to select patients that are thought to benefit from ICB treatment [6, 8]. Other biomarkers that have been identified include but are not limited to, tumor-infiltrating lymphocytes (TILs), CD8⁺ T-cells, T-cell receptor clonality and IFN- γ -related gene signatures [6, 9, 10, 21, 24, 33, 37]. It is thought that ICB has the highest likelihood of success in tumors that have an inflamed phenotype [44, 45]. These inflamed phenotypes typically have a tumor microenvironment with functional CD8⁺ TILs, functional antigen presentation machinery proteins, and T-helper type 1 cytokines and chemokines such as IFN- γ and IL-2 [27, 29, 46]. While there is an active immune response, inhibitory factors may also be present. Potential inhibitory factors are large densities of Tregs, MDSCs, and anti-inflammatory T-helper type 2 cytokines, such as TGF- β and IL-10 [47]. Other immunological phenotypes that can be found in the tumor microenvironment include a phenotype which is completely deprived of immune cells (immune desert), or a phenotype in which the immune cells are unable to infiltrate the tumor properly (immune-excluded tumors) [46, 48, 49]. These tumors lack infiltration of competent T-cells, rarely express checkpoint inhibitor molecules, have a low mutational load, and have low expression of antigen presentation machinery markers [48]. These two phenotypes rarely respond to ICB monotherapy [19]. In order to convert these immune deserts or immune-excluded tumors into inflamed tumors, combination therapy with either other immunotherapies or different treatment modalities [50], including chemotherapy, may be an option [48].

Table 1. Predictive factors for checkpoint inhibition therapy.

Type	Predictive factor	Effect	Cancer type	Checkpoint inhibitor	Reference
Clinical	Clinical condition	High ECOG Performance status is predictive for poor OS	Melanoma, NSCLC	Nivolumab, pembrolizumab, ipilimumab	Nakamura et al. [6], Bagley et al. [7]
	Clinical chemistry	High LDH is predictive of poor OS	Melanoma, TNBC	Nivolumab, ipilimumab	Nakamura et al. [6] Nanda et al. [8], Loi et al. [9], Martens et al. [10]
		High C-reactive protein is predictive of poor OS	Melanoma	Nivolumab, ipilimumab	Nakamura et al. [6], Simeone et al. [11]
		High levels of soluble CD73 is associated with poor OS and PFS	Melanoma	Nivolumab	Morello et al. [12]
	Tumor mutational burden	High mutational load correlates with improved OR, durable clinical benefit, PFS and OS	Various	Pembrolizumab, nivolumab, ipilimumab, atezolizumab	Hugo et al. [13], Rizvi et al. [14], Snyder et al. [15], Rosenberg et al. [16]
Tumor	Mismatch repair status	Mismatch repair deficiency correlates with response	Any solid tumor with mismatch repair deficiency	Pembrolizumab	Le et al. [17]
	Tumor PD-L1 expression	PD-L1 expression correlates with response	Various tumor types	Pembrolizumab, nivolumab, atezolizumab	Gettinger et al. 2016[18]; Herbst et al. 2014[19] Fuchs et al. 2018[20]
	Viral etiology	Human Papilloma Virus positivity correlates with response	Head and neck cancer	Pembrolizumab	Chow et al. 2016[21]
		Epstein-Bar virus positivity correlates with response	Gastric	Pembrolizumab	Kim et al. 2018[22]
	Immunological	Tumor infiltrating lymphocytes	Baseline peritumoral and intratumoral PD-1 expression on CD8 ⁺ T-cells correlates with response and improved survival	Melanoma	Pembrolizumab, nivolumab
High level of stromal TILs correlates with response			Melanoma, TNBC	Pembrolizumab	Loi et al. 2017[9], Tumeah et al. 2014[24]
PD-L1 expression on TILs correlates with response			Various tumor types	Atezolizumab, pembrolizumab	Herbst et al. 2014[19],Dirix et al. 2018[25]. Tumeah et al. 2014[24]

		High baseline FoxP3 and IDO expression correlates with clinical activity	Melanoma	Ipilimumab	Hamid et al. 2011[26]
		More clonal TCR repertoire correlates with response	Melanoma	Pembrolizumab	Tumeh et al. 2014[24]
	Peripheral blood	Low number baseline Ki67 EOMES ⁺ CD8 ⁺ T-cells is associated with relapse	Melanoma	Ipilimumab	Wang et al. 2012[27]
		High percentage of baseline memory CD45RO ⁺ CD8 ⁺ T-cells correlates with improved survival	Melanoma	Ipilimumab	Tietze et al. 2017[28]
		Lower baseline level of peripheral NK cells correlates with improved survival	Melanoma	Ipilimumab	Tietze et al. 2017[28]
		High Neutrophil-to-Lymphocyte ratio is predictive of poor OS	NSCLC, melanoma	Nivolumab, ipilimumab	Bagley et al. 2017[7], Cassidy et al. 2017[30]
		Low absolute and relative lymphocyte count is predictive of poor OS	Melanoma	Nivolumab, ipilimumab	Nakamura et al. 2016[6], Simeone et al. 2014[11], Martens et al. 2016 [10]
		Low leukocyte count at baseline correlates with response	Melanoma	Ipilimumab	Gebhardt et al 2015[31]
		Low neutrophil count is associated with improved OS	Melanoma, NSCLC	Ipilimumab, nivolumab	Bagley et al. 2017[7], Ferrucci et al. 2016[32]
		Low baseline MDSCs correlates with improved OS	Melanoma	Ipilimumab	Kitano et al. 2014[33], Sade-Feldman et al. 2016[34]
		High levels of serum IFN- γ , IL-6, and IL-10 are associated with response	Melanoma	Nivolumab	Yamazaki et al. 2017[35]
		High frequencies of circulating Tregs is associated with improved OS	Melanoma	Ipilimumab	Martens et al. 2016[10]
		Low absolute monocyte count correlates with OS	Melanoma	Ipilimumab	Martens et al. 2016[10]
		High frequency of CD14 ⁺ CD16 ⁺ HLA-DR ^{hi} monocytes correlates with response	Melanoma	Nivolumab, pembrolizumab	Krieg et al. 2018[36]

Immune gene expression	Upregulated IFN- γ signaling correlates to better response rates and better PFS rates	Head and neck cancer, melanoma, urothelial cancer, NSCLC, cell	Pembrolizumab, nivolumab, atezolizumab	Ribas et al. 2015[37], Ayers et al. 2017[38], O'Donnell et al. 2017[39], Prat et al. 2017[40] Fehrenbacher et al. 2016[41].
	Upregulated T helper type 1 gene expression at baseline correlates to response	Various	Atezolizumab	Herbst et al. 2014[19]
	Upregulated genes regarding antigen presentation machinery correlates to better response rates and better PFS rates	Head and neck cancer, melanoma, urothelial cancer, NSCLC, cell	Pembrolizumab, nivolumab	O'Donnell et al. 2017[39], Prat et al. 2018[40]
	Upregulated genes regarding T-cell cytotoxic function correlates to better response rates and better PFS rates	Head and neck cancer, melanoma, urothelial cancer, NSCLC, cell	Pembrolizumab, nivolumab	O'Donnell et al. 2017[39], Prat et al. 2019[40]

Chemotherapy was previously thought to be solely immunosuppressive, but recent data show that it may also possess immunostimulatory properties [51, 52]. It has the potential to induce favorable immunogenic conditions within the tumor microenvironment, which may be difficult to achieve by just targeting immune cells [51, 52]. In this review, we describe these immunomodulatory effects for different classes of chemotherapy. Each compound exerts unique immunological effects, which may be either beneficial or detrimental to treatment with ICB. Furthermore, this review discusses the compounds and treatment schedules in ongoing combination studies.

IMMUNOMODULATORY EFFECTS OF CHEMOTHERAPY

Chemotherapy comprises a large group of molecules which target proliferating cells. Although chemotherapy predominantly affects cancer cells, proliferating benign cells such as immune cells may also be affected. For this reason, it was long assumed that chemotherapy is merely immunosuppressive. Indeed, chemotherapy may lead to myelosuppression and leukocytopenia. However, recent findings demonstrate that many forms of chemotherapy also exhibit immunostimulatory effects. Here, we discuss the immunomodulatory effects of the four main groups of chemotherapy: topoisomerase inhibitors, antimicrotubule agents, alkylating agents and antimetabolites (Figure 1). We searched PubMed for preclinical and clinical trials published before 13 December 2018. Interim analysis and early-release publications of American Society of Clinical Oncology (ASCO) and European Society for Medical Oncology (ESMO) were also reviewed. Only articles in English were included. The search terms were ‘immune checkpoint inhibitors’, ‘anti-PD-(L)1’, ‘anti-CTLA-4’, and the names of the ICB available to date, ‘immunomodulation’ and the specific actors of the immune responses, ‘topoisomerase inhibitors’, ‘antimicrotubule agents’, ‘alkylating agents and antimetabolites’ and the specific agents per group. We only discuss chemotherapeutic compounds which are used for the treatment of solid tumors. Abstracts were reviewed and relevant articles were assessed in full.

Topoisomerase inhibitors

Topoisomerase inhibitors block the action of topoisomerases, enzymes controlling topological changes in DNA structures. Type I topoisomerases cut one strand of a DNA double helix, whereas type II topoisomerase cut both strands. Important topoisomerase inhibitors in the treatment of solid cancers of which immunomodulatory effects are described include topoisomerase I inhibiting camptothecin derivatives and topoisomerase II inhibiting anthracyclines.

Camptothecin derivatives

Irinotecan and topotecan are camptothecin derivatives commonly used in the treatment of a wide variety of solid tumors. Preclinical findings suggest that they may enhance T-cell recognition of tumor cells. In melanoma, they are capable of upregulating tumor-specific antigens. In vitro models demonstrated that treatment with topoisomerase I inhibitors led to increased expression of the antigens melan-a/MART-1 and TP53INP1. Overexpression of these antigens led to improved recognition of tumor cells by T-cells, and subsequently

increased T-cell-mediated killing of these tumor cells [53, 54]. Another in vitro experiment revealed upregulation of the danger-associated molecular patterns (DAMPs) high mobility group box 1 protein (HMGB1) and heat shock protein 70 (HSP70) after irinotecan treatment [55]. DAMPs have the potential to induce dendritic cell maturation leading to an inflammatory antitumor response. Tumor cells surviving topotecan treatment have upregulated major histocompatibility complex I (MHC I) and Fas expression, making them more sensitive to effector T-cell killing [56, 57].

Clinical studies determining the impact of camptothecin derivatives and individual drug doses and schedules on the immune system are limited in number. Small studies have been carried out monitoring changes in immune cell subsets in patients undergoing treatment. Camptothecin derivatives appear to impact the composition of immune cells in peripheral blood little, compared with other chemotherapeutic drugs. Topotecan treatment did not significantly impact absolute lymphocyte count nor T-cell and B-cell numbers in ovarian cancer patients with advanced disease [58]. However, the naive T-cell subpopulation was decreased upon treatment in chemotherapy naive patients, whereas the proportion of memory T-cells remained the same [58].

Anthracyclines

Anthracyclines are topoisomerase II inhibitors capable of inducing immunogenic cell death (ICD), a form of apoptosis which can induce an effective antitumor immune response through activation of DCs and the subsequent activation of specific T-cell responses. It is characterized by the expression of DAMPs, such as calreticulin, ATP, HMGB1 and HSP70 [59, 60]. In vitro studies demonstrated that DAMPs could be detected after 12 h of treatment and remained elevated through 24 h [61]. The dosage needed for induction of ICD, however, was generally higher than the dose needed for cytotoxicity [62]. ICD may also lead to the production of immunostimulatory cytokines, such as IFN- γ [62]. Inhibition of caspase, or depletion of DCs or CD8⁺ T-cells may abolish anthracycline-mediated antitumor immune response [63]. Doxorubicin, epirubicin and idarubicin are all known to induce ICD [52].

Apart from ICD, other immunomodulatory effects of anthracyclines have been investigated as well. For instance, anthracyclines are able to elicit an immune response in a similar manner as induced by viral pathogens [64]. An in vivo experiment using fibrosarcomas in mice demonstrated that intratumoral doxorubicin increased levels of transcripts associated with viral infections, including IFN-stimulated genes, genes involved in the recruitment and activation of leukocytes, and *Cd274* (encoding PD-L1). Anthracyclines have also been shown to selectively deplete immunosuppressive cells. Administration of 5 mg/kg doxorubicin intraperitoneally Q3W may lead to decreased MDSCs numbers in vivo, which in turn lead to increased numbers of CD4⁺ and CD8⁺ T-cells, as well as increased expression of IFN- γ , granzyme B and perforin [65]. Epirubicin impairs the function of Tregs by blocking the interaction between FoxP3 and the NF- κ B subunit p65 in vitro [66]. This has resulted in blocking Treg-mediated suppression of CD8⁺ T-cells.

The potential negative effects of anthracyclines on the immune system have been investigated in small studies. A single dose of epirubicin appeared to not significantly decrease blood lymphocyte numbers [67]. Daunorubicin has been shown to induce cell

death in both resting and active peripheral blood lymphocytes after 20 h of incubation. This may be a potential negative effect for ICB combination [68]. Assessment of dose and schedule dependency of the aforementioned effects in cancer patients is warranted.

Anti-microtubule agents

Antimicrotubule agents exert neoplastic effects by disrupting microtubules. The most widely used antimicrotubule agents are the taxanes and vinca-alkaloids.

Taxanes

Docetaxel and paclitaxel are the most commonly used taxanes in the treatment of cancer. Taxanes are known for inducing leukocytopenia, depleting both lymphocytes and neutrophils, which has been described previously in a model [69]. Given as a 3-weekly standard of care, taxane-induced leukocytopenia typically starts 10 days after infusion and restores to baseline levels ~3 weeks after infusion. Neutrophils are depleted more than lymphocytes [69], thereby improving the neutrophil-to-lymphocyte ratio to a more favorable one for ICB treatment [30]. However, various types of lymphocyte subsets are depleted, including CD3⁺, CD4⁺, CD8⁺, CD56⁺ and CD45RO⁺ cells [70]. As some of these cells are positively correlated with ICB response [28], further research is necessary to understand whether and how leukocytopenia affects ICB outcome.

Taxane treatment reduces the number of lymphocytes, but it is debatable whether they impact the functionality of cytotoxic T cells. One study found that T-cell-mediated cytotoxicity was found to be impaired upon paclitaxel treatment [71]. In contrast, another study found no effect, [72], while others even found that taxane treatment led to increased NK and lymphokine activated killer cell activity [73]. Additionally, pro-inflammatory cytokines, such as IFN- γ , IL-2, IL-6 and GM-CSF were found to be upregulated after six cycles of standard taxane treatment [73].

Taxanes appear to selectively reduce immunosuppressive cells. Both docetaxel and paclitaxel have been shown to selectively decrease Treg and MDSC numbers, while unaffected CD4⁺ and CD8⁺ viability [74–77]. Not only the number, but also the inhibitory function of Tregs is diminished. Expression of FoxP3, one of the key regulators of the immune system, was lowered in PBMCs which were incubated with paclitaxel for 24 h [77]. Another study found the anti-inflammatory cytokine IL-10 to be significantly decreased in patients with advanced disease after 4 weeks of paclitaxel treatment [72].

Taxane treatment may lead to induction of TILs [78]. A small prospective study showed that in breast cancer patients, tumors were non-inflamed before treatment. However, after four treatment cycles of 200 mg/m² Q2W neoadjuvant paclitaxel treatment, surgery was carried out and one-third of the patients demonstrated immune infiltrates in their tumor biopsies. Interestingly, only the patients with a partial or complete response demonstrated TILs after treatment.

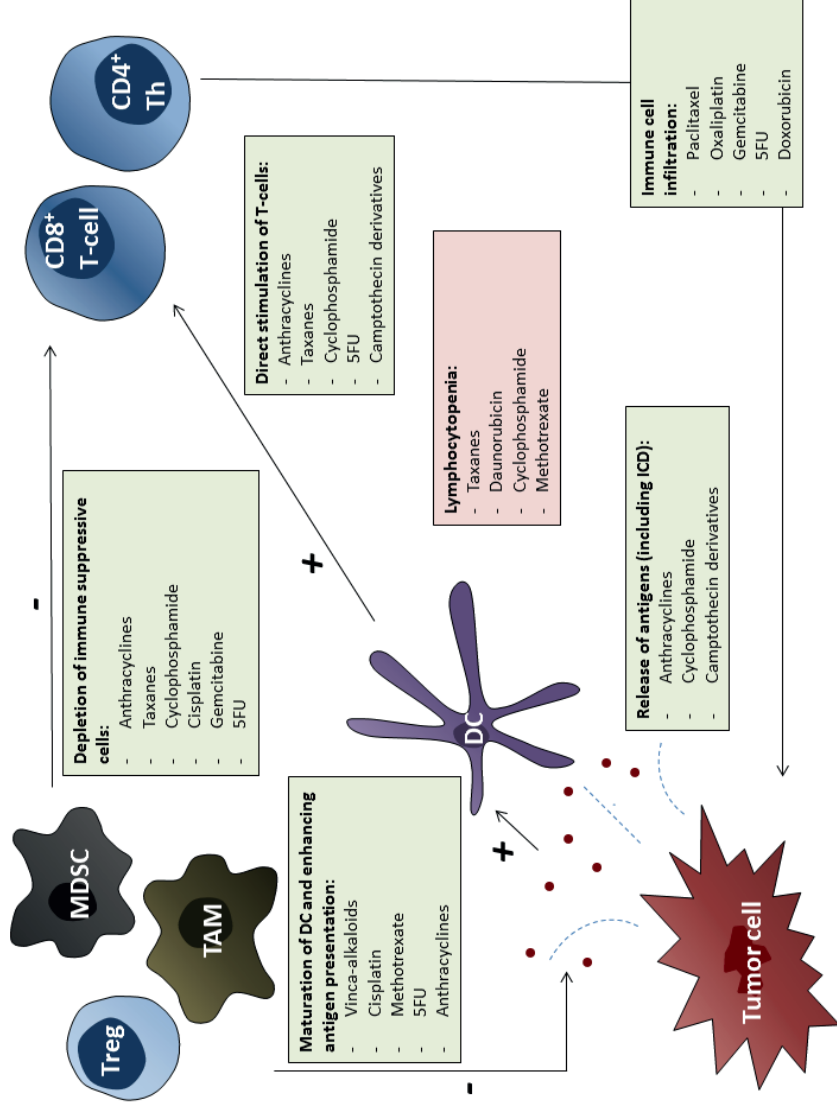


Figure 1. Immunomodulatory effects of chemotherapy. DC = dendritic cells. 5FU = 5-fluorouracil. ICD = immunogenic cell death. MDSC = myeloid derived suppressor cell. TAM = tumor associated macrophages. Th = T helper cell. Tregs = regulatory T-cells.

Vinca-alkaloids

Few studies have been carried out to assess the impact of vinca-alkaloids on the immune system. Vincristine suppresses the activity of immunosuppressive tumor-associated macrophages, whilst upregulating pro-inflammatory cytokines, and downregulating PD-L1 in PBMCs of healthy donors [79]. Vinorelbine generates reactive oxygen species and nitrogen species in vivo, which kills a significant number of immune cells [80], an effect which might negatively impact outcome of ICB. Vinblastine was identified as a compound capable of inducing maturation of DCs in an in vitro drug screen. Subsequent in vivo experiments revealed that administration of vinblastine enhanced CD8+ clonal expansion and cytotoxic function [81]. Here, vinblastine was administered subcutaneously twice, with 1 week between injections.

Alkylating and platinum-based anticancer agents

Alkylating agents inhibit a.o. the transcription of DNA into RNA, thereby stopping protein synthesis. We discuss the most widely used compounds of this class of drugs: cyclophosphamide, dacarbazine and platinum-based chemotherapeutic drugs.

Cyclophosphamide

Cyclophosphamide is extensively investigated for its immunomodulating effects. Similar to anthracyclines, cyclophosphamide is capable of inducing ICD [52]. Furthermore, cyclophosphamide may trigger DC homeostasis [82]. Mice which were injected with a single dose of intraperitoneal 100 mg/kg cyclophosphamide exhibited tumor cell death with immunogenic features, tumor infiltration and engulfment of apoptotic tumor cells by DCs, and subsequent cross priming of CD8+T-cells by DCs.

The dosage may be crucial when combining cyclophosphamide with immunotherapy. While higher dosages of cyclophosphamide induce myelosuppression [83], metronomic low dosing may boost the immune system [84–86]. Patients receiving a daily dose of 100 mg oral cyclophosphamide showed decreased numbers and percentages of Treg cells, whereas there was no significant decrease in other lymphocyte counts [85]. Interestingly, doubling the dose of cyclophosphamide depleted all lymphocyte subpopulations. Next to decrease of Treg cells, effector functions are increased in patients receiving a metronomic dose. Both NK and T-cell activity were increased [85]. Furthermore, in vivo experiments show that a single low dose of cyclophosphamide leads to a shift from T-helper type 2 to type 1 cytokines, with enhanced IL-2 and IFN- γ production, and decreased IL-10 and TGF- β production after treatment compared with pretreatment [86]. A clinical trial investigating a modified vaccine Ankara-5T4 (MVA-5T4) further demonstrated the potential abilities of cyclophosphamide to deplete Treg cells. Patients were randomized to receive 50 mg twice daily cyclophosphamide or not, and MVA-5T4 or not [87]. In both cyclophosphamide group and the cyclophosphamide plus MVA-5T4 group, FoxP3 Treg cells were depleted. These depletions were noted at week three of treatment, which was associated with a longer progression-free survival (PFS). In the cyclophosphamide only group, Treg numbers returned to baseline at day 29. Although various studies illustrated positive effects of metronomic low dosing of cyclophosphamide, other studies showed no difference or even increase in Treg levels upon treatment [88, 89].

Next to the dosage and schedule, the tumor type may play a role as well in triggering a drug induced-immune response. Treg depletion was observed in breast cancer and CRC [87, 90], but not in melanoma patients [91]. Cyclophosphamide eliminated MDSCs in CRC [92], but in prostate cancer patients, metronomic cyclophosphamide treatment led to an increase of MDSC [91].

Dacarbazine

Dacarbazine is currently only used in melanoma patients for which the newer therapies are contra-indicated or who progressed on other therapies. Dacarbazine upregulates NKG2D receptors in human melanoma cells, which leads to activation of NK cells and release of IFN- γ : Increased levels of IFN- γ results in upregulation MHC I-expression on tumor cells, which is necessary for the recognition by T-cells [93].

Platinum derivatives

Well-known platinum derivatives are cisplatin, oxaliplatin and carboplatin. Cisplatin is the best studied platinum derivative regarding immunomodulatory effects. Cisplatin was shown to upregulate tumor cell expression of PDL1, e.g. in head and neck squamous cell carcinoma patients receiving standard cisplatin treatment [94]. This suggests a postexposure anticancer T-cell response, hampered by coinciding PD-L1 expression. High doses of cisplatin significantly reduced IFN- γ production by T-cells in vitro [95], and reduced the cytotoxicity of NK cells in ovarian cancer patients [96]. Lower doses impaired T-cell function less significantly [95]. Conversely, aside from the immunosuppressive effects through PD-L1 upregulation, cisplatin has been shown to have immunostimulatory properties as well, demonstrated by upregulation of MHC class I expression on antigen presenting cells [97, 98], recruitment of effector cells to the tumor site, triggering their proliferation [99], and downregulation of the immunosuppressive microenvironment by depleting MDSCs and Tregs [100].

Less data are available regarding the effect on the immune system of oxaliplatin and carboplatin. Oxaliplatin induces upregulation of PD-L1 on DCs [101], and carboplatin PD-1 mRNA expression [102]. Oxaliplatin may induce novel T-cell infiltration of the tumor. A single dose of oxaliplatin increased immune-cell infiltration in a CRC mouse model [103]. Furthermore, oxaliplatin is a known ICD inducer [104] and upregulates DAMPs [105].

Clearly, also of this class of oncolytics optimal dose and schedule for boosting ICD needs to be further established.

Antimetabolites

Antimetabolites interfere with essential biochemical pathways for DNA synthesis, often acting as a substitute or competitor of the natural substrates in physiological metabolism. We focused on the compounds that are often used in solid tumors: gemcitabine, methotrexate and 5-fluorouracil (5FU).

Gemcitabine

The immunomodulating properties of gemcitabine are mainly investigated when applied at the standard dose. Administration of this dose decreases the number of MDSCs, while enhancing cross-presentation of malignant antigens [106]. In pancreatic cancer patients, standard dose gemcitabine led to the depletion of Tregs, which lasted until 2 weeks after the last dose of chemotherapy [107]. Interestingly, no other lymphocyte subtypes significantly decreased after treatment. In ovarian cancer, a single dose of gemcitabine increased the CD8⁺ T-cell tumor infiltration and PD-L1 expression both in vitro and in vivo [107, 108]. This effect was observed during the first 5 days after treatment, but not after 2 weeks of treatment [102]. Due to this time-dependent effect, ICB could best be given 1 week after gemcitabine administration. The impact of dose on immunomodulatory effects require further investigation.

Methotrexate

Methotrexate targets rapidly dividing cells by inhibiting the formation of nucleotides, thereby impairing proliferation. Although high-dose methotrexate causes bone marrow suppression [109], low-dose methotrexate has shown immunostimulating properties. In an in vitro experiment, low-dose noncytotoxic concentrations of methotrexate boosted the maturation of DCs by upregulating CD40, CD80 and CD83 [110]. In return, the DCs stimulated proliferation of T-cells [110], which could lead to a greater antitumor response. This suggests that low-dose methotrexate could be used as an immunostimulating agent. However, more research evaluating the impact of methotrexate on the immune system is needed to confirm whether it is indeed a suitable combination partner for ICB, as the currently available data are too limited.

5-Fluorouracil

5FU functions as antimetabolite of pyrimidine by inhibiting the synthesis of DNA and RNA. 5FU is the most extensively investigated oncolytic compound for its immunomodulating effects. A standard dose of 5FU may exert immune stimulatory effects, e.g. by facilitating antigen uptake by DCs. In an in vitro experiment, DCs were incubated with a gastric cancer cell line which was pretreated with 5FU. The isolated DCs showed higher IL-12 production when incubated with the gastric cancer cell line pretreated with 5FU compared with the control. Subsequently, the cytotoxic T-lymphocytes generated by these DCs showed higher cytotoxicity compared with the control [111]. Furthermore, 5FU also selectively kills MDSCs in vivo, while sparing the other lymphocyte subtypes [108]. Effects were seen in the spleen and tumor of mice, 5 days after the intraperitoneal injection. Selective depletion of MDSCs was associated with greater CD8⁺ T-cell tumor infiltration and T-cell-dependent antitumor responses.

COMBINATION THERAPY

Various studies investigating combination therapy with chemotherapy and checkpoint inhibitors have been carried out. Both in vivo and clinical studies are showing promising results [103, 112, 113].

In vivo experiments allow for swift testing of different regimens by varying both the doses and the order of administration of the drugs. One study tested three different regimens using the combination of gemcitabine and ipilimumab in non-immunogenic mouse models [114]. Gemcitabine was given either 15 days before anti-CTLA-4, concomitantly, or 3 days after anti-CTLA-4. Synergistic effects were only observed in the concomitant regimen, while omitting the first dose of gemcitabine drastically decreased antitumor effects. In another in vivo study combining cyclophosphamide and anti-CTLA-4 similar results were obtained [115]. Immunological antitumor responses were seen when cyclophosphamide was given 1 day before anti-CTLA-4 treatment. However, when reversing the order, CD8⁺ T-cells underwent massive apoptosis and antitumor effects of anti-CTLA-4 were attenuated. These findings suggest that indeed there is a need for a chemotherapy induction phase before administering ICB.

An overview of clinical trials of which data are available is presented in Table 2. Combination therapy in the clinic is mostly well tolerated, and durable responses have been observed in various trials. Currently, three combinations have been approved for first-line treatment, all for advanced NSCLC [120, 147, 148].

In the majority of clinical trials, chemotherapy and ICB are administered concurrently and at full doses. Few trials have explored the optimal dose, or sequence of administration, while preclinical data have shown that these parameters might affect outcome. For example, an induction phase of chemotherapy can modify the tumor microenvironment thereby optimizing it for ICB [152]. A study in metastatic triple negative breast cancer (TNBC) patients investigated induction therapy with various types of chemotherapy [153, 154]. For the induction phase, low doses of chemotherapy were given for 2 weeks: 50 mg daily cyclophosphamide, twice 40 mg/m² cisplatin or twice 15 mg doxorubicin. Response rates with chemotherapy appear higher in the cohorts where low-dose chemotherapy was used as induction, compared with nivolumab alone. Thus far, response rates appear most promising in the doxorubicin and cisplatin induction arms. Biomarker analysis carried out in this trial showed that indeed upon treatment with these two compounds, upregulation is found in key immunological pathways associated with response to anti-PD-1, and this effect is further increased after nivolumab administration. Furthermore, the number of intratumoral T-cells as well as the T-cell clonality is found to be higher after treatment with these drugs, compared with no induction phase [155]. Another study that investigates the impact of order of administration is a large phase II study of ipilimumab with paclitaxel and carboplatin in NSCLC patients [129]. Three different regimens were tested: a phased regimen in which chemotherapy is given before ipilimumab, a concurrent regimen, and a control group of placebo and chemotherapy. The primary end point of improved PFS was only met in the phased regimen, suggesting again that there is indeed a need for a chemotherapy induction phase.

Conversely, a potential immunotherapy induction phase may also be useful. This type of induction could prevent the adverse effects of chemotherapy on the immune system and could improve the overall response rate of combination therapy [121]. A study in TNBC showed that an induction phase with durvalumab followed by combination therapy of weekly nab-paclitaxel for 12 weeks followed by four cycles of combination therapy with epirubicin

and cyclophosphamide resulted into a higher pathological CR rate when compared with chemotherapy alone (53.4% versus 44.2%, respectively) [123]. As there was no chemotherapy induction arm in this trial, it remains to be elucidated whether an immunotherapy or chemotherapy induction phase is most effective.

CONCLUSIONS AND FUTURE PERSPECTIVES

Checkpoint blockade therapy is effective in a variety of tumor types. However, to further increase the number of suitable tumor types, ICB may be combined with compounds which are able to convert non-inflamed tumors into inflamed ones. This in return may render these tumors more sensitive to ICB therapy. Preclinical studies demonstrate that the majority of chemotherapeutic drugs has been shown to exert immunostimulatory effects, either by inhibiting immunosuppressive cells and/or activating effector cells, or by increasing immunogenicity and increasing T-cell infiltration. Although preclinical data have proved to be useful for identifying immunomodulating effects, extrapolation to the clinic should be done cautiously. For example, drug concentrations used in these experiments and drug exposure over time often do not correspond to observed exposure in the clinic. Preferably, preclinical experiments should mimic as much as is possible the clinical situation. An additional potential confounder is that the majority of studies investigate the immunomodulating effects of chemotherapy in peripheral blood and not in the tumor microenvironment. Although some peripheral factors contribute to a response to ICB, intratumoral immunological factors such as CD8+ T-cell infiltration, PD-L1 expression and IFN- γ secretion may be even more crucial and representative of observed effects. Therefore, it is warranted to further investigate the impact of chemotherapy in the tumor micro-environment. For this, it will be essential to draw pre- and on-treatment tumor biopsies during clinical trials, as they may reflect changes in the immunological status of the tumor better than peripheral markers.

In addition to choosing the ideal drugs for combination, it is crucial to investigate the optimal regimen for combination treatment. Current practice is that full-dose chemotherapy is administered with ICB on the same day. However, preclinical research suggests that for certain chemotherapeutic agents timing and sequence of administration of both modalities is important. Furthermore, during combination treatment, chemotherapy is now often administered at the maximum tolerated dose. For the majority of chemotherapeutic compounds, treatment at these doses results in bone marrow toxicity and may lead to altered immune cell function, while metronomic doses have been shown to augment immunotherapeutic activity [85, 156, 157]. Early signs of improved outcome of combined modality of chemotherapy and ICB in patients encourage more advanced approaches in identifying representative preclinical models, optimal drug combinations, sequence effects and ideal concentration–time profiles. This outcome should be the template for translation to clinical proof of concept studies, which should incorporate extensive pre- and on-treatment biomarker assessment, which may leverage pivotal studies, ultimately leading to novel standards of care.

Table 2. Clinical combination trials.

Drugs Immunotherapy		Chemotherapy		Regimen		Tumor Type		Reference		Major findings/issues	
Atezolizumab		Nab-paclitaxel		Atezolizumab 800 mg Q2W (d1,15) and nab-paclitaxel 125 mg/m ² Q1W (d1,8,15) in cycles of 4 weeks	TNBC	Adams et al. 2018[116]		Median PFS 5.5 months, OS 14.7months			
Atezolizumab		Carboplatin, paclitaxel, nab-paclitaxel		Atezolizumab 15mg/kg (in a later amendment 1200mg flat dose) + carboplatin AUC6 + paclitaxel 200mg/m ² Q3W(Arm C), atezolizumab + carboplatin + pemimetrexed 500mg/m ² Q3W(Arm D), or atezolizumab + carboplatin Q3W + nab-paclitaxel 100mg/m ² QW (Arm E) for 4–6 cycles followed with atezolizumab maintenance	NSCLC	Liu et al. 2018[117]		Confirmed ORRs were 36% Arm C, 68% Arm D (one complete response [CR]) and 46% Arm E (four CRs). Median PFS was 7.1 months, 8.4 months and 5.7 months, respectively. Median OS was 12.9 months, 18.9 months and 17.0 months, respectively			
Atezolizumab		Carboplatin and etoposide		Carboplatin AUC5 + etoposide 100mg/m ² Q3W + atezolizumab 1200mg or placebo Q3W	NSCLC	Horn et al. 2018[118]		The median OS was 12.3 months in the atezolizumab group and 10.3 months in the placebo group (hazard ratio for death, 0.70; 95% CI, 0.54 to 0.91; P=0.007). The median PFS was 5.2 months and 4.3 months, respectively (hazard ratio for disease progression or death, 0.77; 95% CI, 0.62 to 0.96; P=0.02).			
Atezolizumab, durvalumab, nivolumab or pembrolizumab		Carboplatin, pemimetrexed, bevacizumab, docetaxel, ramucirumab, vinorelbine, gemcitabine, paclitaxel		Any ICB before any chemotherapy	NSCLC	Grigg et al.2017[119]		Durable responses after treatment. Lack of control arm			
Atezolizumab		Carboplatin, paclitaxel, bevacizumab		Atezolizumab 1200 mg + Carboplatin AUC 6 + Paclitaxel 200 mg/m ² (Arm A) or atezolizumab + bevacizumab 15 mg/kg + Carboplatin + Paclitaxel (Arm B) vs bevacizumab + carboplatin + paclitaxel (Arm C) IV q3w for 4 or 6 cycles per investigator discretion, then maintenance atezolizumab, atezolizumab + bevacizumab or bevacizumab, respectively.	NSCLC	Reck et al. 2017[120]		Clinically meaningful PFS benefit with atezolizumab + bevacizumab + chemotherapy versus bevacizumab + chemotherapy. Approved for first line treatment of metastatic non-squamous NSCLC.			
Avelumab		Carboplatin, gemcitabine		2 cycles of induction avelumab prior to combining carboplatin-gemcitabine plus	Urothelial cancer	Vida et al. 2018[121]		Induction phase with ICB. "Priming the immune response			

			avelumab for 6 cycles						before chemotherapy could prevent the detrimental effect of chemotherapy on immune cells; reduction of tumor burden with chemotherapy may allow immunotherapy to be more effective"
Avelumab		Cisplatin	Avelumab 10mg/kg on Day 1 of the Lead-in Phase; Days 8, 25, and 39 of the chemoradiation therapy phase; and q2w for 12 months during the maintenance phase. •Cisplatin 100 mg/m ² IV; Days 1, 22, and 43 of the chemoradiation therapy phase. Radiation therapy 70 Gy/35 fractions/7 weeks.	Head and neck cancer	Yu et al. 2018[122]			No results yet	
Durvalumab		Nab-paclitaxel, cyclophosphamide, eprubicin	Durvalumab 1.5 g or placebo Q4W. placebo monotherapy (0.75 g) was given for the first 2 wks (window phase), and durvalumab/placebo + nab-paclitaxel 125 mg/m ² QW for 12 wks, followed by durvalumab/placebo + eprubicin/cyclophosphamide Q2W for 4 cycles	TNBC	Loibl et al. 2018[123]			Combination therapy resulted in a high CR rate in TNBC. Induction therapy with durvalumab seemed beneficial	
Durvalumab		Eribulin	A fixed dose of durvalumab (1.12g) is given on day 1 of each cycle. The starting dose is 1.1mg/m ² with dose escalation to 1.4mg/m ² on day 1 and day 8 Q3W	TNBC	Landry et al. 2018[124]			No results yet	
ICB		Carboplatin, paclitaxel, temozolomide, nab-paclitaxel	Not specified in abstract/poster	Melanoma	Aguilera et al. 2018[125]			Patients who received chemo-immunotherapy had a median OS of 5 years (95% CI: 2-NR) versus 1.8 years (95% CI: 0.9-2; p = 0.002) for those who received either ICB (n = 9) or chemotherapy alone (n = 15), with ORR of 61% versus 17% (p = 0.001), respectively	
Ipilimumab		Dacarbazine	Ipilimumab 10mg/kg + dacarbazine 850mg/m ² or dacarbazine + placebo Q3W followed by dacarbazine monotherapy	Melanoma	Robert et al. 2011[126]			Combination therapy resulted into a higher OS (11.2 months vs. 9.1 months). In another phase II study ipilimumab monotherapy resulted into an OS of 11.1 month, even in pre-treated patients[127]	
Ipilimumab		Dacarbazine	Ipilimumab 3mg/kg Q4W alone or with dacarbazine 250mg/m ² /day up to 6x5day	Melanoma	Hersh et al, 2011[128]			Objective response rate was 14.3% vs 5.4% for the	

Ipilimumab	Paclitaxel, carboplatin	cycles Concurrent: 4x ipilimumab 10mg/kg + paclitaxel 175mg/m ² + carboplatin AUC6 followed by 2x placebo + paclitaxel + carboplatin Phased: 2x placebo + paclitaxel + carboplatin followed by 4x ipilimumab + paclitaxel + carboplatin. Control: placebo + paclitaxel + carboplatin	NSCLC	Lynch et al. 2012[129]	combination therapy. OS was 20.9 and 16.4 respectively Only phased regimen leads to improved PFS compared to control
Ipilimumab	Gemcitabine, cisplatin	2x gemcitabine 1000mg/m ² + cisplatin 70mg/m ² followed by 4x ipilimumab 10mg/kg + gemcitabine + cisplatin	Urothelial cell carcinoma	Galsky et al. 2017[130]	No changes in composition and frequency of peripheral immune cells after gemcitabine. Expansion of CD4 ⁺ cells after combination therapy. No ipilimumab monotherapy cohort
Ipilimumab	Paclitaxel, carboplatin	Phased ipilimumab paclitaxel + carboplatin followed by 4x 10mg/kg ipilimumab + paclitaxel + carboplatin	NSCLC	Govindan et al. 2017[131]	No prolonged OS compared to chemotherapy alone
Ipilimumab, nivolumab	Trabectedin	Ipilimumab (1mg/kg Q12W), nivolumab (3mg/kg Q2W), and escalating doses of trabectedin (1.0, 1.3, 1.5 mg/m ² Q3W)	STS	Gordon et al. 2018[132]	No results yet
Nivolumab	Gemcitabine, cisplatin, pemetrexed, paclitaxel, carboplatin, docetaxel	Arm A: nivolumab 10mg/kg + gemcitabine 1250mg/m ² + cisplatin 80mg/m ² Arm B: nivolumab + pemetrexed 500mg/m ² + cisplatin 75mg/m ² Arm C: nivolumab + paclitaxel 200mg/m ² + carboplatin AUC6 + bevacizumab 15mg/kg Arm D: nivolumab + docetaxel 75mg/m ²	NSCLC	Kanda et al. 2016[133]	Full dose was given. Difficult to compare response rates: different lines of treatment, different and low patient numbers
Nivolumab	Gemcitabine-cisplatin, pemetrexed-cisplatin, paclitaxel-carboplatin	10 mg/kg nivolumab gemcitabine-cisplatin, 10 mg/kg nivolumab pemetrexed-cisplatin, 10 mg/kg nivolumab paclitaxel-carboplatin 5 mg/kg nivolumab paclitaxel-carboplatin	NSCLC	Rizvi et al 2016[134]	Chemotherapy doses not defined. Most promising results in nivolumab- paclitaxel-carboplatin group
Nivolumab	Carboplatin	Carboplatin (AUC6) with or without nivolumab (360 mg) Q3W	TNBC	Garrido et al. 2018[135]	No results yet
Nivolumab	Paclitaxel	Nivolumab (Q4W, 3mg/kg on days 1 and 15 for level 1 and 1mg/kg for level -1) with fixed doses of paclitaxel and ramucirumab (Q4W, 80mg/m ² on days 1.8 and 15 and 8mg/kg on days 1 and 15, respectively)	Gastric cancer	Nishina et al. 2018[136]	No results yet
Nivolumab	Paclitaxel	Nivolumab 240mg/body on day 1, 15, paclitaxel 90mg/m ² on day1, 8, 15, and bevacizumab 10mg/kg on day 1, 15 Q4W	HER2 negative breast cancer	Ozaki et al. 2018[137]	No results yet

Nivolumab	Cisplatin, pemetrexed or cisplatin, gemcitabine	Cisplatin 75mg/m ² Q3Wx3 plus either pemetrexed 500 mg/m ² Q3Wx3 or gemcitabine 1250mg/m ² d1, d8 Q3Wx3 plus nivolumab 360mg Q3Wx3	NSCLC	Evans et al. 2018[138]	No results yet
Nivolumab	Trabectedin	Trabectedin (1.5mg/m ²) Q3W, and nivolumab (3mg/kg) Q3W	STS	Chawla et al. 2018[139]	Paired administration of trabectedin and nivolumab is safe, and that this combined chemo-immuno-therapy approach may have synergistic activity
Nivolumab	Cisplatin, pemetrexed	Cisplatin (75 mg/m ²), pemetrexed (500 mg/m ²), and nivolumab (360 mg) q3w.	Mesothelioma	Fujimoto et al. 2018[140]	No results yet
Pembrolizumab	Paclitaxel, doxorubicin, cyclophosphamide, carboplatin	Cohort A: pembrolizumab 200mg Q3W + nab-paclitaxel 100-125mg/m ² QW followed by Q3W pembrolizumab 200mg + cyclophosphamide 600mg/m ² + doxorubicin 60mg/m ² . Cohort B: pembrolizumab 200mg + nab-paclitaxel 100-125mg/m ² QW + carboplatin AUC6 Q3W followed by Q3W pembrolizumab 200mg + doxorubicin 60mg/m ² + cyclophosphamide 600mg/m ² .	TNBC	Bhatti et al. 2017[141]	Both regimens showed promising anti-tumor activity with manageable toxicity. Addition of carboplatin resulted in more grade 3 or 4 toxicities, mainly neutropenia
Pembrolizumab	Gemcitabine, docetaxel, nab-paclitaxel, vinorelbine, irinotecan, liposomal doxorubicin	Arm 1: pembrolizumab 2mg/kg Q3W + gemcitabine 1000mg/m ² D1 and D8 Q3W Arm 2: pembrolizumab + gemcitabine 900mg/m ² D1 and D8 + docetaxel 75mg/m ² D8 Q3W Arm 3: pembrolizumab + gemcitabine 1000mg/m ² + nab-paclitaxel 125mg/m ² D1 and D8 Q3W Arm 4: pembrolizumab + gemcitabine 1000mg/m ² + vinorelbine 25mg/m ² D1 and D8 Q3W Arm 5: pembrolizumab + irinotecan 300mg/m ² Q3W Arm 6: pembrolizumab + liposomal doxorubicin 30mg/m ² Q3W	All solid tumor types	Weiss et al. 2017[142]	All advanced solid tumor types included. Full doses of chemotherapy are used. Recommended phase 2 dose determined as maximum tolerated dose. Partial responses observed in arm 3 – 6.
Pembrolizumab	Carboplatin, pemetrexed,	Carboplatin AUC5mg/mL + pemetrexed 500mg/m ² Q3W for 4 cycles followed by optional pemetrexed 500mg/m ² +/- pembrolizumab 200mg Q3W for 2 years	NSCLC	Papadimitrakopoulou et al. 2017[113]; Langer et al.2016[143]	All drugs administered on same day. Improved efficacy over chemotherapy alone. Approved for first line treatment of metastatic non-squamous NSCLC.
Pembrolizumab	5FU, cisplatin	Pembrolizumab 200mg Q3W + cisplatin	Gastric cancer	Bang et al.2017[20]	Full dose given. Promising anti-

			80mg/m ² Q3W + 5FU 800mg/m ² Q3W or capecitabine 1000mg/m ² BID Q3W					tumor activity irrespective of PD-L1 expression.
Pembrolizumab	Carboplatin, gemcitabine		Pembrolizumab 200mg Q3W, and carboplatin (AUC2) + gemcitabine (800mg/m ²) on days 1 and 8	TNBC		Obeid et al 2017[144]		Two out of three patients showed effective immune stimulation
Pembrolizumab	Eribulin		eribulin 1.4mg/m ² on day 1 and 8, pembrolizumab Q3W	TNBC		Tolaney et al 2017[145]		Median PFS 4.2 months, OS 17.7 months
Pembrolizumab	Capecitabine or paclitaxel		Pembrolizumab 200mg Q3W and 1 st or 2 nd line paclitaxel (80mg/m ² qW) or oral capecitabine (2000mg BID, weekly 1 on/1 off)	TNBC		Page et al. 2018[146]		Three out of nine patients showed a partial response, of whom two had metastatic disease.
Pembrolizumab	Pemetrexed, cisplatin, carboplatin		Pemetrexed and a platinum-based drug +200mg pembrolizumab or placebo Q3W for 4 cycles followed by 35 cycles of pembrolizumab or placebo + pemetrexed	NSCLC		Gandhi et al. 2018[147]		OS at 12 months was 69.2% in the pembrolizumab-combination group versus 49.4% in the placebo-combination group, regardless of PD-L1 status. PFS survival was 8.8 vs 4.9 months respectively. The incidence of grade 3 rAEs was comparable between the 2 groups.
Pembrolizumab	Carboplatin, nab-paclitaxel		Pembrolizumab at 200mg/week plus carboplatin AUC6 Q3W and paclitaxel at 200mg/m ² Q3W or nanoparticle albumin-bound (nab)-paclitaxel at 100mg/m ² QW for 4 cycles vs the same chemotherapy plus placebo	NSCLC		Paz-Ares et al 2018.[148, 149]		Improved overall survival (15.9 months vs 11.3 months), response rates, and duration of response (PFS if 6.4 months vs 4.8 months) in the group with chemo-immunotherapy compared to chemotherapy alone. Approved for first line treatment of metastatic squamous NSCLC.
Pembrolizumab	Docetaxel or gemcitabine		Pembrolizumab 200mg and either docetaxel 75 mg/m ² (arm A) or gemcitabine 1000 mg/m ² on day 1 and 8 (arm B) q3w	Urothelial cell cancer		Parikh et al. 2018[150]		Arm A had an ORR of 50% and DCR of 67%, whereas arm B had an ORR of 33% and DCR of 50%. Median PFS was 4.8, 5.7, and 3.7 months for the overall cohort, arm A, and arm B, respectively.
Tremelimumab	Gemcitabine		Gemcitabine (1000 mg/m ² on days 1, 8, and 15 of each 28-day cycles) + tremelimumab (6, 10, or 15 mg/kg) on day 1 of each 84-day cycle for a maximum of 4 cycles	Pancreatic cancer		Aglietta et al. 2014[151]		Full dose gemcitabine, MTD of tremelimumab 15mg/kg. Two partial responses

REFERENCES

1. Larkin J, Minor D, D'Angelo S et al. Overall survival in patients with advanced melanoma who received nivolumab versus investigator's choice chemotherapy in CheckMate 037: a randomized, controlled, open-label phase III trial. *J Clin Oncol* 2018; 36: 803–390.
2. Weber JS, D'Angelo SP, Minor D et al. Nivolumab versus chemotherapy in patients with advanced melanoma who progressed after anti-CTLA-4 treatment (CheckMate 037): a randomised, controlled, open-label, phase 3 trial. *Lancet Oncol* 2015; 16: 375–384.
3. Motzer RJ, Escudier B, McDermott DF et al. Nivolumab versus everolimus in advanced renal-cell carcinoma. *N Engl J Med* 2015; 373(19):1803–1813.
4. Ning Y, Suzman D, Maher VE et al. FDA approval summary: atezolizumab for the treatment of patients with progressive advanced urothelial carcinoma after platinum-containing chemotherapy. *Oncologist* 2017; 22(6): 743–749.
5. Sul J, Blumenthal GM, Jiang X et al. FDA approval summary: pembrolizumab for the treatment of patients with metastatic non-small cell lung cancer whose tumors express programmed death-ligand 1. *Oncologist* 2016; 21(5): 643–650.
6. Nakamura Y, Kitano S, Takahashi A, Tsutsumida A. Nivolumab for advanced melanoma: pretreatment prognostic factors and early outcome markers during therapy. *Oncotarget* 2016; 7(47): 77404–77415.
7. Bagley SJ, Kothari S, Aggarwal C et al. Pretreatment neutrophil-to-lymphocyte ratio as a marker of outcomes in nivolumab-treated patients with advanced non-small-cell lung cancer. *Lung Cancer* 2017; 106: 1–7.
8. Nanda R, Chow LQM, Dees EC et al. Pembrolizumab in patients with advanced triple-negative breast cancer: phase Ib KEYNOTE-012 study. *J Clin Oncol* 2016; 34(21): 2460–2467.
9. Loi S, Adams S, Schmid P et al. Relationship between tumor infiltrating lymphocyte (TIL) levels and response to pembrolizumab (pembro) in metastatic triple-negative breast cancer (mTNBC): results from KEYNOTE-086. *Ann Oncol* 2018; 28: 605–649.
10. Martens A, Wistuba-Hamprecht K, Geukes Foppen M et al. Baseline peripheral blood biomarkers associated with clinical outcome of advanced melanoma patients treated with ipilimumab. *Clin Cancer Res* 2016; 22: 2908–2918.
11. Simeone E, Gentilcore G, Giannarelli D et al. Immunological and biological changes during ipilimumab treatment and their potential correlation with clinical response and survival in patients with advanced melanoma. *Cancer Immunol Immunother* 2014; 63: 675–683.
12. Morello S, Capone M, Sorrentino C et al. Soluble CD73 as biomarker in patients with metastatic melanoma patients treated with nivolumab. *J Transl Med* 2017; 15: 244.
13. Hugo W, Zaretsky JM, Sun L et al. Genomic and transcriptomic features of response to anti-PD-1 therapy in metastatic melanoma. *Cell* 2016; 165: 35–44.
14. Rizvi NA, Hellmann MD, Snyder A et al. Mutational landscape determines sensitivity to PD-1 blockade in non-small cell lung cancer. *Science* 2015; 348: 124–128.
15. Snyder A, Makarov V, Merghoub T et al. Genetic basis for clinical response to CTLA-4 blockade in melanoma. *N Engl J Med* 2014; 371: 2189–2199.
16. Rosenberg JE, Hoffman-Censits J, Powles T et al. Atezolizumab in patients with locally advanced and metastatic urothelial carcinoma who have progressed following treatment with platinum-based chemotherapy: a single-arm, multicentre, phase 2 trial. *Lancet* 2016; 387: 1909–1920.
17. Le DT, Uram JN, Wang H et al. PD-1 blockade in tumors with mismatch-repair deficiency. *N Engl J Med* 2015; 372(26): 2509–2520.
18. Gettinger S, Rizvi NA, Chow LQ et al. Nivolumab monotherapy for first-line treatment of advanced non-small-cell lung cancer. *J Clin Oncol* 2016; 34: 2980–2987.
19. Herbst RS, Soria J-C, Kowanetz M et al. Predictive correlates of response to the anti-PD-L1 antibody MPDL3280A in cancer patients. *Nature* 2014; 515: 563–567.
20. Bang Y-J, Muro K, Fuchs CS et al. KEYNOTE-059 cohort 2: safety and efficacy of pembrolizumab (pembro) plus 5-fluorouracil (5-FU) and cisplatin for first-line (1L) treatment of advanced gastric cancer. *J Clin Oncol* 2017; 35: 4012.
21. Chow LQM, Haddad R, Gupta S et al. Antitumor activity of pembrolizumab in biomarker-unselected patients with recurrent and/or metastatic head and neck squamous cell carcinoma: results from the phase Ib KEYNOTE-012 expansion cohort. *J Clin Oncol* 2016; 34:3838–3845.

22. Kim ST, Cristescu R, Bass AJ et al. Comprehensive molecular characterization of clinical responses to PD-1 inhibition in metastatic gastric cancer. *Nat Med* 2018; 1: 1449–1458.
23. Vilain RE, Menzies AM, Wilmott JS et al. Dynamic changes in PD-L1 expression and immune infiltrates early during treatment predict response to PD-1 blockade in melanoma. *Clin Cancer Res* 2017; 23(17):5024–5033.
24. Tumeah PC, Harview CL, Yearley JH et al. PD-1 blockade induces responses by inhibiting adaptive immune resistance. *Nature* 2014; 515: 568–571.
25. Dirix LY, Takacs I, Jerusalem G et al. Avelumab, an anti-PD-L1 antibody, in patients with locally advanced or metastatic breast cancer: a phase 1b JAVELIN Solid Tumor study. *Breast Cancer Res Treat* 2018; 167: 671–686.
26. Hamid O, Schmidt H, Nissan A et al. A prospective phase II trial exploring the association between tumor microenvironment biomarkers and clinical activity of ipilimumab in advanced melanoma. *J Transl Med* 2011; 9:204.
27. Wang W, Yu D, Sarnaik AA et al. Biomarkers on melanoma patient T cells associated with ipilimumab treatment. *J Transl Med* 2012; 10: 146.
28. Tietze JK, Angelova D, Heppt MV et al. The proportion of circulating CD45RO + CD8 + memory T cells is correlated with clinical response in melanoma patients treated with ipilimumab. *Eur J Cancer* 2017; 75: 268–279.
29. Tietze JK, Angelova D, Heppt MV et al. Low baseline levels of NK cells may predict a positive response to ipilimumab in melanoma therapy. *Exp Dermatol* 2017; 26: 622–629.
30. Cassidy MR, Wolchok RE, Zheng J et al. Neutrophil to lymphocyte ratio is associated with outcome during ipilimumab treatment. *EBioMedicine* 2017; 18: 56–61.
31. Gebhardt C, Sevko A, Jiang H et al. Myeloid cells and related chronic inflammatory factors as novel predictive markers in melanoma treatment with ipilimumab. *Clin Cancer Res* 2015; 21: 5453–5459.
32. Ferrucci PF, Ascierto PA, Pigozzo J et al. Baseline neutrophils and derived neutrophil-to-lymphocyte ratio: prognostic relevance in metastatic melanoma patients receiving ipilimumab. *Ann Oncol* 2016; 27: 732–738.
33. Kitano S, Postow MA, Ziegler CGK et al. Computational algorithm-driven evaluation of monocytic myeloid-derived suppressor cell frequency for prediction of clinical outcomes. *Cancer Immunol Res* 2014;2: 812–821.
34. Sade-Feldman M, Kanterman J, Klieger Y et al. Clinical significance of circulating CD33⁺CD11b⁺HLA-DR⁻ myeloid cells in patients with stage IV melanoma treated with ipilimumab. *Clin Cancer Res* 2016; 22: 5661–5672.
35. Yamazaki N, Kiyohara Y, Uhara H et al. Cytokine biomarkers to predict antitumor responses to nivolumab suggested in a phase 2 study for advanced melanoma. *Cancer Sci* 2017; 108: 1022–1031.
36. Krieg C, Nowicka M, Guglietta S et al. High-dimensional single-cell analysis predicts response to anti-PD-1 immunotherapy. *Nat Med* 2018; 24: 144–153.
37. Ribas A, Robert C, Hodi FS et al. Association of response to programmed death receptor 1 (PD-1) blockade with pembrolizumab (MK-3475) with an interferon-inflammatory immune gene signature. *J Clin Oncol* 2015; 33: 3001.
38. Ayers M, Lunceford J, NebozhynMet al. Relationship between immune gene signatures and clinical response to PD-1 blockade with pembrolizumab (MK-3475) in patients with advanced solid tumors. *J Immunother Cancer* 2015; 3:80.
39. O'Donnell PH, Grivas P, Balar AV et al. Biomarker findings and mature clinical results from KEYNOTE-052: first-line pembrolizumab in cisplatin-ineligible advanced urothelial cancer. *J Clin Oncol* 2017; 35: 4502–4502.
40. Prat A, Navarro A, Paré L et al. Immune-related gene expression profiling after PD-1 blockade in non-small cell lung carcinoma, head and neck squamous cell carcinoma, and melanoma. *Cancer Res* 2017; 77: 3540–3550.
41. Fehrenbacher L, Spira A, Ballinger M et al. Atezolizumab versus docetaxel for patients with previously treated non-small-cell lung cancer (POPLAR): a multicentre, open-label, phase 2 randomised controlled trial. *Lancet* 2016; 387: 1837–1846.
42. U.S. Food and Drug Administration. Opdivo (nivolumab) Prescribing information, 2015. Reference ID: 4198384.
43. U.S. Food and Drug Administration. Keytruda (pembrolizumab) 2018: 1–53; Reference ID: 4276421.

44. Alexandrov LB, Nik-Zainal S, Wedge DC et al. Signatures of mutational processes in human cancer. *Nature* 2013; 500: 415–421.
45. Sclafani F. PD-1 inhibition in metastatic dMMR/MSI-H colorectal cancer. *Lancet Oncol* 2017; 18: 1141–1142.
46. Ji R-R, Chasalow SD, Wang L et al. An immune-active tumor microenvironment favors clinical response to ipilimumab. *Cancer Immunol Immunother* 2012; 61: 1019–1031.
47. Lindau D, Gielen P, Kroesen M et al. The immunosuppressive tumour network: myeloid-derived suppressor cells, regulatory T cells and natural killer T cells. *Immunology* 2013; 138: 105–115.
48. Hegde PS, Karanikas V, Evers S. The where, the when, and the how of immune monitoring for cancer immunotherapies in the era of checkpoint inhibition. *Clin Cancer Res* 2016; 22(8): 1865–1874.
49. Higgs BW, Robbins PB, Blake-Haskins JA et al. 15LBA high tumoral IFN γ mRNA, PD-L1 protein, and combined IFN γ mRNA/PD-L1 protein expression associates with response to durvalumab (anti-PD-L1) monotherapy in NSCLC patients. *Eur J Cancer* 2015; 51: S717
50. Ribas A, Dummer R, Puzanov I et al. Oncolytic virotherapy promotes intratumoral T cell infiltration and improves anti-PD-1 immunotherapy. *Cell* 2017; 170: 1109–1119
51. Sakai H, Kokura S, Ishikawa T et al. Effects of anticancer agents on cell viability, proliferative activity and cytokine production of peripheral blood mononuclear cells. *J Clin Biochem Nutr* 2013; 52: 64–71.
52. Pol J, Vacchelli E, Aranda F et al. Trial Watch: immunogenic cell death inducers for anticancer chemotherapy. *Oncoimmunology* 2015; 4: 1008866
53. Haggerty TJ, Dunn IS, Rose LB et al. Topoisomerase inhibitors modulate expression of melanocytic antigens and enhance T cell recognition of tumor cells. *Cancer Immunol Immunother* 2011; 60: 133–144.
54. McKenzie JA, Mbofung RM, Malu S et al. The effect of topoisomerase I inhibitors on the efficacy of T-cell-based cancer immunotherapy. *J Natl Cancer Inst* 2018; 110: 777–786.
55. Frey B, Stache C, Rubner Y et al. Combined treatment of human colorectal tumor cell lines with chemotherapeutic agents and ionizing irradiation can in vitro induce tumor cell death forms with immunogenic potential. *J Immunotoxicol* 2012; 9: 301–313.
56. Alagkiozidis I, Facciabene A, Tsiatas M et al. Time-dependent cytotoxic drugs selectively cooperate with IL-18 for cancer chemo-immunotherapy. *J Transl Med* 2011; 9: 77.
57. Wan S, Pestka S, Jubin RG et al. Chemotherapeutics and radiation stimulate MHC class I expression through elevated interferon-beta signaling in breast cancer cells. *PLoS One* 2012; 7:e32542
58. Ferrari S, Rovati B, Cucca L et al. Impact of topotecan-based chemotherapy on the immune system of advanced ovarian cancer patients: an immunophenotypic study. *Oncol Rep* 2002; 9: 1107–1113.
59. Galluzzi L, Buque A, Kepp O et al. Immunogenic cell death in cancer and infectious disease. *Nat Rev Immunol* 2017; 17: 97–111.
60. Martins I, Tesniere A, Kepp O et al. Chemotherapy induces ATP release from tumor cells. *Cell Cycle* 2009; 8: 3723–3728.
61. Fucikova J, Kralikova P, Fialova A et al. Human tumor cells killed by anthracyclines induce a tumor-specific immune response. *Cancer Res* 2011; 71: 4821–4833.
62. Showalter A, Limaye A, Oyer JL et al. Cytokines in immunogenic cell death: applications for cancer immunotherapy. *Cytokine* 2017; 97: 123–132.
63. Casares N, Pequignot MO, Tesniere A et al. Caspase-dependent immunogenicity of doxorubicin-induced tumor cell death. *J Exp Med* 2005; 202: 1691–1701.
64. Sistigu A, Yamazaki T, Vacchelli E et al. Cancer cell-autonomous contribution of type I interferon signaling to the efficacy of chemotherapy. *Nat Med* 2014; 20(11): 1301–1309.
65. Alizadeh D, Trad M, Hanke NT et al. Doxorubicin eliminates myeloid-derived suppressor cells and enhances the efficacy of adoptive T-cell transfer in breast cancer. *Cancer Res* 2014; 74: 104–118.
66. Kashima H, Momose F, Umehara H et al. Epirubicin, identified using a novel luciferase reporter assay for Foxp3 inhibitors, inhibits regulatory T cell activity. *PLoS One* 2016; 11: 0156643.
67. Lissoni P, Tancini G, Archili C et al. Changes in T lymphocyte subsets after single dose epirubicin. *Eur J Cancer* 1990; 26: 767–768.

68. Ferraro C, Quemeneur L, Fournel S et al. The topoisomerase inhibitors camptothecin and etoposide induce a CD95-independent apoptosis of activated peripheral lymphocytes. *Cell Death Differ* 2000; 7: 197–206.
69. Quartino AL, Friberg LE, Karlsson MO. A simultaneous analysis of the time-course of leukocytes and neutrophils following docetaxel administration using a semi-mechanistic myelosuppression model. *Invest New Drugs* 2012; 30: 833–845.
70. Kotsakis A, Sarra E, Peraki M et al. Docetaxel-induced lymphopenia in patients with solid tumors: a prospective phenotypic analysis. *Cancer* 2000; 89: 1380–1386.
71. Chuang LT, Lotzova E, Heath J et al. Alteration of lymphocyte microtubule assembly, cytotoxicity, and activation by the anticancer drug taxol. *Cancer Res* 1994; 54: 1286–1291.
72. Tong AW, Seamour B, Lawson JM et al. Cellular immune profile of patients with advanced cancer before and after taxane treatment. *Am J Clin Oncol* 2000; 23: 463–472.
73. Tsavaris N, Kosmas C, Vadiaka M et al. Immune changes in patients with advanced breast cancer undergoing chemotherapy with taxanes. *Br J Cancer* 2002; 87: 21–27.
74. Kodumudi KN, Woan K, Gilvary DL et al. A novel chemoimmunomodulating property of docetaxel: suppression of myeloid-derived suppressor cells in tumor bearers. *Clin Cancer Res* 2010; 16: 4583–4594.
75. Li J-Y, Duan X-F, Wang L-P et al. Selective depletion of regulatory T cell subsets by docetaxel treatment in patients with nonsmall cell lung cancer. *J Immunol Res* 2014; 2014: 286170.
76. Roselli M, Cereda V, di Bari MG et al. Effects of conventional therapeutic interventions on the number and function of regulatory T cells. *Oncoimmunology* 2013; 2: 27025.
77. Zhang L, Dermawan K, Jin M et al. Differential impairment of regulatory T cells rather than effector T cells by paclitaxel-based chemotherapy. *Clin Immunol* 2008; 129: 219–229.
78. Demaria S, Volm MD, Shapiro RL et al. Development of tumorinfiltrating lymphocytes in breast cancer after neoadjuvant paclitaxel chemotherapy. *Clin Cancer Res* 2001; 7: 3025–3030.
79. Fujimura T, Kakizaki A, Kambayashi Y et al. Cytotoxic antimelanoma drugs suppress the activation of M2 macrophages. *Exp Dermatol* 2018; 27: 64–70.
80. Thomas-Schoemann A, Lemare F, Mongaret C et al. Bystander effect of vinorelbine alters antitumor immune response. *Int J Cancer* 2011; 129: 1511–1518.
81. Tanaka H, Matsushima H, Nishibu A et al. Dual therapeutic efficacy of vinblastine as a unique chemotherapeutic agent capable of inducing dendritic cell maturation. *Cancer Res* 2009; 69: 6987–6994.
82. Schiavoni G, Sistigu A, Valentini M et al. Cyclophosphamide synergizes with type I interferons through systemic dendritic cell reactivation and induction of immunogenic tumor apoptosis. *Cancer Res* 2011; 71: 768–778.
83. Food and Drug Administration. Cyclophosphamide Prescribing Information 2013; 1–18. Reference ID: 3304966.
84. Wu J, Jordan M, Waxman DJ. Metronomic cyclophosphamide activation of anti-tumor immunity: tumor model, mouse host, and drug schedule dependence of gene responses and their upstream regulators. *BMC Cancer* 2016; 16: 623.
85. Ghiringhelli F, Menard C, Puig PE et al. Metronomic cyclophosphamide regimen selectively depletes CD4+CD25+ regulatory T cells and restores T and NK effector functions in end stage cancer patients. *Cancer Immunol Immunother* 2007; 56: 641–648.
86. Matar P, Rozados VR, Gervasoni SI, Scharovsky GO. Th2/Th1 switch induced by a single low dose of cyclophosphamide in a rat metastatic lymphoma model. *Cancer Immunol Immunother* 2002; 50: 588–596.
87. Scurr M, Pembroke T, Bloom A et al. Effect of modified vaccinia Ankara-5T4 and low-dose cyclophosphamide on antitumor immunity in metastatic colorectal cancer a randomized clinical trial. *JAMA Oncol* 2017; 3: 1–9.
88. Kwa M, Li X, Novik Y et al. Serial immunological parameters in a phase II trial of exemestane and low-dose oral cyclophosphamide in advanced hormone receptor-positive breast cancer. *Breast Cancer Res Treat* 2018; 168: 57–67.
89. Audia S, Nicolas A, Cathelin D et al. Increase of CD4⁺CD25⁺ regulatory T cells in the peripheral blood of patients with metastatic carcinoma: a phase I clinical trial using cyclophosphamide and immunotherapy to eliminate CD4⁺CD25⁺ T lymphocytes. *Clin Exp Immunol* 2007; 150: 523–530.

90. Ge Y, Domschke C, Stoiber N et al. Metronomic cyclophosphamide treatment in metastasized breast cancer patients: immunological effects and clinical outcome. *Cancer Immunol Immunother* 2012; 61: 353–362.
91. Ahlmann M, Hempel G. The effect of cyclophosphamide on the immune system: implications for clinical cancer therapy. *Cancer Chemother Pharmacol* 2016; 78: 661–671.
92. Medina-Echeverez J, Fioravanti J, Zabala M et al. Successful colon cancer eradication after chemoimmunotherapy is associated with profound phenotypic change of intratumoral myeloid cells. *J Immunol* 2011; 186: 807–815.
93. Ugurel S, Paschen A, Becker JC. Dacarbazine in melanoma: from a chemotherapeutic drug to an immunomodulating agent. *J Invest Dermatol* 2013; 133: 289–292.
94. Ock C-Y, Kim S, Keam B et al. Changes in programmed death-ligand 1 expression during cisplatin treatment in patients with head and neck squamous cell carcinoma. *Oncotarget* 2017; 8: 97920–97927.
95. Tran L, Allen CT, Xiao R et al. Cisplatin alters antitumor immunity and synergizes with PD-1/PD-L1 inhibition in head and neck squamous cell carcinoma. *Cancer Immunol Res* 2017; 5: 1141–1151.
96. Garzetti GG, Ciavattini A, Muzzioli M, Romanini C. Cisplatin-based polychemotherapy reduces the natural cytotoxicity of peripheral blood mononuclear cells in patients with advanced ovarian carcinoma and their in vitro responsiveness to interleukin-12 incubation. *Cancer* 1999; 85: 2226–2231.
97. Jackaman C, Majewski D, Fox SA et al. Chemotherapy broadens the range of tumor antigens seen by cytotoxic CD8(+) T cells in vivo. *Cancer Immunol Immunother* 2012; 61: 2343–2356.
98. Nio Y, Hirahara N, Minari Y et al. Induction of tumor-specific antitumor immunity after chemotherapy with cisplatin in mice bearing MOPC-104E plasmacytoma by modulation of MHC expression on tumor surface. *Anticancer Res* 2000; 20: 3293–3299.
99. Hu J, Kinn J, Zirakzadeh AA et al. The effects of chemotherapeutic drugs on human monocyte-derived dendritic cell differentiation and antigen presentation. *Clin Exp Immunol* 2013; 172: 490–499.
100. Huang X, Cui S, Shu Y. Cisplatin selectively downregulated the frequency and immunoinhibitory function of myeloid-derived suppressor cells in a murine B16 melanoma model. *Immunol Res* 2016; 64: 160–170.
101. Tel J, Hato SV, Torensma R et al. The chemotherapeutic drug oxaliplatin differentially affects blood DC function dependent on environmental cues. *Cancer Immunol Immunother* 2012; 61: 1101–1111.
102. Peng J, Hamanishi J, Matsumura N et al. Chemotherapy induces programmed cell death-ligand 1 overexpression via the nuclear factor- κ B to foster an immunosuppressive tumor microenvironment in ovarian cancer. *Cancer Res* 2015; 75: 5034–5045.
103. Wang W, Wu L, Zhang J et al. Chemoimmunotherapy by combining oxaliplatin with immune checkpoint blockades reduced tumor burden in colorectal cancer animal model. *Biochem Biophys Res Commun* 2017; 487: 1–7.
104. Terenzi A, Pirker C, Keppler BK, Berger W. Anticancer metal drugs and immunogenic cell death. *J Inorg Biochem* 2016; 165: 71–79.
105. Tesniere A, Schlemmer F, Boige V et al. Immunogenic death of colon cancer cells treated with oxaliplatin. *Oncogene* 2010; 29: 482–491.
106. Liu WM, Fowler DW, Smith P, Dalglish AG. Pre-treatment with chemotherapy can enhance the antigenicity and immunogenicity of tumours by promoting adaptive immune responses. *Br J Cancer* 2010; 102: 115–123.
107. Homma Y, Taniguchi K, Nakazawa M et al. Changes in the immune cell population and cell proliferation in peripheral blood after gemcitabine based chemotherapy for pancreatic cancer. *Clin Transl Oncol* 2014; 16: 330–335.
108. Vincent J, Mignot G, Chalmin F et al. 5-Fluorouracil selectively kills tumor-associated myeloid-derived suppressor cells resulting in enhanced T cell-dependent antitumor immunity. *Cancer Res* 2010; 70: 3052–3061.
109. Grosflam J, Weinblatt ME. Methotrexate: mechanism of action, pharmacokinetics, clinical indications, and toxicity. *Curr Opin Rheumatol* 1991; 3: 363–368.
110. Kaneno R, Shurin GV, Tourkova IL, Shurin MR. Chemomodulation of human dendritic cell function by antineoplastic agents in low noncytotoxic concentrations. *J Transl Med* 2009; 7: 58.

111. Galetto A, Buttiglieri S, Forno S et al. Drug- and cell-mediated antitumor cytotoxicities modulate cross-presentation of tumor antigens by myeloid dendritic cells. *Anticancer Drugs* 2003; 14: 833–843.
112. Cui S. Immunogenic chemotherapy sensitizes renal cancer to immune checkpoint blockade therapy in preclinical models. *Med Sci Monit* 2017; 23: 3360–3366.
113. Papadimitrakopoulou V, Gadgeel SM, Borghaei H et al. First-line carboplatin and pemetrexed (CP) with or without pembrolizumab (pembro) for advanced nonsquamous NSCLC: updated results of KEYNOTE-021 cohort G. *J Clin Oncol* 2017; 35: 9094.
114. Lesterhuis WJ, Salmons J, Nowak AK et al. Synergistic effect of CTLA-4 blockade and cancer chemotherapy in the induction of anti-tumor immunity. *PLoS One* 2013; 8:61895.
115. Iida Y, Harashima N, Motoshima T et al. Contrasting effects of cyclophosphamide on anti-CTL-associated protein 4 blockade therapy in two mouse tumor models. *Cancer Sci* 2017; 108(10): 1974–1984.
116. Adams S, Diamond JR, Hamilton EP et al. Phase Ib trial of atezolizumab in combination with nab-paclitaxel in patients with metastatic triple-negative breast cancer (mTNBC). *J Clin Oncol* 2016; 34: 1009.
117. Liu SV, Camidge DR, Gettinger SN et al. Long-term survival follow-up of atezolizumab in combination with platinum-based doublet chemotherapy in patients with advanced non-small-cell lung cancer. *Eur J Cancer* 2018; 101: 114–122.
118. Horn L, Mansfield AS, Szczesna A et al. First-line atezolizumab plus chemotherapy in extensive-stage small-cell lung cancer. *N Engl J Med* 2018; 379: 2220–2229.
119. Grigg C, Reuland BD, Sacher AG et al. Clinical outcomes of patients with non-small cell lung cancer (NSCLC) receiving chemotherapy after immune checkpoint blockade. *J Clin Oncol* 2017; 35: 9082.
120. Reck M, Socinski MA, Cappuzzo F et al. Primary PFS and safety analyses of a randomized phase III study of carboplatin + paclitaxel +/- bevacizumab, with or without atezolizumab in 1L non-squamous metastatic nscl (IMPOWER150). *Ann Oncol* 2018; 13:77-78.
121. Vida AR, Mellado B, del MXG et al. Phase II randomized study of first line avelumab with carboplatin-gemcitabine versus carboplatin-gemcitabine alone in patients with metastatic urothelial carcinoma ineligible for cisplatin-based therapy. *J Clin Oncol* 2018; 36:4591.
122. Yu Y, Lee NY. JAVELIN Head and Neck 100: a phase III trial of avelumab and chemoradiation for locally advanced head and neck cancer. *Futur Oncol* 2019; 15:687-694
123. Loibl S, Untch, M, Burchardi, N et al. Randomized phase II neoadjuvant study (GeparNuevo) to investigate the addition of durvalumab to a taxane-anthracycline containing chemotherapy in triple negative breast cancer (TNBC). *J Clin Oncol* 2018; 36:104.
124. Landry CA, Guziel JM, Ru M et al. A phase Ib study evaluating the safety and tolerability of durvalumab in combination with eribulin in patients with HER2-negative metastatic breast cancer and recurrent ovarian cancer. *J Clin Oncol* 2018; 36:3116.
125. Vera Aguilera J, Paludo J, Bangalore A et al. Chemoimmunotherapy combination after PD-1 inhibitor failure to improve clinical outcomes in metastatic melanoma patients. *J Clin Oncol* 2018; 36: 9558.
126. Robert C, Thomas L, Bondarenko I et al. Ipilimumab plus dacarbazine for previously untreated metastatic melanoma. *N Engl J Med* 2011; 364: 2517–2526.
127. Wolchok JD, Neyns B, Linette G et al. Ipilimumab monotherapy in patients with pretreated advanced melanoma: a randomised, doubleblind, multicentre, phase 2, dose-ranging study. *Lancet Oncol* 2010; 11: 155–164.
128. Hersh EM, O'Day SJ, Powderly J et al. A phase II multicenter study of ipilimumab with or without dacarbazine in chemotherapy-naïve patients with advanced melanoma. *Invest New Drugs* 2011; 29: 489–498.
129. Lynch TJ, Bondarenko I, Luft A et al. Ipilimumab in combination with paclitaxel and carboplatin as first-line treatment in stage IIIB/IV non-small-cell lung cancer: results from a randomized, double-blind, multicenter phase II study. *J Clin Oncol* 2012; 30: 2046–2054.
130. Galsky MD, Wang H, Hahn NM et al. Phase 2 trial of gemcitabine, cisplatin, plus ipilimumab in patients with metastatic urothelial cancer and impact of DNA damage response gene mutations on outcomes. *Eur Urol* 2017; 73: 751–759.
131. Govindan R, Szczesna A, Ahn M-J et al. Phase III trial of ipilimumab combined with paclitaxel and carboplatin in advanced squamous non-small- cell lung cancer. *J Clin Oncol* 2017; 35: 3449–3457.

132. Gordon EM, Chua-Alcala VS, Kim K et al. Phase 1/2 study of safety/efficacy using trabectedin, ipilimumab, and nivolumab as first-line treatment of advanced soft tissue sarcoma (STS). *J Clin Oncol* 2018; 36:46.
133. Kanda S, Goto K, Shiraishi H et al. Safety and efficacy of nivolumab and standard chemotherapy drug combination in patients with advanced non-small-cell lung cancer: a four arms phase Ib study. *Ann Oncol* 2016; 27: 2242–2250.
134. Rizvi NA, Hellmann MD, Brahmer JR et al. Nivolumab in combination with platinum-based doublet chemotherapy for first-line treatment of advanced non-small-cell lung cancer. *J Clin Oncol* 2016; 34: 2969–2979.
135. Garrido-Castro AC, Barry WT, Traina TA et al. A randomized phase II trial of carboplatin with or without nivolumab in first- or second-line metastatic TNBC. *J Clin Oncol* 2018; 36:1118.
136. Nishina T, Hironaka S, Kadowaki S et al. An investigator initiated multicenter phase I/II study of paclitaxel, ramucirumab with nivolumab as the second-line treatment in patients with metastatic gastric cancer. *J Clin Oncol* 2018; 36: 4131.
137. Ozaki Y, Matsumoto K, Takahashi M et al. Phase II study of a combination therapy of nivolumab, bevacizumab and paclitaxel in patients with HER2-negative metastatic breast cancer as a first-line treatment (WJOG9917B, NEWBEAT trial). *J Clin Oncol* 2018; 36: 1110.
138. Evans NR, Cowan S, Solomides C et al. Nivolumab plus cisplatin/pemetrexed or cisplatin/gemcitabine as induction in resectable NSCLC. *J Clin Oncol* 2018; 36(Suppl 15): TPS8582.
139. Chawla SP, Sankhala KK, Ravicz J et al. Clinical experience with combination chemo-immunotherapy using trabectedin and nivolumab for advanced soft tissue sarcoma. *J Clin Oncol* 2018; 36:23568.
140. Fujimoto N, Aoe K, Kozuki T et al. A phase II trial of first-line combination chemotherapy with cisplatin, pemetrexed, and nivolumab for unresectable malignant pleural mesothelioma: a study protocol. *Clin Lung Cancer* 2018; 19:705–707.
141. Bhatti S, Heldstab J, Lehn C et al. Safety and efficacy study of pembrolizumab (MK-3475) in combination with chemotherapy as neoadjuvant treatment for participants with triple negative breast cancer (TNBC) (MK-3475-173/KEYNOTE 173). *J Clin Oncol* 2017; 35: 556–556.
142. Weiss GJ, Waypa J, Blaydorn L et al. A phase Ib study of pembrolizumab plus chemotherapy in patients with advanced cancer (PembroPlus). *Br J Cancer* 2017; 117: 33–40.
143. Langer CJ, Gadgeel SM, Borghaei H et al. Carboplatin and pemetrexed with or without pembrolizumab for advanced, non-squamous nonsmall- cell lung cancer: a randomised, phase 2 cohort of the open-label KEYNOTE-021 study. *Lancet Oncol* 2016; 17: 1497–1508.
144. Obeid E, Zhou C, Macfarlane A et al. Combining chemotherapy and programmed death 1 (PD-1) blockade to induce a T-cell response in patients with metastatic triple negative breast cancer (mTNBC). *J Clin Oncol* 2017; 35: 11563.
145. Tolaney SM, Kalinsky K, Kaklamani V et al. Abstract PD6-13: phase 1b/2 study to evaluate eribulin mesylate in combination with pembrolizumab in patients with metastatic triple-negative breast cancer. *Cancer Res* 2018; 78: 6–13.
146. Page DB, Kim IK, Sanchez K et al. Safety and efficacy of pembrolizumab (pembro) plus capecitabine (cape) in metastatic triple negative breast cancer (mTNBC). *J Clin Oncol* 2018; 36: 1033.
147. Gandhi L, Rodri'guez-Abreu D, Gadgeel S et al. Pembrolizumab plus chemotherapy in metastatic non-small-cell lung cancer. *N Engl J Med* 2018; 378: 2078–2092.
148. Paz-Ares L, Luft A, Vicente D et al. Pembrolizumab plus chemotherapy for squamous non-small-cell lung cancer. *N Engl J Med* 2018; 379: 2040–2051.
149. Paz-Ares LG, Luft A, Tafreshi A et al. Phase 3 study of carboplatin/paclitaxel/nab-paclitaxel (Chemo) with or without pembrolizumab (Pembro) for patients (Pts) with metastatic squamous (Sq) non-small cell lung cancer (NSCLC). *J Clin Oncol* 2018; 36: 105.
150. Parikh M, Pan C-X, Beckett LA et al. Pembrolizumab combined with either docetaxel or gemcitabine in patients with advanced or metastatic platinum-refractory urothelial cancer: results from a phase I study. *Clin Genitourin Cancer* 2018; 16: 421–428
151. Aglietta M, Barone C, Sawyer MB et al. A phase I dose escalation trial of tremelimumab (CP-675, 206) in combination with gemcitabine in chemotherapy-naive patients with metastatic pancreatic cancer. *Ann Oncol* 2014; 25: 1750–1755.
152. Pfirschke C, Engblom C, Rickelt S et al. Immunogenic chemotherapy sensitizes tumors to checkpoint blockade therapy. *Immunity* 2016; 44: 343–354.

153. Adaptive phase II randomized non-comparative trial of nivolumab after induction treatment in triple negative breast cancer: TONIC-trial. *Ann Oncol* 2017; 28: 605–649
154. Kok M, Voorwerk L, Horlings H et al. Adaptive phase II randomized trial of nivolumab after induction treatment in triple negative breast cancer (TONIC trial): final response data stage I and first translational data. *J Clin Oncol* 2018; 36:1012.
155. Gray A, de la Luz Garcia-Hernandez M, van West M et al. Prostate cancer immunotherapy yields superior long-term survival in TRAMP mice when administered at an early stage of carcinogenesis prior to the establishment of tumor-associated immunosuppression at later stages. *Vaccine* 2009; 27: 52–59.
156. Ehrke MJ. Immunomodulation in cancer therapeutics. *Int Immunopharmacol* 2003; 3: 1105–1119.
157. Maccubbin DL, Wing KR, Mace KF et al. Adriamycin-induced modulation of host defenses in tumor-bearing mice. *Cancer Res* 1992; 52: 3572–3576.

Chapter 7

Conclusions and future perspectives

CONCLUSIONS AND FUTURE PERSPECTIVES

With the approval of checkpoint inhibition therapy, anti-cancer immunotherapy has taken a leap forward. This thesis described how treatment with immunotherapy could be further improved by investigating novel therapies (chapter 1 and 2), broadening the range of tumors for existing therapies (chapter 3), developing assays for identifying novel biomarkers (chapter 4), identifying potential pitfalls (chapter 5) and designing rational strategies for combination treatment (chapter 6).

Novel therapies

Although no one doubts the impact checkpoint inhibitors have had in the field of anti-cancer immunotherapy, still only subsets of patients show responses to treatment. Indeed, a need for novel therapies in order to treat an even broader range of cancers is necessary. **Chapter 1** described novel antibodies which target immune cells to the tumor site, with the aim of triggering novel and local immune responses. **Chapter 1.1** showed that a CEA targeting bispecific monoclonal antibody was able to generate an anti-tumor immune response in microsatellite stable colorectal cancers, a phenomenon not achieved by checkpoint inhibition therapy alone. **Chapter 1.2** described two tumor targeting immunocytokines which contain a variant of IL-2. For CEA-IL2v, imaging studies have confirmed the selective and targeted tumor accumulation in another study. Anti-tumor responses were seen in melanoma patients and head and neck squamous cell cancer types. Further investigation is required to assess the added value of the targeting component of these immunocytokines in regards to efficacy. **Chapter 2** described monoclonal antibodies targeting co-stimulatory receptor molecules. Targeting OX40 is currently explored in the clinic by multiple pharmaceutical companies. **Chapter 2.1 and 2.2** described the OX40 monoclonal antibody from GSK and Pfizer respectively. Both compounds were deemed safe and tolerable. Anti-tumor responses were seen in both monotherapy and combination therapy, and currently the focus for these compounds is to identify the most suitable combination partner. **Chapter 2.3** described the anti-CD40 antibody selicrelumab in combination with either atezolizumab or vanucizumab. The main toxicity seen was injection site reactions due to the subcutaneous administration of the compound. Efficacy is currently assessed in expansion cohorts of selected tumor types.

Broadening the range of tumors for existing therapies.

In the past years, approval of pembrolizumab has expanded rapidly across tumor types. Approval started with melanoma and non-small cell lung cancer, and has expanded to head and neck squamous cell carcinoma, Merkel cell carcinoma, urothelial cell carcinoma, gastric cancer, classical Hodgkin lymphoma, B-cell lymphoma, MSI-H/dMMR cancers, hepatocellular carcinoma and cervical cancer. KEYNOTE-158 is a large study which is still ongoing and which determines the efficacy of pembrolizumab in advanced rare tumor types. Approval of pembrolizumab in PD-L1 positive cervical cancer is based on efficacy data of KEYNOTE-158 and is described in **Chapter 3.1**. Modest efficacy results were observed, with an objective response rate of 12.2% (95% CI, 6.5% - 20.4). A safety and efficacy analysis of patients with rare tumors treated at the Netherlands Cancer Institute was described in **Chapter 3.2**. Efficacy was seen in a broad range of tumor types including MSI-H tumors, anal cancer, small cell lung cancer, and cervical cancer.

Developing assays for identifying novel biomarkers

Much research is done to identify relevant biomarkers in order to select those patient populations who respond to treatment. However, the assays that are used in these studies are often poorly described, which may explain differences in findings. Therefore, there is a need for well-validated assays of which both the merits and limitations are known. **Chapter 4.1** described an enzyme linked immunosorbent assay which is capable of measuring nivolumab and pembrolizumab in human serum and cerebrospinal fluid. This is the first assay describing nivolumab concentrations in cerebrospinal fluid. This assay can be used for further studies investigating the relation between nivolumab concentrations and responses seen in brain metastases. **Chapter 4.2** described a multiparameter flow cytometry assay for quantification of immune cell subsets, PD-1 expression levels and PD-1 receptor occupancy by nivolumab and pembrolizumab. Together, these two assays can be used to set up a large study in patients treated with nivolumab or pembrolizumab to assess the relationship between (1) serum or cerebrospinal fluid concentrations and response or toxicity, (2) receptor occupancy and response, (3) PD-1 expression levels on various immune cell subsets and efficacy.

Designing rational strategies for combination treatment

Combination treatment is a potential strategy to broaden the indication range of anticancer immunotherapy. However, rather than combining all novel immunotherapies with checkpoint inhibitors, the focus should be on designing rational strategies. An example for this is the tumor-targeting immunocytokine FAP-IL2v, which was described in **Chapter 1.2**. This molecule will continue development with combination partners that show antigen-dependent cell mediated toxicity. Biomarker data revealed that FAP-IL2v showed high proliferation and activation of peripheral natural killer cells upon treatment. Natural killer cells can bind to tumor cell-bound antibodies, resulting into degranulation and eventually death of the tumor cells by apoptosis. Cetuximab and trastuzumab are antibodies which can bind to tumor cells and promote antigen-dependent cell mediated killing by natural killer cells. These combination trials are currently ongoing, so far showing promising results.

As described in this thesis, the efficacy of the monoclonal antibodies targeting co-stimulatory molecules show modest efficacy in monotherapy. A potential reason for this is that co-stimulatory receptors typically only stimulate already ongoing immune responses. Therefore, the ideal combination partner might be those that trigger novel anti-tumor immune responses. As described in **Chapter 6**, preclinical and retrospective clinical studies of chemotherapeutic compounds have shown that this class of drug might trigger novel immune responses. Quite recently, pembrolizumab has been approved both by FDA and EMA for combination treatment with pemetrexed and platinum in non-squamous NSCLC as first line treatment (August 2018), and with carboplatin and paclitaxel in squamous NSCLC, also as first line treatment (October 2018).

Identifying potential pitfalls

As drug development is remarkably expensive, it is of utmost importance to identify and overcome potential pitfalls of drug development as soon as possible.

One potential pitfall is anti-drug antibody (ADA) formation against biological agents, and a review describing this phenomenon is described in **Chapter 5**. ADAs appear to not significantly impact registered biologicals, however they may impact efficacy and safety of drugs currently in development. A high incidence was seen in the monoclonal antibodies investigated in this thesis that contain a CEA-binding region. The high incidence of ADAs not only showed loss of exposure in several patients, but also impacted safety. The problem was identified early, and patients were given the anti-CD20 antibody obinituzumab in order to prevent ADA formation.

Another potential pitfall observed in phase I immunotherapy studies described in this thesis is the high incidence of severe toxicities, such as infusion related reactions, capillary leak syndrome and cytokine release syndrome. Although these toxicities were not necessarily dose-limiting, the high incidence and severity requires specialized trained staff (both nurses and physicians) to identify and treat these symptoms. These toxicities may make it unable to treat patients in non-academic hospitals, and therefore less suitable to treat a broad range of patients. In addition, patients often experience significantly more fatigue or require prolonged hospital stays. It is crucial to find not just the maximal tolerated dose, but also a dose which gives patients an acceptable quality of life.

Anti-cancer immunotherapy is an exciting field which develops rapidly. Already in the four years during this PhD, checkpoint blockade therapy has been expanded in numerous tumors. However, as this thesis shows, exciting new challenges remain for improving immunotherapy.

Appendix

Summary

Nederlandse samenvatting

List of publications

Dankwoord

Curriculum vitae

Summary

The research in this thesis focuses on the early stage of clinical development of immunotherapeutic compounds.

Chapter 1 focuses on novel tumor targeting anti-tumor immunotherapies. By not only activating the immune system, but also targeting the immune cells to the tumor, a more favorable safety and efficacy profile might be reached. **Chapter 1.1** describes CEA-TCB, a novel bi-specific antibody which binds both CEA on the tumor, and CD3 on the T-cell. This chapter describes the dose-escalation portion of the trial, and shows that CEA-TCB effectively increases immune responses within the tumor. Anti-tumor responses were seen even in microsatellite stable colorectal patients, an achievement not seen with checkpoint inhibition therapy. **Chapter 1.2** describes clinical trials investigating immunocytokines which contain a variant of IL-2. This variant has an abolished α subunit of the IL-2 receptor, which prevents the immunocytokine to preferentially activate regulatory T-cells. Two different immunocytokines are described: FAP-IL2v targets fibroblast activating protein in the tumor stroma, and CEA-IL2v targets carcinoembryonic antigen on tumor cells. Tolerability was moderate, with many patients experiencing infusion related reactions and having prolonged hospital stays. However, treatment was more tolerable in subsequent cycles, and durable anti-tumor responses were seen in multiple patients.

Chapter 2 focuses on monoclonal antibodies which target co-stimulatory receptor molecules. **Chapter 2.1 and 2.2** describe phase I studies investigating anti-OX40 treatment. **Chapter 2.1** investigates GSK3174998 as monotherapy and in combination with pembrolizumab. The drug was well tolerable and an anti-tumor response was seen in a heavily pre-treated soft tissue sarcoma patient. **Chapter 2.2** investigates the phase I study of PF-04518600 in selected tumor types. No dose-limiting toxicities occurred in this trial, and three patients achieved an objective response. Biomarker analysis revealed proliferation and activation of CD4+ cells, clonal expansion of CD4+ and CD8+ cells, and upregulation of genes of the inflammatory response pathway. **Chapter 2.3** investigates selicrelumab in combination with either atezolizumab or vanucizumab. In these trials, selicrelumab was administered subcutaneously. This led to a more favorable pharmacokinetic and safety profile as compared to intravenous administration. However, nearly all patients experienced injection site reactions. These reactions were manageable with topical corticosteroid treatment. Modest efficacy was seen in the trials, with responses seen in microsatellite instable colorectal cancer, squamous cell carcinoma of unknown origin, and ovarian cancer.

Chapter 3 describes results of the KEYNOTE-158 study, a study which investigates pembrolizumab in advanced rare cancers. **Chapter 3.1** describes pembrolizumab in cervical cancer. Based on this data, pembrolizumab has been approved for the treatment of patients with PD-L1 positive cervical cancer which have progressed on or after chemotherapy. The observed responses were exclusively seen in PD-L1 positive patients. **Chapter 3.2** describes results of the KEYNOTE-158 study of patients treated at the Netherlands Cancer Institute. Durable (> 6 months) responses were seen in a wide variety of tumor types, including anal carcinoma, cervical cancer, small cell lung cancer, and microsatellite instable tumors.

Chapter 4 describes the development of two assays which can be used in the clinic to measure anti-PD-1 monoclonal antibody serum concentrations and receptor occupancy levels. These assays can be used for further immunomonitoring studies to investigate the effect of pharmacokinetics, receptor occupancy levels, and proportion of immune cell subsets on clinical outcome.

Chapter 5 discusses an important phenomenon seen in drug development of biologicals: the formation of anti-drug antibodies. As the name implies, these antibodies bind to the therapeutic agent and may impact exposure, pharmacodynamics, or safety of the drug. The majority of biologicals trigger anti-drug antibody formation. However, the clinical relevance of these ADAs are often not described. This chapter aimed at raising awareness to consistently report the incidence and impact of ADA formation, as well as using well-validated assays which only measure parameters that are relevant to drug development.

Chapter 6 discusses a controversial partner for immunotherapy, namely chemotherapy. Chemotherapy is notoriously known for being immunosuppressive. However, current (mainly preclinical) research suggests that they exert immunological effects which may be beneficial for immunotherapy. For example, some forms of chemotherapy selectively deplete immunosuppressive cells, whereas others induce an immunological form of apoptosis – immunogenic cell death. Chapter 6 discusses each class of drug in the light of being a combination partner for immunotherapy. In addition, currently ongoing clinical trials are examined in regards to design and results.

Finally, **Chapter 7** ends this thesis with conclusions and future perspectives of immunotherapy.

Nederlandse samenvatting

Het onderzoek in dit proefschrift richt zich op de vroeg-klinische ontwikkeling van immunotherapeutische geneesmiddelen.

Hoofdstuk 1 richt zich op nieuwe tumorgerichte anti-tumor immunotherapieën. Door niet alleen het immuunsysteem te activeren, maar ook de immuuncellen naar de tumor te richten, kan een beter veiligheids- en effectiviteitsprofiel worden bereikt. **Hoofdstuk 1.1** beschrijft CEA-TCB, een nieuw bi-specifiek antilichaam welke bindt aan zowel CEA op de tumor, en CD3 op de T-cel. Dit hoofdstuk beschrijft het dosisescalatie gedeelte van de trial, en laat zien dat CEA-TCB effectief immuun responsen opwekt in de tumor. Anti-tumor responsen werden vastgesteld in microsatelliet stabiele colorectaal patiënten, iets wat nog niet gezien is bij checkpoint blokkade therapie. **Hoofdstuk 1.2** beschrijft klinische trials welke nieuwe immuuncytokinen onderzoeken. Deze immuuncytokinen bevatten een variant van IL-2, welke niet meer in staat is te binden aan de α subeenheid van de IL-2 receptor. Hierdoor bindt de immuuncytokine niet langer preferentieel aan regulatoire T-cellen. Twee verschillende immuuncytokinen worden beschreven: FAP-IL2v bindt aan Fibroblast Activating Protein, een eiwit in de stroma van de tumor. CEA-IL2v bindt aan carcinoembryonic antigen op de tumor cellen. De tolerabiliteit van beide middelen was matig. Menig patient ondergingen een infuusreactie en verbleven langere tijd in het ziekenhuis. Toediening werd tolereerbaarder in vervolgcycli, en anti-tumor activiteit werd gezien in meerdere patiënten

Hoofdstuk 2 focust zich op monoclonale antilichamen welke binden aan co-stimulatorische receptor moleculen. **Hoofdstuk 2.1 en 2.2** beschrijven fase I studies welke anti-OX40 behandeling onderzoeken. **Hoofdstuk 2.1** onderzoekt GSK3174998 als monotherapie en in combinatie met pembrolizumab. Het medicijn werd goed verdragen, en anti-tumor responsen werden gezien in een zwaar voorbehandelde patiënt met sarcoom van de weke delen. **Hoofdstuk 2.2** onderzoekt de fase I studie van PF-04518600 als monotherapie en in combinatie met utomilumab in voorgeselecteerde tumor typen. In deze trial werden geen dosis-limiterende toxiciteiten gezien, en responsen werden vastgesteld in melanoompatiënten en een patiënt met hepatocellulair carcinoom. Biomarker analyse liet zien dat er proliferatie en activatie optreedt in CD4+ cellen, klonale expansie van CD4+ en CD8+ T cellen, en opregulatie van genen betrokken bij ontstekingsreacties. **Hoofdstuk 2.3** onderzoekt selicrelumab in combinatie met atezolizumab of vanucizumab. Selicrelumab werd subcutaan toegediend bij patiënten, wat leidt tot een beter farmacokinetisch- en veiligheidsprofiel. Echter, bijna alle patiënten vertoonden een huidreactie op de plaats van injectie. Deze reactie was goed behandelbaar met corticosteroïdezalf. Responsen traden op bij microsatelliet instabiele colorectaal kanker, epitheelcelkanker van onbekende origine en ovariumkanker.

Hoofdstuk 3 beschrijft de resultaten van KEYNOTE 158, een studie welke pembrolizumab onderzoekt in zeldzame tumoren. **Hoofdstuk 3.1** beschrijft pembrolizumab in baarmoederhalskanker. Gebaseerd op deze data is pembrolizumab goedgekeurd voor de behandeling van patiënten met PD-L1 positieve baarmoederhalskanker die progressie

vertoonden op chemotherapie. Responsen werden exclusief gezien in PD-L1 positieve tumoren. **Hoofdstuk 3.2** beschrijft de resultaten van de KEYNOTE-158 studie van patiënten die behandeld zijn in het Nederlands Kanker Instituut. Duurzame (> 6 maanden) anti-tumor responsen werden gezien in anuscarcinoom, baarmoederhalskanker, kleincellig long kanker, en microsatelliet instabiele tumoren.

Hoofdstuk 4 beschrijft de ontwikkeling van twee analytische methodes welke in de kliniek gebruikt kunnen worden om anti-PD-1 monoclonale antilichaam serum concentraties en receptorbezetting te meten. Deze technieken kunnen gebruikt worden voor immunomonitoring studies welke de effecten van farmacokinetiek, receptor bezetting en verhouding van de verscheidene typen immuuncellen onderzoeken in relatie tot klinische uitkomst.

Hoofdstuk 5 beschrijft een belangrijk fenomeen dat wordt gezien in de klinische ontwikkeling van biologische middelen: anti-geneesmiddel antilichamen (ADAs). Zoals de naam zegt, binden deze ADAs zich aan het therapeutische geneesmiddel, wat een effect kan hebben op de blootstelling, farmacodynamiek of veiligheid van het middel. Echter, de klinische relevantie van deze ADAs worden vaak niet beschreven. Dit hoofdstuk heeft als doel bewustwording van het fenomeen, en de noodzaak om consistent de incidentie en impact van ADAs te rapporteren.

Hoofdstuk 6 beschrijft een controversiële partner voor immunotherapie: chemotherapie. Chemotherapie is bekend om zijn immunosuppressieve eigenschappen. Echter, nieuwe (voornamelijk preklinische) studies laten zien dat chemotherapie ook gunstige eigenschappen kunnen hebben op het immuunsysteem. Zo zouden bepaalde chemotherapieën selectief de immunosuppressieve cellen vernietigen. Weer andere chemotherapieën zorgen voor een immunologische vorm van apoptose: immunogenische celdood. **Hoofdstuk 6** beschrijft elke klasse van chemotherapie en bekijkt welke soorten geschikt zijn als combinatiepartner voor checkpoint blokkade therapie. Verder worden huidige klinische studies onder de loep genomen wat betreft studieopzet en resultaten.

Tenslotte sluit **hoofdstuk 7** dit proefschrift af met conclusies en toekomstperspectieven.

LIST OF PUBLICATIONS

Articles

Chung, H. C., **Ros, W.**, Delord, J-P , Perets, R., Italiano, A., Shapira-Frommer, R., Manzuk, L., Piha-Paul S. A., Xu L., Zeigenfuss, S., Pruitt, S K., Leary A. Efficacy and safety of pembrolizumab in previously treated advanced cervical cancer: results from the phase II KEYNOTE-158 study.

Journal of Clinical Oncology 2019;37:1470-1478

Heinhuis, K.M*, **Ros, W.***, Kok, M., Steeghs, N. Beijnen, J., Schellens, J.H.M. Enhancing anti-tumor response by combining immune checkpoint inhibitors with chemotherapy in solid tumors.

Annals of Oncology 2019 Feb 1;30:219-235.

Pluim, D*, **Ros, W*.**, van Bussel, M. T. J., Brandsma, D., Beijnen, J. H., & Schellens, J. H. M.. Enzyme linked immunosorbent assay for the quantification of nivolumab and pembrolizumab in human serum and cerebrospinal fluid.

Journal of Pharmaceutical and Biomedical Analysis 2019; 164:128–134.

van Brummelen, E.M.J*, **Ros, W*.**, Wolbink, G., Beijnen, J.H., and Schellens, J.H.M. (2016). Antidrug Antibody Formation in Oncology: Clinical Relevance and Challenges.

The Oncologist. 2016;21: 1260 - 1268

Van den Wollenberg, D.J.M., Dautzenberg, I.J.C., **Ros, W.**, Lipińska, A.D., van den Hengel, S.K., and Hoeben, R.C. . Replicating reoviruses with a transgene replacing the codons for the head domain of the viral spike.

Gene Therapy 2015; 22, 267–279.

Diab A, Hamid O, Thompson JA, **Ros W**, Eskens F, Doi T, Hu-Lieskovan S, Klempner SJ, Ganguly B, Fleener C, Joh T, Liao K, Turich Taylor C, Chou J, El-Khoueiry A. A first in human phase 1 and pharmacological study of the OX40 agonist PF-04518600 in patients with selected locally advanced or metastatic cancers

Submitted

Pluim D*, **Ros W***, Miedema IHC, Beijnen JH, Schellens JHM. Multiparameter flow cytometry assay for quantification of immune cell subsets, PD-1 expression levels and PD-1 receptor occupancy by nivolumab and pembrolizumab.

Cytometry Part A [In press.]

***Shared first author**

Abstracts

Melero I, Segal NH, Saro Suarez JM, **Ros W**, Martinez Garcia M, Calvo E, Moreno V, Ponce Aix S, Marabelle A, Cleary JM, Hurwitz H, Eder JP, Jamois C, Belousov A, Bouseida S, Sandoval F, Bacac M, Nayak TK, Karanikas V, Argiles G. Pharmacokinetics (PK) and pharmacodynamics (PD) of a novel carcinoembryonic antigen (CEA) T-cell bispecific antibody (CEA CD3 TCB) for the treatment of CEA-expressing solid tumors. *Journal of Clinical Oncology* 2017;35:2549.

Segal NH, Saro J, Melero I, **Ros W**, Argiles G, Marabelle A, Rodriguez Ruiz ME, Albanell J, Calvo E, Moreno V, Cleary JM, Eder JP, Karanikas V, Bouseida S, Sandoval F, Sabanes D, Sreckovic S, Hurwitz H, Paz-Ares L, Tabernero J. Phase I Studies of the Novel Carcinoembryonic Antigen CD3 T-Cell Bispecific (CEA-CD3 TCB) Antibody as a Single Agent and in Combination With Atezolizumab: Preliminary Efficacy and Safety in Patients With Metastatic Colorectal Cancer (mCRC). *Annals of Oncology* 2017;28:10.

Tabernero, J., Melero, I., **Ros, W.**, Argiles, G., Marabelle, A., Rodriguez-Ruiz, M.E., Albanell, J., Calvo, E., Moreno, V., Cleary, J.M., et al. (2017). Phase Ia and Ib studies of the novel carcinoembryonic antigen (CEA) T-cell bispecific (CEA CD3 TCB) antibody as a single agent and in combination with atezolizumab: Preliminary efficacy and safety in patients with metastatic colorectal cancer (mCRC). *J. Clin. Oncol.* 2017; 35, 3002.

Soerensen MM, **Ros W**, Rodriguez-Ruiz ME, Robbrecht D, Rohrberg KS, Martin-Liberal J, Lassen UN, Melero Bermejo I, Lolkema MP, Tabernero J, Boetsch C, Piper-Lepoutre H, Waldhauer I, Charo J, Evers S, Teichgräber V, Schellens JHM. Safety, PK/PD, and anti-tumor activity of RO6874281, an engineered variant of interleukin-2 (IL-2v) targeted to tumor-associated fibroblasts via binding to fibroblast activation protein (FAP). *Journal of Clinical Oncology* 2018;36:e15155

Melero I, Castanon Alvarez E, Mau Sorensen M, Lassen U, Lolkema M, G Robbrecht D, A Gomez-Roca C, Martin-Liberal J, Tabernero J, **Ros W**, Ahmed S, Isambert N, Piper Lepoutre H, Boetsch C, Charo J, Evers S, Teichgräber V, H M Schellens J. Clinical activity, safety, and PK/PD from a phase I study of RO6874281, a fibroblast activation protein (FAP) targeted interleukin-2 variant (IL-2v). *Annals of Oncology* 2018;29: 133-148.

El-Khoueiry AB, Hamid O, Thompson J, **Ros W**, Eskens F, Doi T, Hu-Lieskovan S, Chou J, Liao K, J Ganguly B, Fleener C, Joh T, Diab A. The relationship of pharmacodynamics (PD) and pharmacokinetics (PK) to clinical outcomes in a phase I study of OX40 agonistic monoclonal antibody (mAb) PF-04518600 (PF-8600). *Journal of Clinical Oncology* 2017; 35:3027

Hamid O, **Ros W**, Thompson JA, Rizvi NA, Angevin E, Chiappori A, Ott PA, Ganguly BJ, Fleener C, Liao K, Joh T, Dell V, Chou J, Hu-Lieskovan S, Eskens FALM, Diab A, Doi T, Wasser J, Spano J-P, El-Khoueiry A. Safety, pharmacokinetics (PK) and pharmacodynamics (PD) data from a phase I dose-escalation study of OX40 agonistic monoclonal antibody (mAb) PF-04518600 (PF-8600) in combination with utomilumab, a 4-1BB agonistic mAb.

Annals of Oncology 2017;28: v403-v427.

Diab A, Hamid O, Thompson JA, **Ros W**, Eskens FALM, Doi T, Hu-Lieskovan S, Long H, Joh T, Potluri S, Wang X, Fleener C, Taylor CT, Ganguli BJ, Chou J, El-Khoueiry AB. Pharmacodynamic (PD) changes in tumor RNA expression and the peripheral blood T cell receptor (TCR) repertoire in a phase I study of OX40 agonistic monoclonal antibody (mAb) PF-04518600 (PF-8600).

Cancer Research 2018; 78:CT010

Emiliano Calvo, Jan Schellens, Ignacio Matos, Elena Garralda, Morten Mau-Soerensen, Aaron Hansen, Maria Martinez-Garcia, Martijn Lolkema, Jehad Charo, Chiara Lambertini, Christoph Mancao, Katrijn Bogman, Cristiano Ferlini, Martin Sern, **Ros W**. Combination of subcutaneous selicrelumab (CD40 agonist) and vanucizumab (anti-Ang2/VEGF) in patients with solid tumors demonstrates early clinical activity and a favorable safety profile.

Journal for ImmunoTherapy of Cancer 2018;115:386

Chung HC, Lopez-Martin JA, Kao SC-H, Miller WH, **Ros W**, Gao B, Marabelle A, Gottfried M, Zer A, Delord J-P, Penel N, Jalal SI, Xu L, Zeigenfuss S, Pruitt SK, Piha-Paul SA. Phase 2 study of pembrolizumab in advanced small-cell lung cancer (SCLC): KEYNOTE-158.

Journal of Clinical Oncology 2018;36:8506.

Dankwoord

Graag wil ik iedereen bedanken die er aan heeft bijgedragen dat ik de afgelopen vier jaar met veel plezier en voldoening naar mijn werk ging.

Te beginnen met de personen waar het allemaal om draait: **de patienten en hun families**. Bedankt voor het vertrouwen in het AvL en ik wens jullie veel sterkte toe.

Veel dank aan mijn promotor **Jos Beijnen** en voormalig promotor **Jan Schellens**. Dankzij jullie heb ik deze fantastische mogelijkheid gekregen om mijn PhD in klinische farmacologie te doen. Ook veel dank aan **Frans, Serena, Marloes, Sofie** en **Neeltje**. Mede dankzij jullie kritische blik is dit boekje tot stand gekomen.

Ik wil graag mijn mede-OiO's bedanken voor de gezelligheid. We hebben de afgelopen vier jaar veel meegemaakt en we hebben onszelf er toch maar door heen geslagen. **Linda, Emilie, Vincent, Robin, Bart, Ruud, Maikel, Anke, Remy, Aurelia, Lotte, Roos, Cynthia en Didier**, bedankt voor de gezellige tijd. Verder wens ik iedereen veel succes met het afronden van hun eigen promotie: **Merel, Julie, Jonathan, Semra, Jorn, Karen, Nikki, Paniz, Ignace, Hedvig, Maarten, Evelien, Jeroen, Maaïke, Margarida, Sven, Luka en Diewertje**. Roomies: **Steffie, Laura, Marit, Kimberley, en Arthur**, bedankt voor de gezelligheid op de kamer, het was nooit stil. **Sanne en Jill**, ik ga jullie missen. **Mark**, samen begonnen, samen de finish-line bereikt. En uiteraard **Rene**: bedankt voor het tijdelijk overnemen van mijn studies.

Een speciale vermelding voor de top-analist **Dick Pluim**, die verantwoordelijk is voor het tot stand komen van maar liefst twee artikelen in mijn boekje. Jouw doorzettingsvermogen voor het opzetten van de immunologische assays was bewonderlijk, en ik vraag me af of ik dit had kunnen afronden zonder jou.

Verder wil ik graag de **verpleegkundigen van de CRU** bedanken. Ik heb veel respect voor jullie werkethiek. Jullie zullen nooit de kantjes er van af lopen. **Yvonne, Bianca, Tessa, Martine, Sofie, Jolien** – het was erg leuk het laatste half jaartje met jullie op de kamer te zitten. Ook dank aan **Brenda, Pascal, Fauzia, Jamie en Marja**.

Triallab en Pathology – hartelijk dank voor de prettige samenwerking!

Immunologiegroep: bedankt voor de regelmatige bezoeken aan jullie groep en jullie goede adviezen. Ook dank aan de groepleiders werkende op de afdeling Farmacologie: **Olaf, Alfred en Alwin Huitema.**

Collega's van het trialbureau – **Lidwina, Danja, Rebecca, Lisette, Floor, Christiane, Abi, Josien, Michiel, Lydia, Annelies, Gerda, Lindsey, Jeltje, Marjolein, Marjolijn, Ernst, Ludy, Lindsay, Dayenne, Marieke, Aysegul en Anja** – Nu ik zelf datamanager ben, zie ik hoeveel werk jullie verrichten voor de klinische studies. Heel veel dank daarvoor!

Paranimfen, maar vooral goede vriendinnen, **Laura en Charissa**, dank voor jullie vriendschap.

Mam, pap, zus en broer – jullie weten nog steeds niet wat ik precies doe, maar dat doet er ook niet toe. Dear **family from across the Atlantic Ocean**, thanks for always making me feel welcome in your home and supporting my pursue of the PhD degree.

Last but not least, I want to thank the single most important person in my life – my husband **Matt La Fontaine**. I cannot wait to see what the future holds for us.

Veel dank aan iedereen,
Willeke

Curriculum vitae

Willeke Ros was born on February 28th 1990 in Leiden. After graduating from high school 'Andreas College location Pieter Groen', she went to study for her Bachelors degree in Biology at the University of Leiden. Here, she conducted her internship at the Department of Molecular Biology at the Gorlaeus Laboratory. After this, she went to pursue her Masters degree in Biomedical Sciences at the Leiden University Medical Center (LUMC), which she received *cum laude*. She conducted various internships: generating a genetically modified reovirus at the department of Virus- and Stem Cell Biology at the LUMC, modelling the neurological disease lissencephaly in patient-derived neuro-epithelial stem cells at the Karolinska Institute, Stockholm (Sweden) and conducting pharmacodynamics assays for a clinical trial at the University of Wisconsin, Madison (U.S.A). Subsequently, she started her PhD research at the department of Pharmacology at the Netherlands Cancer Institute – Antoni van Leeuwenhoek Ziekenhuis, supervised by Prof. dr. J.H. Beijnen. and Prof. dr. J.H.M. Schellens. Her PhD research resulted in this thesis, which she will defend at Utrecht University on September 18th, 2019.